DOCTORAL THESIS

Investigation of the role of WIP and WASP in regulating myeloid cells migration during mild hyperthermia

Ciccioli, Mariacristina

Award date:
2020

Awarding institution:
University of Roehampton

Investigation of the role of WIP and WASP in regulating myeloid cells migration during mild hyperthermia

by

Mariacristina Ciccioli BSc, MSc

A thesis submitted in partial fulfilment of the requirements for the degree of PhD

Department of Life Sciences
University of Roehampton
2019

Abstract

Local mild hyperthermia stimulates the activity of immune cells including prompting leukocyte migration and trafficking, but the molecular mechanisms involved in this process are poorly understood. The Wiskott Aldrich Syndrome Protein (WASP) and the WASP interacting protein (WIP) work as a functional unit that plays a major role in assembly and disassembly of myeloid cell adhesions termed podosomes by binding both F-actin and other actin-related proteins. Besides, WIP can also regulate actin dynamics by modulating the lipid composition of the plasma membrane, as recently shown in neurons. In various organisms, the lipid composition and fluidity of the cell membrane work as a thermosensor that regulates the cellular response to changes in temperature. This study aimed to investigate whether WIP or WASP may regulate the migratory response to mild hyperthermia as in local inflammation or during a febrile event.

Results showed that mild hyperthermia (40°C) promoted random cell migration correlating with the assembly of more robust and dynamic podosomes with increased matrix degradation capability in a WASP and WIP-dependent manner. We observed that this response is dependent on the actin polymerising activity and the nuclear translocation of WASP.

Our data also indicate that increased membrane fluidity, like the one induced by hyperthermia, can trigger a migratory response in myeloid cells. Following hyperthermia, WIP delivers changes in monocytic cells membrane lipid composition to maintain fluidity homeostasis in the plasma membrane, particularly in podosomal areas at adhesion sites, triggering the increased invasive migratory capacity. The modulation of the lipid composition of the plasma membrane is mediated by the WIP-dependent regulation of genes involved in lipid biosynthesis and rafts formation in response to hyperthermia. These genes include NSMAF, OSBPL5 and regulators of cholesterol biosynthesis. In response to hyperthermia, WIP also controls the upregulation of Heat Shock protein 90 (HSP90), a protein previously associated with podosome formation. This process is independent of WASP.

Taken together, our data show a role of both WIP and WASP in the increased migratory phenotype of myeloid cells in response to mild hyperthermia.

Table of contents

List of figures

List of tables

Acknowledgements

First, my gratitude goes to my supervisor and Director of Studies, Dr. Yolanda Calle, for the continuous support, encouragement and guidance received throughout the whole PhD journey. Yolanda's supervision and training strongly contributed to my academic and professional development, making me a better scientist.

Besides, I would like to thank:

My second supervisor, Dr. Michal Letek, for the critical reading of this thesis, the knowledge shared, and the assistance provided, especially during the cloning development.

Dr. Jorge Bernardino de la Serna, who gave me the opportunity to join his team and access to outstanding research facilities. Jorge's experience contributed to an important part of this research.

Dr. Ines Anton, for constantly providing research advice and for the collection of primary samples.

The technical team at University of Roehampton for the continuous assistance.

The students and interns whose lab work contributed to the data collection, in particular Laura, Ricardo, Caera and Ricardo.

My fellow labmates and PhD students for sharing the laughs and the sorrows, in particular Natalia, Simone, Marie-Claire, Antonella and Myrto.

My family, whose sacrifice and support throughout my education allowed me to reach this goal.

Marco, for the graphical advice and more importantly for the patience, the daily support and for helping me believe in myself.

Author’s declaration

I declare that the worked included in this thesis is original, except where indicated by references in the text. The work was conducted by me, unless otherwise stated.

The thesis has not been presented to any University for examination, with the exception of the podosomes enumeration and matrix degradation work presented in Chapter 3, which was carried out with Ricardo Carlos Diaz Cuffin towards his BSc’s thesis, under my supervision.

Common abbreviations

3D – Three-dimensional

APC – Antigen Presenting Cell

Apo – Apolipoprotein

ARAP3 – Ankyrin Repeat and PH Domain 3

Arp – Actin related protein

ATP – Adenosine triphosphate

BA – Benzyl alcohol

BM – Basement membrane

Btk – Bruton's tyrosine kinase

BSA – Bovine serum albumin

CCR2 - CC-chemokine receptor 2

Cdc42 – Cell division control protein 42 homolog

CO2 – Carbon dioxide

CRIB – Cdc42 and Rac-interactive binding domain

DAPI – 4', 6-diamidino-2-Phenylindole

DC – Dendritic cell

DMEM – Dulbecco's Modified Eagle Medium

DNA – Deoxyribonucleic acid

ECM – Extracellular matrix

ERK – Extracellular signal-regulated kinase

F-actin – Filamentous actin

FA – Focal adhesion

FAK – Focal adhesion kinase

FBP – Formin binding protein

FCS – Foetal calf serum

FDR – false discovery rate

FN- fibronectin

G-actin – Globular actin

GAP – GTPase-activating proteins

GAPDH – Glyceraldehyde 3-phosphate dehydrogenase

GDP – Guanosine diphosphate

GP – Generalized polarization

GEF – Guanine nucleotide exchange factor

GFP – Green fluorescent protein

GTP – Guanosine triphosphate

HSE- Heat shock element

HSF – Heat shock factors

HSG – Heat shock genes

HSP – Heath shock protein

HEK – Human embryonic kidney

IF – Immunofluorescence

IL – Interleukin

Ig G – Immunoglobulin G

JMY – Junction-Mediating Regulator Protein

KO – Knockout

LFA – Lymphocyte Function Antigen

LPS – Lipopolysaccharide

MCP – Monocyte Chemoattractant Protein

MHC – Major Histocompatibility process

MLC – Light Chain Myosin

MMP – Matrix metalloprotease

MOI – Multiplicity of Infection

MRTFA – Myocardin-related transcription factor

N-WASP – Neural Wiskott Aldrich Syndrome protein

Nck – Non-catalytic region of tyrosine kinase adaptor protein

NES – Nuclear export signal

NLS – Nuclear localization signal

NPF – Nucleation-promoting factor

NK – Natural Killer

OSBPL5 – Oxysterol Binding Protein Like 5

ORP5 – Oxysterol-binding protein-related 5

PBS – Phosphate buffered saline

PECAM - platelet/endothelium cells adhesion molecule

PIP2 – Phosphatidylinositol 4,5-biphosphate

PL – Poly-L-Lysine

PI – Propidium Iodide

RES - Resistant

Rho – Ras homolog family member

ROCK – Rho-associated coiled-coil containing protein kinase

RICS – Raster image correlation spectroscopy

SDS – Sodium dodecyl Sulfate

SRF – Serum response factor

SRBPs – sterol regulatory binding proteins

N-SM – neutral sphingomyelin

SMase – sphingomyelinase

TBS-T – Tris-buffered saline and Tween 20

TCR – T-cell receptor

TGF-ß – Transforming growth factor beta

Tyr - tyrosine

TNF – Tumour necrosis factor

TRP - Transient receptor potential channels

VCA – Verprolin Central Acidic domain

VSV-G – Vesicular stomatitis virus-protein G

Was – Wiskott-Aldrich syndrome

Wasp – Wiskott-Aldrich syndrome protein

Wave – Wasp family verprolin homologs

WB – Western Blot

WIP – Wasp interacting protein

wt – Wild type

Chapter 1: Introduction

1 Introduction

In many biological events, both physiological and pathological, cells respond to a stimulus by trafficking. In physiological conditions, cell migration and invasion are seen in tissue repair, immune response and morphogenesis (Aman and Piotrowski, 2010; Trepat, Chen and Jacobson, 2012; Qu, Guilak and Mauck, 2019), while in pathological situations, cells invasion of the surrounding matrix can result into a metastatic event (van Zijl, Krupitza and Mikulits, 2011; Bravo-Cordero, Hodgson and Condeelis, 2012; Tahtamouni *et al.*, 2019). In both cases, migration is strictly dependent on actin cytoskeleton remodelling and adhesion to the extracellular matrix (Huttenlocher, Sandborg and Horwitz, 1995; Linder and Aepfelbacher, 2003; O'Neill, 2009; Parsons, Horwitz and Schwartz, 2010; Shafaq-Zadah *et al.*, 2016). Following an external stimulus, migrating cells tend to polarize and define a leading edge to guide the direction of locomotion (Calle *et al.*, 2006). However, the kind of protrusion assembled can vary based on the nature of the cell and on the type of surrounding matrix (Bershadsky *et al.*, 2006; van den Dries, Bolomini-Vittori and Cambi, 2014). Protrusions are assembled thanks to actin cytoskeleton polymerization and are stabilized through adhesion to the extracellular matrix (Huttenlocher and Horwitz, 2011). Adhesion structures can be more or less dynamic, and disassembly events are fundamental to allow cells detachment and progression (Destaing *et al.*, 2003; Calle *et al.*, 2006; Macpherson *et al.*, 2012).

1.1 Podosomes: structure, molecular composition and regulation

Podosomes take their name from the first description as cell feet in Rous sarcoma virus-transformed fibroblast that goes back to 1985 (Tarone et al., 1985). Since then, several discoveries unveiled their molecular structure and functions. Podosomes are now described as highly dynamic adhesion structures assembled at the border between the lamellipodium and the lamellum by myeloid lineage cells like macrophages, monocytes, dendritic cells, migratory phase osteoclasts and megakaryocytes (Evans et al., 2003; Calle et al., 2006; Chou et al., 2006; Luxenburg et al., 2006). Podosomes are dot shaped, with a diameter of 0.5-1μm, 0.6μm high and a lifetime of 2 to 12 minutes (Jones, 2008). They can organize to form superstructures, according to the cell type (Figure 1.1). Migratory phase macrophages and dendritic cells assemble evenly distributed podosomes behind lamellipodia in the leading edge (Evans et al., 2003; Monypenny et al., 2011), while osteoclasts, in their immature state, can assemble belt or ring-shaped podosomes clusters, identified as precursors to specialized sealing zones (Luxenburg et al., 2007). In addition to myeloid cells, podosomal-like structures were also found in non-myeloid cells as endothelial cells exposed to the transforming growth factor β (TGF- β) (Varon et al., 2006) and virus Src-transformed fibroblasts, where podosomes are distributed in large ring-shaped clusters known as rosettes (Pan et al., 2013). Although podosomes structural organization might differ (Figure 1.1), a striking evidence of podosomes presence is the typical subdivision between the F-actin core (Chou et al., 2006) and the integrin-associated ring structure (Staszowska et al., 2017). Other hallmarks of podosomes are the high turnover (Macpherson et al., 2012) and the ability to degrade basement membranes through the secretion of proteases (Bañón-Rodríguez et al., 2011). It is mainly for this capability that

podosomes have been related to other structures such as invadopodia, mainly produced by metastatic cancer cells (Linder, 2009).

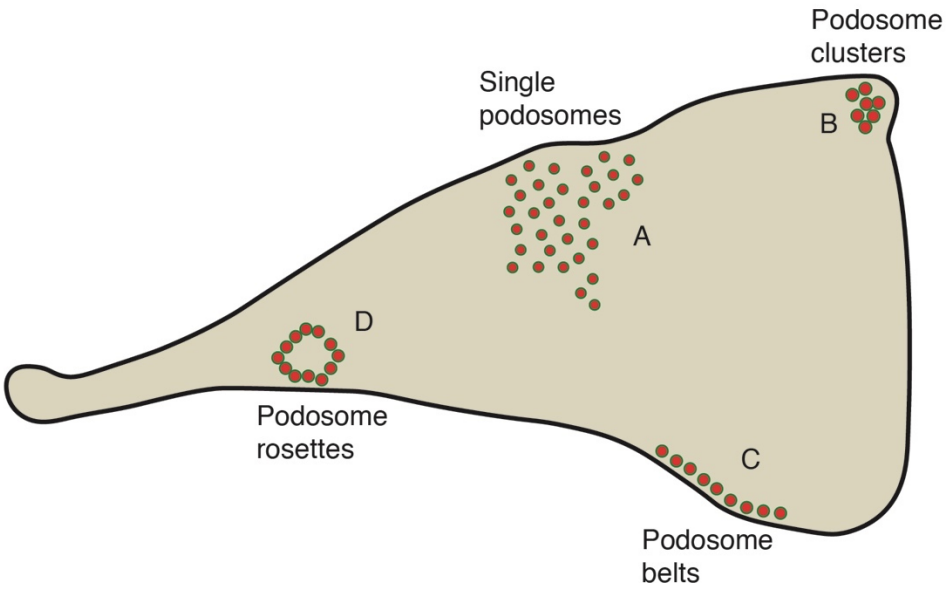

Figure 1.1. Different podosomes organization patterns.

Figure shows schematic podosomes structural organizations observed in different cell types. Podosomes actin core is shown in red and it is surrounded by a vinculin ring in green. Evenly distributed podosomes found in migrating macrophages and dendritic cells are shown as single podosomes (A), although they might be connected through the cytoskeleton network. Podosomes clusters (B) and podosomes belts (C) are usually found in osteoclast in the base of their differentiative stage, while podosomes rosettes (D) are distributed in Src transformed fibroblasts or endothelial cells. Figure was adapted from Schachtner et al., 2013.

1.1.1 Molecular components and regulation of the podosome core

The podosome core is mainly formed by actin and actin related proteins that are necessary to lead the actin nucleating process (Linder *et al.*, 2005). Actin assembly in the core is a highly dynamic process and depends on the formation of actin branched networks from the Actin-related protein 2/3 complex (Arp2/3) that works upon activation of WASP downstream to extracellular signalling by Rho GTPases (Luan *et al.*, 2018). In addition, bundled actin filaments can be found in the podosomes core and they are mainly produced by formins, whose activity was previously associated only to stress-fibres and filopodia (Lew, 2002). Lately, formins were found to be

responsible for connecting the podosomes core with the adhesion proteins of the ring structure and single podosomes with each other (Cox *et al.*, 2012; Panzer *et al.*, 2016). In the next sections, I will discuss the role played by the proteins involved in the extracellular signalling regulating actin nucleation and by the main actin related proteins in the podosome core.

1.1.1.1 Rho family GTPases

Rho GTPases play a major role in controlling actin remodelling steps necessary for cell migration (Nobes and Hall, 1999; Ridley, 2000) and they have also been involved in regulation of podosome formation.

In humans, at least 20 Rho GTPases were identified. Among these proteins, the ones that were mainly associated with cell migration processes are RhoA/B, Rac1/2 and Cdc42 (Sit and Manser, 2011). Rho GTPases main feature is the ability to cycle from the inactive GDP-bound form to the active GTP-bound form, following hydrolysis of GTP through activation of the catalytic enzymes guanine-nucleotide-exchange factors (GEFs) and GTPase-activating proteins (GAPs) (Etienne-Manneville and Hall, 2002; Sit and Manser, 2011). When Rho proteins are found in the active form, they activate signalling cascades to start several cellular processes. In particular, Rho GTPases were found to be involved in the different events occurring during cells migration: from the extension of lamellipodia and adhesions formations to body contraction and tail detachment (Ridley, 2001).

Lamellipodia extension and formation of membrane ruffles were mainly attributed to Rac proteins and require polymerization of branched actin through activation of the ARP2/3 complex (Kiosses *et al.*, 1999; Rottner, Hall and Small, 1999; Royal *et al.*, 2000). Humans possess three Rac isoforms: Rac1, Rac2 and Rac3. Rac1 is ubiquitously expressed (Liu, Kapoor and Leask, 2009) while Rac2 and Rac3 are

respectively expressed in haematopoietic cells (Gu *et al.*, 2002) and in the brain (Hwang *et al.*, 2005). The importance of Rac1 was clearly underlined by the finding that Rac1-deficient embryos are lethal (Sugihara *et al.*, 1998). Tissue-specific depletion of Rac1 caused defects in migration in certain cell types (Nobes and Hall, 1995; Knight *et al.*, 2000), due to a fault in lamellipodia extension (Allen *et al.*, 1998), although in macrophages the defects observed in migration were minimal (Wheeler *et al.*, 2006). Rac2 is involved in haematopoietic cells migration, as evident in neutrophils from Rac2 deficient mice that displayed defects in the response to chemoattracts resulting in actin polymerization and chemotaxis deficiency (Roberts *et al.*, 1999). Rac3 controls neuronal development and interneurons migration (de Curtis, 2019). Rac proteins were also implicated in the assembly of adhesion structures and, vice versa, Rac activation is induced by cells adhesion to the extracellular matrix. For example, plating cells on fibronectin induces Rac and Cdc42 activation (Price *et al.*, 1998). Rac1 KO DCs fail to assemble podosomes (Burns *et al.*, 2001), while macrophages can compensate and still assemble podosomes, although the ring structure is highly defective and lack associated paxillin (Wheeler *et al.*, 2006). On the contrary, Rac2 seems to be essential for podosomes formation in macrophages. Although $Rac2^{-/-}$ macrophages lack podosomes, migration speed is similar than in WT cells and invasion through matrigel is not impaired (Wheeler *et al.*, 2006). How Rac activates actin polymerization is still unclear. There are evidences that Rac can interact with the ARP2/3 complex (Pollard, Blanchoin and Mullins, 2000), through activation of one of its targets, IRSp53, which in turn interacts with the SH3 domain of WAVE (Miki *et al.*, 2000). IRSp53 was also found to be fundamental for linking GTPases to SH3 binding partners, including N-WASP. When the IRSp53 Rac-binding domain is

overexpressed, podosomes formation is impaired, highlighting the importance of Rac controlled expression in mediating podosome assembly (Oikawa *et al.*, 2013).

The process of cell contraction is mainly regulated by Rho isoforms. The three Rho isoforms, RhoA, RhoB and RhoC have homologous sequences (Heasman and Ridley, 2008) and interact with ROCK (Rho-kinases) to phosphorylate MLC (Light chain myosin) and activate actomyosin contractile forces (Bhadriraju *et al.*, 2007). In cells expressing large focal adhesion, inhibiting Rho activity can have a positive effect on migration by lowering adhesions and a negative one by stopping body contraction (Cox, Sastry and Huttenlocher, 2001). On the contrary, in highly motile cells such as macrophages and neutrophils, migration is affected negatively by Rho inhibition, impeding cell body contraction and, consequently, translocation (Allen *et al.*, 1998). In addition, a RhoA role in podosome assembly in osteoclasts and DCs was described (Burns *et al.*, 2001; Ory *et al.*, 2008). RhoA expression is not depleted in Src transformed fibroblasts, where stressed fibers are replaced by podosomes. Surprisingly, it has been observed that RhoA functions are not disrupted by Src transformation and, on the contrary, RhoA activation is fundamental for podosomes assemble and podosomes mediated matrix degradation. In particular, RhoA colocalizes with F-actin and cortactin in the podosomes core and might play a role in localising Src to podosomes (Berdeaux *et al.*, 2004). RhoA can also induce podosomes formation in osteoclast by increased production of PIP_2 (Chong *et al.*, 1994; Chellaiah *et al.*, 2000), whose role in binding WASP and assisting its activation was previously described (Higgs and Pollard, 2000).

Among all the Rho GTPases, Cdc42 role in podosomes formation, as well as chemotaxis and cell polarization, was widely studied. Cdc42 can regulate actin polymerization by binding with effector proteins such as PAK and WASP/N-WASP

(Zicha *et al.*, 1998; Higgs and Pollard, 2000). The importance of Cdc42 in podosomes assemble is underlined by the fact that KO DCs fail to assemble podosomes and lose polarity (Linder *et al.*, 1999, 2000; Burns *et al.*, 2001). Cdc42 interaction with WASP to induce podosomes formation will be described in the next sections.

1.1.1.2 The role of the ARP2/3 complex and Formins in F-actin nucleation

Podosomes formation requires nucleation of branched actin filaments. During the actin nucleation process, globular actin monomers (G-actin) are assembled into a growing filament, with a pointed end and a barbed end, where the elongation takes place (Mullins, Heuser and Pollard, 1998). There are two models of actin nucleation: the tip model and the convergent elongation model. These models do not exclude each other. The first one is mainly operated by formins that work as dimers to assemble filopodia, stress fibers and actin cables (Mellor, 2010). Formins cluster with the plasma membrane and can initiate bundle actin filaments polymerization that are subsequently stabilized by fascins crosslinking (Young, Heimsath and Higgs, 2015). Lately, formins were found to be important in stabilizing podosomes (Mersich *et al.*, 2010; Panzer *et al.*, 2016). In particular, Formin FRL1 is localized in the core tip and can be immunoprecipitated together with integrins (Mersich *et al.*, 2010). Formins KD cells have reduced adhesion and podosomes formation capability (Mersich *et al.*, 2010). Furthermore, the Formin-binding protein (FBP17) localizes in podosomes and, together with Dynamin, recruits the WASP-WIP complex to the plasma membrane (Tsuboi *et al.*, 2009).

The ARP2/3 complex is the orchestrator of the second model seen in lamellipodia formation. In mammals, it is composed of 7 subunits: the actin related subunits Arp2 and Arp3 and the actin-related protein complex-1 to 5 called ARPC-1, ARPC-2, ARPC-3, ARPC- 4, ARPC-5 (Mullins, Heuser and Pollard, 1998). The ARP2/3

complex on its own is inefficient and requires binding to proteins presenting a WCA domain known as nucleation promoting factors (NPFs) (Goley *et al.*, 2004). The WCA domain contains a WH2 domain to bind G-actin and a central acidic region to bind the ARP2/3 complex (Disanza and Scita, 2008; Tyler, Allwood and Ayscough, 2016). Upon activation and conformational change, the ARP2/3 complex can elongate filaments at a 70° angle to form the branched actin network (Chereau *et al.*, 2005). A 3D reconstruction of the actin branch conducted by electron tomography suggested that the subunits Arp2 and Arp3 relate with the pointed end of the daughter filament while ARPC2 and ARPC4 interact with the mother filament (Rouiller *et al.*, 2008). However, the function of the specific subunits still requires a better understanding. The ARP2 subunit, together with actin, is responsible of ATP hydrolysis that promotes debranching and recycling of the ARP2/3 complex (Goley and Welch, 2006). Other proteins, known as actin depolymerizing factors (ADF), have been reported as responsible of debranching by binding to actin and mediating structural changes that will reduce affinity with the ARP2/3 complex (Chan, Beltzner and Pollard, 2009) or by binding directly to the ARP2/3 complex and inhibiting the growth of the new filament (Gandhi *et al.*, 2010; Nakano *et al.*, 2010).

In podosomes, the ARP2/3 complex activity is strictly dependent on the NPFs WASP and is essential for podosomes maintenance (Mizutani *et al.*, 2002; Tyler, Allwood and Ayscough, 2016). Inhibition of ARP2/3 activity through the small molecule CK666 caused severe podosome defects in both monocytes and megakaryocytes (Nolen *et al.*, 2009; H. Schachtner *et al.*, 2013).

1.1.1.3 The WASP/WAVE family of proteins

Proteins belonging to the WASP/WAVE family are essential for actin cytoskeleton remodelling, being able to activate the ARP2/3 complex downstream to GTPases signals (Goley *et al.*, 2004). The family comprises 5 subfamilies (Figure 1.2): WASP and N/WASP, the WAVE/SCAR family including WAVE1/SCAR1, WAVE2/SCAR2 and WAVE3/SCAR3 (Kurisu and Takenawa, 2009), WASP homolog associated with actin, membranes and microtubules (WHAMM), WASP and SCAR homolog (WASH) and the junction-mediating regulator protein (JMY) (Alekhina, Burstein and Billadeau, 2017).

WASP was firstly studied in 1994 as the product of the gene mutated in an X-linked human disease known as the Wiskott Aldrich syndrome characterized by eczema, thrombocytopenia and recurrent infections (Ochs *et al.*, 1980; Derry, Ochs and Francke, 1994; Jin *et al.*, 2004). WASP is only expressed in haematopoietic cells thanks to a 137-bp regions upstream of the transcription site, that contains fundamental motifs for the binding of many haematopoietic transcription factors (Petrella *et al.*, 1998). Instead, Neural WASP (N-WASP) is ubiquitously expressed, with higher abundance in the brain (Ho *et al.*, 2001). WAVE1, WAVE2 and WAVE3 are located on different chromosomes and show a unique expression pattern. WAVE2 appears to be ubiquitously expressed in mammals, while WAVE1 and WAVE3 are fundamentally found in the brain (Pilpel and Segal, 2005; Stovold, Millard and Machesky, 2005; Miyamoto *et al.*, 2013). All the members of the family have a similar aminoacidic sequence, with a length in between 498 and 559 amino acids. They all share a proline-rich motif and the VCA domain, a carboxy-terminal homologous sequence containing a Verprolin homology domain (WH2) and a central-acidic region necessary for ARP2/3 and actin binding (Alekhina, Burstein and Billadeau, 2017). The

WASP subfamily proteins are characterized by a WH1 domain in the N-terminal region that is involved in protein-protein interactions and the CRIB domain that is the mediator of WASP interaction with Rho GTPases (Bompard and Caron, 2004). The WAVE subfamily has a different regulation because its members do not have the CRIB domain. Their activity is strictly dependant on the presence of an intact pentameric complex made of SRA1, NAP1, Abl and HSPC300 (Chen *et al.*, 2014). This complex is found in lamellipodium protrusions and has a major role in migration following activation of SRA1 by the GTPase RAC (Chen *et al.*, 2017). Furthermore, Abl was found in invadopodia and has an important role in regulating extracellular matrix degradation (Stradal *et al.*, 2001).

WHAMM structure is characterized by an N-terminal membrane interaction domain (WMD), a coiled-coil (CC) microtubule binding domain, a proline rich sequence and an actin nucleation domain defined as WWCA on the C-terminal (Campellone *et al.*, 2008). WHAMM localizes in the endoplasmic reticulum and it was shown that interaction with RhoD controls its cargo function in transporting vesicles from the Golgi to the plasma membrane (Blom *et al.*, 2015). The interaction of WHAMM-CC domain with microtubules causes conformational changes necessary to initiate its transport function. In fact, following microtubule binding, the N-terminal domain can bind the membrane, masking the C-terminal and, in turns, preventing actin polymerization (Liu *et al.*, 2017).

WASH possesses a WASH homology domain (WHD1) on the N-terminal, a tubulin binding domain (WHD2), and a proline rich region and a WCA on the C-terminal (Gomez and Billadeau, 2009). WASH alone is inactive and belongs to the SHRC pentameric complex, which is similar in size and shape to the WAVE complex but localizes in endosomes (Jia *et al.*, 2010). WASH activation is achieved through K63-

polyubiquitylation, which allows exposure of the WCA domain and regulates architecture and trafficking in the endosomal system (Hao *et al.*, 2013). WASH importance is underlined by the fact that WASH depleted mutants in mice are lethal and several diseases are associated with defects in endosomal protein trafficking (Gomez *et al.*, 2012). WASH role as a F-actin nucleation factor was described in centrosomes (Farina *et al.*, 2016).

JMY contains a coiled-coil domain at the N-terminal region, a proline rich domain and a WCA domain with three WH2 domain on the C-terminal (Zuchero *et al.*, 2009). The presence of tandem WH2 domains allows JMY to polymerize actin independently of ARP2/3. However, its ARP2/3-dependant actin polymerization capability has also been described (Zuchero *et al.*, 2009). Upon DNA damage, actin polymerization is increased, and, in turns, monomeric actin is sequestered into the growing filament. The NLS sequence, localized among the WH2 domains, becomes accessible and JMY is translocated into the nucleus where it regulates the gene expression of p-53 (Zuchero *et al.*, 2012).

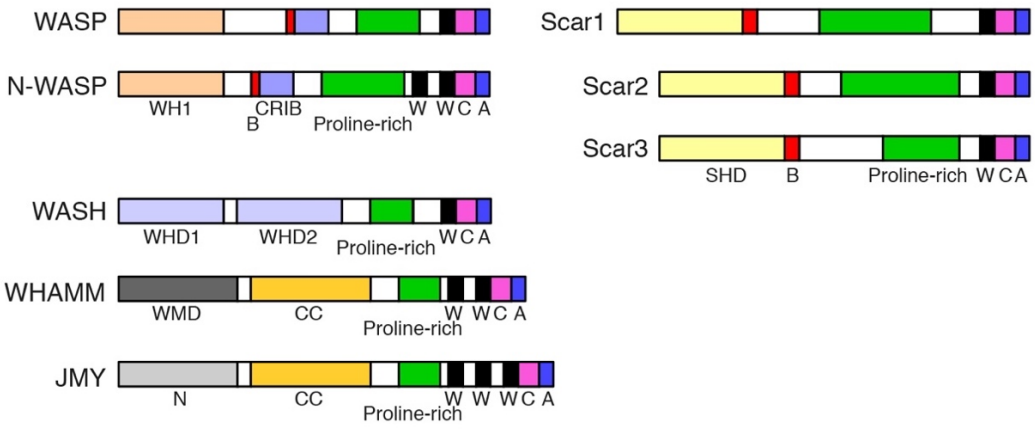

Figure 1.2. Schematic representation of WASP/WAVE family of proteins.

Domain organization of WASP/Wave family of proteins showing the major protein interaction sites. All members share a pppp, proline rich domains, the VCA, verprolin cofilin homology domains/acidic region and a WH2, WASP homology 2 domain. The WASP subfamily proteins are characterized by a WH1 domain in the amino-terminal region and CRIB, Cdc42 and Rac interactive domain. The WAVE subfamily of proteins does not have the CRIB domain. WHAMM possesses a membrane interaction domain (WMD) on the N-terminal and a coiled-coil (CC) microtubule binding domain. WASH possesses a WASH homology domain (WHD1) on the N-terminal and a tubulin binding domain (WHD2), while JMY contains a coiled-coil domain at the N-terminal, a proline rich domain and on the C-terminal a WCA domain with three WH2 sites.

1.1.1.4 The Wiskott Aldrich syndrome protein (WASP)

WASP is located in the podosomes core, at the very basal level of podosomes, in contact with the plasma membrane (Chou *et al.*, 2006), and was found to be essential for podosome formation in dendritic cells (Bouma *et al.*, 2011), macrophages (Tsuboi, 2007) and osteoclasts (Calle, Jones, *et al.*, 2004). The WH1 (WASP-Homology 1) domain, the region of WASP-WIP interaction, will be described in the next section.

In resting cells, WASP is found in its autoinhibited conformation in which the CRIB domain is bound through hydrophobic interaction to the VCA domain, blocking the site for interface with the ARP2/3 complex (Calle, Chou, *et al.*, 2004). Following external stimuli, the Rho GTPase Cdc42 can bind to the CRIB domain allowing the release of the VCA domain (Higgs and Pollard, 2000; Kim *et al.*, 2000). Additionally, the interaction of Toca-1 with WIP and active Cdc42 seems to be essential in

promoting the actin polymerizing process (Ho *et al.*, 2004). Once WASP is activated, the VCA region can interact with monomeric actin and the ARP2/3 complex to start de novo actin polymerization (Figure 1.3). An additional regulatory mechanism of WASP is mediated by the phosphorylation of the tyrosine residue Y291 (Y293 in mice) by Src family kinases and Btk kinase (Blundell *et al.*, 2009). It was shown that Y291 phosphorylation induces conformational changes in WASP, stabilizing the open conformation and improving filopodia formation in a Cdc42-independent manner (Cory *et al.*, 2002; Blundell *et al.*, 2009). More recently it was demonstrated that WASP tyrosine phosphorylation promotes podosomes disassembly by inducing WASP-calpain dependent degradation (Macpherson *et al.*, 2012). For instance, the expression of WASP Y291E (human phosphomimetic mutant) in myeloid cells leads to assembly of smaller podosomes with a shorter life span. This phenotype can be reversed by inhibiting calpain activity, indicating that phosphorylation of WASP Tyr291 facilitates its degradation by calpains during podosomes disassembly (Macpherson *et al.*, 2012). Another important domain of WASP is the proline rich region, which is involved in signal transduction and WASP activation through interactions with Src homology 3 (SH3) containing proteins such as NCK, Grb2 and Src-family kinases (Fukuoka *et al.*, 2001; Rohatgi *et al.*, 2001).

WASP role in podosome formation is undisputed and it cannot be replaced by N-WASP activity. Partial (50%) protein KD is sufficient to abolish podosome formation (Olivier *et al.*, 2006) and myeloid cells (both macrophages and DCs) of WAS patients completely fail to assemble podosomes, contributing to defects in migration and chemotaxis *in vivo* and *in vitro* (Linder *et al.*, 1999). DCs lacking podosomes form dysmorphic lamellipodia, assemble focal adhesions-like structures and present β2-integrin dispersion throughout the cell surface impairing adhesion (Burns *et al.*, 2001;

Calle *et al.*, 2004). Similar defects were found in WASP-null mouse models, where a reduced number of podosomes were assembled and they appeared smaller, highly disorganized and lacking the presence of vinculin rings (Jones, 2008). Not surprisingly, patients affected by the Wiskott Aldrich syndrome are prone to infectious diseases (such as respiratory, ear, sinus infections and pneumonia) and autoimmune disorders (such as haemolytic anaemia, idiopathic thrombocytopenic purpura and vasculitis), due to abnormal myeloid cell trafficking and adhesion (Ochs and Thrasher, 2006). A normal phenotype can be restored in WAS patients myeloid cells with *in vitro* gene transfer (Jones *et al.*, 2002). All these observations are evidence that WASP function is not limited to its polymerizing activity, but it works as an adaptor protein being able to recruit vinculin and cluster integrins necessary for adhesion to the ECM (Burns and Thrasher, 2004; Calle *et al.*, 2006; Bouma *et al.*, 2011).

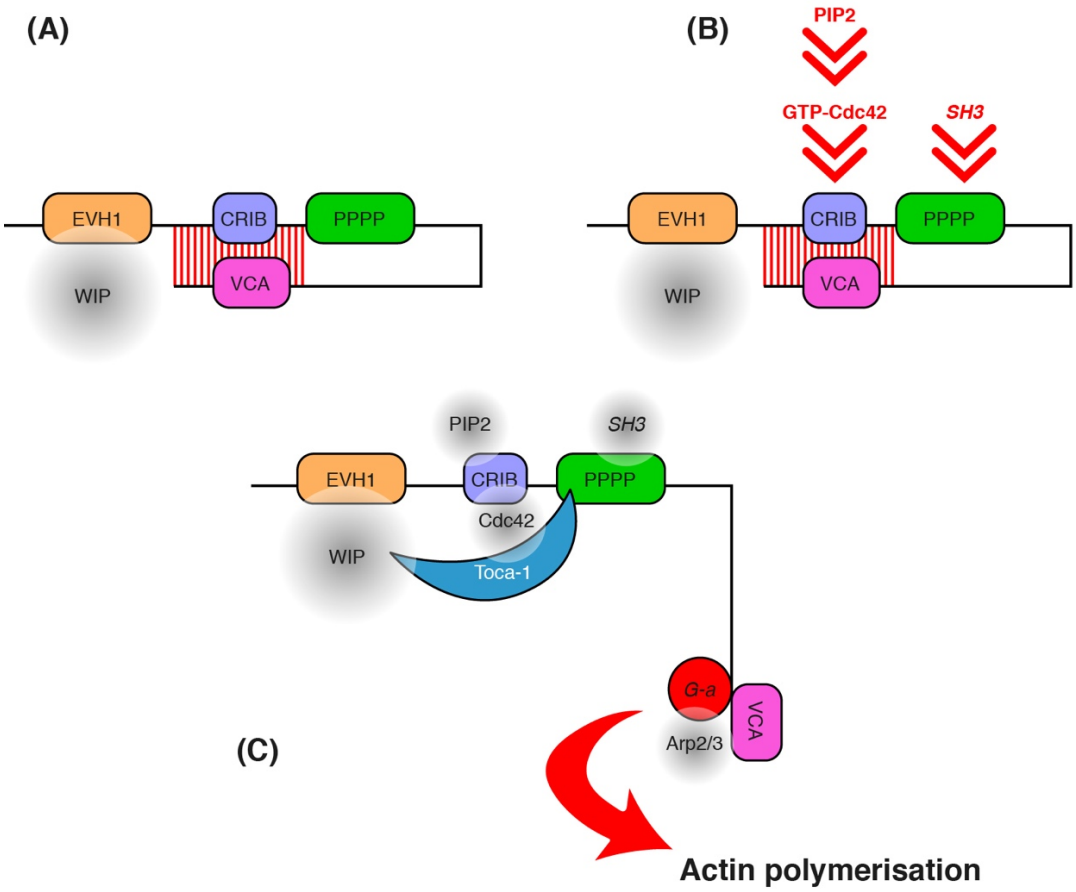

Figure 1.3. Schematic representation of WASP activation.

(A) In resting cells, WASP is found in its autoinhibited conformation, in which the CRIB domain is bound to the C-terminal domain and WIP interacts with the WH1 domain. (B) Following external stimuli, the Rho GTPase Cdc42 binds to the CRIB domain allowing the release of the VCA domain. (C) The interaction of Toca-1, WIP, Cdc42 and SH3-containing proteins with the proline-rich domain of WASP contributes promoting the actin polymerization process. Once WASP is activated, the VCA region can interact with monomeric actin and the ARP2/3 complex starts actin polymerization *de novo*. Figure was adapted from Calle et al., 2008.

1.1.1.5 The WASP interacting protein (WIP)

Approximately 80% of the mutations causing WAS disease are localized in the WH1 domain of WASP, which is essential for WASP-WIP interaction (Volkman *et al.*, 2002). This finding underlies the relevance of WIP in regulating WASP activity. WIP belongs to the WASP interacting/verprolin family of proteins (Figure 1.4), together with CR16 and WICH/WIRE. WIP shares 30-40% of its sequence with WICH/WIRE and 25% with CR16. All the members of the family present a region rich in prolines,

a verprolin-homology region in the N-terminus that can bind actin, and a further homology sequence in the C-terminus that can bind to the WH1 domain of both WASP and N-WASP (Aspenströ, 2005). Each protein is differentially tissue distributed. Although WIP is ubiquitously present in all tissues, it is predominantly expressed in haematopoietic cells while the other members of the family are mainly expressed in the brain (Ho *et al.*, 2001; Aspenström, 2004; Tsuboi, 2006; García *et al.*, 2016). A WIP isoform that was later described is mini-WIP, derived from a truncated transcription of WIPF1 gene and lacks the WASP binding domain, whose function remains unknown (Friedl *et al.*, 2014).

WIP-WASP interaction is thought to be essential in regulating WASP activity, stability and subcellular localization (Fried *et al.*, 2014). WIP and WASP coexist as a complex in which WIP protects WASP from calpain and proteasome degradation (de la Fuente *et al.*, 2007; Chou *et al.*, 2006). When WIP is phosphorylated on tyrosine residues by the Bruton's tyrosine kinases (BTK), the complex is released and WASP is rapidly degraded, leading to podosomes disassemble. This event controls podosomes turnover (Vijayakumar *et al.*, 2015). DCs from WIP-null mouse fail to form podosomes and show defects in migration, chemotaxis and polarity (Chou *et al.*, 2006). WIP-null phenotype resembles WASP-null phenotype (Antón and Jones, 2006), although when WASP levels are restored using calpain inhibitors, podosomes are still not formed. Furthermore, when WIP-WASP interaction is blocked, actin polymerization takes place at inappropriate sites and cell polarization is defective (Tsuboi, 2006). Therefore, WIP must have an important role in regulating WASP localization in sites of active actin polymerization at the plasma membrane (Chou *et al.*, 2006). WIP activity is not only limited to its interaction with WASP, but it stabilizes F-actin by localizing in stress fibers and filopodia, it is involved in actin

bundling and it controls actin dynamics by interacting with other cytoskeleton proteins such as NCK and cortactin (Martinez-Quiles *et al.*, 2001). An additional role attributed to WIP, cortactin-dependent matrix degradation, will be discussed in the next section.

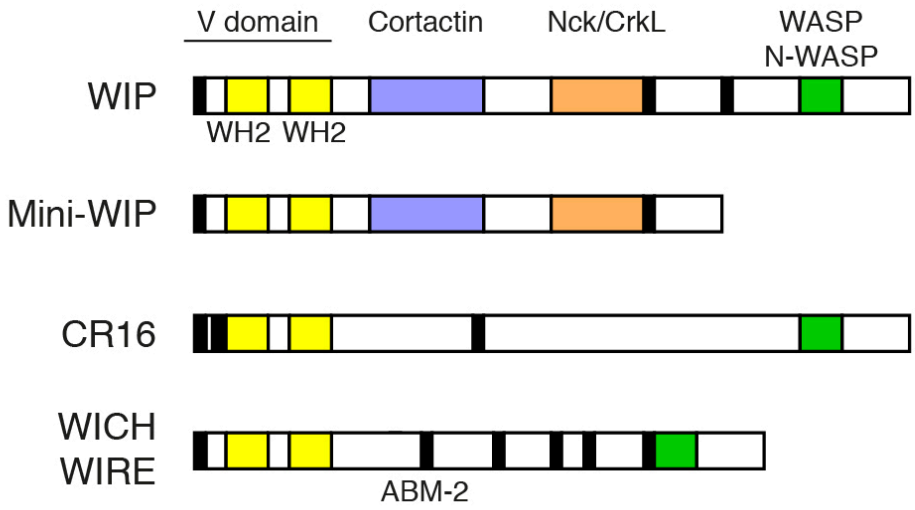

Figure 1.4. Schematic representation of WIP family proteins. WIP belongs to the WASP interacting/verprolin family of proteins, together with CR16 and WICH/WIRE.

All the members of the family have a verprolin-homology region in the N-terminus that can bind actin and a homology sequence in the C-terminus that can bind to the WH1 domain of both WASP and N-WASP. Additionally, the verprolin domain is followed by regions rich in prolines for cortactin and Nck binding. Mini-WIP derives from a truncated transcription of WIPF1 gene and lacks the WASP binding domain. There are in between two and six actin-based motility 2 domains (ABM-2) for profilin binding in all the proteins. Figure was adapted from Calle et al., 2008.

1.1.1.6 Cortactin

Cortactin is an actin binding protein, that plays an important role in cell motility and invasion (Wu and Parsons, 1993; MacGrath and Koleske, 2012). Its amino acidic sequence comprises five main domains: an N-terminal region containing a binding site for the ARP2/3 complex, 6 tandems 37 amino acid repeating segments known as cortactin repeats that bind actin, an α-helical motif whose function is not clear, a proline-rich domain abundant in tyrosine, serine and threonine residues to interact with kinases such as PAKs and ERK (Vidal *et al.*, 2002; Martinez-Quiles *et al.*, 2004), and

a Src homology (SH) 3 domain at the carboxyl terminus (Cosen-Binker and Kapus, 2006; Shvetsov *et al.*, 2009). This last domain is the key region for cortactin interaction with podosome proteins like WIP, WASP and N-WASP (Kinley *et al.*, 2003). Cortactin is ubiquitously expressed, with haematopoietic cells being the only exception. Haematopoietic cells express HS1, a protein structurally similar to cortactin, but containing only 3 complete tandem repeats (Uruno, Zhang, *et al.*, 2003; Thomas *et al.*, 2017).

Cortactin possesses high affinity for actin and enhances actin polymerization in several ways (Uruno, Liu, *et al.*, 2003). It can bind the ARP2/3 complex through the N-terminal domain inducing actin nucleation (Uruno *et al.*, 2001) and stabilizes branched actin filaments connecting them through the ARP2/3 complex (Pant *et al.*, 2006). Furthermore, cortactin can act synergistically with the VCA domain of WASP or N-WASP (Weaver *et al.*, 2001) and with WIP through the SH3 domain to improve the efficiency of ARP2/3-dependent actin polymerization (Kinley *et al.*, 2003). Cortactin is localized in migrating cells protrusions such as lamellipodia, invadopodia and podosomes (MacGrath and Koleske, 2012). It was shown that cortactin depletion results in failure in invadopodia formation and consequently matrix degradation, suggesting a role of cortactin in metalloproteases secretion in invadopodia that was subsequently confirmed (Clark *et al.*, 2007; Clark and Weaver, 2008). The role of the interaction between WIP and cortactin in podosomes formation and matrix degradation was extensively studied in DCs. Podosomes are specialized structures for ECM degradation through secretion of MMPs. Cortactin localizes in the podosomes core but in the absence of WIP it is found distributed all over the cell body. WIP KO DCs assemble focal adhesions and show impaired gelatinases activity due to defects in MMPs production. It was shown that in the absence of cortactin podosomes are

assembled but they appear smaller and poorly organized, suggesting a role of cortactin not in podosomes initiation but in their maturation and stabilization. When WIP/Cortactin binding is impaired, MMPs are not secreted, indicating that WIP-cortactin binding is a necessary step for MMPs localization at cell-substratum adhesion (Bañón-Rodríguez *et al.*, 2011).

1.1.2 Molecular components and regulation of the podosome ring structure

The ring structure in podosomes is mainly characterized by cytoskeleton adaptors proteins (e.g. vinculin, paxillin and talin) linked to cell adhesion molecules (integrin family) and assembled to create rings surrounding the central actin core (Wernimont *et al.*, 2008; Staszowska *et al.*, 2017). For a long time, it was considered a unique symbol of podosomes but it was recently identified into invadopodia in breast cancer cells (Branch, Hoshino and Weaver, 2012). Protein kinases such as Src family kinases and protein kinase C (PKC) (Teti *et al.*, 1992) are also localized in the podosomes ring, together with adhesion proteins. In the next sections, we will describe the main components of podosomes rings cited above.

1.1.2.1 Integrins

Integrins are heterodimer transmembrane glycoproteins formed of two subunits, an α- and a β-subunit (Campbell and Humphries, 2011). The extracellular integrin globular head region establishes contact with the extracellular matrix (ECM), and is involved in ligand binding and cascade signalling. Two 75aa long stalk regions connect the globular head to the cell cytoplasmic region (Berman, Kozlova and Morozevich, 2003; Humphries, Symonds and Mould, 2003). There are 24 members in the integrin family, and each one of them is built on a different combination of α- and a β-subunits

(Barczyk, Carracedo and Gullberg, 2010). ECM components such as laminin, collagen and fibronectin have adhesions site for integrins. The interaction mainly occurs through the Arg-Gly-Asp (RGD) domain found in several ECM proteins (Schwartz, 2010). Some integrins can mediate interaction with other cells through immunoglobulin like receptors (Borghi *et al.*, 2010) or bacterial LPS (Monick *et al.*, 2002) and viruses (Stewart and Nemerow, 2007).

Integrin regulation and activation depends on conformational shape changes. In the inactive form, the α- and β-tails interact with each other. Activation is achieved when this binding is disrupted (Luo, Carman and Springer, 2007). Following integrin activation and formation of adhesions such as podosomes, cells continue to extend membrane protrusions that are necessary for cell migration and adhesion to the ECM (DeMali and Burridge, 2003). The formation of these adhesion structures is determined by complex signalling cascade events that will remodel cytoskeleton and activate Rho family GTPases. Integrins β1-, β2- and β3- are found in podosomes, with the first one being localized in the podosomes core and the latter two in the ring structure (Destaing *et al.*, 2010; Gawden-Bone *et al.*, 2014; Griera *et al.*, 2014; Peláez *et al.*, 2017). Although it was thought that multiple integrins are important in podosome formation (Linder, 2009), the critical role played by β2 integrin has been recently highlighted (Gawden-Bone *et al.*, 2014). It was shown that, while focal adhesions were not affected, DCs lacking β2 integrin fail to assemble podosomes and that this event was due to the absence of NPxF motifs and threonine residues, necessary for binding to talin, kindlin-3 and other integrin partners (Gawden-Bone *et al.*, 2014). Furthermore, it was shown that activation of integrins can start a phosphorylation cascade involving protein kinases as Src family kinases, interacting with Cdc42, that in turn will start the actin nucleation process mediated by WASP and

the ARP2/3 complex (Luxenburg *et al.*, 2006) and induce MMPs recruitment (Gálvez *et al.*, 2002).

To initiate podosomes formation, both DCs and macrophages need to be stimulated by cytokine and/or chemokines. In fact, when cells are plated in the absence of chemotactic signals on a substrate containing integrin ligands, (e.g. fibronectin or ICAM-1) they fail to assemble a leading edge and podosomes, developing predominantly focal adhesions. Whereas in the presence of chemotactic factors the formation of actin cores and accumulation of β2 integrins around the core is induced, thus allowing for the organisation of integrins in rings (Monypenny *et al.*, 2011).

Finally, the podosomes mechanosensing properties are mediated by integrins, which are able to sense matrix tension and stiffness and reorganize accordingly to modulate cell behaviour and fate (Peng *et al.*, 2012).

1.1.2.2 Src kinases

The Src family comprises nine non-receptor tyrosine kinases (Parsons and Parsons, 2004). They are involved in tyrosine residue phosphorylation to activate/deactivate specific proteins (Luxenburg *et al.*, 2006; Zhou *et al.*, 2006; Xu *et al.*, 2018). In particular, Src has an essential role in regulating cells migration and integrin signalling (Sanjay *et al.*, 2001; Alper and Bowden, 2005). The importance of Src in podosome formation was highlighted by the fact that the expression of the oncogenic form of Src, v-Src, induces rearrangement of actin fibers into podosomes in fibroblasts (Tarone *et al.*, 1985). In addition, podosomes belts are defective in Src-deficient osteoclasts (Sanjay *et al.*, 2001).

The nine proteins of the family share a similar structure, made up by several domains including an amino-terminal myristoylation domain that allows Src-membrane binding, and the Src-homology domain 2 (SH2) and Src-homology domain 3 (SH3)

involved in protein binding and a tyrosine catalytic region SH1 (Parsons and Parsons, 2004). In the inactive state, Src is found in a closed conformation in which the SH2 domain binds phosphorylated tyrosine 527 and SH3 binds a junction domain between SH1 and SH2. Activation takes place when Y527 is dephosphorylated or when SH2 or SH3 interaction is displaced by binding with protein partners (Bernadó *et al.*, 2008). Src can also be activated by phosphorylation in Y416. In fact, the maximum activation of Src is achieved upon phosphorylation of Y416 and dephosphorylation of Y527 (Irtegun *et al.*, 2013).

Src can be activated following integrin clustering (Luxenburg *et al.*, 2007) and it is involved not only in podosome formation but also in structure organization, turnover, and the rate of actin polymerization (Destaing *et al.*, 2008). Apart from integrins, several podosomal proteins including WASP, cortactin, Paxillin and focal adhesion kinases were found to be Src interacting partners (Huang *et al.*, 1997; Baba *et al.*, 1999; Mitra and Schlaepfer, 2006). Interestingly, WASP phosphorylation by Src on tyrosine 291 was associated with increased actin polymerization (Macpherson *et al.*, 2012) and was found to be necessary for efficient polymerizing activity and matrix degradation capability (Dovas *et al.*, 2009). At the same time, Src mediated phosphorylation represents a signal towards calpain-dependent WASP degradation, which promotes podosomes disassembly (Calle *et al.*, 2006; Macpherson *et al.*, 2012). WASP interaction with cortactin, which normally stabilizes podosomes formation, is impaired following Src phosphorylation (Martinez-Quiles *et al.*, 2004). Taken together, these studies suggest that Src has an essential role in controlling both podosome assembly and disassembly through interaction with WASP and other actin related proteins and maintains high podosomes turnover. Finally, Src-phosphorylation determines N-WASP conformational changes, allowing its access into the nuclear

exports signal (NES) (Suetsugu and Takenawa, 2003). When N-WASP accumulates into the cytoplasm, HSP90 expression is increased. Similarly, unphosphorylated N-WASP in the nucleus binds to Heath shock element (HSE) inhibiting both HSP90 transcription and Src kinases activity (Suetsugu and Takenawa, 2003).

1.1.2.3 Vinculin and interacting proteins

Vinculin is a membrane-cytoskeletal protein found in podosomes where is organized in the characteristic ring structure (Calle *et al.*, 2006). It represents a unique podosome marker that for a long time was used to differentiate between podosomes and invadopodia (Gimona *et al.*, 2008). However, it has been shown recently that it can form a ring surrounding invadopodia in breast cancer cells (Branch, Hoshino and Weaver, 2012). Its main function is to connect the actin cytoskeleton with transmembrane proteins, mainly integrins, although it is as well involved in several cell migration and invasion processes (Pasapera *et al.*, 2010; Walde *et al.*, 2014). It was demonstrated that the recruitment of vinculin to the podosome ring is mediated by myosin-II-dependent tension on the actin network (van den Dries *et al.*, 2013).

Vinculin is made up of 1066 aa with a globular head and a tail region. The protein presents a N-terminus globular head and a rod-shaped tail in C-terminus separated by a proline rich region (Miller, Dunn and Ball, 2001). It interacts with other ring proteins through its domains. In particular, a talin-binding site is found in the N-terminus domain (Bois *et al.*, 2006; Yao *et al.*, 2015), while α-actinin can bind the proline-rich region (Bois *et al.*, 2006) and Paxillin binds to the tail together with actin (Turner, Glenney and Burridge, 1990). The interaction with all these proteins is essential to support vinculin activity in adhesions formation. In particular, talin works as a connector by binding F-actin and integrins through the globular head region and vinculin through its rod domain. This process creates a crosslink between integrins

and actin filaments, essential for the assembly of both podosomes and focal adhesions (Bois *et al.*, 2006; Walde *et al.*, 2014). Talin binding to integrins is mediated by cooperation of FAK and PIP2 (Gilmore and Burridge, 1996; Atherton *et al.*, 2015). A similar role is played by paxillin, another vinculin-interacting protein, which binds to vinculin through the N-terminal domain creating a connection with F-actin (Turner, Glenney and Burridge, 1990). Paxillin colocalize with integrins in podosomes (Destaing *et al.*, 2003) and it is found at the interface between membrane and cytoskeleton in podosomes, focal adhesions and invadopodia (Subauste *et al.*, 2004; Badowski *et al.*, 2008). When the expression of paxillin is deficient, osteoclasts assemble podosome clusters instead of rosettes, developing defects in matrix degradation (Pfaff and Jurdic, 2001), and a similar effect is caused by the absence of paxillin phosphorylation (Badowski *et al.*, 2008).

1.2 Podosomes comparison with other cell adhesion structures

Podosomes are assembled by myeloid cells, such as macrophages, monocytes, dendritic cells and migratory phase osteoclasts, while most cells assemble integrin-based adhesion structures known as focal contacts (focal complexes and focal adhesions). Other structures, related to podosomes are invadopodia and they are normally linked with tumour metastasis (Gimona *et al.*, 2008). A brief comparison between podosomes and other adhesion structures, including focal adhesions and Invadopodia, will be introduced in the following sections.

1.2.1 Podosomes: comparison with focal adhesions

Focal adhesions (FAs) represent a common actin-integrin linked structure and can be found at the end of stress fibres, localized between the lamellipodia and the lamellae

(Wozniak *et al.*, 2004; Gimona and Buccione, 2006; Kim and Wirtz, 2013). They can be distinguished from podosomes essentially for three features: morphology, lifetime and protein content.

Morphologically, FAs have an elongated fibre-like shape and are associated with stress fibres, highly contractile bundles of actin and myosin, that apply force to FAs to retract the rear of a moving cell (Livne and Geiger, 2016). FAs have slower turnover dynamics than podosomes, with a lifetime between 30 and 60 minutes (Stehbens and Wittmann, 2014). In FAs, integrins are coupled with the actin cytoskeleton via actin-related proteins such as Talin, α-actinin, Paxillin and Vinculin and contractility is modulated by bundles of Myosin-II (Fraley *et al.*, 2010). Furthermore, the activity of the protein kinases FAK is crucial in the development of these structures (llić *et al.*, 1995). Therefore, although podosomes and FAs share a vast majority of proteins, FAs mainly develop thanks to Myosin-II activity and its recruitment of Vinculin to FAs by FAK-mediated regulation of Paxillin (Pasapera *et al.*, 2010), while Myosin-II role in podosomes is limited to their suppression (Mohd Rafiq *et al.*, 2017). Furthermore, mature FAs do not contain WASP, the vinculin ring structure or the Arp2/3 complex (Block *et al.*, 2008). However, it seems that WIP might be related to FAs dynamics, since both WIP deficient fibroblasts (Lanzardo *et al.*, 2007) and DCs results in formation of a higher frequency of focal adhesions, increasing adhesion to the substratum and affecting migration negatively (Mizutani *et al.*, 2002). How WIP controls FA formation is not clear and a hypothesis was formulated that FAs might be a precursor in the formation of podosomes or invadopodia (Oikawa and Takenawa, 2009).

As podosomes, FAs have mechanosensing activity, since their properties can change in response to the type of underlying substrate and mechanical tensions (Riveline *et*

al., 2001). Matrix degradation capability used to be a distinctive podosomes' feature, but it was recently demonstrated in cancer cells that FAs colocalize with ECM degradation sites and FAK kinase activity was found to be essential for MMPs recruitment following phosphorylation by Src family kinases (Wang and McNiven, 2012). Taken together, the distinctive properties found in these two structures make it relatively easy to discriminate between podosomes and FAs (Figure 1.5), while differentiation between podosomes and invadopodia remain still a complicated field.

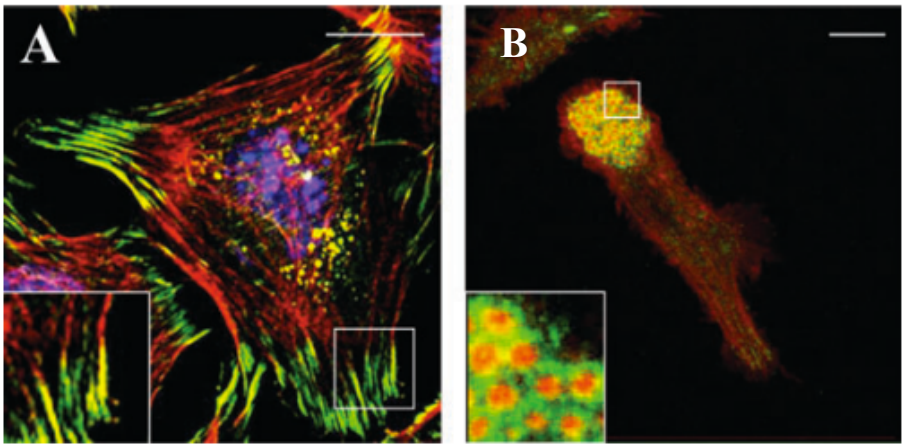

Figure 1.5. Representative images of focal adhesions and podosomes.

Focal adhesions (A), assembled by most cell type including fibroblasts, are seen as elongated stripes localized at the end of stress fibers. F-actin is shown in red and vinculin in green. (B) Podosomes are assembled at the leading edge of macrophages and dendritic cells and present a core of actin (red) surrounded by rings of integrin associated proteins, including vinculin (green). Bar 10 μm. Figure adapted from Calle et al., 2008.

1.2.2 Podosomes: comparison with Invadopodia

Podosomes and invadopodia belong to the category of invadosomes due to their ability to degrade matrix and develop proteolytic migration (Linder, 2009). The fact that they share most of the proteins and both have a dot-shaped actin-rich structure gave space to a debate on the differences between podosomes and invadopodia, with a faction of scientists suggesting they might actually represent the same structure (Linder, 2007). However, more recent studies demonstrated that these structures are indeed

morphologically different, with the invadopodia being wider and taller (up to 8μm in diameter 5μm in height) than podosomes (Linder, Wiesner and Himmel, 2011) and having a greater capability of protruding into the matrix (several microns) (Bowden *et al.*, 1999). Furthermore, it was initially thought that the presence of a vinculin adhesion ring was limited to podosomes (Cox *et al.*, 2012) (Albrechtsen *et al.*, 2011) but vinculin rings were also identified in some instances in invadopodia such as in breast cancer cells (Branch, Hoshino and Weaver, 2012). Besides, while podosomes are highly dynamic, with a half-life shorter than 5 minutes (Starnes, Cortesio and Huttenlocher, 2011), invadopodia are less dynamic in general, with a lifetime that ranges from minutes to several hours (Yamaguchi *et al.*, 2005). Although several actin-related proteins and integrins such F-actin, the Arp2/3 complex, N-Wasp, Cortactin, Fascin, Paxillin, Myosin II, β1- and β3- Integrins, and different MMP and Serine proteases, are present in both the structures (Linder and Aepfelbacher, 2003; Gimona and Buccione, 2006; Weaver, 2006), WASP expression is limited to podosomes (Yolanda Calle *et al.*, 2004; Monypenny *et al.*, 2011). In invadopodia, a similar role to WASP might be played by the ubiquitously expressed N-WASP, since N-WASP deficient cells have decreased invadosomes formation (Lorenz *et al.*, 2004; Gligorijevic *et al.*, 2012).

Functionally, podosomes play an important role in several physiological processes. They are involved in migration and adhesion of immune cells during the inflammatory response (Linder *et al.*, 2000; Jones, 2008) and in bone growth and remodelling (Y. Calle *et al.*, 2004; Luxenburg *et al.*, 2007), while invadopodia are generally found in cancer cells and associated with metastases development and were not proven to be involved in adhesion (Meirson and Gil-Henn, 2018; Williams *et al.*, 2019).

The main similarity shared by the two structures is the ability to degrade ECM using proteases, whose secretion is regulated by the interaction between Cortactin, WIP and N-WASP/WASP (Clark *et al.*, 2007; Bañón-Rodríguez *et al.*, 2011; Siar *et al.*, 2016). Furthermore, in both structures, matrix degradation may be regulated by sensing the stiffness in the environment, showing mechanosensing capability (Alexander *et al.*, 2008; Albiges-Rizo *et al.*, 2009; Parekh and Weaver, 2016). Taken together, all these similarities and the complexity of their protein network, make the differentiation between the two structures an arduous process (Figure 1.6).

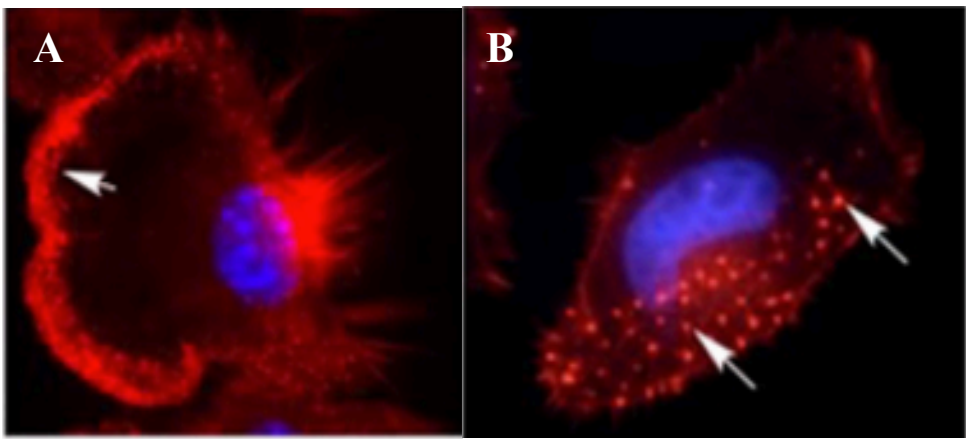

Figure 1.6. Representative images of podosomes and invadopodia.

Podosomes and Invadopodia are visualized by staining with F-actin (red). (A) Podosomes assembled in macrophages; (B) Invadopodia assembled in head and neck squamous carcinoma cells (SCC61). Figure adapted from Murphy et al., 2011.

1.3 Podosome functions

1.3.1 Podosomes in migration

The most compelling evidence of podosomes involvement in migration is the fact that they are only assembled by migratory phase cells. Myeloid leukocytes respond with cell trafficking to a perturbation of homeostasis. In particular, DCs migrate from the tissue where they encounter a pathogen back into the lymph nodes, while monocytes or neutrophils actively migrate and transmigrate through blood vessels to the site of infection (Schmid and Varner, 2007; Gerhardt and Ley, 2015; Iqbal, Fisher and Greaves, 2016). Following the release of chemoattractants by the inflamed tissue, all these cells extend a leading edge, i.e. a lamellipodia, which is stabilized upon adhesion to the substratum and the surrounding ECM through integrin based adhesive structures such as podosomes (Burns and Thrasher, 2004; Cougoule *et al.*, 2010). Less motile cell types assemble stable, long lived adhesions known as focal adhesions, whose anchor to the matrix is firmer and characterized by long bundles of contractile proteins, while podosomes are expressed by highly motile cells as leukocytes, whose functions are strictly dependent on their ability to migrate (llić *et al.*, 1995).

Podosomes are short-lived, distributed in the interface with the matrix and their interaction with the substrate is weaker than in focal adhesion. They are highly dynamic, and their assembly and disassembly allow cell body progression (Linder *et al.*, 2000; Destaing *et al.*, 2003; Götz and Jessberger, 2013). Several studies have underlined the importance of podosomes in both random migration and chemotaxis (Dovas *et al.*, 2009; Burger *et al.*, 2011; Burkhardt Daniel A Hammer *et al.*, 2011; Monypenny *et al.*, 2011). A typical evidence in support of this hypothesis comes from immune cells of patients affected by the Wiskott Aldrich syndrome. DCs and macrophages from these patients or from mice KO for WASP or WIP fail to assemble

podosomes and in turn develop large focal adhesion structures leading to defects in migration and chemotaxis (Linder *et al.*, 1999; Calle *et al.*, 2004; Dovas *et al.*, 2009; García and Machesky, 2012), making WAS patients prone to develop infectious diseases (Chandra *et al.*, 1993; S. Burns *et al.*, 2004). Several steps of migration through the endothelial barrier are defective in the lack of podosomes. Macrophages lacking podosomes show defects in polarization (Linder *et al.*, 2000) and chemotaxis in response to the chemoattractant protein MCP-1 and to the macrophages inflammatory protein (MIP)-1α (Badolato *et al.*, 1998; Zicha *et al.*, 1998). Similarly, WASP KO DCs do not respond to trafficking stimuli *in vivo* due to an alteration in the receptor for CCR7 ligands, leading to defective migration to secondary lymphoid tissues and failure to localize in T-cell areas (de Noronha *et al.*, 2005; Bouma, Burns and Thrasher, 2007). Even a small down regulation of WASP is able to affect podosomes formation impairing motility (Olivier *et al.*, 2006).

1.3.2 Podosomes in adhesion

Several pieces of evidence underline the importance of podosomes as adhesion structures. First of all, podosomes are formed upon cell-substratum interaction on cells ventral surface (Luxenburg *et al.*, 2007; Staszowska *et al.*, 2017). Secondly, they are rich in adhesions proteins, organized in the typical ring structures containing integrins that are linked to actin and actin-related proteins in the podosomes core (Wernimont *et al.*, 2008). Integrins present in the podosomes ring are substrate specific, being able to determine the type of matrix the cells will adhere to (Destaing *et al.*, 2010; Griera *et al.*, 2014; Peláez *et al.*, 2017). At the same time, type and rigidity of the substrate can influence cell shape and integrin clustering to form specific adhesion structures or activate signalling cascades such as MMPs secretion (Gálvez *et al.*, 2002; Albiges-Rizo *et al.*, 2009). Therefore, a question arises on whether podosomes are only formed

as an artefact due to culturing on a rigid substrate, and therefore the chosen substrate becomes an important factor in the study of these adhesion structures. With the aim to mimic physiological conditions, it was shown that monocytes cultured on endothelial cells or osteoclasts cultured on bone lamina assembled podosomes similarly to cells cultured on a rigid substrate, confirming that podosome formation is likely to be a physiological process (Linder and Aepfelbacher, 2003). Furthermore, macrophages cultured in a 3D collagen I gel assemble podosomes-like protrusions rich in several podosomes markers, despite that a vinculin ring structure was not identified in these structures (Van Goethem *et al.*, 2010).

Macrophages from WAS patients cannot assemble podosomes and, therefore present highly deficient adhesion capability (Linder *et al.*, 1999). In fact, in podosomes-deficient leukocytes the rapid attachment and detachment in specific anchorage point through β2 integrins interaction with endothelial ICAM-1 is impaired, determining defects in cells diapedesis and transmigration. Furthermore, both macrophages and DCs deficient in podosomes show abnormal adhesion kinetics determining faults in transendothelial migration (Siobhan Burns *et al.*, 2004).

1.3.3 Podosomes in matrix degradation

The main evidence of podosomes being involved in matrix degradation is the fact that they are typically found in cells that need to cross boundaries to function (Chen *et al.*, 1984; Van Goethem *et al.*, 2011). Matrix degradation studies showed that podosomes colocalized with sites of matrix degradation, confirming the hypothesis that podosomes are sites of ECM degradation thanks to their ability to secrete matrix metalloproteases (MMPs) (Linder, 2009; Linder, Wiesner and Himmel, 2011).

MMPs are zinc containing endopeptidases that can be distinguished between soluble and membrane bound MMPs. There are 25 human MMPs and they share a similar

structure. They are composed of a pro-domain with an autoinhibitory function that prevents catalytic activity, a catalytic domain and a hemopexin domain in the C-terminal region that is required for substrate recognition an interaction (Birkedal-Hansen *et al.*, 1993; GILL and PARKS, 2008; Wiesner *et al.*, 2014). They are initially secreted as inactive zymogen, where the zinc in the active site interacts with the cysteine residue in the pro-domain preventing binding of the substrate, and they are activated following cleavage of the pro-domain (Ra and Parks, 2007).

Due to their wide heterogeneity, MMPs are able to degrade numerous types of extracellular substrates and, therefore, are involved in several biological processes. The two main MMPs that were found in monocyte, macrophages and DCs upon FN-dependent activation are MMP2 and MMP9 (Medeiros *et al.*, 2017). In podosomes, proteins that are located in the actin core were found to be essential for MMPs-dependent matrix degradation. For example, DCs from patients with WAS disease or WAS KO mice are unable to assemble podosomes and consequently they fail to degrade matrix (Isaac *et al.*, 2010). A similar defect was seen in WIP KO DCs and it was demonstrated that WIP KO DCs produce MMPs in a comparable way to WT cells but only a minimal amount of them is secreted, suggesting a role of WIP in controlling MMPs secretion (Bañón-Rodríguez *et al.*, 2011). WIP KO DCs assemble alternative structures similar to focal adhesions but none of these were able to compensate for the absence of podosomes and failed to secrete MMPs (Chou *et al.*, 2006). Furthermore, the essential role of cortactin in both invadopodia and podosome-mediated matrix degradation was recently underlined (Clark *et al.*, 2007; Clark and Weaver, 2008). Cortactin is richly localized in the podosomes core where it can bind to WIP. When the WIP-cortactin interaction is disrupted, cortactin is dispersed throughout the cell's body, it can still bind to MMP2, but secretion does not take place (Bañón-Rodríguez

et al., 2011). All the findings are supporting the idea that the interaction between WIP and cortactin is essential for MMPs secretion. In fact, a WIP mutant lacking the cortactin binding site in DCs leads to non-functional podosomes unable to localize MMPs at the interface between the cell and the substratum (Bañón-Rodríguez *et al.*, 2011).

1.3.4 Mechanosensor activity of podosomes

A mechanosensor activity was initially identified in other adhesion structures such as focal adhesions (Riveline *et al.*, 2001; Albiges-Rizo *et al.*, 2009). Lately, evidence showed that podosomes have a mechanosensor function too. Not only substratum composition is sensed, but also the physical properties as rigidity and topography. The physical properties of the surrounding matrix can influence podosome lifetime and rearrangements. For instance, it was demonstrated that substrate flexibility does not affect podosome size or shape, but lifespan and distance between podosomes can be altered. In particular, in a stiffer environment, podosomes are more stable and less defined, appearing more separated from each other (Collin *et al.*, 2006). Similarly, osteoclasts assembled a small and poorly firm sealing zone on smooth substrates and a large and firm one on rough substrates (Geblinger *et al.*, 2010). Furthermore, in 3D studies, macrophages assembled podosomes only when cultured in a dense collagen matrix (Van Goethem *et al.*, 2011). The mechanism that allows cells to sense the stiffness of the substrate is still poorly understood, although it appears evident that integrins play a major role in modulating cells response to the extracellular matrix physical properties (Peng *et al.*, 2012).

All the functions described above are fundamental for myeloid cells recruitment. In the next section, myeloid cells migration and activation will be introduced.

1.4 Myeloid cells

Myeloid cells represent the first host defence mechanism being the main effector of innate immunity and comprises cells deriving from a common haematopoietic progenitor in the bone marrow, whose differentiation is guided by distinct transcription factors (Kondo, 2010). The myeloid progenitor can differentiate into red blood cells, megakaryocytes or a common precursor for white blood cells, including monocytes, macrophages, dendritic cells and granulocytes (eosinophils, basophils and neutrophils) (Gupta *et al.*, 2014; Weiskopf *et al.*, 2016).

Monocytes and dendritic cells share a common progenitor (Figure 1.7) in the latest stages of development known as the macrophage/dendritic progenitor (MDP) (Ginhoux and Jung, 2014; Schlitzer, McGovern and Ginhoux, 2015). Monocytes and a common dendritic progenitor (CDP) derive from the MDP. Pre-conventional DCs are derived from the CDP and they can leave the bone marrow to enter circulation before localizing into tissues and differentiating in mature DCs (Lee *et al.*, 2015). In mice, the MDP differentiation into monocytes or dendritic cells is respectively fms-like tyrosine kinase 3 (Flt3L) independent or dependant. Flt3-L, also known as hematopoietin, is an essential growth factor for DCs proliferation and mobilization, through binding to the Flt3 receptor (CD135) (Strobl *et al.*, 1997; Karsunky *et al.*, 2003). In humans, DCs and monocytes differentiation is still poorly understood due to the lack of reliable markers and the limited access to cells and human tissue (Ziegler-Heitbrock *et al.*, 2010).

Following differentiation into their mature forms, dendritic cells and monocytes circulate in the bloodstream and respond to the release of chemokines by the inflamed tissue by trafficking towards the site of inflammation (Kawamoto and Minato, 2004). Since their function is mainly dependant on their ability to migrate, it is becoming

apparent the importance of understanding the molecular mechanisms that are driving myeloid cells migration during the immune response.

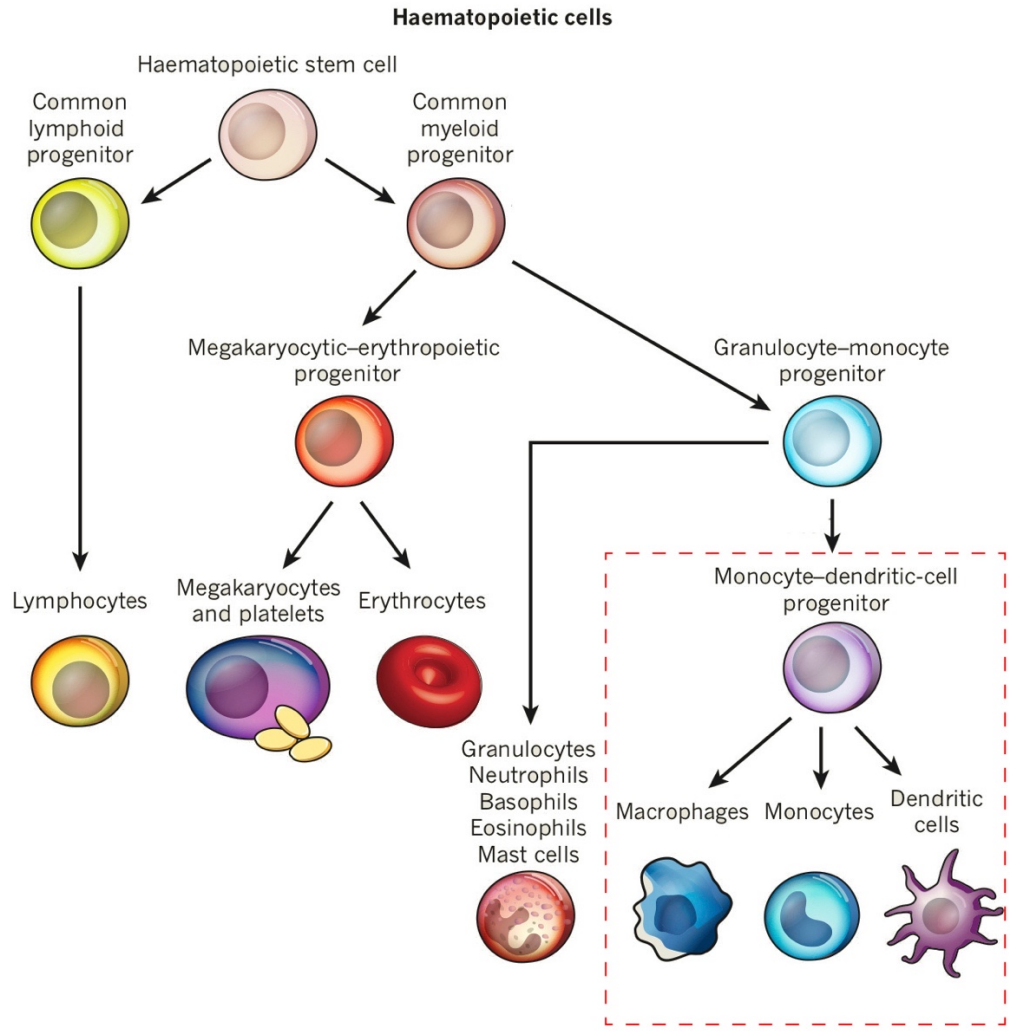

Figure 1.7. Schematic representation of haematopoietic cells differentiation.

Haematopoietic stem cells differentiate into lymphoid and myeloid progenitors. The myeloid progenitor can differentiate into red blood cells, megakaryocytes or a common precursor for white blood cells. Monocytes and dendritic cells share a common progenitor in the latest stages of development known as the macrophage/dendritic progenitor (MDP). Figure was adapted from Ransohoff et al., 2010.

1.4.1 Monocytes recruitment during an inflammatory process

Following monocytes development in the bone marrow, mature cells migrate into the bloodstream where they will reside. In response to different perturbations, monocytes leave the bloodstream and are recruited to sites of inflammation, where they will

differentiate in macrophages and dendritic cells (Chomarat *et al.*, 2000). The directed migration through tissues is thus essential for their function and dysregulation in monocytes activation or trafficking can lead to a wide variety of inflammatory diseases (Fujiwara and Kobayashi, 2005; Porcheray *et al.*, 2005).

Monocytes can be classified on the basis of the expression of chemokine receptors and surface molecules. In particular, human monocytes are divided into the following classes:

- classical monocytes ($CD14^{high}CD16^{null}$), expressing high levels of CC-chemokine receptor 2 (CCR2), can rapidly be recruited to the site of inflammation (Ziegler-Heitbrock *et al.*, 2010). CCR2 deficiency leads to defects in monocytes recruitments to the inflamed tissue (Tsou *et al.*, 2007). Many tissues, following infection, can induce the high expression of MCP-1 (CC-chemokine ligand 2) and MCP-3 (CC-chemokine ligand 7) and upon response to these pro inflammatory cytokines, monocytes can emigrate from the bone marrow to the site of infection (Serbina and Pamer, 2006).
- non-classical monocytes, $CD14^{low}CD16^{high}$, expressing low levels of CCR2 and high levels of CX_3C-chemokine ligand 1 (CX_3CL1), adhere along the luminal surface of endothelial cells in healthy tissues, with a patrolling function (Ziegler-Heitbrock *et al.*, 2010). The adhesion is mediated by the CX_3CL1 ligand, which is membrane-bound on endothelial cells. Resident patrolling monocytes can respond rapidly to a tissue invasion and mediate early immune response by differentiating into macrophages and releasing tumour necrosis factor and cytokines (Auffray *et al.*, 2007; Leuschner *et al.*, 2011). They can also migrate towards the site of inflammation and contribute to wound healing (Shi and Pamer, 2011);

- intermediate monocytes ($CD14^{high}CD16^{high}$), with a pro-inflammatory role. They were described as transition monocytes from classical to non-classical (Ziegler-Heitbrock *et al.*, 2010).

Monocytes recruitment follow the general process of rolling, adhesion and transmigration (Ley *et al.*, 2007). Integrins, together with other adhesion molecules, mediate monocyte interaction with the endothelium to establish tight adhesions. Classical monocytes express P-selectin glycoprotein ligand 1 (PSGL1), which interacts with endothelium P-selectin, E-selectin and L-selectin. L-selectin binds to the endothelium cell-expressed peripheral node addressin (PNAd), mediating monocytes rolling phase on the venules endothelium (Leon and Ardavin, 2008). The rolling process is followed by the formation of tighter adhesions. The transition from rolling to slow rolling and adhesion is dependent on endothelial cells expression of VCAM-1, which can arrest monocytes through an interaction with integrins (Luscinskas *et al.*, 1994; Huo, Hafezi-Moghadam and Ley, 2000). Proper monocytes activation is achieved through interaction with the endothelial Duffy antigen receptor for chemokines (DARC), that is able to transport CCL2 across the endothelium (Pruenster *et al.*, 2009). At this point, monocytes crawl in the endothelium looking for an optimal spot for transmigration. Inter-endothelial adhesive junctions need to be disassembled to allow leukocytes transmigration. Monocytes transmigration causes downregulation of Vascular Endothelia-cadherin (VE-cadherin) and exploits pre-existing VE-cadherin gaps to extend pseudopodia and achieve transmigration (Su *et al.*, 2002). During transmigration, the platelet/endothelium cells adhesion molecule-1 (PECAM-1) expressed on the surfaces of leukocytes and endothelial cells is upregulated and interacts to pull the cell through the endothelium (Muller *et al.*, 1993; Abraham *et al.*, 2016). Following paracellular migration across the endothelial

junctions, the basement membrane needs to be penetrated to allow cells progression. This event is achieved through proteolytic activity, thanks to the production of matrix metalloproteases (Shankavaram *et al.*, 2001), and through mechanical reorganization of cells cytoskeleton. Interestingly, it has been recently demonstrated that macrophages may employ different invasive mechanisms on the basis of the type of barrier they have to cross. For instance, when macrophages are faced with porous membranes, they tend to get deformed and squeeze in; in contrast, macrophages employ proteolytic enzymes when they are faced with more rigid barriers (Friedl and Wolf, 2010).

1.4.2 Role of WIP and WASP in monocytes migration and immune response

In response to extracellular signals, monocytes, macrophages and dendritic cells polarize and assemble a leading edge and a contractile rear to allow cell body progression (Linder *et al.*, 2000; Burns *et al.*, 2001; Evans *et al.*, 2003). Actin polymerization at the leading edge drives podosome development to mediate adhesion to the extracellular matrix, migration and transendothelial invasion (Calle *et al.*, 2006; Tsuboi, 2007; Linder, 2009). However, only certain subsets of these cells assemble podosomes. In particular, they are mainly assembled by immature dendritic cells and alternatively activated macrophages (M2), that are mainly involved in wound healing and tissue repair (Gawden-Bone *et al.*, 2010; Cougoule *et al.*, 2012). Podosome formation is highly dynamic since new podosomes are formed as the lamellae extend and are disassembled at the back of the cell (Starnes, Cortesio and Huttenlocher, 2011). Each cell can assemble from several dozen to hundreds of podosomes. The high number of podosomes assembled from these cells make them a good model for understanding podosomes dynamics and structural organization. Podosomes are also

formed in the monocytic like cell line THP-1 (Tsuboi, 2006; Burger *et al.*, 2011; Okamoto *et al.*, 2018), following differentiation with TGFβ-1 and integrins activation through seeding on fibronectin-coated surfaces. It was demonstrated that podosomes studies on THP-1 cells are highly reproducible in primary murine dendritic cells (Macpherson *et al.*, 2012). Therefore, THP-1 cells can be used as a valuable cell line model for the study of myeloid podosomes in vitro.

In monocytes, podosomes were associated with several fundamental functions described in the previous sections (Andersen *et al.*, 2016). Macrophages and DCs from WAS patients cannot form podosomes, developing defects in migration and chemotaxis and in turn providing the basis for immunodeficiency (Jones *et al.*, 2002; S. Burns *et al.*, 2004). WAS patients present a wide variety of symptoms that correlate with the different type of mutations found in WAS gene. Several WASP domains are important for normal podosomes development, interacting with molecular partners: WAS binding to CdC42 is essential for both podosomes assembly and disassembly (Linder *et al.*, 1999) and WAS interaction with the ARP2/3 complex is necessary to start branch actin polymerization as described above (Burns *et al.*, 2001). Furthermore, mutations in WASP N-terminal region, containing the binding site for WIP, are among the most common in WAS patients. Abolishing WASP/WIP interaction in THP-1 cells and primary monocytes leads to loss of polarization (Tsuboi, 2006), defects in adhesion turnover (Vijayakumar *et al.*, 2015), migration, chemotaxis and polarity as seen in WASP-null cells (Zicha *et al.*, 1998; Jones *et al.*, 2002). Podosomes are also involved in monocytes transmigration and matrix degradation through WIP/cortactin interaction as described in previous sections (Bañón-Rodríguez *et al.*, 2011). While most of the time transmigration within the endothelium is achieved paracellularly at endothelial junctions, podosomes in monocytes mediate transcellularly transmigration

through endothelial cells by integrins interaction with endothelial ICAM1 (Andersen *et al.*, 2016). Taken together, all these data suggest that the WIP-WASP complex works as a functional unit that regulates actin and adhesion dynamics changes during podosomes mediated migration in monocytic cells (Chou *et al.*, 2006).

WASP possesses epigenetic control on adaptive immunity genes through histone methylation (Taylor *et al.*, 2010) and WIP can regulate N-WASP nuclear translocation interfering with cytoskeleton dynamics in rat fibroblasts (Vetterkind *et al.*, 2002). WIP can also regulate gene expression indirectly through the regulation of actin dynamics, which in turn determine the nuclear localisation of the transcription co-factor MRTF-A (Ramesh *et al.*, 2014). Previous data obtained in Dr. Calle's lab showed that both WASP and WIP can be localised in the nucleus of myeloid cells and play a role in the formation of complexes containing tyr-phosphorylated proteins and histones, which suggests a possible direct role of WASP and/or WIP in the nucleus leading to modulation of gene expression (Calle et al., unpublished data). Recently the nuclear entry and exit sequences employed by WASP was identified and it was underlined the importance of a nuclear ARP2/3-VCA independent function of WASP (Sadhukhan *et al.*, 2014). Also, N-WASP, the ubiquitously expressed form of WASP, can localize in the nucleus. Its nuclear localization is controlled by phosphorylation by Src kinases and HSP90 expression (Suetsugu and Takenawa, 2003). Therefore, motility is not only dependent on actin dynamic but is also regulated through gene expression, as actin remodelling and gene expression can influence each other (Sotiropoulos *et al.*, 1999; Posern, Sotiropoulos and Treisman, 2002). However, the role of these proteins in the nucleus remains unclear.

1.5 Effect of mild hyperthermia on regulation of the immune response

Heat is a cardinal sign of inflammation and the correlation infection/increased temperature is highly conserved in plants' (Zhu *et al.*, 2011) and animals' evolution (Vaughn, Bernheim and Kluger, 1974; Bernheim and Kluger, 1976). Body temperature increase of 1 to 4°C provides a survival advantage during infections and the use of antipyretic drugs was associated with a higher rate of mortality in critically ill patients (Ryan and Levy, 2003; Earn, Andrews and Bolker, 2014). On the other hand, fever is not beneficial in diseases characterized by excessive inflammation (Almeida *et al.*, 2006; Liu *et al.*, 2012) or sepsis (Launey *et al.*, 2011). Migration of immune cells represents a crucial step in the host defence mechanism and several studies showed that fever is able to promote several steps involved in both innate and adaptive immunity, including leukocytes activation and migration (Jiang *et al.*, 1999; Rice *et al.*, 2005). However, the mechanism by which mild hyperthermia is able to promote immune cell migration is still poorly understood.

1.5.1 Role of mild hyperthermia in activation and migration of innate immunity cells

Fever has a strong impact on innate immunity (Jiang *et al.*, 1999; Evans, Repasky and Fisher, 2015). Researches performed in animal models of hyperthermia showed that fever range temperatures can have an anti-tumour effect increasing granulocytes respiratory burst and therefore leading to enhanced neutrophils activation and bacteriolytic activity (Takada *et al.*, 2000; Ostberg, Ertel and Lanphere, 2005). Furthermore, mild hyperthermia can induce the fast release of neutrophils from the bone marrow and high recruitment of peripheral neutrophils, inducing neutrophilia, following the overproduction of granulocyte colony-stimulating factor (G-CSF)

(Takada *et al.*, 2000; Ellis *et al.*, 2005). Neutrophil recruitment to distant infected tissues is also augmented in a CXC-chemokine ligand 8 (CXCL8)-dependant way during hyperthermia (Singh *et al.*, 2008) and improved by reduced endothelial integrity in response to ERK1/ERK2 kinases signalling during hyperthermia that facilitate neutrophils extravasation (Tulapurkar *et al.*, 2012).

Fever-range hyperthermia effect on Natural Killer (NK) cells was similar to what was seen in neutrophils. In particular, *in vivo* studies demonstrated that hyperthermia can increase NK cell cytotoxicity on tumour sites, upon upregulation of specific NK ligands on tumour cells (Ostberg *et al.*, 2007), downregulation of MHC class I molecules expression in tumour cells (Dayanc *et al.*, 2008) and upregulation of HSP70 (Dayanc *et al.*, 2008).

Macrophages response to febrile-range hyperthermia has been extensively studied. Whole body heating, up to 39.5°C, increases macrophage production of several cytokines as TNF, IL-1 and IL-6 in mice exposed to LPS (Jiang *et al.*, 1999; Ostberg *et al.*, 2000), improving bacterial clearance. Macrophage activation in response to hyperthermia is induced by upregulation of HSP70 (Multhoff *et al.*, 1995) that leads to phosphorylation of IKK and IκB and nuclear translocation of NFκB (Repasky, Evans and Dewhirst, 2013). In the nucleus, NFκB will bind to the TNF-α promotor increasing its release (Repasky, Evans and Dewhirst, 2013). Furthermore, following exposure to heat, HSP70 can be released extracellularly (Gupta *et al.*, 2013), where it can bind to membrane receptors mediating the production not only of cytokines but also of nitric oxide and inducible nitric oxide synthase (Pritchard, Li and Repasky, 2005).

Similarly, heath can enhance innate immunity stimulating DCs response to pathogens, by improving phagocytic capability (van Bruggen, Robertson and Papadimitriou,

1991; Djaldetti and Bessler, 2015), upregulating MCH class I/II molecules (Knippertz *et al.*, 2011) and Heath Shock protein 70 (HSP70), improving TNF-α production and ability of priming naïve $CD8^{high}$ T cells (Knippertz *et al.*, 2011). DCs can also promote higher proliferation of $CD4^{high}$ T cells and their differentiation towards Th1 subset through secretion of polarizing cytokines as IL-12, increasing their cytotoxic influence (Hatzfeld-Charbonnier *et al.*, 2007). DCs and APCs migration towards lymph nodes was also accelerated by febrile temperature (Ostberg *et al.*, 2000; Hatzfeld-Charbonnier *et al.*, 2007), due to increased responsiveness to the CCR7 ligand through regulation by the CCR7-CCL21 axis (Schumann *et al.*, 2010; Tal *et al.*, 2011).

1.5.2 Role of mild hyperthermia in activation and migration of adaptive immunity cells

The efficient activation of adaptive immunity cells depends on the encounter of an antigen presented by DCs or APCs (den Haan, Arens and van Zelm, 2014). Therefore, a high rate of migrating lymphocytes through lymphoid organs is a crucial event. It was shown that the number of peripheral blood lymphocytes is highly reduced in mice or humans exposed to fever range temperatures, indicating a possible localization into lymphoid organs (Ostberg and Repasky, 2000; Evans *et al.*, 2001). T and B lymphocytes enter into lymph nodes through high endothelial venules (HEVs) in a multistep process similar to monocyte migration towards the invaded tissue described above (Girard, Moussion and Förster, 2012; Griffith, Sokol and Luster, 2014). The process includes L-selectin dependent slow rolling on endothelial venules (Wang *et al.*, 1998), interaction between vessels chemokines and activated chemokines receptors on lymphocytes (Evans *et al.*, 1999), formation of tighter adhesions by interaction with CCL21 and ICAM1 and transendothelial migration mediated by β2 integrin leukocyte-function associated antigen-1 (LFA-1)- intercellular adhesion

molecules-1 and 2 (ICAM-1 and 2) binding (Chen *et al*., 2006; Chen *et al*., 2009). Fever can influence each of those steps. It can promote leukocyte slow rolling on the endothelium by increasing the affinity of L-selectin with its endothelial receptor PNAd (Girard, Moussion and Förster, 2012) and similarly improving the binding activity of α4β7 integrin with the endothelial mucosal addressin cell adhesion molecule-1 (MAdCAM-1) (Picker and Butcher, 1992). Fever induced stress can promote the stabilization of tighter adhesions by augmenting the endothelial expression of CCL21 (Chen *et al.*, 2006). While ICAM-2 is not affected by thermal stimulation, ICAM-1 expression is significantly increased in the intravascular regions, promoting both cells arrest and trans endothelial migration (Chen *et al.*, 2009). Similarly to TNF, thermal effect also increased endothelial expression of CCL21 and ICAM1, while no effect was yet demonstrated on LFA1 or CCR7. This evidence suggests that HEVs play a critical role in the controls of thermal response. Furthermore, during local inflammation, HEVs open gates to lymphoid organs allowing the entrance of additional immune cells such as monocytes and NK cells, increasing their trafficking to lymph nodes in response to CXCL9 and CXCL10 (Janatpour *et al.*, 2001; Martín-Fontecha *et al.*, 2004).

Not only trafficking is augmented by fever in leukocytes by also their ability to respond to inflammatory signals. In particular, both *in vivo* and *in vitro* T-cells exposed to fever-range temperatures show higher differentiation into a cytotoxic subset and higher secretion of INF-γ (Mace *et al.*, 2012). Thermal stress can also cause clustering in cholesterol-enriched domains of immunological components in $CD8^{high}$T cells such as TCR. In $CD4^{high}$ T-cells, heat-induced membrane fluidity changes leads to a macromolecular clustering able of inducing cells activation and IL-2 production without additional CD28 stimulation (Gombos and Vígh, 2015).

1.6 Molecular regulation of the plasma membrane in response to mild hyperthermia

Plasma membranes in eukaryotic cells are essential in establishing a barrier between the cytoplasm and the external compartments allowing, at the same time, communication and signalling exchange with the environment (Owen *et al.*, 2010). It is organized in lipid domains and lipid/proteins clusters, whose distribution and dynamics are essential in regulating cells response and activity (Ingólfsson *et al.*, 2014; Jacobson and Liu, 2016). In particular, immune cells, whose functions are regulated upon recognition of antigens and response to environmental stimuli, require complex plasma membrane interactions between lipids and proteins (Jerry and Sullivan, 1976; He and Marguet, 2008; Owen *et al.*, 2010; Lillemeier and Davis, 2011; Mace *et al.*, 2012). Membrane lipids are organized into a permeable bilayer and it was initially believed that proteins and lipids are randomly distributed throughout the plasma membrane to create a "fluid mosaic" (Singer and Nicolson, 1972). Several varieties of lipids are included in the plasma membrane comprising phosphatidylcholine, phosphatidylethanolamine, phosphatidylserine and sphingomyelin (Ingólfsson *et al.*, 2014). The outer leaflet mainly consists of highly saturated fatty acids and sphingolipids, while the inner leaflet is predominately made of phosphatidylethanolamine and phosphatidylserine and its minor component phosphatidylinositol. This structure, presenting hydrophobic fatty acids in the interior layer, creates a barrier between the two aqueous compartments impeding the access of water-soluble molecules and ions (Pörn, Ares and Slotte, 1993; Dowhan and Bogdanov, 2002; Ejsing *et al.*, 2009; Bevers and Williamson, 2016). Furthermore, the high amount of double bonds in the fatty acids tails confers to the lipid bilayer a viscous fluid more than a solid appearance (Owen *et al.*, 2010).

Membrane fluidity can be influenced by several events, including temperature variations and cholesterol content (Horváth *et al.*, 1998; de Meyer and Smit, 2009; Dawaliby *et al.*, 2015). Hyperthermia generally induces an increment in membrane fluidity that cells try to compensate by increasing the saturation of fatty acid tails, while low temperatures are normally associated with more rigid membranes (Lepock *et al.*, 1983; Laszlo, 1992). Cholesterol can have different outcomes on membrane fluidity based on temperature. During hyperthermia, it impedes the movement of phospholipid tails making membranes less fluid, while at lower temperature its enclosure into the lipid bilayer avoids membranes stiffening and sustains fluidity (de Meyer and Smit, 2009; Dawaliby *et al.*, 2015). Several physiological events including protein activation and cytoskeleton remodelling are driven by the oscillation in overall membrane fluidity. Local changes in membrane fluidity can also affect cell signalling. In lipid rafts, highly-saturated glycosphingolipids and phospholipids are assembled in domains rich in cholesterol to accommodate specific proteins (Dupré *et al.*, 2002; Pike, 2003; Megha and London, 2004; He and Marguet, 2008; Owen *et al.*, 2010). It is believed that in resting cells these complexes are highly dynamic and composed of few molecules. Upon cell activation, they can associate into larger domains that are stabilized by protein-protein and protein-lipid interactions, which start cell membrane-associated transduction signalling events (Cebecauer *et al.*, 2010; Varshney, Yadav and Saini, 2016). For example, in lymphocytes, the T-cell antigen receptor (TCR) and its activator (Lat) are localized in separate domains during resting phases but they concatenate following T cell activation (Lillemeier *et al.*, 2010).

1.6.1 The plasma membrane as a heat sensor during mild hyperthermia: role of lipids

A membrane sensor hypothesis has been recently introduced (Török *et al.*, 2014). According to this theory, the plasma membrane is responsible for sensing stress signals from the environment and re-establishing homeostasis inducing the expression of heath shock proteins (HSPs), which work as chaperones having the ability to restore protein integrity (Török *et al.*, 2014). Therefore, when cells are exposed to mild thermal stress, the lipid membrane bilayer is modified in a way that leads to the activation of transient receptor potential channels (TRP) (Voets *et al.*, 2004; Dhaka, Viswanath and Patapoutian, 2006). Following the opening of TRP, transduction of membrane-associated signals activates heath shock factors (HSF), in particular HSF1, which in turn is able to induce the expression of heath-shock genes (Fan-Xin *et al.*, 2012; Hsu and Yoshioka, 2015). Lipids can activate thermally-gated TRP channels directly, serving as allosteric modulators, or indirectly, altering the physical properties of the membrane (Taberner *et al.*, 2015). Among the vast heterogeneity of membrane lipids, phosphatidylinositol 4,5-biphosphate (PIP_2) is one of the main regulators of the activation of TRP channels (Suh, Biophys. and al, 2008).

Temperature can also have a major effect on lipid rafts. Even a small thermal oscillation can modify lipids fluidity causing, therefore, a redistribution that can lead to activation of proteins present in the rafts (Simons and Ikonen, 1997; Lingwood and Simons, 2010). Furthermore, cholesterol is another strong effector of TRP channels and several TRP channels can segregate into cholesterol-rich lipid rafts, suggesting that the assembly of rafts macrodomains can influence the gating of TRP channels (Chadwick and Goode, 2004; Morenilla-Palao *et al.*, 2009). In particular, when the channels are displaced form the lipid-rafts, their activation can occur at higher

temperatures (Morenilla-Palao *et al.*, 2009). Finally, thermal stress can alter membrane's and microdomain's fluidity by inducing the release of stress hormones, such as corticosteroid, or altering intermolecular interactions (Dindia *et al.*, 2013).

Taken together, these studies underline the essential role of lipids in modulating the physical properties of the plasma membrane, which can influence the expression of heat stress genes and vice versa. Treatments with membrane fluidizers are widely used to mimic the changes in membrane fluidity induced by mild hyperthermia. In particular, Benzyl Alcohol (BA) can be absorbed into the membrane, replacing water molecules and weakening the van der Waals forces in the lipid acyl chains, mimicking the heat shock (Török *et al.*, 2014). Treatment of K562 cells with BA can initiate the heat shock response inducing the expression of HSP70 at low temperatures, having an outcome comparable to what could be observed after exposure to 42°C (Balogh *et al.*, 2005). Similarly, the membrane fluidizers drug bimoclomol can induce the expression of heat shock genes by increasing the fluidity of negatively charged lipids in the plasma membrane (Vígh *et al.*, 1997; Török *et al.*, 2003; Hesselink JM, 2016). Arimoclomol, a membrane fluidizer drug in trial for use as a treatment in diseases characterized by protein misfolding, can potentiate the heat shock response amplifying the expression of HSP70 (Parfitt *et al.*, 2014; Fog *et al.*, 2018). All of these studies suggest that membrane fluidization and hyperthermia have a similar effect in regulating the expression of molecular chaperones and this may be an important step towards the development of treatments for diseases characterized by protein unfolding.

Besides HSPs activation, membrane fluidity was also associated with enhanced immune cells activation, having an effect comparable to mild hyperthermia (Gombos and Vígh, 2015). When T cells are stimulated by CD28, macrodomains containing

cholesterol and sphingomyelin are assembled in the plasma membrane, IL-2 is secreted and T cells are activated (Beyersdorf, Kerkau and Hünig, 2015). It was demonstrated that both mild hyperthermia and drug-induced increment of membrane fluidity at physiological temperatures can activate T cells without requiring CD28 co-stimulation, inducing both lipids clustering and IL-2 production (Gombos and Vígh, 2015). Interestingly, WASP is recruited in lipid rafts in CD28 activated T cells and plays an important role in lipid rafts movement, since WAS patients have impaired clustering capability and weak T cells proliferation (Dupré *et al.*, 2002). These data fit well with the membrane sensor hypothesis, indicating that plasma membrane is the first upstream regulator of heath shock and at the same time suggest that the fever induced activation of immune cells may be regulated by the shift in membrane fluidity.

1.6.2 Regulation of actin dynamics and cell migration by mild hyperthermia

The alteration of lipids fluidity in the plasma membrane caused by heath stressors leads to the upregulation of HSPs (Török *et al.*, 2014). The effect of these proteins on actin cytoskeleton remodelling and dynamics is still poorly understood, although there are a few pieces of evidence demonstrating that HSPs overexpression can induce molecular changes in actin related proteins leading to enhanced cells migration (Aizawa, Sutoh and Yahara, 1996; Park *et al.*, 2007; Sims, McCready and Jay, 2011). For instance, it was demonstrated that T cells overexpressing HSP70 have reduced phosphorylation of cofilin. Cofilin, is an actin nucleating protein, responsible for lamellipodia extension and the cell's leading edge, controlling cell motile behaviour (Aizawa, Sutoh and Yahara, 1996). Phosphorylation of cofilin Ser3 by LIM Kinase (LIMK) stops the protein activity and stabilizes actin filaments. Therefore, HSP70 expressing T cell showed increased chemotaxis ability (Simard *et al.*, 2011).

Similarly, HSP90 can bind actin (Park *et al.*, 2007) and can associate with another actin related protein, N-WASP (Suetsugu and Takenawa, 2003; Park, Suetsugu and Takenawa, 2005; Park *et al.*, 2007). N-WASP, the ubiquitously expressed form of WASP, can nucleate actin by interacting with the ARP2/3 complex, downstream of Rho GTPases signalling. A first evidence of its association with HSP90 came from the fact that accumulation of unphosphorylated N-WASP in the nucleus can abolish HSP90 transcription by binding with heath shock transcription factors and in turn suppressing the activity of Src kinases (Suetsugu and Takenawa, 2003). HSP90 can also modulate N-WASP/ARP2/3 induced actin polymerization in both filopodia and podosomes formation (Park *et al.*, 2007). In fact, it can bind to N-WASP and F-actin, inducing formation of bundle actin by colocalizing with N-WASP in actin branching points during filopodia formation (Park *et al.*, 2007). Moreover, it has been demonstrated in 3Y1/v-Src cells that HSP90 can increase v-Src dependant N-WASP phosphorylation protecting it from proteasome degradation and amplifying actin polymerization and podosome formation (Park, Suetsugu and Takenawa, 2005).

Interestingly, in cancer cells, HSP90 can induce MMP-2 dependant matrix degradation, through interaction with additional co-chaperons including HSP70. When HSP70 is inhibited, MMP-dependant matrix invasion and cell migration are both reduced (Sims, McCready and Jay, 2011). Taken together, it is possible to hypothesize that in response to mild hyperthermia, as during fever, plasma membrane remodelling in immune cells induces the expression of HSPs able to modulate actin dynamics and to boost their motile capability.

Chapter 2: Materials and Methods

2 Materials and Methods

2.1 Cell culture

2.1.1 Cell lines and culture conditions

THP-1 cells were procured from the American Type Culture Collection (ATCC). THP-1 cells resemble monocytes and are derived from patients with acute monocytic leukaemia. This cell line is commonly used as a model of monocyte and macrophage (differentiated with TGFβ-1) for the study of cell migration (Monypenny *et al.*, 2011; Vijayakumar *et al.*, 2015). Cells were grown in suspension in RPMI medium (Sigma Aldrich, UK) supplemented with 10% foetal calf serum (FCS, GIBCO) until a maximum density of $1x10^6$ cells/ml at 37°C in a 5% CO_2 atmosphere. THP-1 cells differentiation to macrophages was induced by seeding on surfaces coated with fibronectin (10µg/ml) (Sigma Aldrich, UK) and incubation for 16 hours with 1ng/ml TGFβ-1 (R&D Systems), as described in the literature (Monypenny *et al.*, 2011; Vijayakumar *et al.*, 2015; Foxall *et al.*, 2019).

HEK 293T cells were used for lentiviral production as described in the following chapters (3.2.1; 5.2.6). HEK 293T cells were cultured in DMEM (Sigma Aldrich, UK) supplemented with 10% FCS at 37°C in a 5% CO_2 atmosphere for about 6 passages. Cells were then adapted to grow in the culture medium used for transfection consisting of RPMI 10% FCS.

Primary dendritic cells (DCs) were isolated by Dr Calle's collaborators as described in the Appendix (section 8.1).

2.1.2 Analysis of cell viability after exposure to mild hyperthermia

THP-1 cells were exposed for 16 hours to mild hyperthermia (40 °C) and then stained with Annexin V (BD Biosciences) tagged with the fluorophore allophycocyanin (APC - λex 594-633 nm; λem 660 nm) and Propidium Iodide (Sigma Aldrich; λex 530 nm; λem 620 nm), following manufacturer instructions. Annexin V is able to bind to the membrane phospholipid phosphatidyl-serine, which is exposed in the outer plasma cell membrane from the earliest phases of apoptosis, while propidium iodide is not permeant to live cells membrane and was used to detect necrotic cells. Percentages of viable (Annexin V and Propidium Iodide negative population), early apoptotic (Annexin V positive, Propidium Iodide negative population), late apoptotic (Annexin V and Propidium Iodide positive population) and necrotic cells (Propidium Iodide positive, Annexin V negative population) were determined acquiring 5000 events per samples through BD Accuri C6 Flow cytometer (BD Biosciences). APC-tagged Annexin V was excited at 625 nm and the emitted fluorescence was collected at 675 nm. Propidium Iodide was excited at 610 nm and the emitted fluorescence was collected at 620 nm.

2.1.3 Transmigration assay

Trans well-inserts (SLS) with a pore size of 8.0 µm were placed in wells of 24 well plates previously filled with 500 µl of serum free RPMI with or without 50 ng/ml MCP1 (R&D systems). $2x10^6$ THP-1 cells/ml suspended in 500 µl serum free RPMI were seeded in the upper chamber of each insert (Figure 2.1). Plates were incubated for one hour at 37°C or 40°C. After the incubation, THP-1 cells resuspended in the medium in the upper and bottom chamber of the filters were collected carefully in 1.5 ml Eppendorf tube, then centrifuged at 2000 rpm for 5 minutes. Cell pellets were

resuspended in 200 µl PBS and the number of cells in each compartment was determined by flow cytometry. The total number of events in 20 µl of medium of each sample were registered and used for analysis. The number of cells that migrated to the lower chamber of the filter was normalized to the total number of cells seeded.

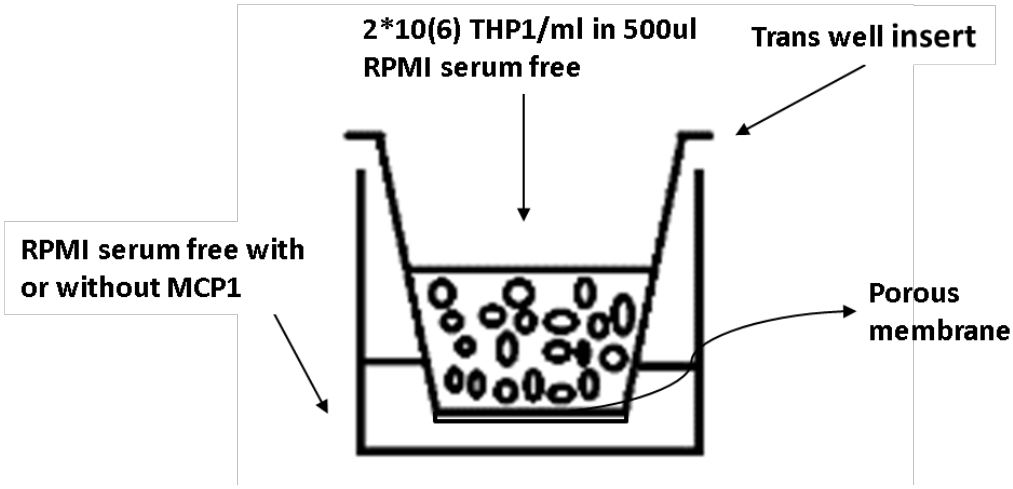

Figure 2.1. Schematic representation of transmigration assay.

$2x10^6$ THP-1 cells/ml were seeded on the upper chamber of the transwell, while the lower chamber was filled with serum free medium alone or supplemented with the chemo attractant protein MCP-1 (50ng/ml) and incubated for one hour at 37°C or 40°C. After the incubation, the number of migrated cells to the lower chamber and remaining cells in the upper chamber was quantified by flow cytometry.

2.2 Protein analysis

2.2.1 Reagents and antibodies

All antibodies used in this study are shown in Table 2.1. All primary antibodies used for Western Blot were diluted in 5% skimmed milk (Sigma) in a 1% Tween 20/PBS solution, while all secondary antibodies were diluted in 2.5% skimmed milk (Sigma) in a 1% Tween 20/PBS solution.

Primary antibodies used for immunofluorescence were diluted in 5% BSA in PBS solution, while secondary antibodies were diluted in 2.5% BSA in PBS solution. Alexa-Fluor-568-conjugated phalloidin (Molecular Probes) was used to stain filamentous actin, while DAPI solution (Molecular Probes, 1:500) was used to stain cells' nuclei. Both phalloidin and DAPI were included during the secondary antibody incubation.

Table 2.1. List of antibodies used in this study

	Species	Type	Dilution	Source	Purpose
Primary antibodies					
WIPF1	Goat	Polyclonal	1:500	Thermo Scientific	Western Blot
WASP B-9	Mouse	Monoclonal	1:500	Santa Cruz Biotechnology	Western Blot
ARP2/3 (p34-Arc/ARPC2)	Rabbit	Polyclonal	1:1000	Millipore	Western Blot
GAPDH 6C5	Mouse	Monoclonal	1:5000	Millipore	Western Blot
ERK1/2	Rabbit	Polyclonal	1:1000	Cell signalling	Western Blot
pThr202/Tyr204-ERK 1/2	Mouse	Polyclonal	1:1000	Cell signalling	Western Blot
WHICH/WIRE (WIPF2)	Rabbit	Polyclonal	1:1000	Sigma	Western Blot
Vincuin	Mouse	Monoclonal	1:1000	Sigma	Western Blot
ILK1	Rabbit	Polyclonal	1:1000	Cell signalling	Western Blot
HSP90 alpha	Rabbit	Polyclonal	1:500	Abcam	Western Blot
GFP	Rabbit	Monoclonal	1:500	Thermo Scientific	Western Blot
Vinculin (hVIN-1)	Mouse	Monoclonal	1:100	Sigma	Immunofluorescence
Secondary antibodies					
Anti-rabbit IgG (H + L), IRDye® 680RD	Donkey		1:5000	Licor	Western Blot
Anti-rabbit IgG (H + L), IRDye® 800CW	Donkey		1:5000	Licor	Western Blot
Anti-goat IgG (H + L), IRDye® 680RD	Donkey		1:5000	Licor	Western Blot
Anti-mouse IgG (H + L), IRDye® 800CW	Donkey		1:5000	Licor	Western Blot
Anti-goat IgG HRP	Rabbit		1:1000	DAKO	Western Blot
Anti-rabbit IgG HRP	Goat		1:1000	DAKO	Western Blot
Anti-mouse IgG HRP	Goat		1:1000	DAKO	Western Blot
Anti-mouse Alexa-Fluor-465	Donkey		1:100	Molecular Probes	Immunofluorescence

2.2.2 Western Blot

Sample preparation. $1x10^7$ THP-1 cells or $2x10^6$ DCs were seeded in 10 cm cell culture petri dishes, previously coated for 1h with 10 µg/ml fibronectin (Sigma Aldrich, UK) and incubated for 16 hours at 37°C or 40° in the presence of 1 ng/ml TGFβ-1 (BD Systems, UK). Cells were lysed in 250 µl 1x Laemmli Buffer (Sigma Aldrich, UK). Lysates were passed through a 0.5x25 mm needle (Terumo Medical Corp.) six times to shred the DNA and then, boiled for 5 minutes at 100°C.

Electrophoresis. Samples and a molecular weight marker (PageRuler™ Plus Pre-stained Protein Ladder, 10 to 250 kDa, ThermoFisher Scientific) were loaded in 12% acrylamide 0.1% SDS PAGE reducing gels. Electrophoresis was performed on a Mini-PROTEAN Tetra cell electrophoresis system (BIORAD) for 90 minutes at 110 constant voltage in 1x running buffer (25 mM Tris Base, 190 mM Glycine, 0.1% SDS).

Transfer of proteins. After electrophoresis, proteins were transferred from the acrylamide gel onto a nitrocellulose membrane (GE Healthcare Life Sciences Nitrocellulose Membrane) using a Mini Trans-Blot (BIORAD) for 3 hours at constant 380 mA in 1x transfer Buffer (25 mM Tris Base, 190 mM Glycine, 20% methanol).

Immune-blot. The membrane was blocked at room temperature for 1 hour in 5% skimmed milk (Sigma) in a 1% Tween 20/PBS solution and then incubated for 16 hours at 4°C with the appropriate concentration of primary antibody in the same blocking solution. The membrane was then washed three times in 1% Tween 20/PBS and incubated with the recommended dilution of secondary antibody in 1% Tween 20/2.5% milk PBS solution at room temperature for 1 hour and washed again three times. Images were acquired employing Odyssey Imaging System (LICOR) and processed and quantified using Image Studio Software (LICOR).

2.2.3 Zymography

Zymography is an electrophoretic technique used for measuring enzymes proteolytic activity (Leber and Balkwill, 1997). In gel zymography, gelatine is included in the polyacrylamide gel. Following electrophoretic run of the cells culture media, the presence of degradation areas in the gel is investigated. Areas of gel degradation correspond to gelatinases, previously secreted by the cells in the media during culturing (Leber and Balkwill, 1997).

$4x10^5$ cells/ml were seeded in 24 well plates' wells previously coated for 1 hour with 10 µg/ml fibronectin (Sigma) with 500 µl serum free RPMI supplemented with 1 ng/ml TGFβ-1 for 16 hours. Plates were incubated either at 37°C or 40°C. The culture medium was collected after 72 hours and centrifuged at 2000 rpm for 5 minutes. Samples were subjected to SDS-electrophoresis in 1x non-reducing sample buffer (250 mM Tris HCl pH 6.8, 25% glycerol, 2.5% SDS) and protein fractionation was carried out on 1 mm SDS-PAGE gels (10% acrylamide, 0.075% gelatine). To allow proteins renaturation and remove SDS, gels were soaked in 2.5% Triton X-100 with gentle shaking for 30 minutes at room temperature and then incubated for 16 hours at 37°C in substrate buffer (0.05 M Tris-HCl pH8.0, 1 mM $CaCl_2$). The following day, gels were stained with Coomassie blue and de-stained in distilled water until bands were visible. Images were acquired using a Gel Doc XR+ (BIO-RAD) and bands intensity was quantified using ImageJ Software. Matrix metalloprotease was identified in base of its molecular weight as inactive pro-MMP9 (92 kDa (Toth and Fridman, 2001)) and active MMP9 (68 kDa (Troeberg and Nagase, 2003)). This technique allows the detection of the zymogen activity due to autocatalytic cleavage, which removes the pro-domain responsible of blocking the active site in MMP9 impeding substrate access (Frankowski *et al.*, 2012).

2.2.4 Biochemical separation of nucleus and cytoplasm

$1x10^7$ THP-1 cells (parental or mutant cells) were seeded for 16 hours at 37°C on 10 cm cell culture petri dishes previously coated for 1 hour with 10 µg/ml fibronectin (Sigma) in the presence of 1ng/ml TGFβ-1. The following day nucleus and cytoplasm were separated using NE-PER™ Nuclear and Cytoplasmic Extraction Reagents (Thermofisher) according to manufacturer instructions. Lysates obtained were diluted in 6x Laemmli Buffer (Sigma Aldrich, UK), boiled for 5 minutes at 100°C and used for Western Blot.

2.3 Microscopy

2.3.1 Immunofluorescence

$2x10^5$ THP-1 cells or DCs were seeded for 16 hours on 13 mm coverslips previously coated for 1h with 10 µg/ml fibronectin (Sigma Aldrich, UK) and placed at the bottom of wells in 24 well plates. Cells were incubated for 16 hours at either 37°C or 40°C in the presence of 1 ng/ml TGFβ-1 (BD Systems, UK). Then, cells were fixed with 4% paraformaldehyde (ThermoFisher Scientific), permeabilized with 0.05% Triton X-100 and blocked in 5% Bovine Serum Albumin (BSA) in PBS. Primary and secondary antibodies were diluted to appropriate concentrations in 2.5% BSA in PBS solution. Alexa-Fluor-568-conjugated phalloidin at 1:100 dilution was added to the secondary antibody mix, together with DAPI at 1:500, to stain filamentous actin and nuclei, respectively. Coverslips were mounted on slides using Fluorsave Reagent (Millipore) and imaged using Nikon Eclipse Ti inverted microscope.

2.3.2 Quantification of podosome formation

THP-1 cells and DCs were immunostained as described above to determine the distribution of actin filaments and vinculin. The percentage of cells with podosomes was quantified in a minimum of three different experiments. Data were obtained analysing 10 fields acquired from at least 2 different coverslips per condition and repeated in at least two different experiments at 60x magnification in Nikon Eclipse Ti inverted microscope. The counting tool in Adobe Photoshop CS6 was used to determine the number of cells with podosomes and the total number of cells per field. The percentage of cells with podosomes was calculated dividing the number of cells presenting at least one podosome by the total number of cells in the field.

2.3.3 Matrix degradation assay

13 mm sterile glass coverslips were coated with fluorescent gelatin according to QCM™ Gelatin Invadopodia Assay (Red) - EMD Millipore protocol. $2x10^5$ THP-1 cells or DCs were seeded on Cy3-gelatin coated coverslips in the presence of 1 ng/ml TGFβ-1 and incubated for 16 hours at either 37°C or 40°C. Coverslips were then stained with FITC-phalloidin and DAPI and mounted as described above. Images were obtained of 10 fields per coverslip chosen at random from at least 3 coverslips per condition at 60x magnification using a Nikon Eclipse Ti inverted microscope. Results were acquired from two different experiments. Photoshop CS6 was used to analyse the images. This method allows to visualize the regions where the cell has degraded matrix to create an area devoid of Cy3 fluorescence. The percentage of cells degrading gelatin was calculated by dividing the number of cells presenting a gelatin degradation area underneath over the total number of cells in the field.

2.3.4 Live cell imaging

Live cell imaging studies were conducted using a Nikon Eclipse Ti inverted microscope. The microscope is supported with an incubation chamber that allows temperature and CO_2 stability. Image acquisition was controlled by NIS Elements Image Software 4.50.

Migration assay. $3x10^4$ cells/ml (1 ml/well) were seeded in 24-well plates previously coated for 1 hour with 10 µg/ml fibronectin (Sigma), in the presence of 1 ng/ml TGFβ-1. Cells were incubated for 16 hours at 37°C. Plates were then inserted in the microscope chamber in which appropriate temperature and 5% CO_2 were maintained. Cells were first filmed at 37°C by taking time-lapse phase contrast photomicrographs every minute for 2 hours at 10x lens magnification. Temperature was then risen to 40°C and cells were allowed to adjust for 30 minutes before starting filming again as described above. Three fields per condition were selected at random for filming. Films were exported as AVI files and analysed using the Manual Tracking plugin in ImageJ-Fiji to determine the velocity and distance travelled by THP-1 cells.

Podosome turnover studies. Podosome turnover studies were performed in WIP KD THP-1 cells expressing eGFP-WIP RES (eGFP WIP RES THP-1 cells). $4x10^4$ cells/ml eGFP WIP RES THP-1 cells were seeded for16 hours in 1 ml RPMI + 10% FCS on 35-mm petri dishes with bottom glass coverslips for cell visualisation, previously coated for 1 hour with 10 µg/ml fibronectin, (Sigma) and in the presence of 1 ng/ml TGFβ-1. The dish was placed in the microscope chamber, in which appropriate temperature and 5% CO_2 were maintained. Cells were first filmed at 37°C by taking time-lapse photomicrographs in the eGFP emission channel every 30 seconds for 30 minutes using a 60x magnification lens. This allows to analyse the distribution of podosome cores over time determined by the localisation of eGFP-WIP in cells.

Temperature was then risen to 40°C and cells were allowed to adjust for 30 minutes before starting filming again as described above. At least 5 cells per condition were filmed per experiment. After careful consideration of the velocity of podosomes formation and disassemble, we decided to select four frames taken every 10 minutes to analyse the turnover of podosomes. Films were exported as AVI files from the NIS Elements Image Software 4.50 and processed with ImageJ-Fiji first to extract images from stacks and then micrographs were processed in Adobe Photoshop CS6. Images were thresholded and then inverted to detect podosomes as a black image on a white background. A grey shade was assigned to the podosomes in each frame by dividing the black value in 4 applying the corresponding opacity value and using the difference function in photoshop. Opacity was calculated as follows: 100 – X in which X is obtained dividing 100 for the total number of frames (4). At this point, images were overlapped using the addition function (add: 100% opacity and invert) to obtain composites containing 4 grey levels. The darkest grey represented more stable podosomes, since it identified pixels present in all the 4 frames, while highest dynamic was identified by lightest greys, corresponding to pixels present in one frame only (Griera *et al.*, 2014). Percentages of pixels corresponding to each grey level were obtained using Adobe Photoshop CS6 and turnover index was calculated as a ratio of light pixels (present in 1 or 2 frames) over dark ones (present in 3 or 4 frames), as previously described (HOLT *et al.*, 2008). Turnover index in directly proportional to podosomes dynamism.

2.4 Gene expression profiling

$5x10^6$ THP-1 or WIP KD THP-1 cells were seeded for 16 hours at either 37°C or 40°C on 10 cm cell culture petri dishes previously coated for 1 hour with 10 µg/ml fibronectin (Sigma) in the presence of 1 ng/ml TGFβ-1. Cells were harvested using cells disassociation media (ThermoFisher Scientific) and mRNA was extracted using mirVana™ miRNA Isolation Kit (ThermoFisher Scientific). Samples, collected in three biological replicates per experimental group (parental THP-1 cells vs WIP KD THP-1 seeded at 37°C and 40°C) were sent to CIC-Biogune, Zamudio (Spain) for total m-RNA sequencing. Details on analysis can be found in the Appendix section 8.2.

2.5 Statistical analysis

GraphPad Prism software was used for the statistical analysis. The test used and the significance for each data set are indicated in the figure legend. Unpaired tests were used since the data were not matched. Non-parametric tests such as Mann Whitney were used to analyse data that failed to follow a Gaussian distribution, while parametric tests such as t-test were used to analyse normally distributed data.

Chapter 3: Role of WIP in myeloid cells migration and invasion in response to mild hyperthermia

3 Role of WIP in myeloid cells migration and invasion in response to mild hyperthermia

3.1 Introduction

Homeostasis is defined as a condition maintained by a biological system when certain variables are kept within acceptable ranges (Buchman, 2002). The human body perceives homeostasis disruption caused by several events, such as infections, allergens or tissue damages, and commonly responds by engaging an inflammatory event (Medzhitov, 2010). Migration of innate immune cells, comprising neutrophils, macrophages and dendritic cells, represents a crucial step in the host defence mechanism. Several studies showed that fever, a cardinal sign of inflammation retained in different organisms, is able to promote innate immunity. For instance, elevated temperature promotes neutrophils activation and recruitment to the site of inflammation (Rice *et al.*, 2005), macrophages secretion of pyrogenic cytokines (Jiang *et al.*, 1999), dendritic cells phagocytosis (Postic *et al.*, 1966) and antigen presenting cells' migration (Ostberg *et al.*, 2001). However, the mechanisms by which mild hyperthermia is able to promote immune cells migration are still poorly understood.

In response to chemokines produced by the inflamed tissue, monocytes are able to extravasate and migrate towards the damaged area (Schenkel, Mamdouh and Muller, 2004; Ingersoll *et al.*, 2011) where they will be activated into their mature phagocytic stage of macrophages (Italiani and Boraschi, 2014). Monocyte motility and adhesion are strictly dependent on F-actin rich structures known as podosomes (Linder *et al.*, 2000; Calle *et al.*, 2006). Podosomes are assembled at the leading edge of some migrating cells including myeloid and cancer cells (Evans *et al.*, 2003). They are comprised of mainly two structures: a core, where proteins involved in actin

polymerization, such as WASP, WIP and the ARP2/3 complex, are located and a surrounding ring, containing integrin associated proteins. In resting cells, the WASP CRIB domain interacts with the VCA domain, inhibiting its actin binding capacity. Downstream of membrane receptor signalling, the Rho-GTPase Cdc42 releases WASP from its autoinhibited conformation, allowing WASP to bind actin monomers and the ARP2/3 complex to start de novo actin filaments (Higgs and Pollard, 1999; Millard, Sharp and Machesky, 2004). WASP stability is strictly dependent on the interaction with WIP (de la Fuente *et al.*, 2007; Chou *et al.*, 2006). Following WIP tyrosine phosphorylation, WASP is released and degraded by calpains and the proteasome (Vijayakumar *et al.*, 2015). In addition to this, WIP presents a myriad of other activities, including binding and stabilizing actin filaments (Martinez-Quiles *et al.*, 2001), mediating metalloproteinase matrix degradation by interacting with cortactin (Bañón-Rodríguez *et al.*, 2011) and contributing to the proper localisation of WASP in the area of actin assembly (Chou *et al.*, 2006; Tsuboi, 2006). Seen all these functions, it is not surprising that 80% of mutation in patients with symptomatic Wiskott Aldrich syndrome resides in the WIP binding domain of WASP (Volkman *et al.*, 2002).

3.2 Hypothesis and aims

Considering this information, we hypothesised that WIP and WASP might work as a functional unit in delivering changes in the actin cytoskeleton, membrane organisation and adhesion dynamics in response to extracellular factors such as the exposure to mild hyperthermia during inflammation. In this chapter we aim to:

- investigate the effect of mild hyperthermia on monocytic cells migration and invasion;
- investigate whether, in response to hyperthermia, WIP is involved in regulating monocytes motile and invasive behaviour by modulating changes in integrin and actin organisation;
- investigate whether the WIP-dependant changes in actin dynamics are involved in the enhancement of the immune response during mild hyperthermia (a local increase of temperature at inflammation sites or during a febrile event).

3.3 Materials and methods

3.3.1 Generation of THP-1-derived mutant cell lines using lentiviral particles

WIP KD THP-1 cells were generated by infection with WIP shRNA lentiviral particles (NM_003387.3-266s1c1 #266 shRNA lentiviral vector, Sigma) at a Multiplicity of Infection (MOI) 5 for two consecutive days. After 48 hours, the medium was replaced with RPMI 10% FCS + 1 µg/ml puromycin for cells selection. Efficiency of transduction was evaluated by detection of WIP by Western Blot.

eGFP-WIP recovered THP-1 cells (RES) and non-target shRNA THP-1 cells (NT) were generated with lentiviral particles produced in our lab using respectively the eGFP-WIP RES transfer vector, previously generated in collaboration with Professor Gareth Jones (Vijayakumar *et al.*, 2015), and the MISSION® pLKO.1-puro Non-Mammalian shRNA Control Plasmid DNA (Sigma Aldrich, UK). Lentiviral particles were produced in 6 wells plates in HEK 293T cells by co-transfecting 1.5 µg interest vector with 1.1 µg pCMV^R8.91 (packaging plasmid) and 0.4 µg pMD.G (envelope plasmid). The three plasmids were mixed in 150 mM NaCl to a final volume of 100 µl and diluted in equal volume of 150 mM NaCl containing 6 µl Jet-PEI (Polyplus). After 30 minutes incubation at room temperature, the Jet-PEI/DNA mix was added to the cells. The following day, the mix was replaced with fresh media and the supernatant harvested after 24h. The supernatant was filtered through a 0.45 µm-pore-size filter and stored at -80°C until transduction. $2x10^5$ THP-1 cells were transduced by suspension in 500 µl of lentiviral supernatant. A second cycle of transfection was performed at 24 h. At 48 hours from the second transfection cycle, cells were transferred to fresh culture medium containing 1 µg/ml puromycin (NT THP-1) or

were eGFP sorted for selection (eGFP WIP RES THP-1) using BD FACSDiva at the Biomedical Research Center at Guy's campus, King's College London.

Table 3.1. List of cells used in this study

Cell lines	Description	Source
THP-1	Human acute monocytic leukemia cell lines	ATCC
WIP KD THP-1	WIP knocked down cell lines derived from THP-1 cells (produced using NM_003387.3-266s1c1 (#266) shRNA lentiviral vector, Sigma)	This study
eGFP WIP RES THP-1	WIP recovered cell lines derived from WIP KD THP-1 cells, carrying eGFP-WIP RES plasmid (Professor Gareth Jones)	This study
Non target shRNA THP-1	THP-1 cells carrying the MISSION® pLKO.1-puro Non-Mammalian shRNA Control Plasmid DNA	This study
Wild type dendritic cells	Primary mouse spleen cells	Dr Ines Anton
WIP KO dendritic cells	Primary WIP KO mouse spleen cells	Dr Ines Anton

3.4 Results

3.4.1 Validation of THP-1 and WIP KD THP-1 cells to study the effect of mild hyperthermia (40°C) on myeloid cell migration

In order to study the possible role of WIP in controlling myeloid cells response to mild hyperthermia, we used THP-1 cells as a model for myeloid cell migration and generated WIP KD THP-1 and NT shRNA cells using lentiviral vectors. WIP protein knock down was successfully achieved as demonstrated by western blot showing that WIP expression is null in the WIP KD THP-1 cells (Figure 3.1). We also demonstrated that expression of WHICH/WIRE, a verprolin family of proteins sharing 30% of its structure with WIP (Aspenström, 2002; Aspenströ, 2005) and able to induce actin filaments formation in a WASP-independent way (Aspenström, 2004), was not affected in WIP KD cells (Figure 3.1), while WIP KD THP-1 cells failed to express significant protein levels of WASP, as previously described (Chou *et al.*, 2006).

Taken together, our results demonstrate that WHICH-WIRE expression is not influenced by WIP levels and that, although WHICH-WIRE can bind WASP (Aspenström, 2002, 2004), it is not able to sustain WASP levels in the absence of WIP (Figure 3.1).

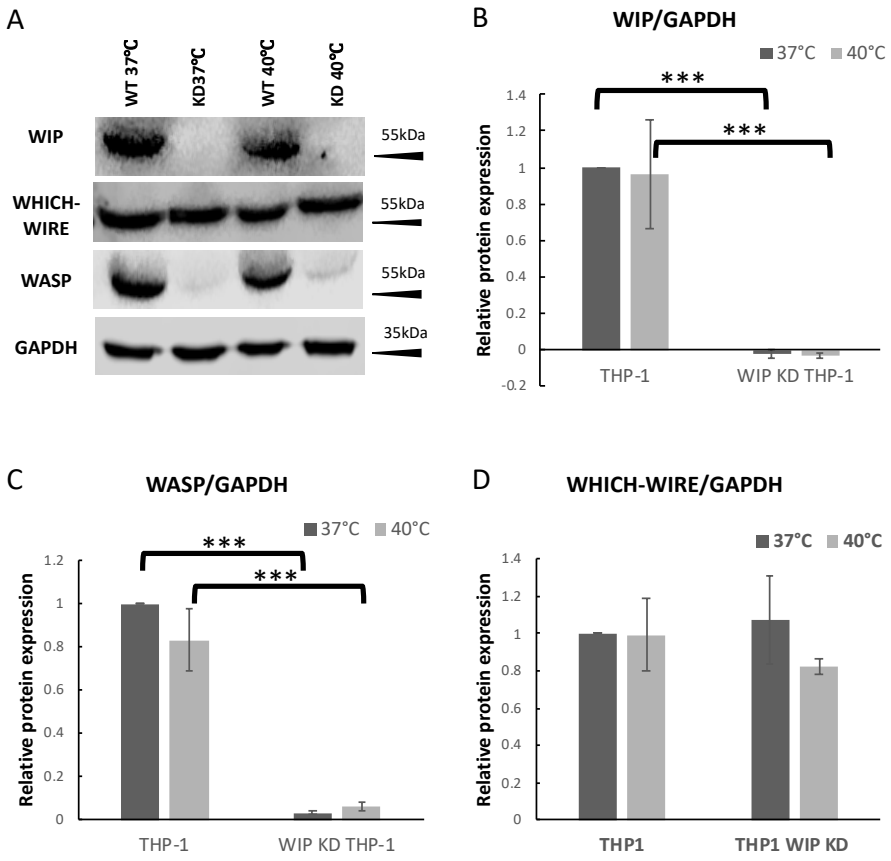

Figure 3.1. Actin related protein expression in THP-1 (WT) and THP-1 WIP KD cells (KD) exposed to febrile temperature.

(A) Representative Immunoblot showing levels of WIP, WASP and WHICH/WIRE in THP-1 and WIP KD THP-1 cells cultured at 37°C or 40°C. GAPDH was used as a loading control. (B, C, D) Quantitative analysis of WIP, WASP and WHICH-WIRE levels, respectively. Bar graphs show average and SE of each protein relative expression to GAPDH and are representative of three biological replicates. Relative protein expression is normalized for GAPDH expression. Unpaired t test was applied (****P<0.001).* Arrows on blots indicate protein ladder closest band (10 to 250 kDa, ThermoFisher Scientific).

Viability of THP-1 and WIP KD THP-1 cells after 16 hours exposure to hyperthermia was tested through Annexin V and Propidium Iodide staining. The percentage of viable and apoptotic cells was determined by flow cytometry. Since both cell lines showed viability of around 90% when exposed to 40°C for 16 hours (Figure 3.2), we can conclude that 16 hours incubation to fever-like temperatures does not impact on the viability of parental or WIP KD THP-1 cells, therefore our experimental hyperthermia approach is valid for further studies.

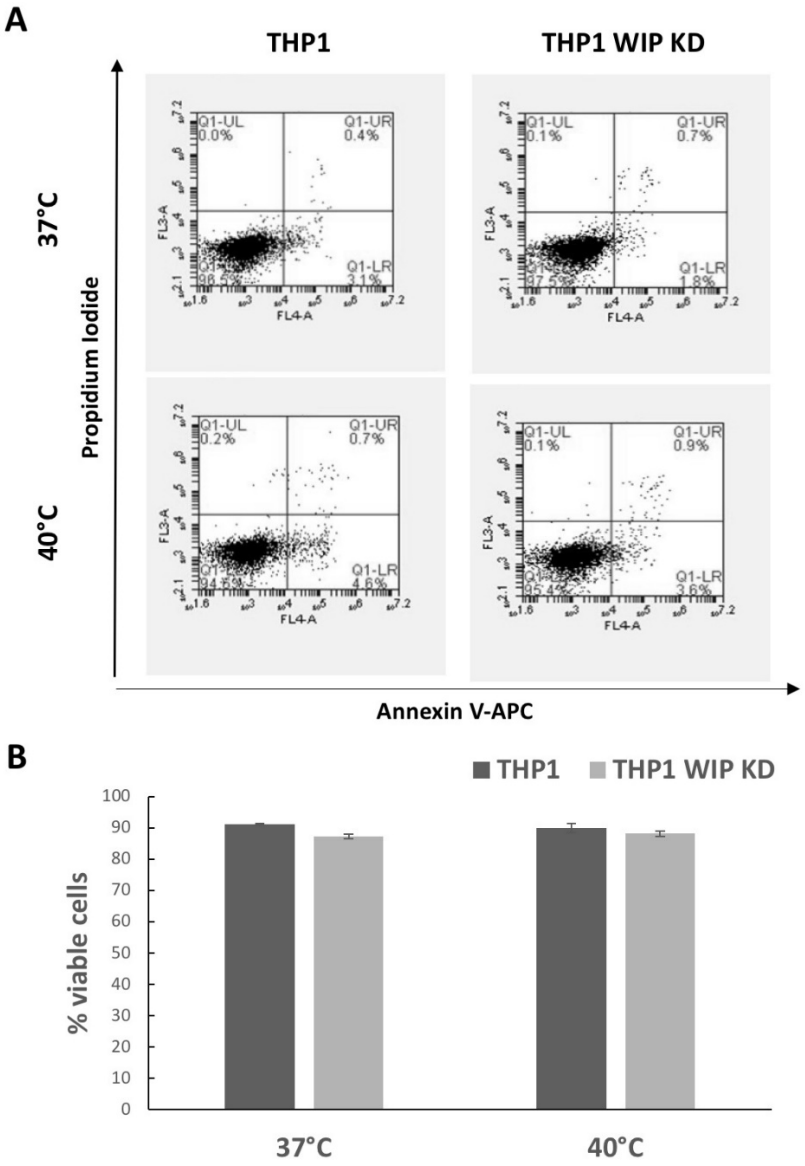

Figure 3.2. Analysis of cell viability of THP-1 and WIP KD THP-1 cells incubated at febrile temperatures (40 °C).

(A) Flow cytometry histograms show the percentage of apoptotic (Annexin V-APC positive) and necrotic (Propidium Iodide positive, Annexin V negative) cells in THP-1 and WIP KD THP-1 cells cultured at 37 °C and 40°C for 16 hours; (B) Histograms showing the average and SE of the percentage of viable (Annexin V and PI negative populations) cells in cultures of THP-1 and THP-1 WIP KD cells incubated at 37 °C and 40°C for 16 hours. Both parental and WIP KD THP-1 cells showed viability of approximately 90% in the cultures cultured at 37 °C and 40°C for 16 hours.

3.4.2 WIP is required for the increased assembly of podosomes in THP-1 and dendritic cells in response to mild hyperthermia (40 °C)

We then investigated the impact of mild hyperthermia on podosome formation in THP-1 cells. At first, the efficiency of THP-1 cells to form podosomes in the presence or absence of TGFβ-1 was studied by analysing podosome formation through immunofluorescence staining of F-actin filaments. TGFβ-1 is a cytokine that has previously been shown to induce differentiation of THP-1 cells towards a macrophage phenotype, including increased formation of podosomes (Monypenny *et al.*, 2011). We observed that podosomes formation in WIP KD THP-1 cells was not influenced by the presence of TGFβ-1, while a significantly higher percentage of parental cells assembled podosomes in the presence of the growth factor (Figure 3.3, 3.4A). Furthermore, although the total number of parental cells per field following incubation with TGFβ-1 suggested a tendency for an increase in the adhesive capability of cells, no statistical significance was found (Figure 3.4B).

Culture of THP-1 cells at 40°C, mimicking mild hyperthermia during inflammation, induced a significant increase in the percentage of cells with podosomes (Figure 3.4A). Additionally, at 40°C podosomes were more robust and numerous (Figure 3.3) with more defined vinculin rings (Figure 3.5). Lack of WIP in WIP KD THP-1 cells, as expected, resulted in loss of podosomes as previously described (Chou *et al.*, 2006) (Figure 3.3, 3.4A) and exposure to 40°C failed to trigger podosome formation (Figure 3.3, 3.4A).

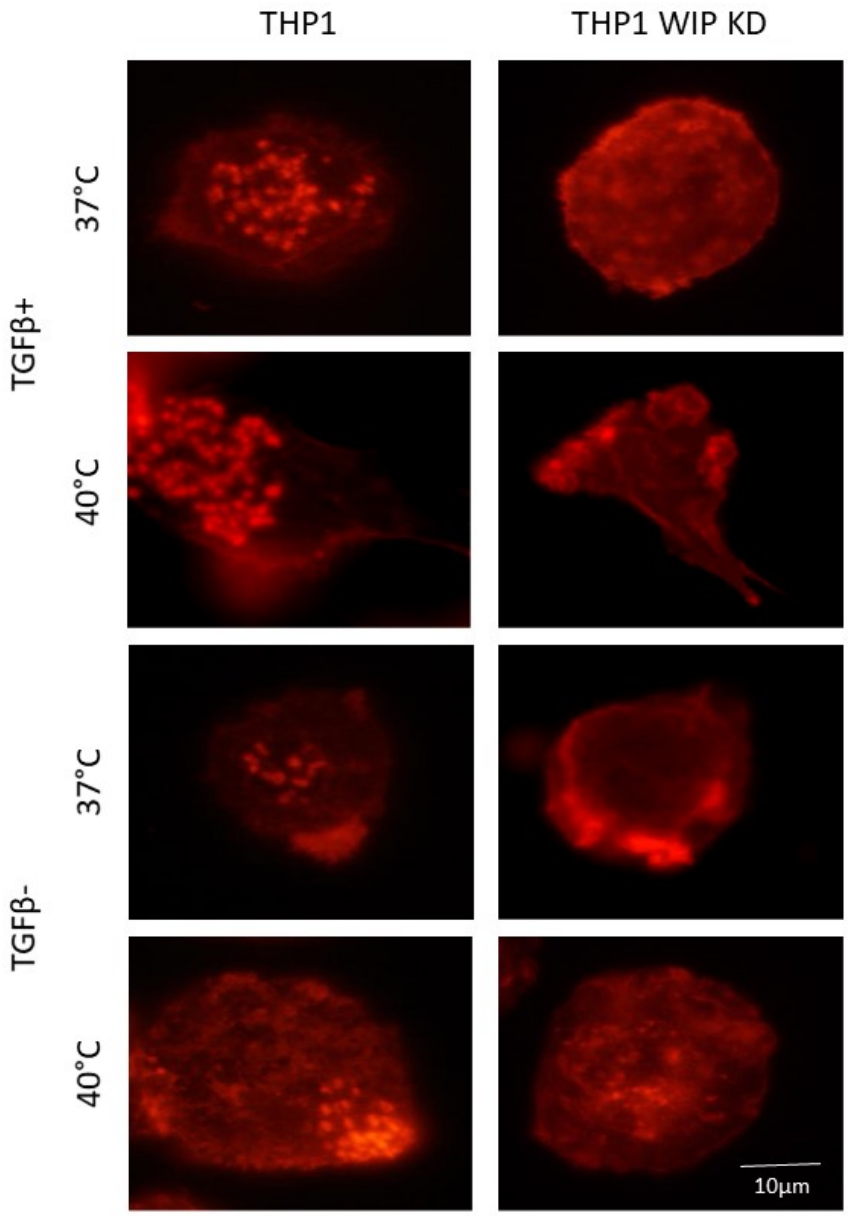

Figure 3.3. Representative Immunofluorescence of parental and WIP KD THP-1 cells stained with red Phalloidin to detect the distribution of F-actin.

THP-1 and WIP KD THP-1 cells were cultured for 16 hours at 37°C and 40°C on fibronectin coated coverslips with or without 1ng/ml TGFβ-1 and stained with Alexa 568nm-labelled phalloidin. Images show filamentous actin distribution in one representative cell for each condition. Podosomes are absent in WIP KD THP-1 cells and rise of temperature increases number of cells with podosomes. Incubation with TGFβ-1 induced podosome formation in THP-1 cells (Bar 10 µm).

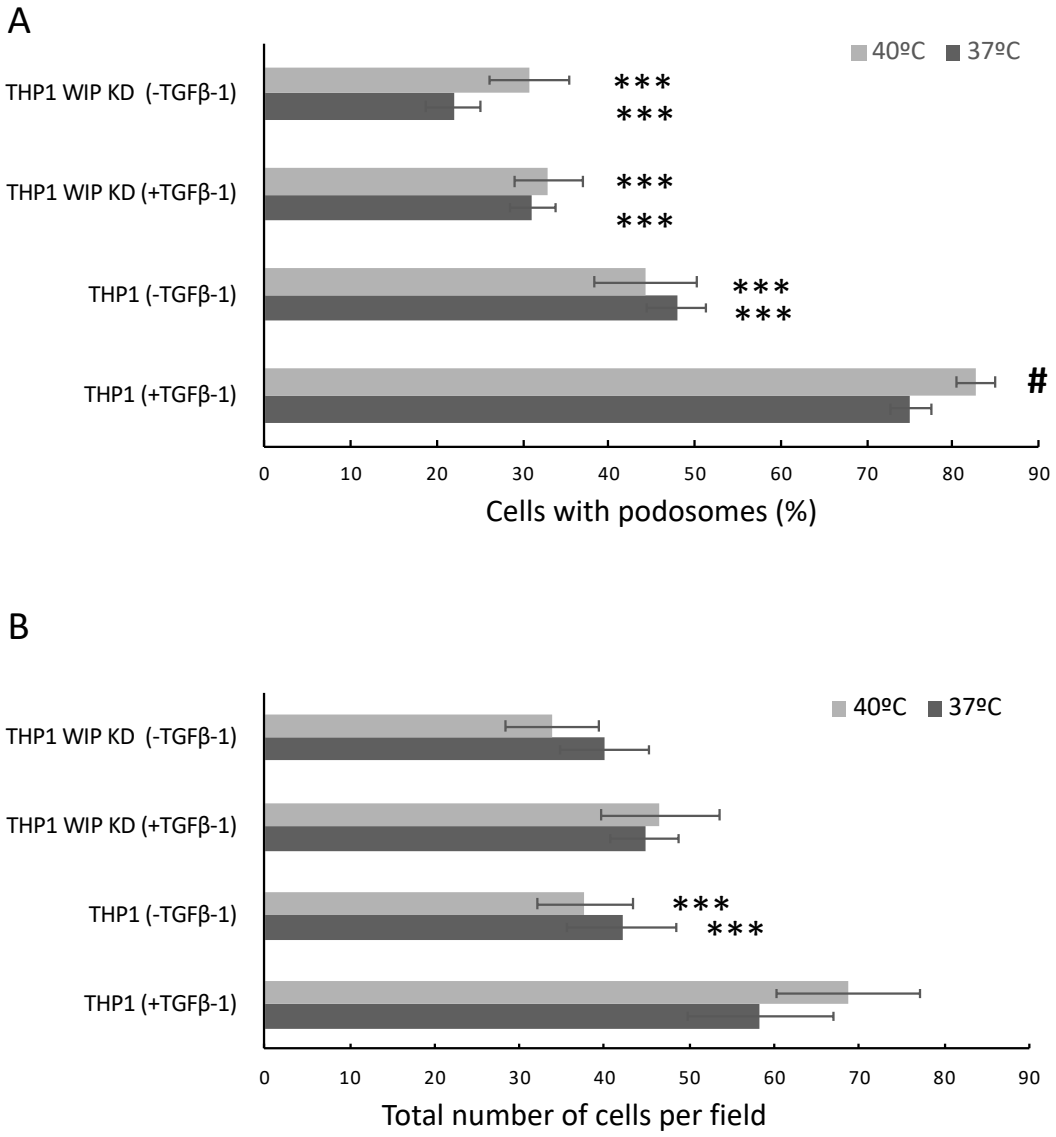

Figure 3.4. Quantitative analysis of number of cells with podosomes and total number of cells per field.

Bar graphs (A) show the average and SE of number of cells with podosomes in THP-1 and WIP KD THP-1 cultured for 16 hours at 37°C and 40°C on fibronectin coated coverslips with and without 1ng/ml TGFβ-1. Data were obtained analysing 10 fields, acquired from at least 3 biological replicates at 40x magnification. # is used to compare differences between 37°C and 40°C, while * indicates differences compared to THP-1 +TGFβ-1, respectively at 37°C and 40°C (Unpaired two tail t test was applied; #P<0.05;***P<0.001); (B) Bar graphs are indicative of the total number of cells observed per field in all the above described conditions. No significant differences were found.

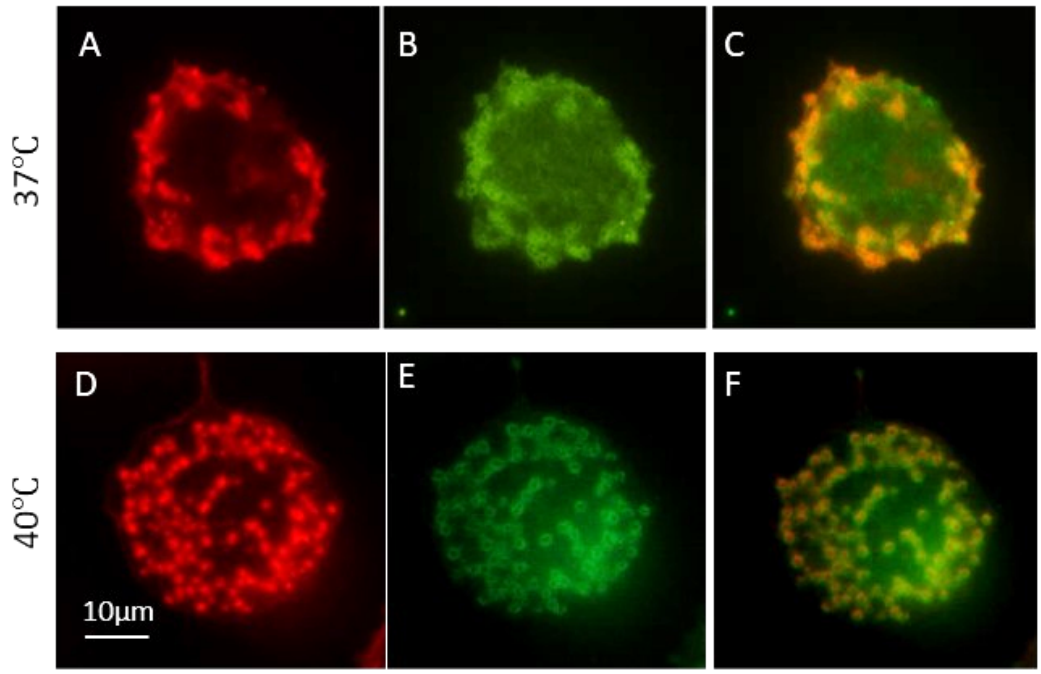

Figure 3.5. Representative images of vinculin rings in THP-1 cells cultured at 37°C and 40°C.

THP-1cells were cultured for 16 hours with 1ng/ml TGFβ-1 at 37°C (A-C) or 40°C (D-F) on fibronectin coated coverslips. Micrographs show the distribution of F-actin in podosome cores in red (A, D) and of vinculin in the podosome rings in green (B, E). Merged images are shown in C and F (Bar 10 µm).

A similar response to heat was observed in primary dendritic cells cultured on poly-L-lysine (PL) or fibronectin (FN) coated surfaces and exposed to mild hyperthermia for 30 minutes, 1 hour or for 16 hours. A short exposure to mild hyperthermia (30 minutes) was sufficient for enhancing podosome assembly in wild type dendritic cells in a comparable way to what was observed after 16 hours incubation (Figure 3.6).

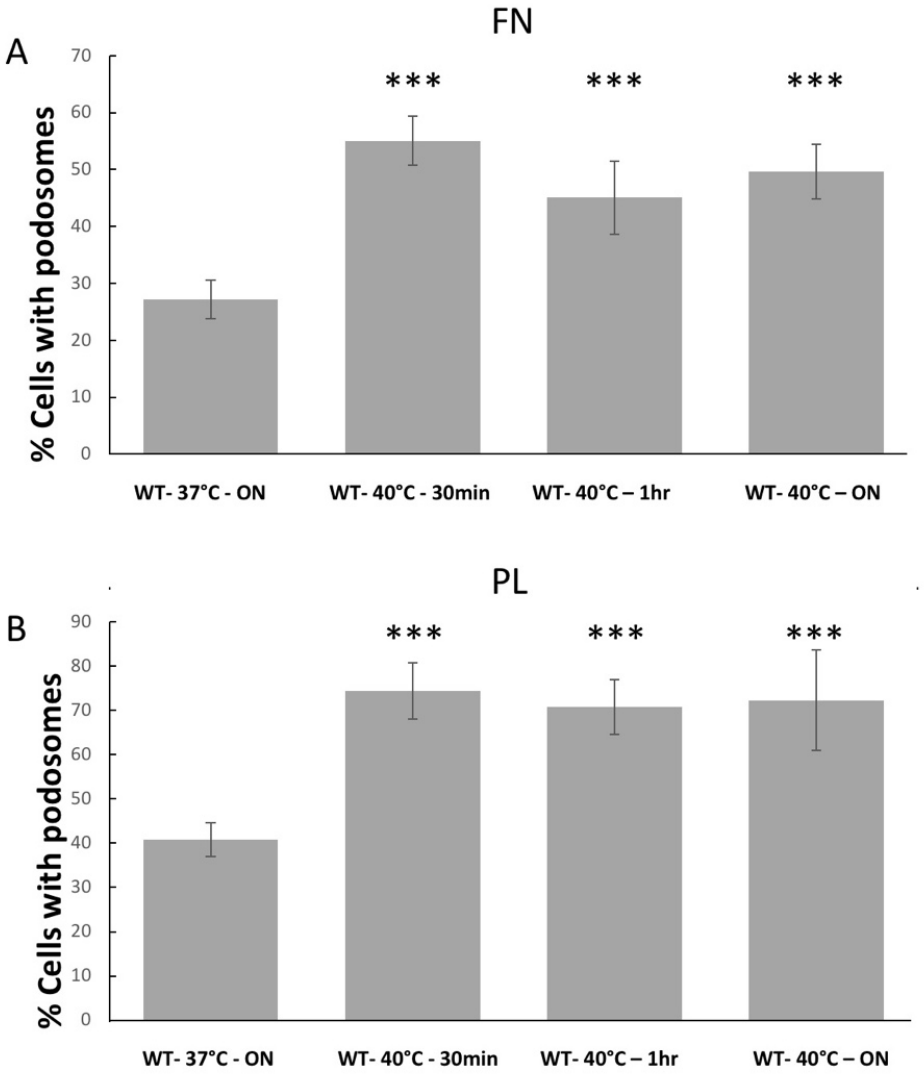

Figure 3.6. Quantitative analysis of number of dendritic cells with podosomes at 37°C and 40°C.

Bar graphs show the average and SE of percentage of wild type (WT) dendritic cells with podosomes when cultured for 16 hours at 37°C or following exposure to mild hyperthermia for 30 minutes, 1 hour or 16 hours on (A) fibronectin (10ug/ml) or (B) poly-L-lysine coated coverslips. 10 fields were acquired for at least 3 coverslips per condition at 60x magnification. Graphs are representative of similar results obtained in two different experiments. On both fibronectin and poly-lysine, increment in temperature is proportional to increment in number of cells producing podosomes, in the three different time frames. * indicates differences compared to WT DCs cultured at 37°C (Unpaired two tail t test was applied. ***P<0.001*)*.

3.4.3 Expression of eGFP WIP RES in WIP KD THP-1 cells recovered the normal parental THP-1 phenotype

In order to further support the role of WIP in migratory and cytoskeletal changes in THP-1 cells in response to febrile temperatures, we generated THP-1 cells that recovered WIP expression by infecting WIP KD THP-1 cells with a lentiviral vector carrying a GFP-fusion WIP sequence with a silent mutation. This mutation prevents targeting by the WIP-shRNA sequence introduced to generate these cells (eGFP-WIP-RES) (Vijayakumar *et al.*, 2015). The selection of cells based on the expression of the eGFP-WIP recovered phenotype was obtained by FACS sorting. FACS sorted cells were 98.7% eGFP positive cells after sorting (Figure 3.7).

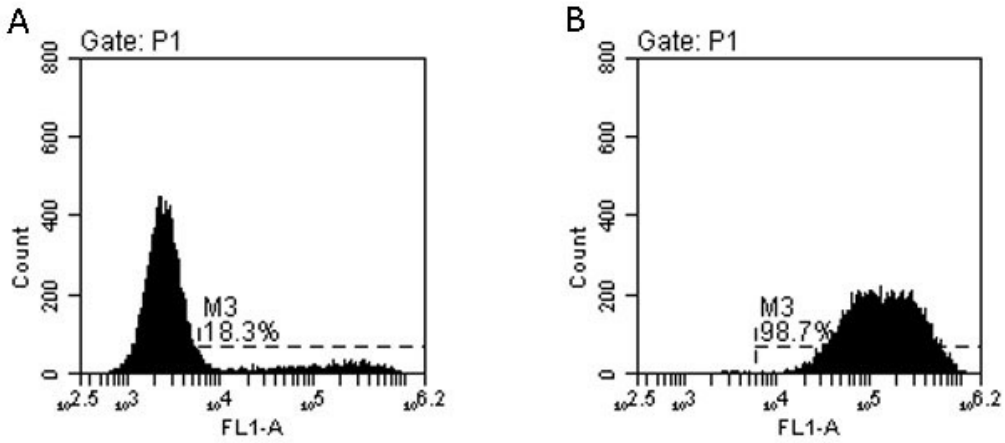

Figure 3.7. Percentages of eGFP positive THP-1 WIP RES cells before and after FACS sorting.

WIP KD THP-1 cells were infected with an eGFP-WIP lentiviral construct carrying a silent mutation in the WIP protein sequence (Vijayakumar *et al.*, 2015). This alternative eGFP-WIP coding sequence is translated into the same WIP amino acids but avoids recognition by the WIP shRNA used to generate WIP KD THP-1 cells. (A) Flow cytometer histogram showing the number of cells expressing eGFP-WIP-RES. After the initial transduction less than 20% of cells were eGFP positive. (B) FACS sorting allowed to select transduced cells that resulted to be almost 100% eGFP-WIP RES positive.

The expression of eGFP-WIP-RES restored the protein concentration of WIP and WASP to wild type levels (Figure 3.8). No significant differences in WIP, WASP or ARP 2/3 proteins concentration were found when THP-1, NT THP-1 cells and eGFP-WIP RES THP-1 cells were compared (Figure 3.8).

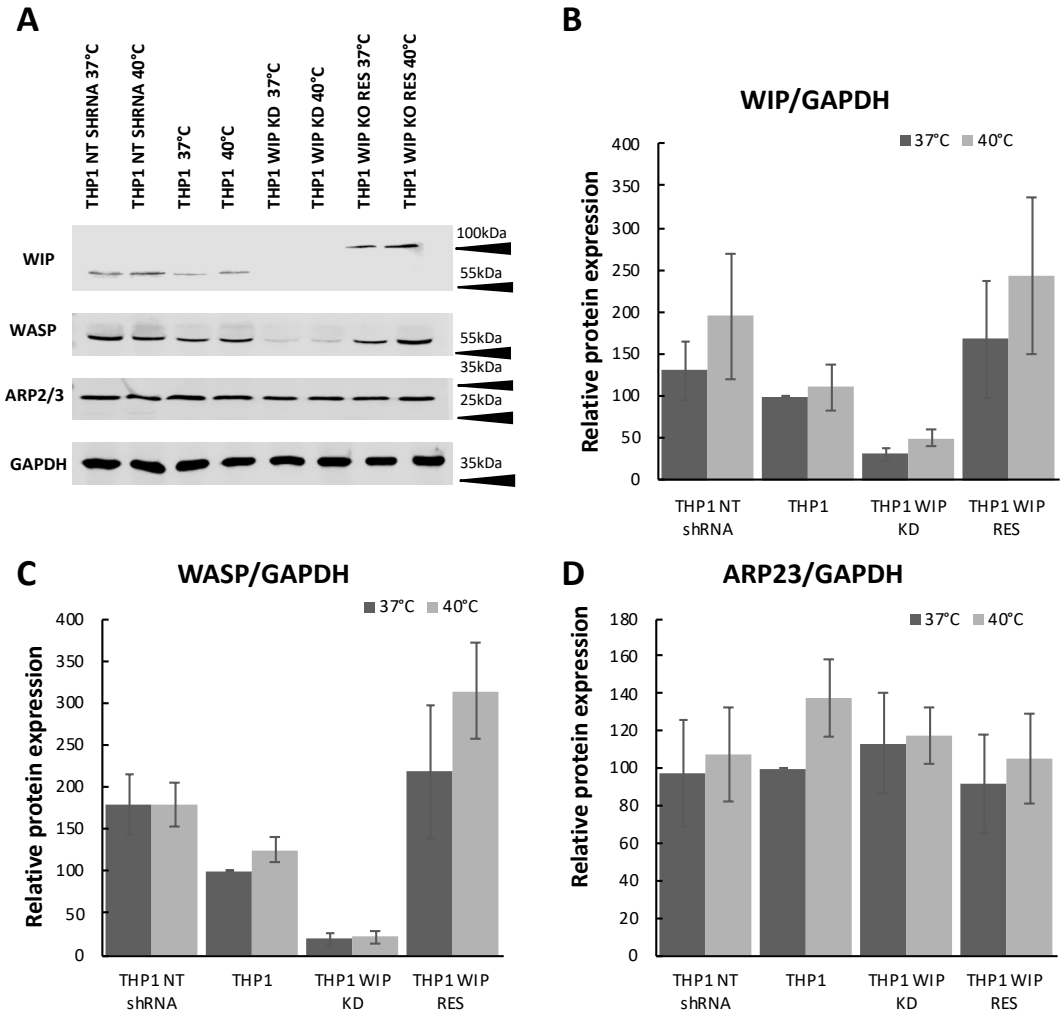

Figure 3.8. Expression of eGFP-WIP in WIP KD THP-1 cells restores WIP and WASP to equivalent levels as in parental cells.

Detection of actin related proteins level in THP-1, WIP KD THP-1, THP-1 non-target shRNA and THP-1 WIP RES cells exposed to mild hyperthermia (40°C). (A) Representative immunoblot of WIP, WASP and ARP2/3 proteins expression in THP-1 cells cultured at 37°C and 40°C. (B-C-D) Bar graphs show average and SE of each protein relative expression and are representative of three biological replicates. Relative protein expression is normalized for GAPDH. Arrows on blots indicate protein ladder closest band (10 to 250 kDa, ThermoFisher Scientific).

Immunofluorescence studies were also performed to confirm the restoration of WIP activity in terms of podosome formation. As expected, eGFP-WIP co-localised with F-actin in the core of podosomes (Figure 3.9). 60% of eGFP-WIP RES THP-1 cells were able to assemble organized podosomes as seen in the parental THP-1 cells.

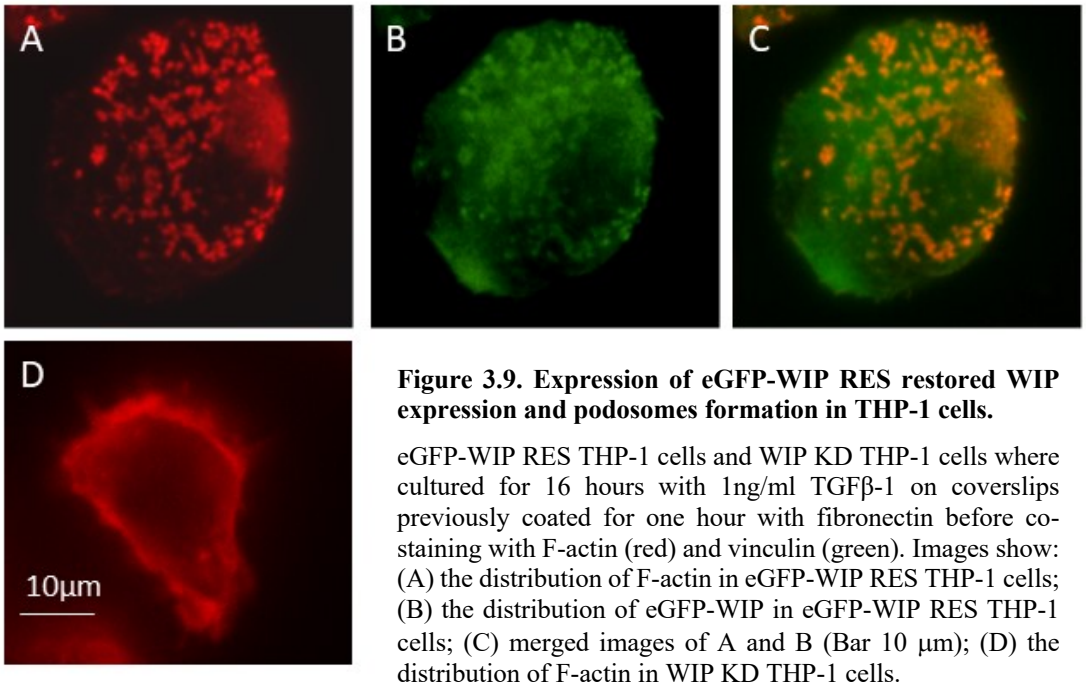

Figure 3.9. Expression of eGFP-WIP RES restored WIP expression and podosomes formation in THP-1 cells.

eGFP-WIP RES THP-1 cells and WIP KD THP-1 cells where cultured for 16 hours with 1ng/ml TGFβ-1 on coverslips previously coated for one hour with fibronectin before co-staining with F-actin (red) and vinculin (green). Images show: (A) the distribution of F-actin in eGFP-WIP RES THP-1 cells; (B) the distribution of eGFP-WIP in eGFP-WIP RES THP-1 cells; (C) merged images of A and B (Bar 10 µm); (D) the distribution of F-actin in WIP KD THP-1 cells.

3.4.4 Protein and gene expression in WIP deficient cells

In order to identify a possible target that plays a role in monocytic cells increased podosomes formation in response to mild hyperthermia, protein expression and activation signalling downstream of integrins was characterised in the generated WIP KD THP-1 cells and in WIP KO dendritic cells. In particular, the phosphorylation of extracellular signal-regulated kinases (ERKs), whose activity is essential for cell adhesion and migration through regulation of integrin signalling, was studied (Klemke *et al.*, 1997; Sawhney *et al.*, 2006). Interestingly, we found that the phosphorylation of both ERK isoforms (ERK1 and ERK2) was significantly increased in response to

16 hours exposure to mild hyperthermia in all the cell lines actively expressing WIP. No statistically significant increase in ERK phosphorylation was observed in WIP KD cells at 40°C. Interestingly, phosphorylation levels were significantly higher at 37°C in WIP KD cells compared to parental cells (Figure 3.10). Furthermore, a similar trend was seen in the expression of the Heat Shock protein 90 (HSP90). At 37°C both WIP KD THP-1 cells (Figure 3.10 A) and WIP KO dendritic cells (Figure 3.11) expressed significantly higher levels of HSP90 compared to parental cells. HSP90 protein levels were significantly enhanced by mild hyperthermia in cells expressing WIP while in WIP KD THP-1 cells HSP90 levels were not altered by this increase in temperature.

No significant reproducible differences in the expression of ARP2/3 (Figure 3.8), vinculin or ILK (Figure 3.10) were found between parental and WIP depleted cells in THP-1 cells or DCs (Figure 3.10-3.11).

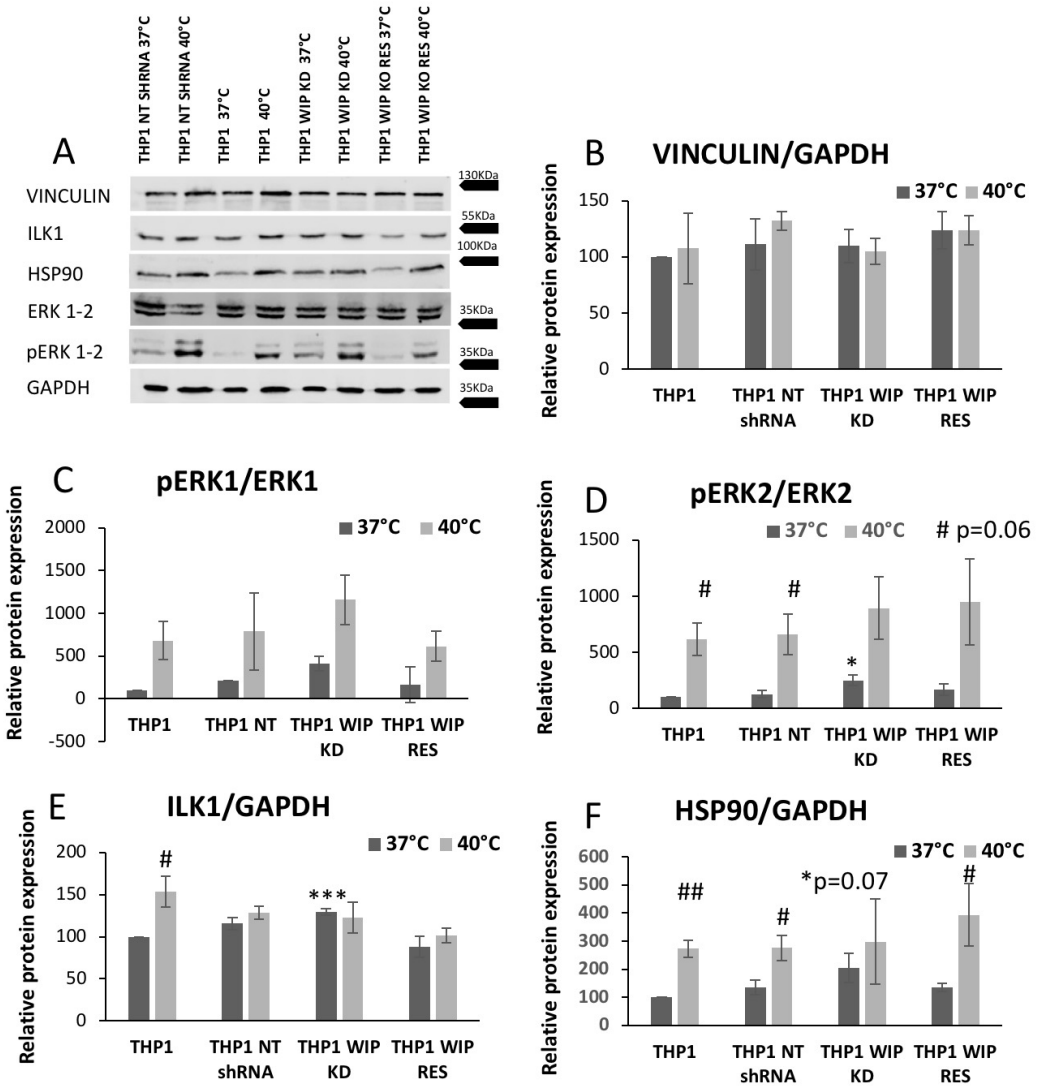

Figure 3.10. Analysis of protein expression in THP-1 WIP mutants.

Representative blots of total cell lysates of THP-1, WIP KD THP-1, THP-1 NT shRNA and THP-1 eGFP-WIP RES mutants after 16 hours incubation on fibronectin coated dishes in the presence of 1ng/ml TGFβ-1 at 37 °C and 40°C. GAPDH was used as loading control. (A) Representative Immunoblot of Vinculin, ILK1, HSP90, ERK and pERK proteins expression in THP-1 cells cultured at 37°C and 40°C. (B-C-D-E-F) Bar graphs show average and SE of each protein relative expression and are representative of three biological replicates. Relative protein expression is normalized for GAPDH. #, t-student test vs control group at 37°C (#$P<0.05$); * t-student test vs corresponding parental THP-1 cells at 37°C or 40°C (*$P<0.05$). Arrows on blots indicate protein ladder closest band (10 to 250 kDa, ThermoFisher Scientific).

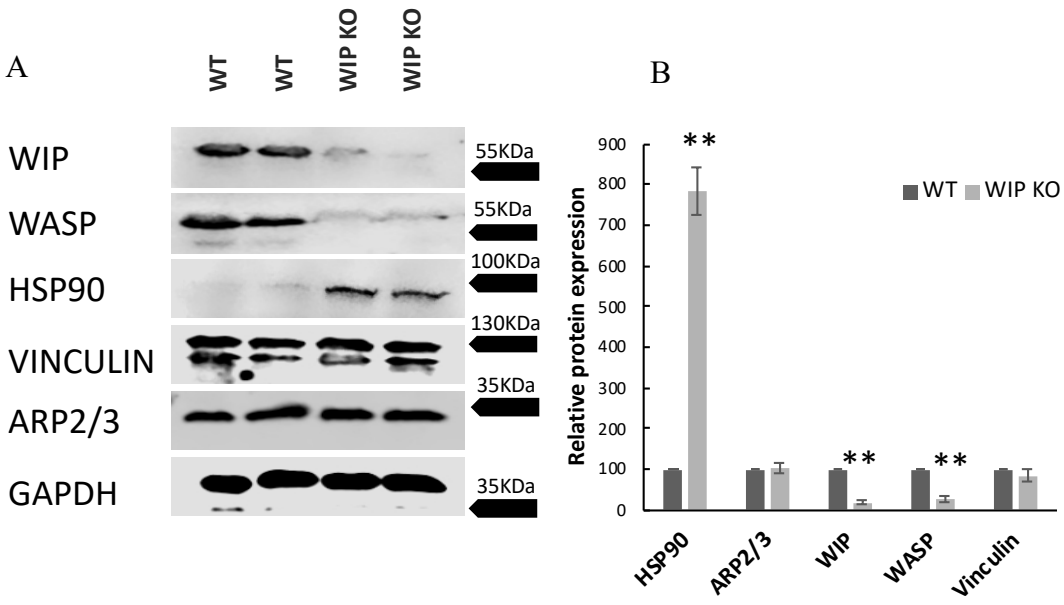

Figure 3.11. Analysis of protein expression in WT and WIP KO dendritic cells.

(A) Representative blots of total cell lysates of WT and WIP KO DCs (two mice per condition) after 16 hours incubation on fibronectin coated dishes in the presence of 1ng/ml TGFβ-1 at 37 °C. GAPDH was used as loading control. (B) Bar graph shows average and SE of each protein relative expression and are representative of two biological replicates. Relative protein expression is normalized for GAPDH. * t-student test vs corresponding WT cells (**P<0.001). Arrows on blots indicate protein ladder closest band (10 to 250 kDa, ThermoFisher Scientific).

HSP90 gene expression was also affected, corresponding to the changes of protein levels detected by western blot. We demonstrated by mRNA sequencing that both HSP90 isoforms (HSP90AA1 and HSP90AB1) were twice more abundant in WIP KD cells and HSP90AA1 expression was significantly increased in response to mild hyperthermia (Figure 3.12). Additionally, we found an upregulation in the expression of genes coding for IL-1β and CCL2 (MCP-1) in WIP KD THP-1 cells (Table 3.2), as observed in the excessive inflammatory phenotype of WAS patients (Lee *et al.*, 2017).

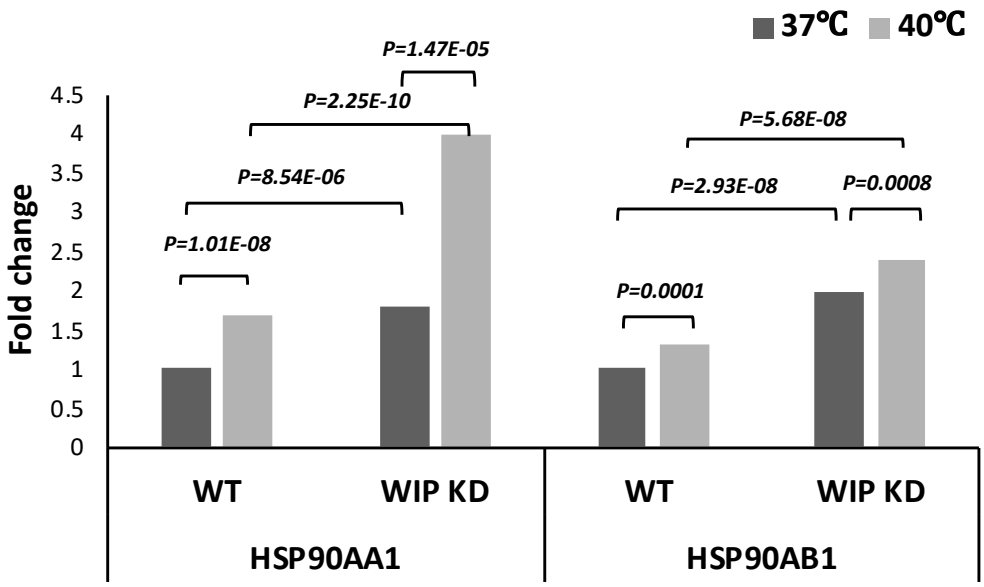

Figure 3.12. HSP90 gene expression in parental and WIP KD THP-1 cells exposed to hyperthermia.

Histograms show fold increase of HSP90 isoforms (HSP90AA1 and HSP90AB1) expression in WIP KD THP-1 cells and parental cells exposed to 37℃ or mild hyperthermia (40℃) relative to parental THP-1 cells at 37 ℃, as determined by mRNAseq. Data were obtained through mRNA sequencing and are representative of three biological replicates.

	THP-1 vs WIP KD THP-1 (37°C)				
Gene	**Fold Change**	**Regulation**	**P-Value**	**mean_WT**	**mean_KD**
CCL2	-5.1877	D	5.19E-09	6.90126	9.27634
IL1β	-2.8735	D	8.82E-09	6.31787	7.84067
	THP-1 (37°C) vs THP-1 (40°C)				
Gene	**Fold Change**	**Regulation**	**P-Value**	**mean_37°C**	**mean_40°C**
CCL2	1.0401	-	0.611386	6.90126	6.84459
IL1β	-1.0714	-	0.239958	6.31787	6.41738
	THP-1 vs WIP KD THP-1 (40°C)				
Gene	**Fold Change**	**Regulation**	**P-Value**	**mean_WT**	**mean_KD**
CCL2	-9.0463	D	1.22E-11	6.84459	10.02192
IL1β	-2.8687	D	1.62E-09	6.41738	7.93777
	WIP KD THP-1 (37°C) vs WIP KD THP-1 (40°C)				
Gene	**Fold Change**	**Regulation**	**P-Value**	**mean_37°C**	**mean_40°C**
CCL2	-1.6767	D	0.00098409	9.27634	10.02192
IL1β	-1.0696	-	0.359449	7.84067	7.93777

Table 3.2. CCL2 and IL-1β genes expression in THP-1 and WIP KD THP-1 cells at 37°C and 40°C.

Data were obtained through mRNA sequencing. The first column shows the name of the genes of interest identified, followed by the fold change value and regulation results, where D, U and – represents a downregulation, upregulation or no differential regulation, respectively. The fourth column represents the p-value obtained comparing three biological replicates in each group and the fifth and sixth columns specify the mean expression value in the population indicated. Each sub-table compares different groups. From top to bottom: WT vs KD at 37°C, WT at 37°C vs WT at 40°C, WT vs KD at 40°C, WIP KD at 37°C vs WIP KD at 40°C.

3.4.5 Nuclear localization of WASP and ARP2/3

We have demonstrated in the previous sections that hyperthermia can induce the expression of genes such as HSP90 and that this event is dependent on the expression of WIP. Previous data suggest a possible role of WIP in regulating gene expression in other myeloid cells such as DCs where WIP is involved in the formation of protein complexes containing the histone H2A.Z. This suggests a possible role of WIP in the formation of nuclear protein complexes involved in DNA packaging and regulation (Calle Y, unpublished data). Additionally, histone H2A.Z allows for detection of changes in environmental temperature in plants, which reinforces the hypothesis of a

possible role of WIP in regulating the response to changes in temperature. With the next set of experiments, we aimed to investigate the possible nuclear localization of WIP or proteins in its interactive network such as WASP or the Arp2/3 complex in response to mild hyperthermia as possible mechanisms of signal transduction to the nucleus mediated by WIP. This would suggest a direct role of these proteins in the nucleus in the detection of increased temperature during the inflammatory response. Unfortunately, WIP nuclear levels detected in our experiments were minimal and there are no available antibodies allowing for a good identification of the protein. Therefore, we focused our studies in investigating whether the nuclear shuttling of some actin related proteins in the WIP network was affected by mild hyperthermia or by perturbation in actin polymerization in parental and WIP KD cells. Parental and WIP KD THP-1 cells were biochemically separated into nuclear and cytosolic fractions following 16 hours exposure to hyperthermia or following incubation with inhibitors of actin polymerization such as Cytochalasin D and Wiskostatin. Cytochalasin D is a potent mycotoxin able to bind F-actin and prevent polymerization of actin monomers (May *et al.*, 1998), while Wiskostatin stabilizes the WASP autoinhibited conformation (Guerriero and Weisz, 2007). We found that the Arp2/3 complex significantly increased shuttling towards the cell nuclear fraction when actin polymerization is impaired, suggesting that WASP mediated actin polymerization promotes the localisation of the Arp2/3 complex in the cytoplasm. Similar levels of the Arp2/3 complex were observed in the nuclear fractions of parental and WIP KD cells at 37°C. However, in response to hyperthermia, Arp2/3 increased its nuclear localization in parental but not in the WIP KD cells. Taken together, our results indicate that WIP regulates the increased nuclear localisation of the Arp2/3 complex in response to mild hyperthermia. Data suggest that WASP might be affected in a similar way as the

ARP2/3 complex when actin polymerization is impaired using Cytochalasin D, however, no significant difference was observed. Furthermore, WASP nuclear levels were not affected by exposure to mild hyperthermia.

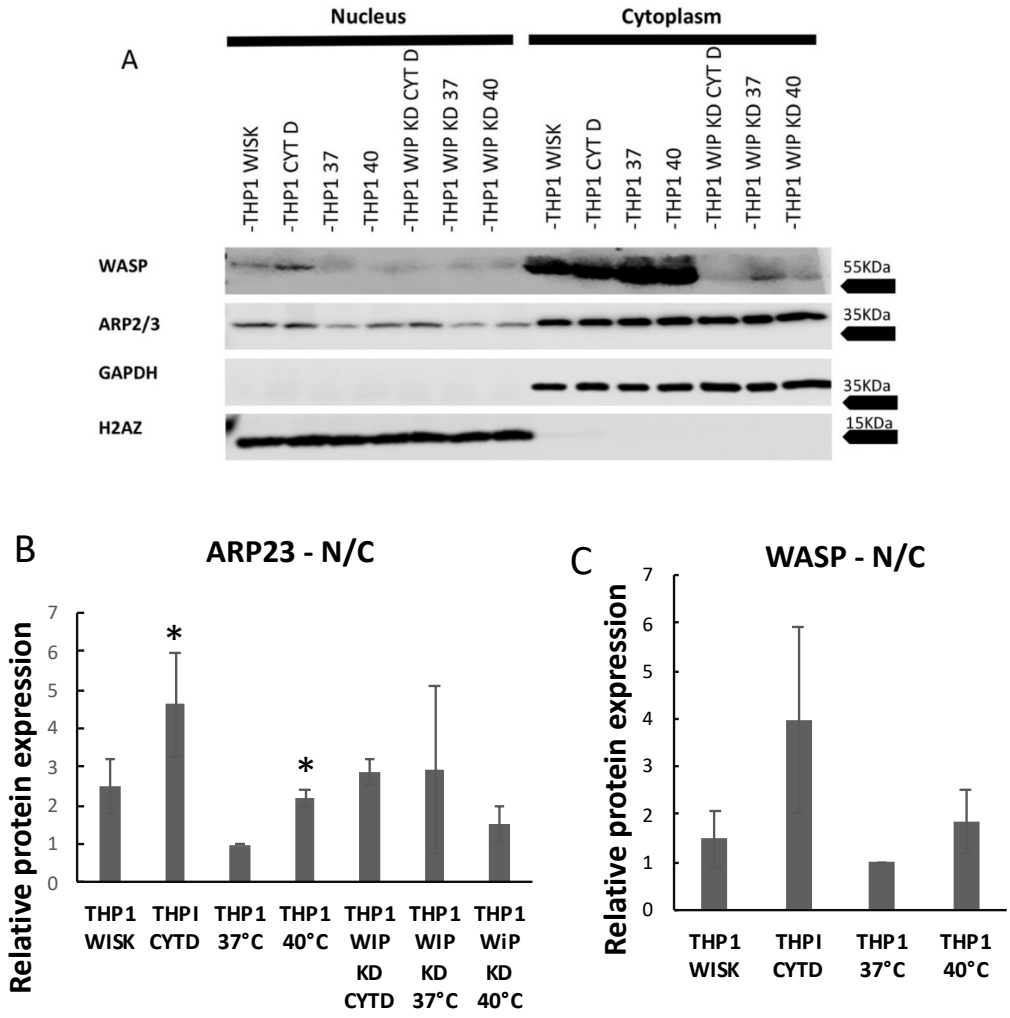

Figure 3.13. Actin related protein translocation between nucleus and cytoplasm in response to febrile temperature (40 °C) and treatment with actin inhibitors drugs.

(A) Representative blots of nuclear and cytoplasmic fractions of THP-1 and WIP KD THP-1 cells. Nucleus/cytoplasmic separation was performed after 16 hours incubation on fibronectin coated dishes in the presence of 1 ng/ml TGFβ-1. Following incubation, cells were treated for 3 hours with Cytochalasin D or Wiskostatin. The effect of febrile temperature was also tested, by incubating cells for 16 hours at 40°C. Separated lysates were used for Western Blotting. H2AZ and GAPDH were used as separation and loading controls. (B-C) Bar graphs show average and SE of each protein relative expression calculated as a ratio between protein expression in the nucleus and protein expression in the cytoplasm. Data are representative of at least three biological replicates. Unpaired two tail t-test was applied (*P<0.05 vs THP-1 37°C). Arrows on blots indicate protein ladder closest band (10 to 250 kDa, ThermoFisher Scientific).

3.4.6 WIP is required for increased cell migration and chemotaxis of THP-1 cells in response to mild hyperthermia (40 °C)

Both neutrophils (Rice *et al.*, 2005) and DCs (Ostberg *et al.*, 2001) have been shown to respond to a febrile event by improving host defence mechanisms, including cell migration towards the tissue of inflammation (Rice *et al.*, 2005). Therefore, we decided to explore how incubation at 40°C for 2 hours (resembling fever or mild hyperthermia during local inflammatory events) would affect monocytic cells' migration using THP-1 cells. At 37 °C, ablation of WIP did not affect the random migration efficiency of THP-1 cells. However, at 40°C, parental THP-1 cells and THP-1 cells transduced with the scrambled shRNA sequence (NT-shRNA THP-1 cell) travelled significantly at higher speed and covered a longer distance compared to 37°C whereas this effect was not observed in WIP KD THP-1 cells (Figure 3.14). Reinstating WIP function in WIP KD THP-1 cells by expression of eGFP-WIP RES recovered the increased random motility in response to incubation at 40°C to the same levels as parental cells.

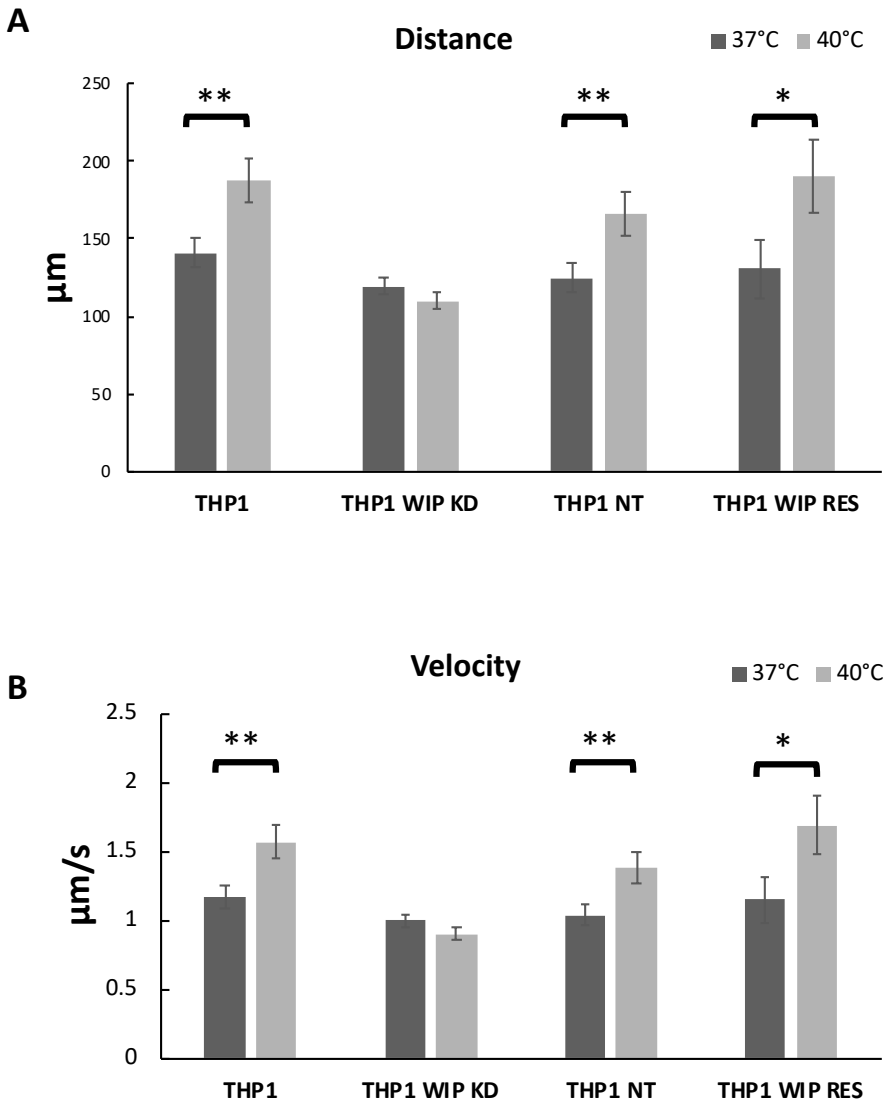

Figure 3.14. Analysis of migration (velocity and distance travelled) of THP-1, WIP KD THP-1 and NT THP-1 cells in response to exposure to 40°C.

The THP-1 cell line variants (parental THP-1, WIP KD THP-1 by transduction with shRNA targeting WIP, THP-1 transduced shRNA scrambled control and WIP KD THP-1 expressing eGFP tagged variant of WIP with a silent mutation that makes it resistant to WIP shRNA) were seeded on fibronectin-coated plates (10 ug/ml) in the presence of 1 ng/ml TGFb1 for 16 hours. Time lapse videos of cells were generated by taking phase contrast micrographs every minute for 2 hours at 37° or 40°C. (A) Histograms show the average and SE of the total distance travelled in two hours by tracked cells; (B) Histograms show the average and SE of cell velocity (µm/second) of tracked cells (n>60). **P<0.01, *P<0.05, 37°C, unpaired two tail t-Student test 37°C vs 40°C.

Furthermore, in the presence of MCP-1 almost double the number of cells transmigrated at 40°C indicating a role of mild hyperthermia in enhancing chemotaxis of THP-1 cells to MCP-1 (Figure 3.15) as well as the general capacity for random migration (Figure 3.14).

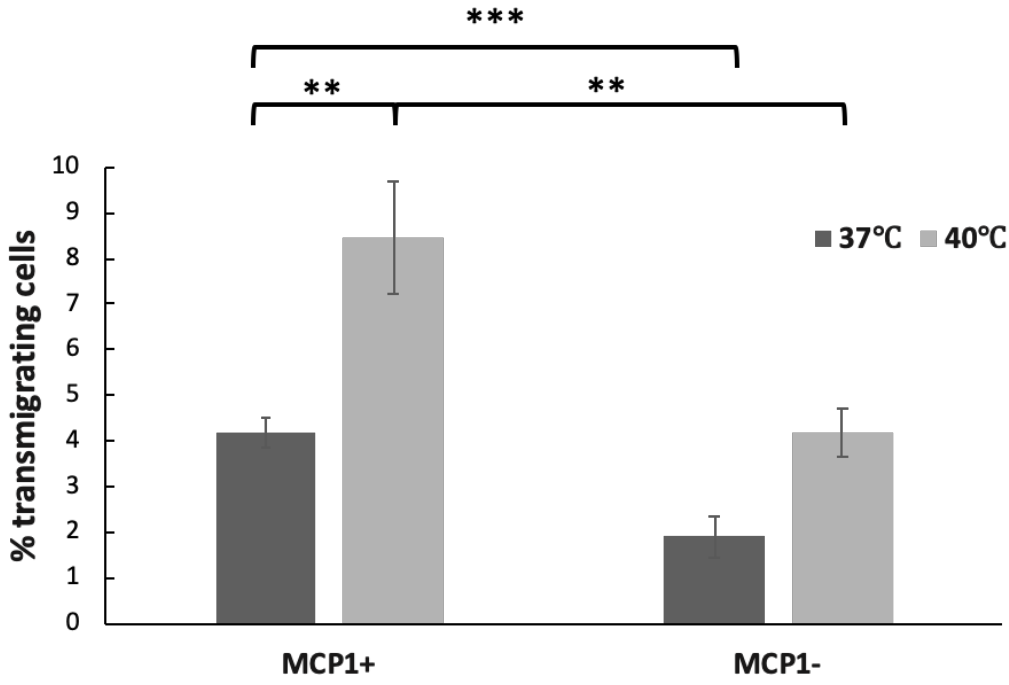

Figure 3.15. Chemotaxis of THP-1 cells towards MCP-1 at 37°C and 40°C.

Bar graphs show average and SE of percentage of the percentage of transmigrated cells towards the bottom of the well in a Boyden chamber in each condition. The increment of the percentage of transmigrated THP-1 cells at 40°C is significantly larger in the presence of chemoattractants, indicating enhanced chemotaxis of THP-1 cells towards MCP-1 at 40°C. *$P<0.05$, **$P<0.01$, ***$P<0.001$, unpaired t-Student test. Results are representative of 5 biological replicates.

3.4.7 Podosome turnover increases in response to mild hyperthermia

We showed above that increased migration of THP-1 cells in response to exposure to 40°C correlated with an impact on podosome formation and this process required WIP. We now aimed to study whether the restoration of WIP levels using our eGFP-WIP construct in WIP KD THP-1 could also restore the increment in podosomes formation seen in the THP-1 cells in response to hyperthermia.

The formation of podosomes was significantly increased in response to exposure to 40°C in THP-1 cells but not in WIP KD cells, as previously observed in this study. Whereas restoration of WIP levels in THP-1 WIP KD cells rescued podosome assembly at 37°C as well as the increase in podosome formation in response to exposure to 40°C (Figures 3.16, 3.17).

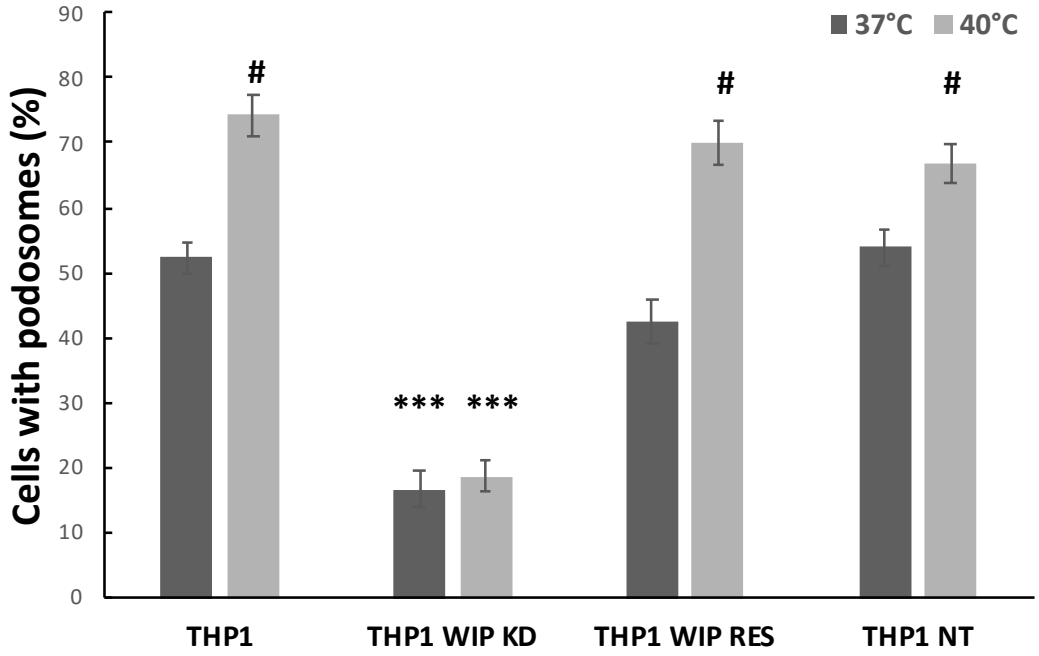

Figure 3.16. Analysis of podosome formation in response to mild hyperthermia in THP-1, WIP KD THP-1, WIP RES THP-1 and NT THP-1.

Quantitative analysis of number of cells with podosomes. Bar graph show the average and SE of number of cells with podosomes in THP-1, WIP KD THP-1, eGFP-WIP RES WIP KD THP-1 and NT THP-1 cells cultured for 16 hours at 37°C and 40°C on fibronectin coated coverslips with 1ng/ml TGFβ. Data were obtained analysing 5 fields, acquired from at least 2 coverslips per condition at 60x magnification and are representative of three biological replicates. #, t-student test vs control group at 37°C (#P<0.05); * t-student test vs parental THP-1 cells at 37°C or 40°C (***P<0.001).

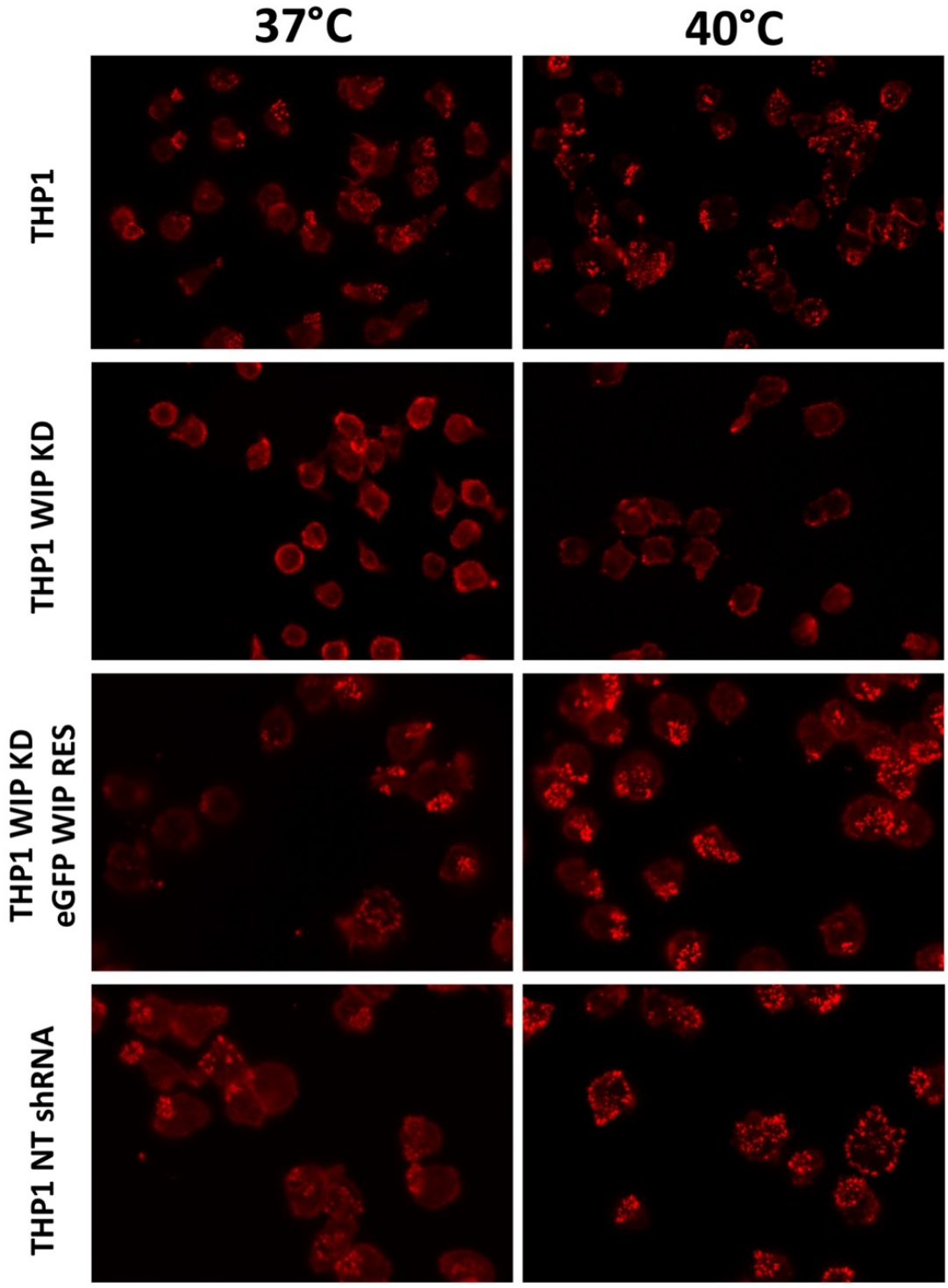

Figure 3.17. Representative micrographs showing podosome formation in response to exposure to 40°C in THP-1, WIP KD THP-1, WIP RES WIP KD THP-1 and NT THP-1.

THP-1 cells were cultured for 16 hours at 37°C or 40°C on fibronectin coated coverslips in the presence of 1ng/ml TGFβ-1 and stained with Alexa 568 nm-labelled phalloidin. Micrographs show filamentous actin distribution in one representative field for each condition (Bar 10 μm).

Migration requires assembly and disassembly of podosomes at the front of the cell, allowing progression of the cell body in the direction of movement (Cramer, 1999). Since we showed that migration velocity and podosome formation are both increasing proportionally with exposure of THP-1 cells to 40°C, we decided to investigate whether podosome turnover was similarly affected. Time lapse imaging of the distribution of eGFP-WIP in the core of podosomes was used to determine podosome localization every 30 seconds for 30 minutes (Figures 3.18, 3.19) allowing for the calculation of the index of podosome turnover (rate of podosome disassembly) (Figure 3.20). Our analysis demonstrated that, during exposure to 40°C, podosomes assembled and disassembled significantly faster with a 1.7-fold increase in the turnover index in cells cultured at 40°C vs cells cultured at 37°C (Figures 3.20).

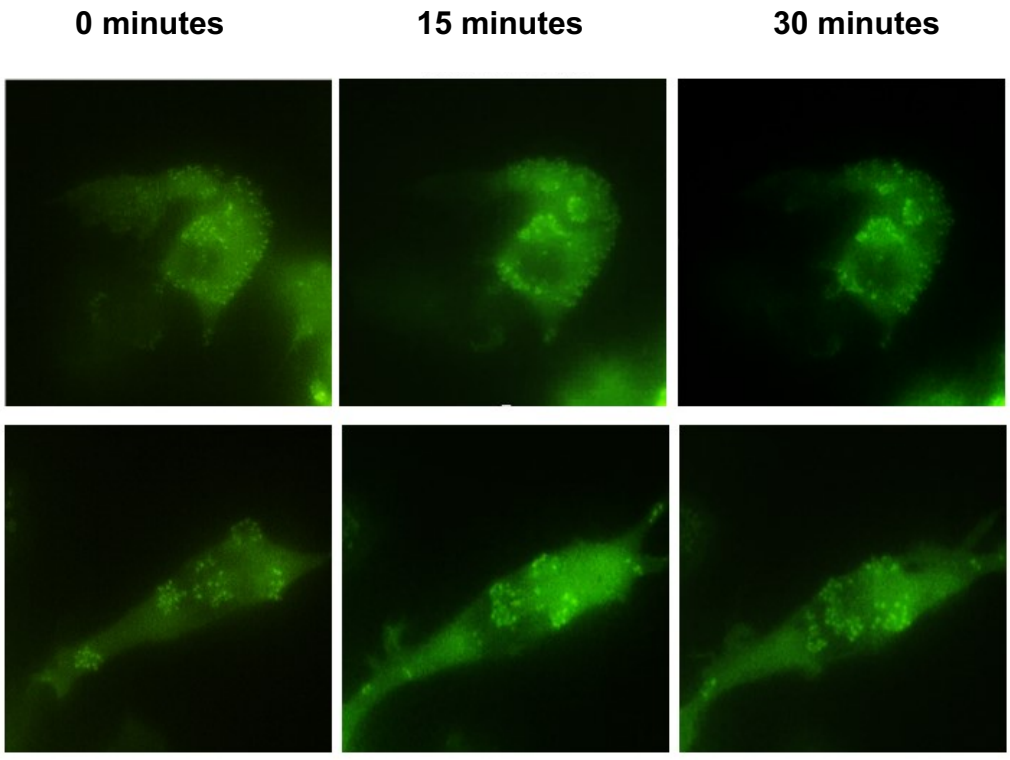

Figure 3.18. Representative micrographs of eGFP WIP distribution in podosomes in THP-1 cells filmed using time-lapse video at 37°C or 40°C for 30 minutes.

Images show eGFP-WIP distribution in THP-1 cells in the core of podosomes in a sequence at different time points of filming at 37°C (top panels) or 40°C (bottom panels). WIP localized in the same position for a longer period over time at 37°C, while it shifted its distribution more frequently when cells were incubated at 40°C, resulting in a faster turnover.

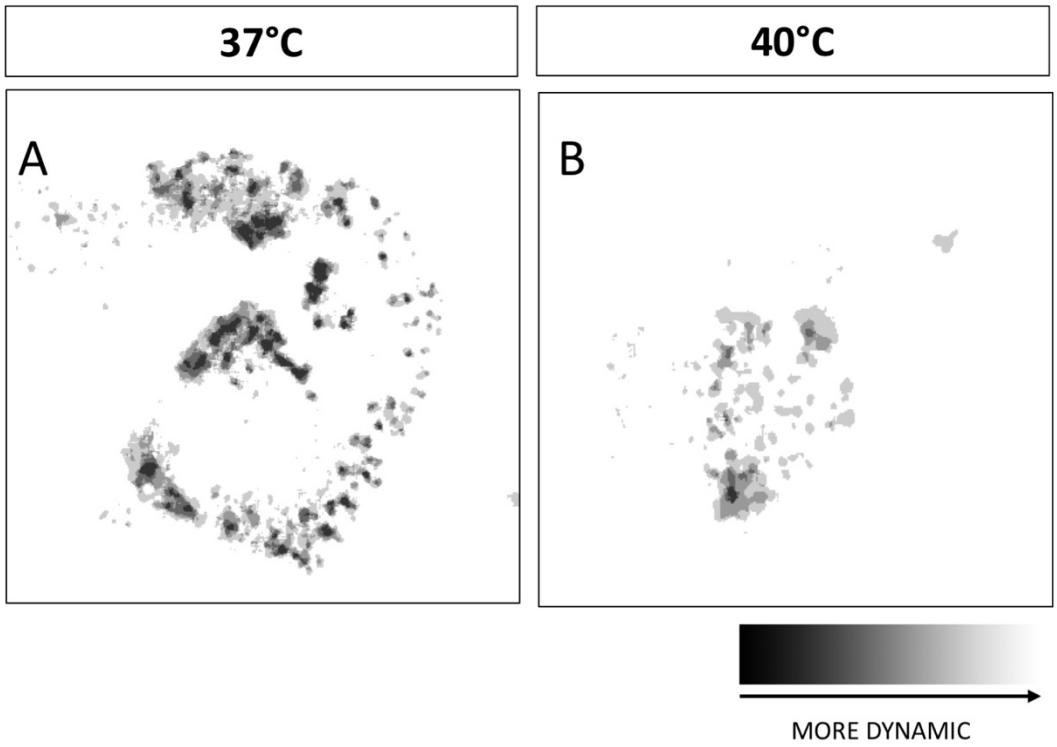

Figure 3.19. Composites for analysis of adhesion turnover.

Areas of light grey colour pixels represent dynamic turnover whereas areas of dark grey and black colour pixels represent more stable podosomes. Example of cell adhesion turnover at 37°C (A) and 40°C (B) showing podosome turnover is more dynamic at 40°C vs 37°C.

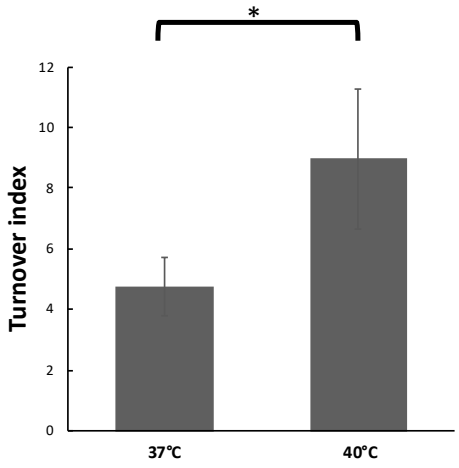

Figure 3.20. Analysis of podosome turnover in eGFP-WIP RES THP-1 cells seeded on fibronectin at 37°C and 40°C.

Histogram shows average and SE of podosome turnover index of cells incubated at 37°C or 40°C (*P<0.05, Mann-Whitney test).

3.4.8 THP-1 and dendritic cells acquire an invasive phenotype in response to mild hyperthermia

Podosomes are sites of matrix degradation and hence, the observed increased podosome formation at 40°C suggested a possible increase in matrix degradation. To investigate the role of temperature on matrix degradation, cells were seeded for 16 hours on red fluorescent gelatine, used to resemble matrix. Cells with an invasive phenotype generated area devoid of fluorescence on the degraded area (Figure 3.21). As previously shown (Bañón-Rodríguez *et al.*, 2011), lack of WIP in WIP KD THP-1 cells resulted in failure of matrix degradation (Figures 3.21 and 3.22). Recovery of WIP expression in WIP KD THP-1 cells restored this capability to equivalent levels as parental THP-1 cells at 37°C. Furthermore, the matrix-degradation potential of THP-1 cells was significantly increased at 40°C (Figure 3.20) and was dependent on the expression of WIP (Figures 3.21 and 3.22).

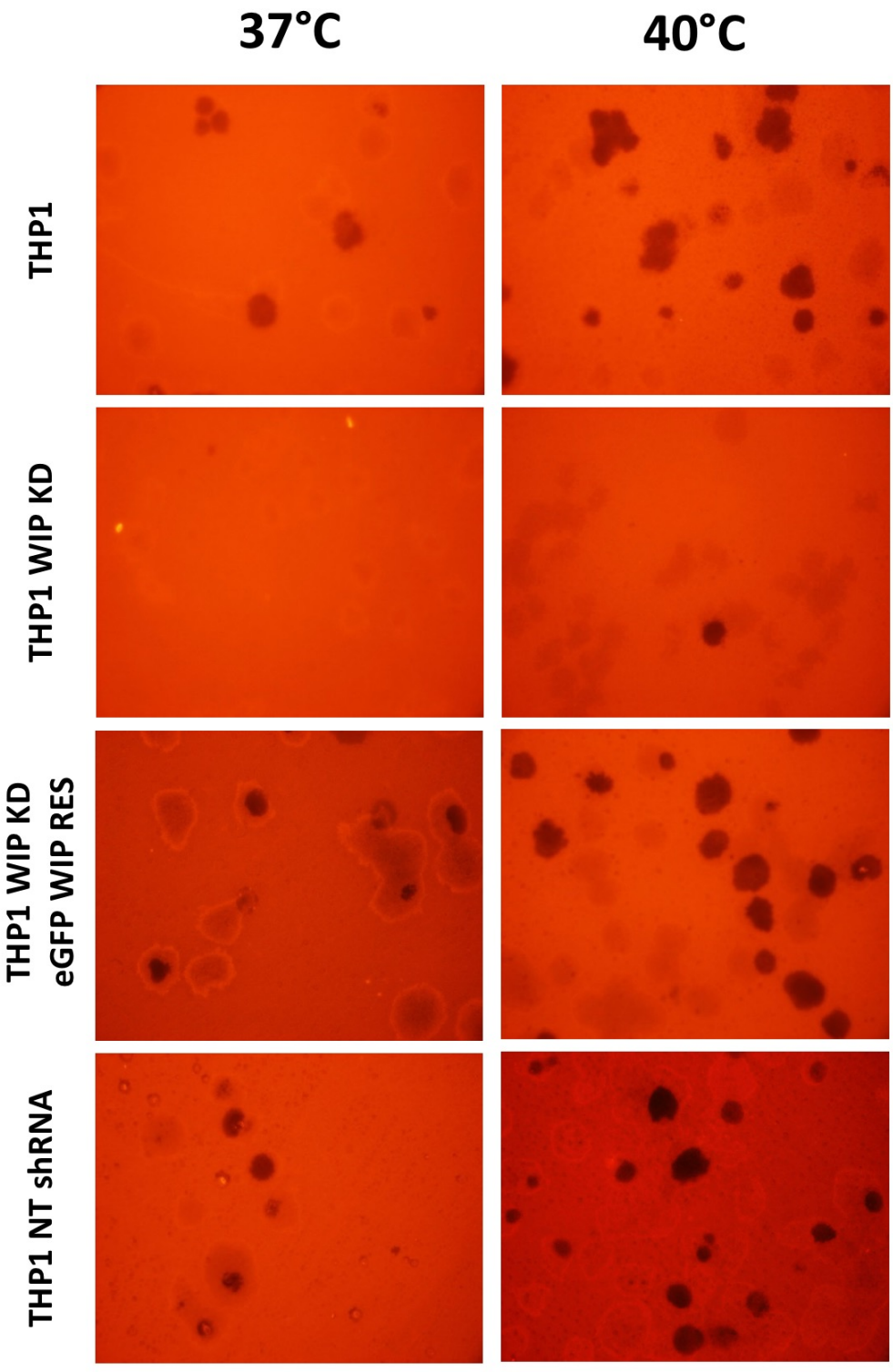

Figure 3.21. Representative fluorescent images of gelatin degradation by THP-1, WIP KD THP-1, eGFP-WIP RES WIP KD THP-1 and THP-1 NT shRNA.

Cells were cultured for 16 hours at 37°C or 40°C on red fluorescent gelatin coated coverslips in the presence of 1ng/ml TFGβ. This method allows to visualize the regions where cells degraded matrix and generated an area devoid of red fluorescence. Images are representative of matrix degradation in each condition.

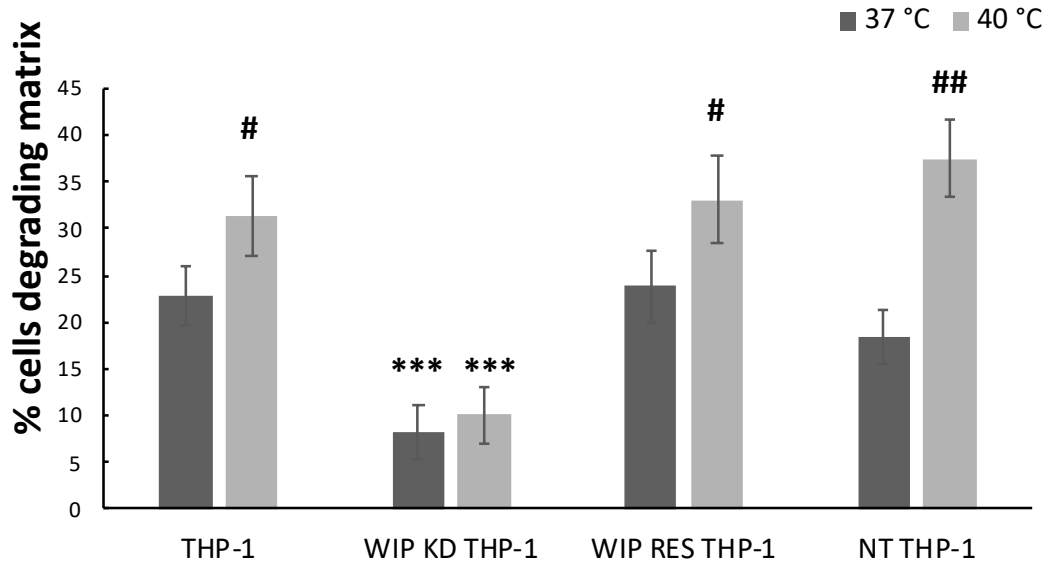

Figure 3.22. Quantitative analysis of the percentage of THP-1 cells degrading matrix.

Bar graph shows the average and SE of percentage of cells with a degradation area beneath per field of view used as a read out of the capacity of THP-1, WIP KD THP-1, eGFP-WIP RES WIP KD THP-1 and THP-1 NT cells to degrade matrix after 16 hours incubation. Data were obtained from 10 fields for at least 3 coverslips per condition at 60x magnification. Graphs are representative of similar results obtained in two different experiments. Unpaired t test was applied. #, t-student test vs control group at 37°C (#P<0.05); * t-student test vs parental THP-1 cells at 37°C or 40°C (***P<0.001).

The results obtained in THP-1 cells were highly reproducible in primary DCs. DCs derived from WIP KO mice showed defects in matrix degradation and WT cells appeared to increase matrix digestion proportionally to the increment in temperature (Figure 3.23, 3.24).

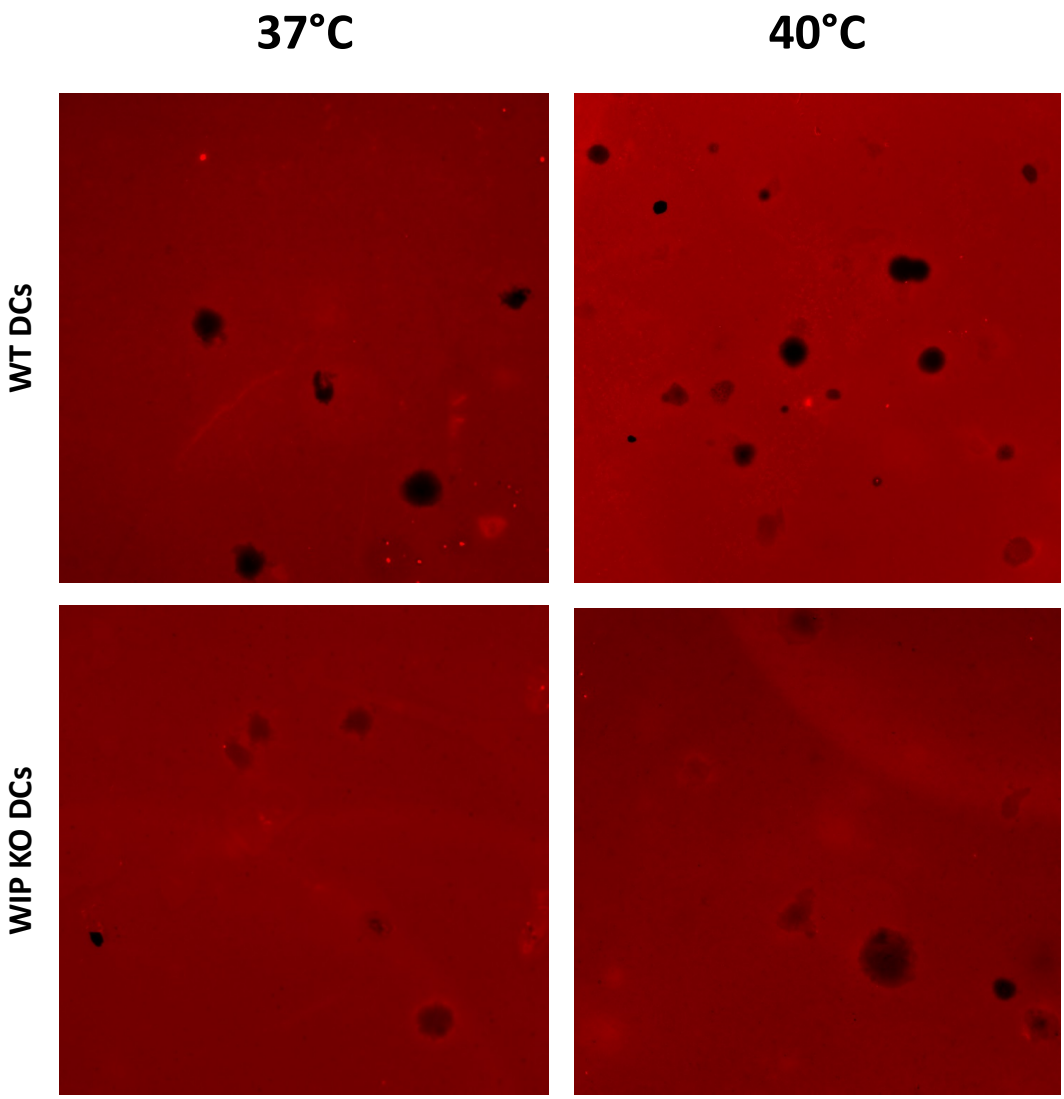

Figure 3.23. Representative fluorescent images of matrix degradation in WT and WIP KO dendritic cells.

Cells were cultured for 16 hours at 37°C or 40°C on red fluorescent gelatin coated coverslips with 1ng/ml TFG-β. This method allows to visualize the regions where the cell has degraded matrix to generate an area devoid of fluorescence. Picture were acquired at 60x magnification and are representative of matrix degradation in each condition.

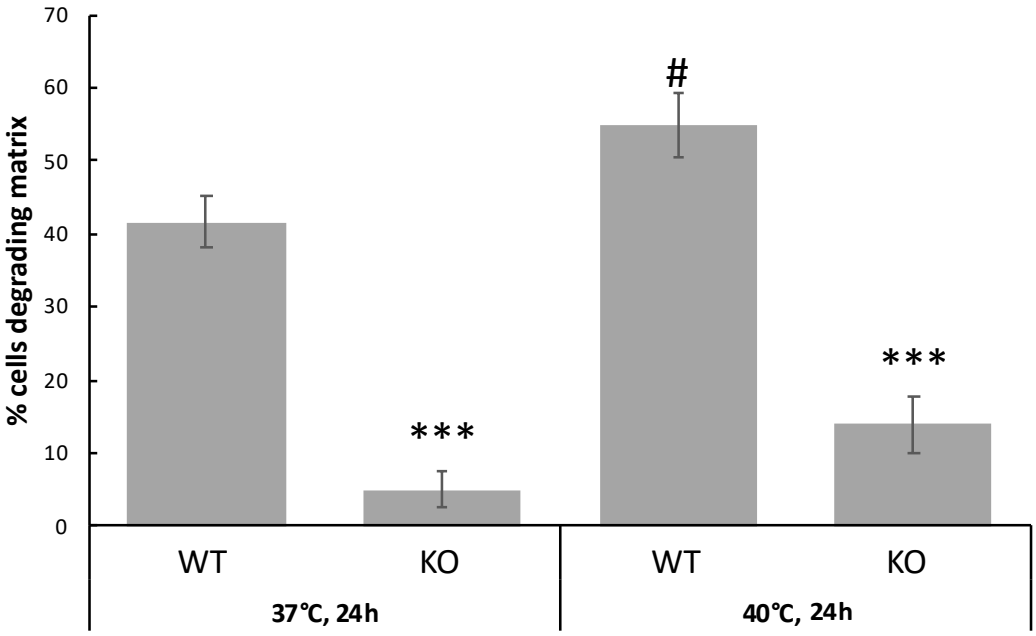

Figure 3.24. Quantitative analysis of number of dendritic cells degrading matrix.

Bar graph shows the average and SE of percentage of cells able to degrade matrix in WT and WIP KO dendritic cells after incubation at febrile condition. 10 fields were acquired for at least 3 coverslips per condition at 60x magnification. WIP KO dendritic cells are not able to degrade matrix and increment in temperature is proportional to increment in degrading capability in WT cells. Unpaired t test was applied. #, t-student test vs control group at 37°C (#P<0.05); * t-student test vs parental cells at 37°C or 40°C (***P<0.001).

Taken together, our results showed that cells exposed to mild hyperthermia assembled and disassembled podosomes at a faster rate, but they were also able to degrade matrix more efficiently. To explain this observation, we hypothesized that cells might degrade matrix more efficiently when incubated at 40°C by increasing the release of metalloproteinases (MMPs). MMPs are the main class of enzyme responsible for matrix degradation (Ohnishi *et al.*, 1998). THP-1 cells, seeded on fibronectin coated surfaces, can secrete in the culture medium MMPs, in particular proMMP-9 and MMP-9, which belong to the class of gelatinases. Our results showed that the zymogen proMMP-9, inactive form, is increasingly converted into active MMP-9 when THP-1 cells were exposed to mild hyperthermia (Figure 3.25).

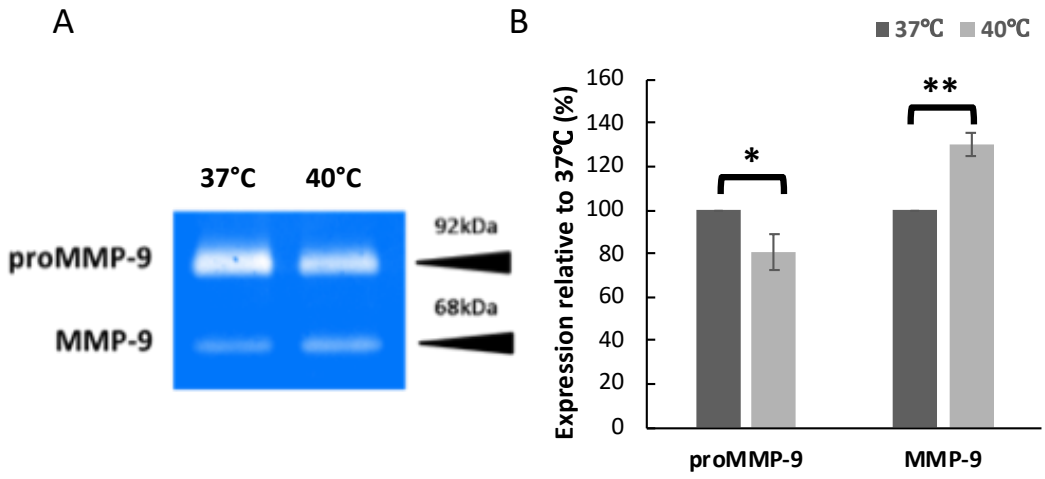

Figure 3.25. Increased levels of secreted active MMP-9 are induced by mild hyperthermia in THP-1 cells.

Supernatants of THP-1 seeded on fibronectin at 37°C or 40° were collected after 48h and subjected to gelatin zymography. (A) Representative zymograph of results obtained in three separate experiments. Pro-MMP-9 and active MMP-9 were visualized as area of degradation on 0.075%gelatin SDS gel stained with Coomassie blue. The bands obtained at 92kDa and 68kDa were identified respectively as proMMP-9 and MMP-9 as previously demonstrated (Troeberg and Nagase, 2003). (B) Bar graphs are showing the average and SE of the intensity of the bands obtained in three different experiments. Data are shown relative to 37°C. Images were analysed using ImageJ Fiji. * $P<0.01$, Student's t-test 37°C vs 40°C.

3.5 Discussion

Little is known about the molecular mechanisms used by the immune cells to integrate signals from their environment leading to their activation and recruitment to the site of inflammation in response to mild hyperthermic temperatures (Evans, Repasky and Fisher, 2015). Fever is a condition characterized by abnormally high body temperature and the correlation infection/temperature increase is retained in the animal and plant's kingdoms (Bernheim and Kluger, 1976; Covert and Reynolds, 1977; Watling *et al.*, 2008). Several evidences are now underlining the importance of fever in boosting the immune system. The use of antipyretics (non-anti-inflammatory) drugs, such as paracetamol, was associated with higher mortality rate in critically ill patients (Schulman *et al.*, 2005) and thermal heat therapy seemed to improve anti-tumour immunity (Mikucki *et al.*, 2013). Furthermore, it was demonstrated that local hyperthermia, occurring during local inflammatory events such as tissue repair and infections (Fieren, 2012; Prats *et al.*, 2016; Mescher, 2017), can stimulate the immune response. For instance, local hyperthermia can induce local macrophages proliferation rather than systemic recruitment (Mescher, 2017) and homing of lymphocytes by increased avidity of lymphocytes for L-selectin lymphocyte-endothelial cell adhesion (Midis, Fabian and Lefor, 1992; Lefor *et al.*, 1994). Local hyperthermic heat is used as a treatment in several tumours, with the aim of inducing cytotoxic T-cell adhesion, increase natural killer cells response to cytokine therapy, improving antigen presentation and boosting innate immunity (Forni *et al.*, 1995; Baronzio *et al.*, 2006; Toraya-Brown and Fiering, 2014; Gao *et al.*, 2016). According to the "Danger model" of immunity (Forsdyke, 1999), tumour cells respond to heat therapy delivering danger signals, that will induce the expression of HSPs and, in turn, the maturation and recruitment of both innate and adaptive immune cells (Forsdyke, 1999). However,

excessive inflammation can lead to the development of various form of arthritis and lowering the temperature through cryotherapy is an efficient method to reduce the pain (Bouzigon *et al.*, 2016). Therefore, understanding the signalling pathways induced by hyperthermia on immune cells may lead to improved personalized treatments for specific diseases related to inflammation. Mild heat stress promotes T-lymphocytes site-directed trafficking and adhesion to the endothelium thanks to the improvement in the expression of adhesion molecules following activation of heat shock proteins (HSP) (Chen and Evans, 2005; Park *et al.*, 2005). In accordance with these findings, this study demonstrated that monocytic cells also migrate faster, travel significantly longer distances and show increase chemotaxis when exposed to hyperthermia.

In monocytes and dendritic cells, migration and adhesion are strictly dependent on podosomes and its formation and dynamics are regulated by WASP and WIP (Guiet *et al.*, 2012; Hannah Schachtner *et al.*, 2013). Hence, we hypothesized that the WIP-WASP functional unit might induce changes in actin dynamics allowing immune cells to reach the site of inflammation in response of the external stimulus of temperature increment.

In response to mild hyperthermia, not only THP-1 parental cells migrated faster but they also produced more numerous and robust podosomes, surrounded by well-defined vinculin rings. Additionally, WIP deficient cells, failed to respond to the temperature stimulus and did not improve their motile or podosome assembling capability. Both events were recovered in WIP KO cells upon reconstitution of WIP levels by expression of eGFP-WIP (RES), pointing out at WIP as a mediator of the changes occurred. Our findings corroborate previous associations between loss of podosomes and reduced migration (Olivier *et al.*, 2006), underlining that podosomes are not only adhesive structures but fundamentally involved in motility. Perhaps, the

fact that WAS patients' immune cells may not be able to respond to the heat stress-induced immunity boost contributes to a worst prognosis during the course of infections (Linder *et al.*, 2000). While increased migration did not reflect an increment in the expression of the main actin related proteins involved in podosomes formation, such as WIP, WASP or ARP2/3, our data indicated that, in response to hyperthermia, ERK phosphorylation was enhanced. Interestingly, ERK activation can modulate cell migration by both regulating the expression of migratory genes (Chen *et al.*, 2009; Hong *et al.*, 2011) or by transducing signals downstream of the cell adhesion molecules of the integrin family by interacting with proteins involved in protrusions and lamellipodia extension as WAVE, cortactin and Src (Martinez-Quiles *et al.*, 2004; Danson *et al.*, 2007; Mendoza *et al.*, 2011).

Levels of HSP90, a protein previously associated with podosome formation and stabilization (Park, Suetsugu and Takenawa, 2005), were also raised in response to the increment in temperature. HSP90 is not only a partner of N-WASP in podosome assembly, protecting N-WASP from degradation (Park, Suetsugu and Takenawa, 2005), but can also regulate signalling mediated by kinases including Src and ERK (Suetsugu and Takenawa, 2003). Our data showed an increase in HSP90 levels that correlated with an activation of ERK phosphorylation in response to mild hyperthermia, confirming the link in between the ERK pathway and HSP90 (Dou, Yuan and Zhu, 2005). Our data also showed a significantly higher expression of HSP90 correlating with increased phosphorylation of ERK in the WIP deficient cells, indicating a role of WIP in restricting HSP90 expression in myeloid cells in the resting state and allowing for its upregulation only in response to mild hyperthermia (and perhaps other inflammatory signals) during an organised immune response. Taken together, our results suggest that dysregulation of the WIP/WASP pathway in immune

cells results in a status that resembles the response to mild hyperthermia, which may contribute to the hyper-reactive autoinflammatory phenotype in WAS patients. In fact, HSP90 can also induce cytokine activation, including IL-1β (Kim *et al.*, 2016), whose hyperactivation is common in WAS patients leading to excessive inflammasome activity and autoimmunity (Lee *et al.*, 2017). Interestingly, the genes coding for IL-1β and CCL2, also known as MCP-1 and involved in the recruitment of monocytes during inflammation (Yoshimura *et al.*, 1989), are both upregulated in the WIP KD cells, possibly causing the autoinflammatory phenotype seen in WAS patients.

Monocytes and dendritic cells trafficking to the site of inflammation is not a random process. The recruitment requires activation of chemokines receptors following production of pro inflammatory cytokines (Linder *et al.*, 2000; Shi and Pamer, 2011; Yang *et al.*, 2014). To investigate the role of mild heat stress on chemotaxis, cells migration towards MCP-1 was studied. MCP-1 is the main regulator of monocytes migration and defects in his sequence are associated with impaired leukocytes recruitment (Yoshimura *et al.*, 1989; Proudfoot *et al.*, 2003). Our findings highlighted once again the importance of temperature, since THP-1 cells significantly transmigrated faster when cultured at 40ºC and as well responded to MCP-1, in the presence of which temperature-induced migration was almost doubled.

Migration requires dynamic assembly and disassembly of adhesion structures (Cramer, 1999). In fact, podosomes are highly dynamic with a half-life ranging from 30 seconds to 10 minutes (Destaing *et al.*, 2003). In addition, live imaging studies allowed us to film podosomes assembly and disassembly during a 30 minutes' time frame by visualizing eGFP-WIP protein co-localized in the podosomes core. In cells exposed to febrile temperature podosomes turnover resulted to be significantly faster, supporting the increased migration findings described above.

Monocytic transendothelial migration is a complex process that involves several steps. Following chemokines release and exposure of adhesion molecules, leukocytes immobilize through tight adhesions with the endothelium and start transmigration via endothelial gaps (Maslin *et al.*, 2005; Muller, 2011). At this point, basement membrane digestion will be necessary to proceed further. Our study revealed that mild hyperthermia is able to enhance monocytic and dendritic cells invasive capability and this process is dependent on the presence of WIP. THP-1 cells cultured at 40ºC degraded significantly more gelatine when compared to cells cultured at 37ºC. WIP deficient cells displayed diminished degrading potential, while recovered cells performed as parental ones. Podosomes are sites for secretion of proteases able to degrade different kind of matrix, including collagen, gelatin and fibronectin (Linder, 2007; Gill and Parks, 2008). Therefore, we could associate the defects observed in the WIP KD cells to the lack of podosomes. In particular, the most interesting proteases studied in association with podosomes are metalloproteases. THP-1 cells were able to secrete proMMP-9 and the active MMP-9 form. Mild hyperthermia augmented the conversion of the inactive zymogen to its active form. A key regulator of MMPs recruitment to adhesion sites is the WIP-cortactin unit that is recruited to the core of podosomes (Artym *et al.*, 2006; Bañón-Rodríguez *et al.*, 2011). Cortactin knocked down cells exhibit a defect in migration (Clark *et al.*, 2007; Lai *et al.*, 2009) and failure in degrading matrix (Bañón-Rodríguez *et al.*, 2011). The complex WIP-cortactin was identified as essential in localizing MMPs to podosomes and starting matrix degradation. It would be interesting to investigate a possible role of WIP and/or cortactin in MMPs activation driven by hyperthermia. Furthermore, the enhanced activation of MMP-9 explained how cells cultured at 40ºC degraded more matrix, although they presented reduced adhesion times since they were travelling

significantly faster.

Furthermore, exposure to mild hyperthermia induces actin related proteins shuttling into the nucleus in a WIP-dependent manner. This demonstrates that hyperthermia may play a role in modulating the nuclear regulation of the actin nucleating process and, therefore, in developing a connection between actin dynamics and the expression of temperature responsive genes. The importance of WIP/WASP in controlling actin remodelling in response to hyperthermia was also underlined by the fact that ARP2/3 nuclear localization was increased in parental but not in WIP KD cells in response to hyperthermia. This finding further corroborates the idea that WIP or WASP are the main regulator of cell fate following the external stimulus of heat and that their mechanism of action includes the control of actin related protein shuttling in the nucleus to possibly affect gene expression. Interestingly, ARP2/3 in the nucleus was found to have a role in regulating gene expression by physically interacting with RNA polymerase II and, in turn, regulating transcription (Yoo, Wu and Guan, 2007).

Taken together, all the results obtained so far are supporting the participation of temperature in controlling monocyte migration during the inflammatory response, affecting particularly migration and invasion events driven by the WIP-WASP functional unit, including enhanced degradation of the ECM that may facilitate the transmigration across the basal lamina of recruited myeloid cells at sites of inflammation. WIP may achieve this regulation through its role in controlling F-actin dynamics as well as the role in regulation of levels of expression of HSP90 that we have identified. In conclusion, our results suggest that in leukocytes, WIP modulates the adequate response to mild hyperthermia in febrile conditions involved in the enhancement of the immune response.

A further WIP role recently discovered associated its function with the regulation of

the membrane lipids composition in neurons, identifying WIP as a possible modulator of lipid metabolism (Franco-Villanueva *et al.*, 2014). The lipid composition and fluidity of cell membranes works as a thermosensor that modulates cells response to temperature changes including expression of Heat Shock Proteins (HSP) (Török *et al.*, 2014) or lipid modulators. To maintain homeostasis, various cell types and microorganisms respond to heat stress by increasing the saturation levels of the fatty acyl tails of their membrane lipids (Larkindale and Huang, 2004).

Given the role of the plasma membrane lipids in thermosensing and the previously described role of WIP in regulating the lipid composition of biological membranes, we decided to study the possible role of WIP in regulating the lipid composition in response to mild hyperthermia in myeloid cells.

Chapter 4: WIP modulates the lipid composition of the plasma membrane in myeloid cells in response to mild hyperthermia

4 WIP modulates the lipid composition of the plasma membrane in myeloid cells in response to mild hyperthermia

4.1 Introduction

Results shown in the preceding chapter confirmed previous studies indicating that mild hyperthermia can enhance the activity of immune cells providing a survival advantage during infection (Park *et al.*, 2005; Simard *et al.*, 2011; Singh and Hasday, 2013). Exposure to febrile-range temperatures enhanced the chemotactic and invasive capabilities of monocytic cells. However, the intracellular signalling involved in fever that activates leukocytes migration remains largely unknown (Evans, Repasky and Fisher, 2015). Our data indicate that WIP is involved in the increased invasive migratory capacity of myeloid cells in response to mild hyperthermia and we now aim to further understand the molecular mechanisms regulated by WIP that are involved in this process.

Temperature can affect the physiology of living cells in several ways: by altering chemical reactions rates and/or affecting the activity of proteins, lipids or nucleic acids by influencing their atoms configuration (Sengupta and Garrity, 2013). Therefore, different cell types and organisms must use sophisticated systems for sensing the thermal fluctuations and responding in a physiological way to maintain homeostasis (Lepock, 1982; Miller and Ziskin, 1989; Armour *et al.*, 1993). According to the "Membrane Sensor Hypothesis" (Török *et al.*, 2014), fever-induced mild heat shock temperatures can cause alterations in the plasma membrane, which consequently modulate transient receptor potential (TRP) channels whose regulation is strictly

dependent on lipid conformation. The resulting cascade of events may affect the expression of heat shock genes (Török *et al.*, 2014).

Lipids represent the key constituent of plasma membranes and are highly heterogenic among organisms, cells and organelles (Spector and Yorek, 1985; Coskun and Simons, 2011; Harayama and Riezman, 2018). Mainly, the matrix of the cell membrane is composed of polar lipids, whose amphipathic structures allow compartmentalization between the internal and external environment, creating a lipid bilayer. Although this description is currently accepted, we must acknowledge that membranes are highly asymmetric, being the internal layer rich in phosphatidylserine (PS) and phosphatidylethanolamine (PE) and the outer layer in phosphatidylcholine (PC) and sphingomyelin (SM) (van Meer and de Kroon, 2011). Furthermore, sphingolipids, cholesterol and proteins can self-assemble into aggregates known as lipid rafts involved in membrane signalling and trafficking (Simons and Ikonen, 1997; Munro, 2003; Pike, 2003).

Segregation is not the only function of membrane lipids. Some lipids can act as messengers for signal transduction or create membrane domains to recruit cytosol proteins and start secondary signalling (van Meer, Voelker and Feigenson, 2008). Furthermore, proteins as receptors and enzymes are embedded in the bilayer. The balance between fatty acids, cholesterol and phospholipids determines membrane physical properties such as fluidity and plasticity. The modification of these properties can affect several cells functions such as phagocytosis, endocytosis, prostaglandin production, and cell growth (Spector and Yorek, 1985).

Membrane fluidity is normally maintained within a certain range and it is dependent on the length of the fatty acids tails, phospholipids saturation levels (absence or presence of double bonds) and content of cholesterol (de Meyer and Smit,

2009; Dawaliby *et al.*, 2015). In response to hyperthermia, molecular forces that hold lipids together are overcome leading to an increment in membrane fluidity (Murata and Los, 1997). Therefore, in response to heat stress, most organisms (bacteria, yeast, plant and mammalian cells) increase the saturation levels of the fatty acyl tails of their membrane lipids (Larkindale and Huang, 2004) to compensate the increment in fluidity and these changes might work as a thermosensor that modulates cells response to temperature (Török *et al.*, 2014). Fluidity can also play an important role in regulating immune cells activation (Schumann, 2012; Mansilla *et al.*, 2004; Hubler and Kennedy, 2016), as seen in T cell where increment in membrane fluidity and exposure to mild hyperthermia can similarly activate the immune response (Gombos and Vígh, 2015). These findings fit with the idea that reorganization of lipid membrane domains can be responsible for the signalling cascade that will determine cells fate following heat shock. Additionally, several studies have shown that the change in membrane fluidity can trigger a cell response by modulating the expression of Heat Shock Genes (Balogh *et al.*, 2005).

It was recently shown that WIP can regulate the lipid composition of the plasma membrane in neurons (Franco-Villanueva, Wandosell and Antón, 2015). Lack of WIP induced upregulation of the expression of neuraminidases resulting in lower levels of sphingomyelin and reorganization of their lipid micro domain leading to changes in the assembly of F-actin (Franco-Villanueva *et al.*, 2014). These results are underlying the WIP role in linking membrane lipid composition and actin dynamics. Furthermore, our preliminary data showed that both WIP and WASP can play a role in the formation of complexes containing tyrosine-phosphorylated proteins and histones (Calle, unpublished data). In particular, we identified histones H2AV and H2AZ in these complexes. H2AZ works as a chromatin thermostat in plants. It controls the access of

RNA polymerase II into the nucleosome and, therefore, the expression of temperature responsive genes (Deal and Henikoff, 2010).

4.2 Hypothesis and aims

Taken together, the current publications and our preliminary data suggest that WIP might play a role in the regulation of immune cell response to mild hyperthermia by modulating fluidity and lipid composition of the plasma membrane.

Therefore, in this chapter, we aim to:

- investigate the possible changes in membrane lipid composition and organization occurring in parental and WIP KD cells exposed to mild hyperthermia;
- investigate the role played by WIP in remodelling the membrane lipid composition in response to hyperthermia;
- investigate the role that may be played by membrane fluidity perturbations and heat shock activation in inducing monocytes migratory and invasive boost;
- verify whether similar outcomes in terms of cells migration and invasion can be determined by exposure to hyperthermia or by altering membrane fluidity using membrane fluidizer drugs. The two drugs tested, Benzyl Alcohol, a local anaesthetic able to interfere with van der Waals forces in the lipid bilayers (Friedlander *et al.*, 1987), and Arimoclomol, a phase II/III clinical trial drug used for the treatment of misfolding disorders (Fog *et al.*, 2018), are Heat shock proteins co-inducers able to interfere with membrane fluidity.

4.3 Materials and methods

4.3.1 Raster Imaging Correlation Spectroscopy (RICS)

Sample Preparation. $1x10^5$ THP-1 and WIP KD THP-1 cells were stained with 1 μM di-4-ANEPDHQ (ThermoFisher Scientific) and seeded for 16 hours at 37°C on fibronectin coated microwell-chambers with high optical quality (Ibidi, Martinsried, Germany) in the presence of 1 ng/ml TGFβ-1. Di-4-ANEPDHQ is a membrane-staining widely used in studies of lipid domains in model membranes and cells (Jin *et al.*, 2005). The following day cells were stained with 1 μM SiR-Actin (SPIROCHROME) and incubated for 1 hour before imaging to fluorescently label F-actin and identify areas of podosome assembly.

Imaging. Cells were imaged at 37°C or 40°C (after 30 minutes incubation time) in 5% CO_2 atmosphere using a Leica TCS SP8 inverted microscope fitted with a HCX PL APO 63x/1.2NA CORR CS2 water immersion objective. This microscope laser scanning function allows the observation of fast biological processes and can be switched from super resolution confocal microscopy to STED nanoscopy, allowing a deep understanding of subcellular architecture. Di-4-ANEPDHQ was excited using a pulsed (80 MHz) super-continuum white laser light (WLL) at 488 nm and the emission signal was detected with a photon counting (HyD) detector at 500-580 nm. SiR-Actin was excited at 640 nm and emission collected with a HyD detector at 640-770 nm. 256x256 pixels images were collected, with a pixel size of 80.4nm and 8μs pixel dwell time (indicating the time spent by the laser in imaging each pixel), for 200 consecutive frames. Pinhole (aperture used to spatially filter the light beam) was set to one Airy unit and PSF (point spread function) was characterised as previously described (Garcia and Bernardino De La Serna, 2018). Dwell time was chosen to allow PSF overlapping in the bases of previously analysed lipid dynamics data.

Raster Image Correlation Spectroscopy. RICS is a technique that allows to measure molecule dynamics using fluorescent laser scanning confocal or STED microscopy images. Laser scanning microscopy allows to trace highly dynamics molecules, such as membrane lipids, on live cells. This is achieved thanks to the ability to scan regions of interest, labelled with a fluorescent probe (in this case the membrane-staining di-4-ANEPDHQ) pixels by pixel, with a dwell time chosen on the basis of the molecular velocity of diffusion. Molecules diffusion will be sensed as a fluctuation of fluorescence from a pixel to the neighbour pixels. A coefficient of diffusion will be obtained using algorithms and spatial-temporal autocorrelation functions (Brown *et al.*, 2008) as described below.

"SIM FCS 4" software was used for the analysis as previously described (Garcia and Bernardino De La Serna, 2018; Rossow *et al.*, 2010). Analysis of di-4-ANEPDHQ emission signal was performed by subtracting a moving average of 10 to discard possible errors due to cells movement. Regions of interests (ROIs) of 128x128 pixels were employed to analyse membrane lipids diffusion in the entire cell plane, while specific regions of interest were squared as 32x32 pixel size. In parental cells, ROIs were chosen in base on the presence of podosomes, to have a comparison among the different structures, while in the WIP KD cells random regions were chosen. After subtracting the moving average, we obtained an autocorrelation 2D map and observed the average intensity trace to discard possible photobleaching events. The autocorrelation 2D map was then fitted, using the previously characterized PSF waist value, line time and pixel time, to obtain a coefficient of diffusion. Data were averaged from at least 5 cells per conditions.

4.3.2 Generalized Polarization (GP) analysis

Sample Preparation. Samples were prepared as described for RICS analysis.

Imaging. Samples were imaged as described for RICS analysis, but two different emission signals were detected for di-4-ANEPDHQ with photon counting (HyD) detectors (500-580 nm and 620-750 nm).

Generalized Polarization. Changes in membrane fluidity in live THP-1 cells were estimated using the polarity sensitive dye di4-ANEPPDHQ (Bernabé-Rubio *et al.*, 2019). Sample preparation and imaging were performed as described above. This probe's emission spectrum can be 60 nm blue-shifted depending on different membrane microenvironmental molecular aspects, such as the surrounding water content or membrane potential, but in both cases rendering information that ultimately can be correlated to the membrane lateral order or lipid packing (Jin *et al.*, 2005). This emission shift can be used to calculate the "GP" (generalised polarisation) value, a relative value used to quantify lipid packing/order and consequently membrane fluidity. Di-4-ANEPDHQ was excited using a pulsed (80MHz) super-continuum white laser light (WLL) at 488nm. Two different emission signals were detected with photon counting (HyD) detectors (500-580 nm and 620-750 nm). The GP value was calculated as:

$$\frac{Em1-Em2}{Em1+Em2} = \text{GP},$$

where Em1 and Em2 are the emission intensity at 520 nm and 690 nm, respectively. Analysis was performed using "SIM FCS 4". Large vectors were split sequentially, and GP localization histograms were generated around the areas of interest. GP value was chosen on the basis of the frequency of counts. For each cell analysed, GP value was averaged from at least 5 consecutive images. Final data were averaged from at least 5 cells per condition.

Statistical Analysis. GP frequency raw data were extracted from SIM FCS and plotted in GraphPad Prism. Using the non-linear regression function, frequency data were fitted to a Gaussian and the mean value of the peak was used as GP valued. Final data were averaged from at least 5 cells per condition.

4.3.3 Drug treatments

Arimoclomol and Benzyl Alcohol (BA) were used to test cells response to increment in membrane fluidity. In the different experiments detailed in section 2, cells were treated with Arimoclomol after attachment to fibronectin coated substrates (approximately 6 hours) and incubated for 16 hours at 37°C with the following Arimoclomol concentrations: 0.1 μM, 0.5 μM, and 1 μM. On the other hand, Benzyl alcohol was added after cells incubation for 16 hours on fibronectin coated surfaces and cells were then treated for 1 hour at the following concentrations: 0.1 mM, 0.5 mM, and 1 mM.

4.3.4 Lipidomics

$5x10^6$ THP-1 cells were seeded on 10 cm cell culture petri dishes for 16 hours at 37°C and 40°C. Cells were harvested using cells disassociation media (ThermoFisher Scientific) and collected by centrifugation. Cell pellets were sent to IMG Pharma for analysis of membrane lipid composition using mass spectrometry. Detail of analysis can be found in appendix section 8.3.

4.4 Results

4.4.1 WIP modulates the lipid composition of the plasma membrane

Alterations of membrane fluidity works as a thermosensor that regulates the cellular response to changes in temperature (Park *et al.*, 2005) and various cell types and microorganisms respond to heat stress increasing the saturation levels of the fatty acyl tails of their membrane lipids, to maintain homeostasis (Larkindale and Huang, 2004). It was recently shown that WIP can regulate the lipid composition of the plasma membrane in neurons, leading to changes in F-actin assembly (Franco-Villanueva *et al.*, 2014). We hypothesized that in myeloid cells, WIP may play a role in inducing changes in actin dynamics and enhance the migratory response in response to mild hyperthermia by regulating membrane lipid composition.

Our data, obtained by lipidomics analysis, showed that reduced levels of WIP in THP-1 WIP KD cells resulted in significant changes in the composition of certain lipids whose levels varied in response to mild hyperthermia in parental THP-1 cells (Figure 4.1). Additionally, levels of some of these lipids did not vary significantly in WIP KD THP-1 cells in response to exposure to 40°C. These results indicate a role of WIP in the regulation of the lipid composition involved in the response to febrile temperatures in THP-1 cells and possibly in other myeloid cells.

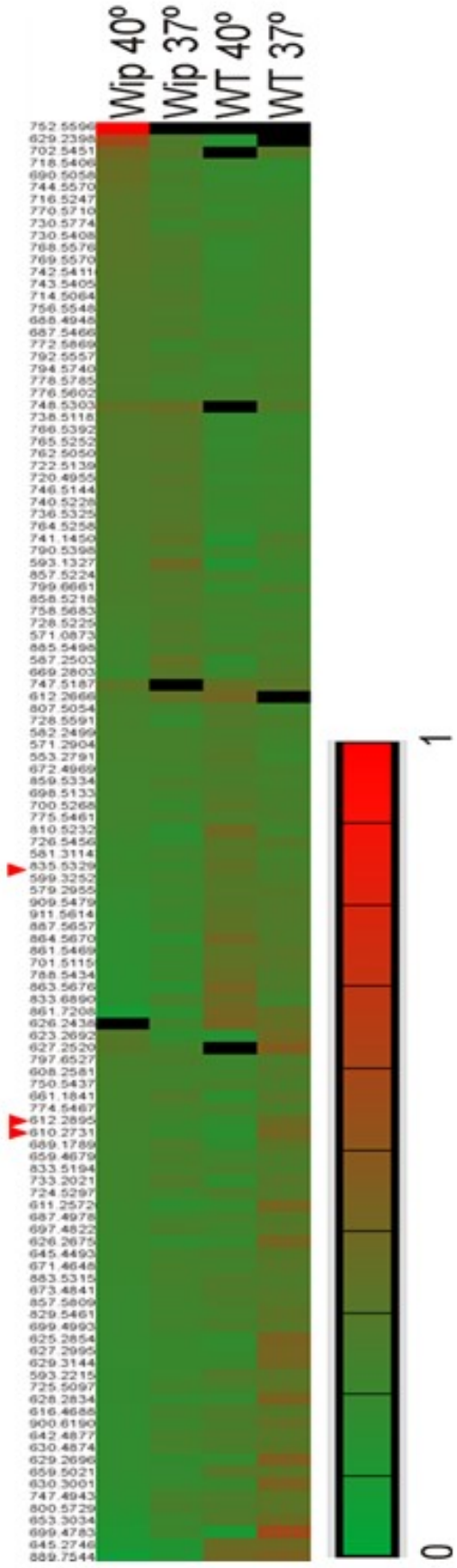

Figure 4.1. Changes in lipid composition in THP-1 cells regulated by WIP and by exposure to mild hyper thermic febrile temperatures.

Lipidomics analysis of membrane extracts of THP-1 parental and WIP KD cells seeded on fibronectin in the presence of 1ng/ml TGFβ-1 and incubated for 16 hours at 37°C and 40°C. Mean comparisons between the samples is shown in the Heatmap, where the sum of the z values of the peaks in each sample for each mass channel is normalized to sum one and the value of the relative amount of lipid for each sample at the corresponding mass channel is represented by a colour in a scale from close to zero (green) to 1 (red). 0 values are shown in black. Numbers on the left side identify the mass values of each peak. Arrows correspond to some of the peaks that significantly varied with temperature in the THP-1 parental cells and that appeared deregulated in WIP KD cells.

We performed the identification of three lipids whose levels were highly de-regulated in WIP KD THP-1 cells in comparison to parental THP-1 cells and that also changed levels in response to exposure to 40°C (Figure 4.1, red arrows). The identified lipids comprised two Phosphatidyl Inositol (PI) non-saturated derivatives, PI_24:6 and PI_24:5 whose levels decreased in parental THP-1 cells (Figure 4.2 A and 4.2 B) and one PI monounsaturated derivative (PI_34:1) whose levels increased in parental THP-1 cells when cultured at 40°C (Figure 4.2 C). These changes in saturation of fatty acids are common in response to higher temperatures in various plants (Larkindale and Huang, 2004): increasing the amount of saturated fatty acids and reducing the non-saturated ones to compensate the increase in membrane fluidity induced by mild hyperthermia.

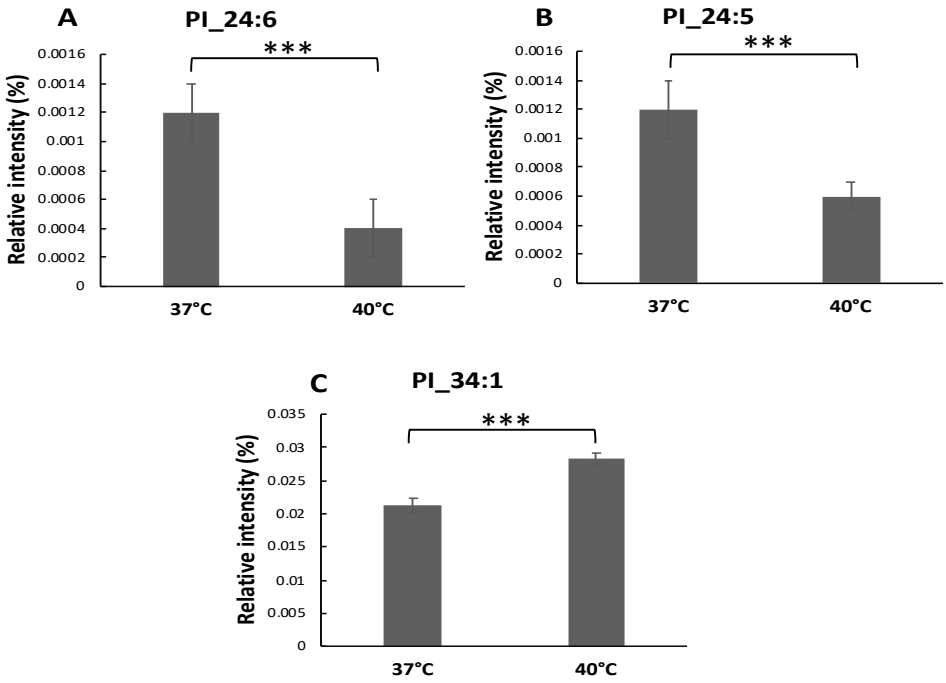

Figure 4.2. Examples of lipid changes in THP-1 cells exposed to hyperthermia.

Bar graphs are showing average and SD of relative peaks intensity obtained in the main significant lipids changing levels in parental THP-1 cells in response to exposure to 40C that where deregulated and did not vary in levels at 40C in WIP KD cells, pointed with red arrows in Figure 4.1. THP-1 cells responded to mild hyperthermia (exposure to 40°C) by decreasing the levels of **(A)** PI_24:6 and **(B)** PI_24:5, two lipids containing non-saturated fatty acids and increasing the levels of **(C)** PI_34:1, a long lipid containing saturated fatty acids *(p***<0.001).*

4.4.2 WIP regulates the fluidity of the plasma membrane at adhesion sites in resting myeloid cells and in response to activation by mild hyperthermia

The cell membrane is an intricate structure, whose main constituents are phospholipids and cholesterol. Fluidity studies can be performed by electron spin resonance, nuclear magnetic resonance and fluorescence anisotropy (8). In this section, we performed a study of cell membrane fluidity by indirectly measuring molecules diffusion using Raster Image Correlation Spectroscopy (RICS) and lipid packing using polarity sensitive dyes (generalized polarization, GP). We hypothesized that the observed WIP-dependent changes in the lipid composition of the plasma membrane may correlate with variations in homeostasis of membrane fluidity that may be related to the increased migration velocity and adhesions turnover observed in parental cells exposed to mild hyperthermia.

In order to determine the possible role of WIP in regulating fluctuations in membrane fluidity, we analysed the lipid spatiotemporal diffusion in THP-1 and WIP KD THP-1 cells at 37°C and 40°C by using RICS. RICS analysis was performed on two different cell planes: basal (region of cell adhesion to the substrate) and apical. Clear differences in diffusion were found between parental and WIP KD cells in the basal adhesion plane. WIP KD THP-1 cells presented a more rigid basal adhesion plane with a diffusion coefficient almost two-fold lower as determined by RICS analysis (Figure 4.3A Figure 4.4) and a significantly 5-fold higher GP index (Figure 4.4) when compared to parental cells.

The effect of mild hyperthermia on lipid diffusion in parental and WIP KD cells was then compared. Incubation of THP-1 parental cells at 40°C resulted in a tendency of an increase in the diffusion index that was not statistically significant as determined by RICS analysis using confocal microscopy (Figure 4.3A, 4.5), while STED

microscopy underlined a small but significant increase in diffusion (diffusion coefficient increased from 1.2 to 1.5) (Figure 4.3B). Unlike parental cells, WIP KD cells responded to incubation at 40°C by increasing lipid diffusion, with a higher significant increase of 1.8-fold in diffusion vs a 1.2-fold increase detected in parental THP-1 cells using confocal microscopy (Figure 4.3A, Figure 4.5).

In addition, RICS analysis allows extracting information on diffusion coefficient at specific regions of interest. Thanks to SiR-actin staining, we were able to clearly visualize podosomes regions in parental cells and compare lipid diffusion associated to different actin structures. In particular, we found lipids in regions associated with podosomes to have a significantly higher coefficient of diffusion compared to regions without podosomes (Figure 4.3C, Figure 4.4, Figure 4.5). In Figure 4.4, ROIs “i” and “ii” in THP-1 cells represent regions with podosomes, showing higher diffusion compared to regions “iii” and “iv”, without podosomes. In Figure 4.5, ROIs “iii” and “iv” in THP-1 cells represent regions with podosomes, showing higher diffusion compared to regions “i” and “ii”, without podosomes.

Furthermore, the changes in fluidity observed on the overall basal plane in WIP KD cells vs parental cells were also observed when we analysed smaller selected regions. At 40°C, parental cells maintained the distinction in diffusion observed between podosomal and non-podosomal regions at lower temperatures (Figure 4.3C, D). However, in WIP KD cells lipid diffusion observed in smaller regions selected randomly increased by 2.2-fold after incubation at 40°C in a similar way as the one observed in the total basal plane region (Figure 4.3D, 4.4, 4.5). Despite this major increase in lipid diffusion in WIP KD cells in response to raised temperatures, these values remained lower in comparison to parental cells (Figure 4.3 D). No statistically

significant differences were observed at the apical region between parental THP-1 and WIP KD cells at 37°C or upon exposure to 40°C in (Figure 4.3E, Figure 4.6).

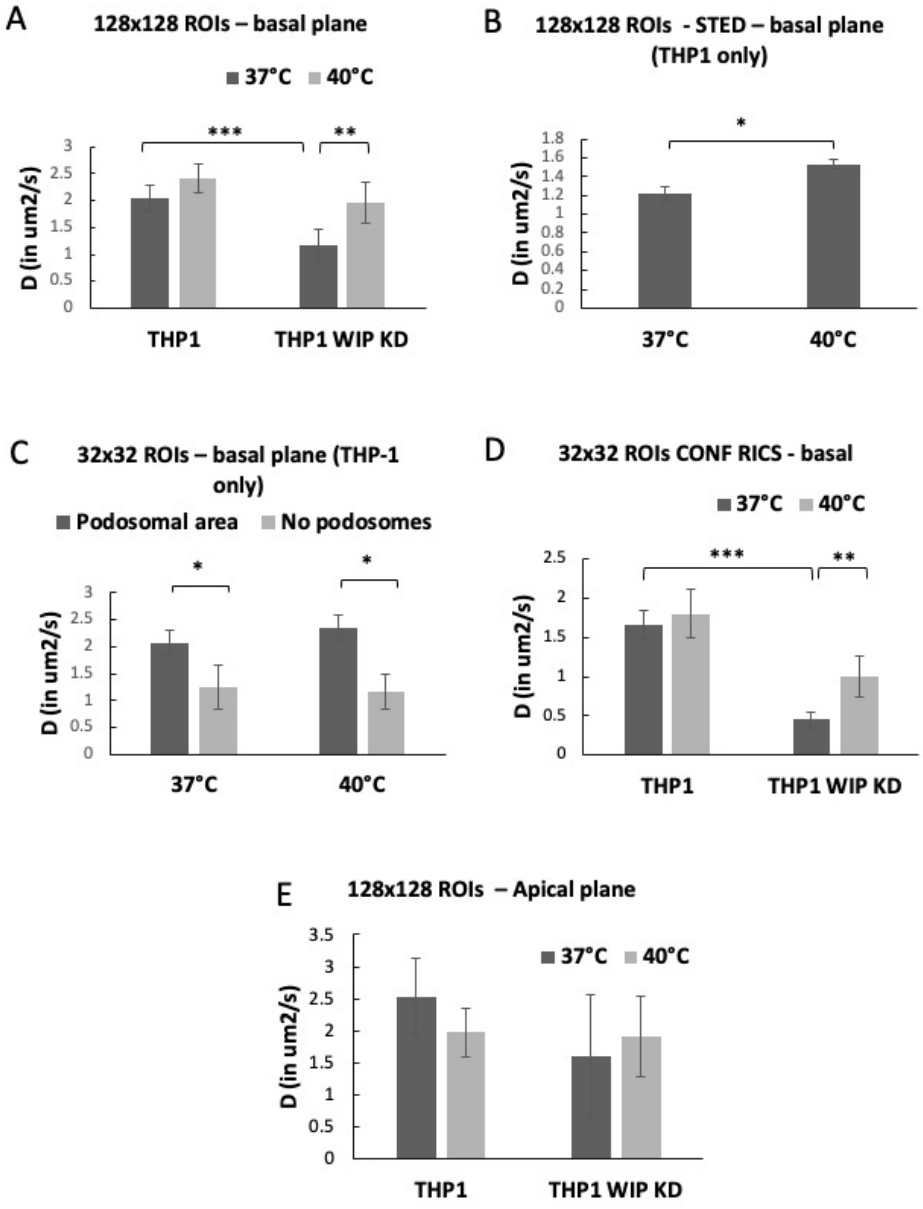

Figure 4.3. Bar graphs show average and SE of the coefficient of diffusion (D) obtained with laser scanning imaging *(RICS).*

RICS analysis was performed over 200 frames (approximately 7 minutes) and coefficient of diffusion was averaged from at least 5 cells per condition. (A) Histogram compares diffusion in parental and WIP KD cells at 37°C and 40°C on the cell basal plane in 128x128 ROIs using confocal laser scanning microscopy; (B) Histogram compares diffusion in parental cells at 37°C and 40°C on the cell basal plane in 128x128 ROIs. Only in this case cells were imaged using STED microscopy; (C) Histogram compares diffusion in parental cells between podosomal and non podosomal 32x32 ROIs at 37°C and 40°C; (D) Histogram compares diffusion between parental and WIP KD cells at 37°C and 40°C on the cell basal plane in 32x32 ROIs; (E) Histograms compare diffusion between parental and WIP KD cells at 37°C and 40°C on the cell apical plane in 128x128 ROIs;

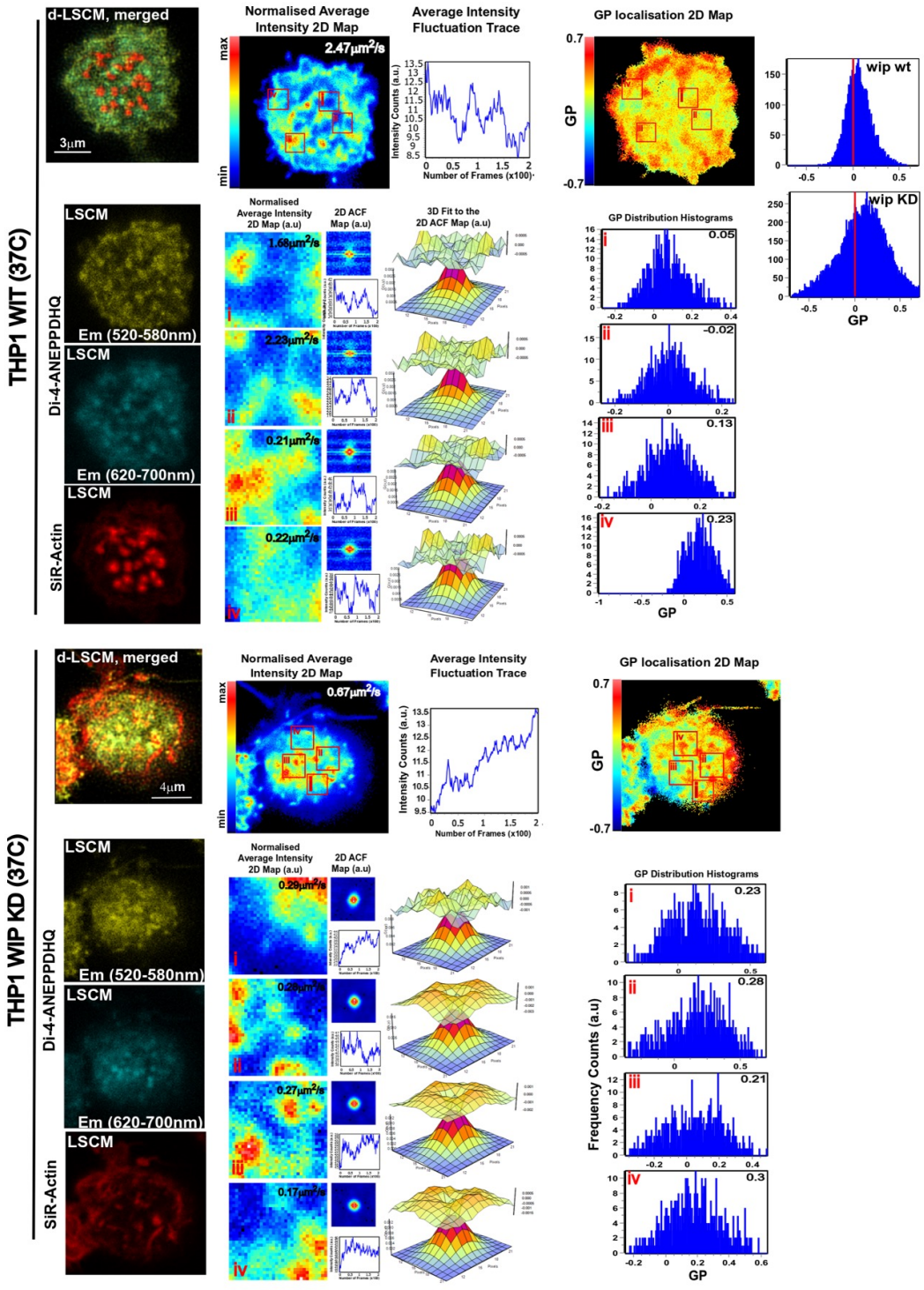

Figure 4.4. RICS and GP analysis on THP-1 and WIP KD THP-1 at 37°C on the basal plane.

THP-1 and WIP KD THP-1 cells were grown for 24h on fibronectin coated chambers and stained with 1μM di-4-ANEPDHQ (ThermoFisher Scientific) in the presence of 1ng/ml TGFβ-1. The following day cells were stained with 1μM SiR-Actin (Spirochrome) and incubated for 1 hour before imaging at 37°C. RICS analysis was performed over 200 frames, while 5 frames per cell were averaged in the GP analysis. From the left: laser scanning confocal microscope merged di-4-ANEPDHQ and SiR-actin images (separated images shown below), representative normalized intensity maps (below: normalized intensity 2D map, 2D autocorrelation function (ACF) maps and average intensity fluctuation traces for

each 32x32 pixels ROIs in which ROIs i and ii in the THP-1 cells represents regions with podosomes and ROIs iii and iv represents regions without podosomes), average intensity fluctuation traces (below: fit to ACF for each 32x32 pixels ROIs), GP Localization 2D map (below: GP distribution histograms in each 32x32 pixels ROIs) and GP distribution histograms in the whole THP-1 (top) or WIP KD THP-1 cell (bottom). Both analyses show distinct lipid fluidity properties among the two cell lines, indicating a higher fluidity in parental cells. In particular, non podosomal areas (ROIs iii and iv in THP-1 WT) resulted to be more packed and organized compared to regions presenting podosomes.

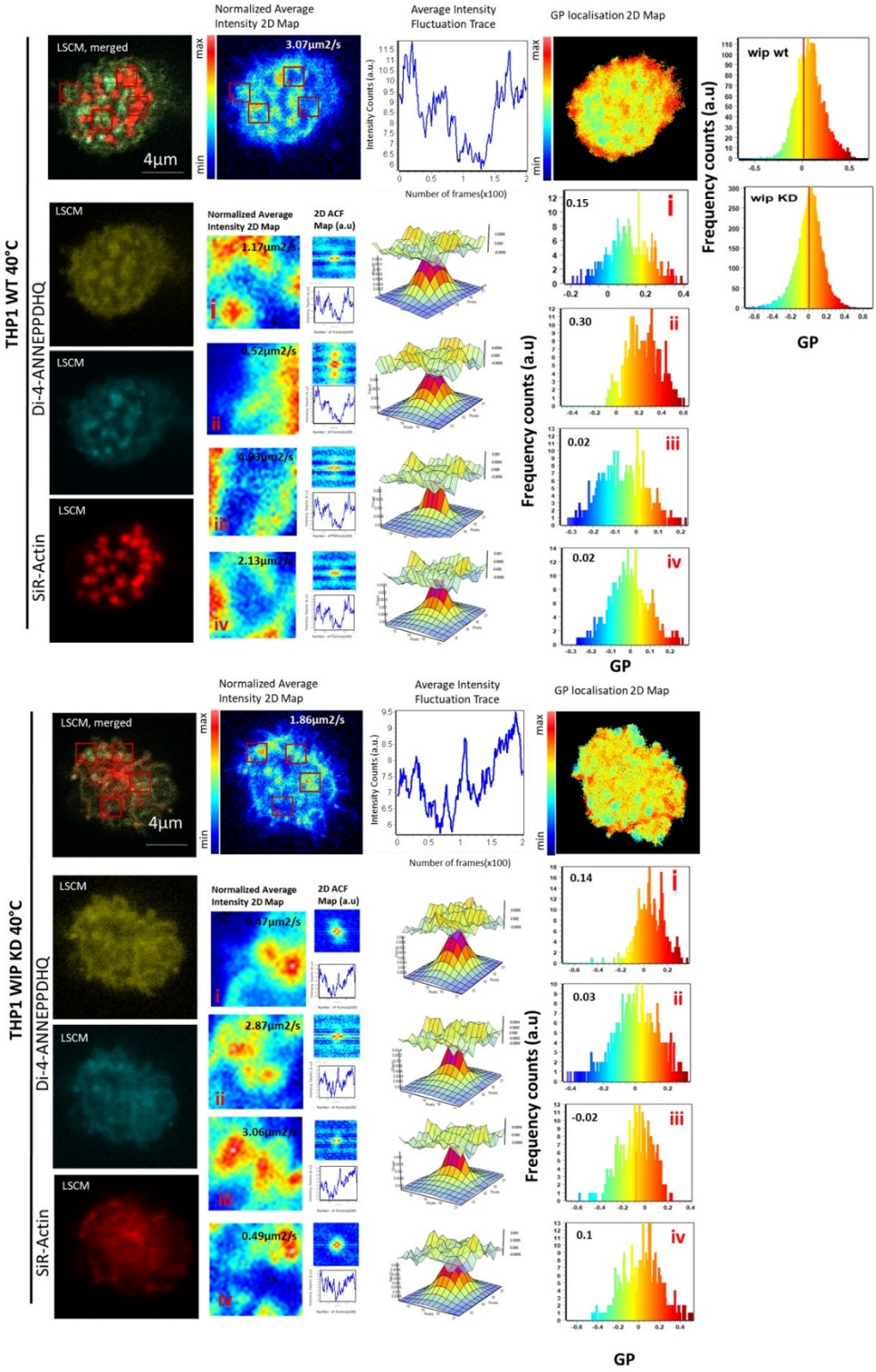

Figure 4.5. RICS and GP analysis on THP-1 and WIP KD THP-1 cells exposed to mild hyperthermia (40°C) in the basal plane.

THP-1 and WIP KD THP-1 cells were grown for 24h on fibronectin coated chambers and stained with 1 µM di-4-ANEPDHQ (ThermoFisher Scientific) in the presence of 1 ng/ml TGFβ-1. The following day cells were stained with 1 µM SiR-Actin (Spirochrome) and incubated for 1 hour before imaging at 37°C. RICS analysis was performed over 200 frames, while 5 frames per cell were averaged in the GP

analysis. From the left: laser scanning confocal microscope merged di-4-ANEPDHQ and SiR-actin images (separated images shown below), representative normalized intensity maps (below: normalized intensity 2D map, 2D autocorrelation function (ACF) maps and average intensity fluctuation traces for each 32x32 pixels ROIs in which ROIs iii and iv in the THP-1 cells represents regions with podosomes and ROIs i and ii represents regions without podosomes), average intensity fluctuation traces (below: fit to ACF for each 32x32 pixels ROIs), GP Localization 2D map (below: GP distribution histograms in each 32x32 pixels ROIs) and GP distribution histograms in the whole THP-1 (top) or WIP KD THP-1 cell (bottom). Both RICS and GP analysis in parental cells showed no difference compared to previous observations at 37°C, while WIP KD THP-1 cells significantly increased diffusion and decreased general polarization, indicating a role of temperature in incrementing fluidity only in the WIP KD cells.

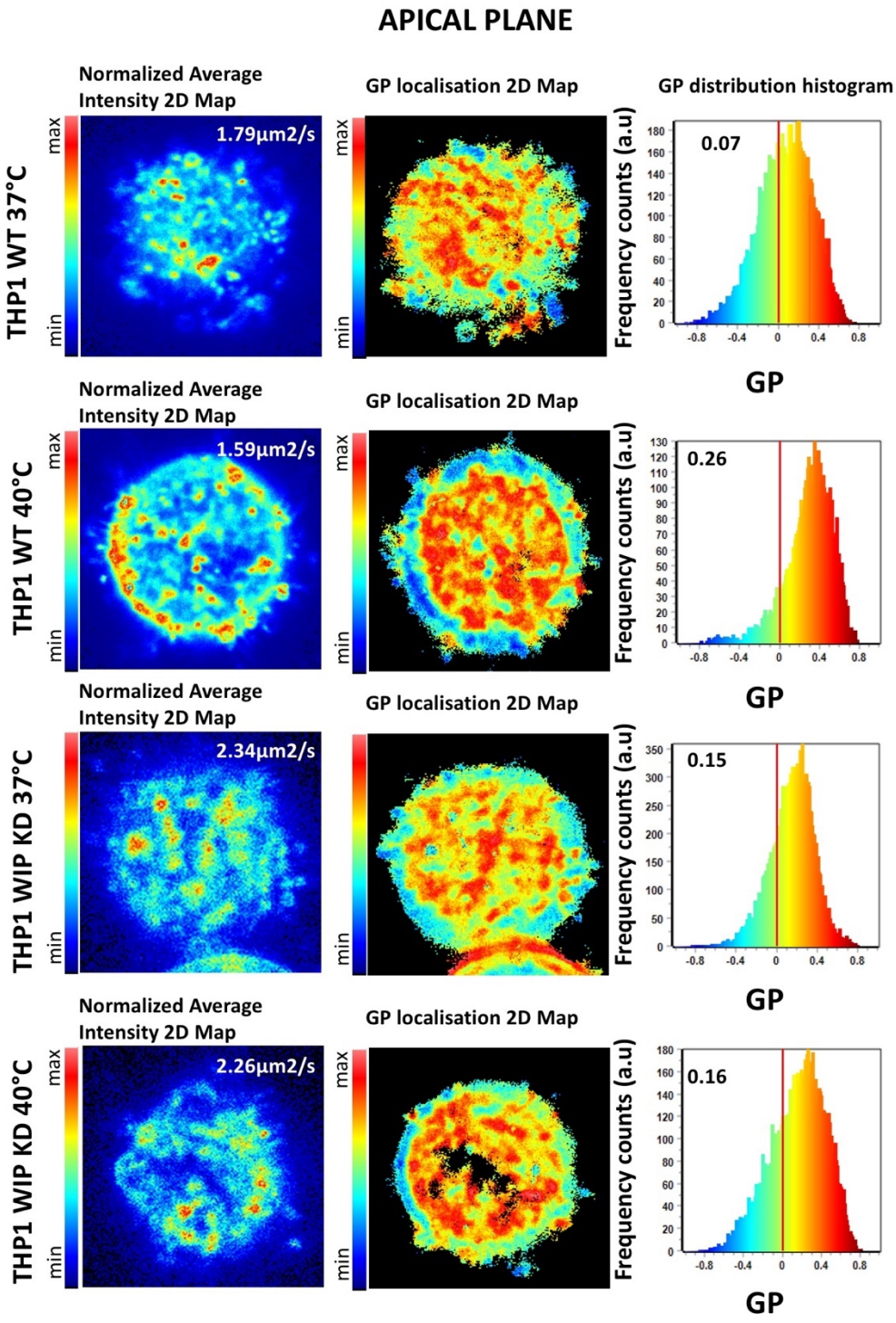

Figure 4.6. RICS and GP analyses show no difference in lipids behaviours at the apical plane in THP-1 and WIP KD THP-1 cells exposed to hyperthermia.

THP-1 and WIP KD THP-1 cells were grown for 24h on fibronectin coated chambers and stained with 1 µM di-4-ANEPDHQ (ThermoFisher Scientific) in the presence of 1 ng/ml TGFβ-1. The following day cells were stained with 1µM SiR-Actin (SPIROCHROME) and incubated for 1 hour before imaging at 37°C or 40°C. RICS analysis was performed over 200 frames, while 5 frames per cell were averaged in the GP analysis. From the left: representative maximum intensity projection maps and coefficient of diffusion, GP Localization 2D map and GP distribution histogram.

All the results obtained by RICS analysis were then correlated with further data on GP of the cell membrane by staining with a polarity-sensitive dye, di-4-ANEPPDHQ, whose emission spectrum depends on the lipid lateral packing and water content. GP studies allowed to reveal the different membrane fluidity and dynamic properties in each condition in a more consistent manner. In cell membranes, the polarity depends on the hydration level of the bilayer. Packed membranes are formed by highly saturated fatty acids, allowing a low water content (GP high) in between phospholipids' adjacent polar head groups while highly disordered membranes, rich in unsaturated fatty acids, results in less packed phospholipid and, in turns, in higher water content (GP low). The di-4-ANEPPDHQ dye presents two kinds of emission with a 60-nm emission shift from a liquid-ordered to a liquid-disordered phase and was used to calculate the GP. The data obtained with the GP analysis validated the diffusion data acquired by RICS, as there is a direct correlation between high membrane order or lateral packing and low lateral diffusion.

WIP KD cells showed higher GP, corresponding to a higher level of lipid packing compared to parental cells (Figure 4.4, 4.5, 4.7A). After exposure to hyperthermia parental cells decreased the GP value at the basal end slightly but not significantly in both confocal (Figure 4.4, 4.5, 4.7A) and STED microscopy (Figure 4.7B) while WIP KD cells became more fluidic in response to hyperthermia in the total basal region (Figure 4.4, Figure 4.5, 4.7A).

Similarly to the results obtained using RICS, podosomal regions presented lower GP values indicating higher membrane fluidity compared to other actin regions devoid of podosomes and these differences were sustained at the same level when cells were incubated at 40°C (Figure 4.7C). Additionally, the analysis of smaller regions of interest at the basal level in WIP KD cells showed higher GP values in comparison to

parental cells (Figure 4.7D) reflecting a higher level of lipid packaging and reduced membrane fluidity. In response to increased temperature, while parental cells sustained the GP values indicating a tight control of homeostasis of lipid packaging, WIP KD cells showed a significant decrease in GP. No significant differences or changes in GP were observed between parental and WIP KD cells or in response to increase temperature at the apical plane (Figure 4.7E).

Taken together, the results using RICS and GP analysis show that the lack of WIP results in lower fluidity of the cell membrane in areas of attachment. Additionally, in response to mild hyperthermia, our data show that WIP is required to counteract the increase in fluidity induced by increased temperatures in order to sustain the adequate levels of membrane fluidity at adhesion sites.

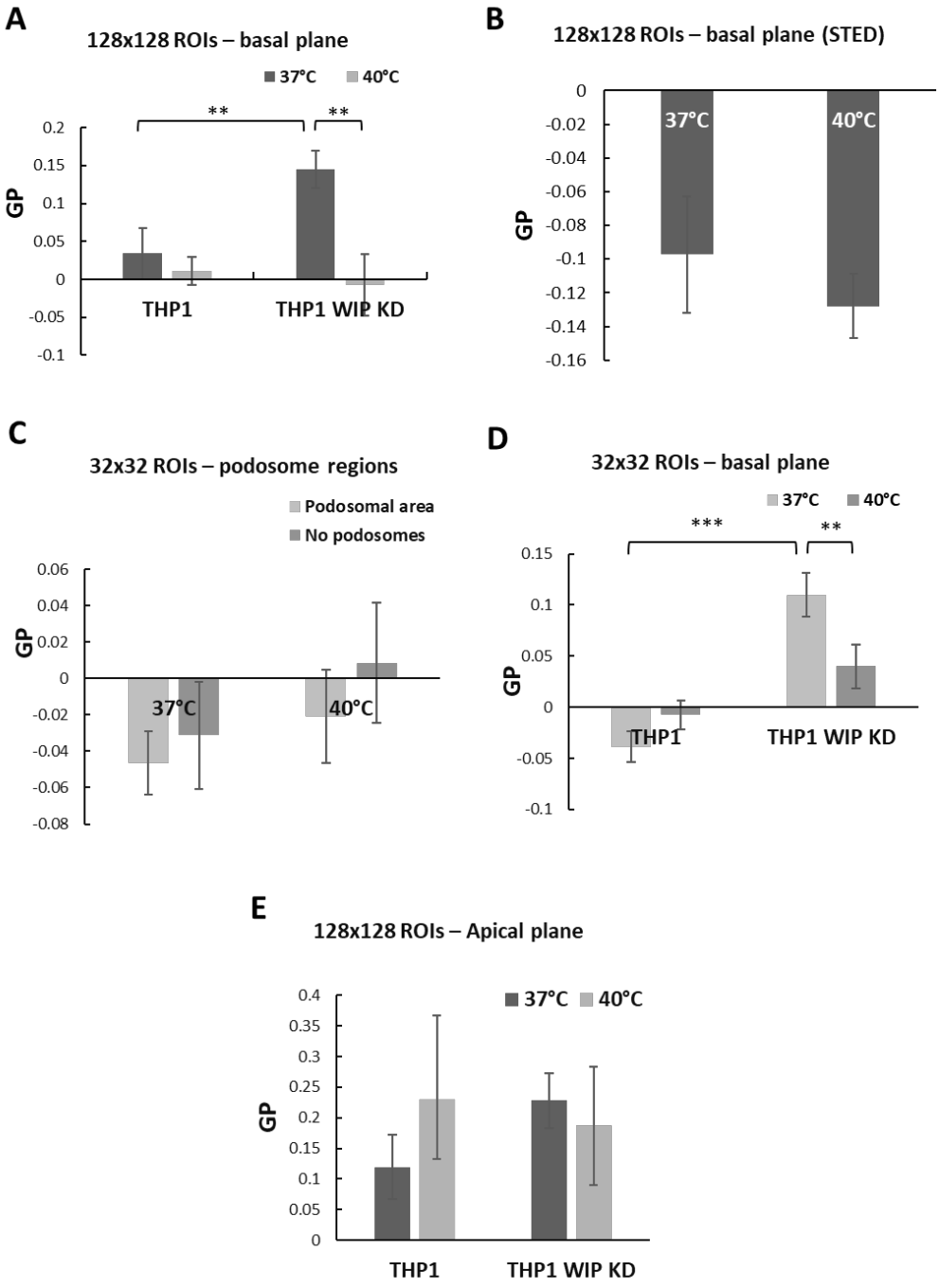

Figure 4.7. Bar graphs show average and SE of the General Polarization (GP) index obtained analysing at least 5 cells per condition after staining with di-4-ANEPDHQ.

GP analysis was performed averaging 5 frames per cell. (A) Histogram compares GP between parental and WIP KD cells at 37°C and 40°C on the cell basal plane in 128x128 ROIs; (B) Histogram compares GP between parental cells at 37°C and 40°C on the cell basal plane in 128x128 ROIs. Only in this case cells were imaged using STED microscopy; (C) Histograms compare GP in parental cells between podosomal and non podosomal 32x32 ROIs at 37°C and 40°C; (D) Histogram compares GP between parental and WIP KD cells at 37°C and 40°C on cell basal plane in 32x32 ROIs; (E) Histogram compares GP between parental and WIP KD cells at 37°C and 40°C on the cell apical plane in 128x128 ROIs;

4.4.3 Membrane fluidizing drugs induce changes in migration mimicking mild hyperthermia

Taken together, our results so far show that incubation of THP-1 cells at 40°C, significantly increase cell migration and promotes an invasive phenotype. This correlates with a WIP-dependent maintenance of membrane homeostasis that would counteract the increase in membrane fluidity promoted by exposure to higher temperatures. Since changes in membrane fluidity have been proposed as a mechanism for thermosensing (Saita and de Mendoza, 2015), we hypothesised that exposure of myeloid cells to hyperthermia will result in an initial increase in membrane fluidity that in turn will trigger cell migration while counteracting membrane fluidity to maintain membrane homeostasis.

To test this hypothesis, we studied whether by increasing membrane fluidity with membrane fluidizer compounds, the migration and matrix degradation capabilities of THP-1 parental cells would also increase.

We first optimised the concentration of the chosen compounds and evaluated their possible toxic effect in our cultures. We initially found that concentrations of Benzyl Alcohol higher than 5 mM, as used to increase membrane fluidity in a similar way than during a thermal shift up to 42°C (Balogh *et al.*, 2005), would cause cell detachment from fibronectin coated substrates resulting, therefore, impossible to be used for migrations studies with THP-1 cells. Following this finding, we decided to evaluate cell viability after 1-hour treatment with Benzyl Alcohol concentrations lower than 5 mM in cells grown in the presence or absence of 10% FCS. Those conditions were chosen to mimic the conditions that would be later used to perform migration and transmigration experiments. We tested growing concentrations of Benzyl Alcohol, from 0.5 mM to 5 mM, and found that, in all the cultures, THP-1 cells

showed viability higher than 90%, perfectly comparable to the one obtained when cells are cultured in the absence of the drug. Furthermore, culturing cells in serum free medium for one hour did not affect cell viability (Figure 4.8). We also investigated the effect of Arimoclomol on cells detachment and found that 1 μM was the maximum permissive concentration to be used in our experiments.

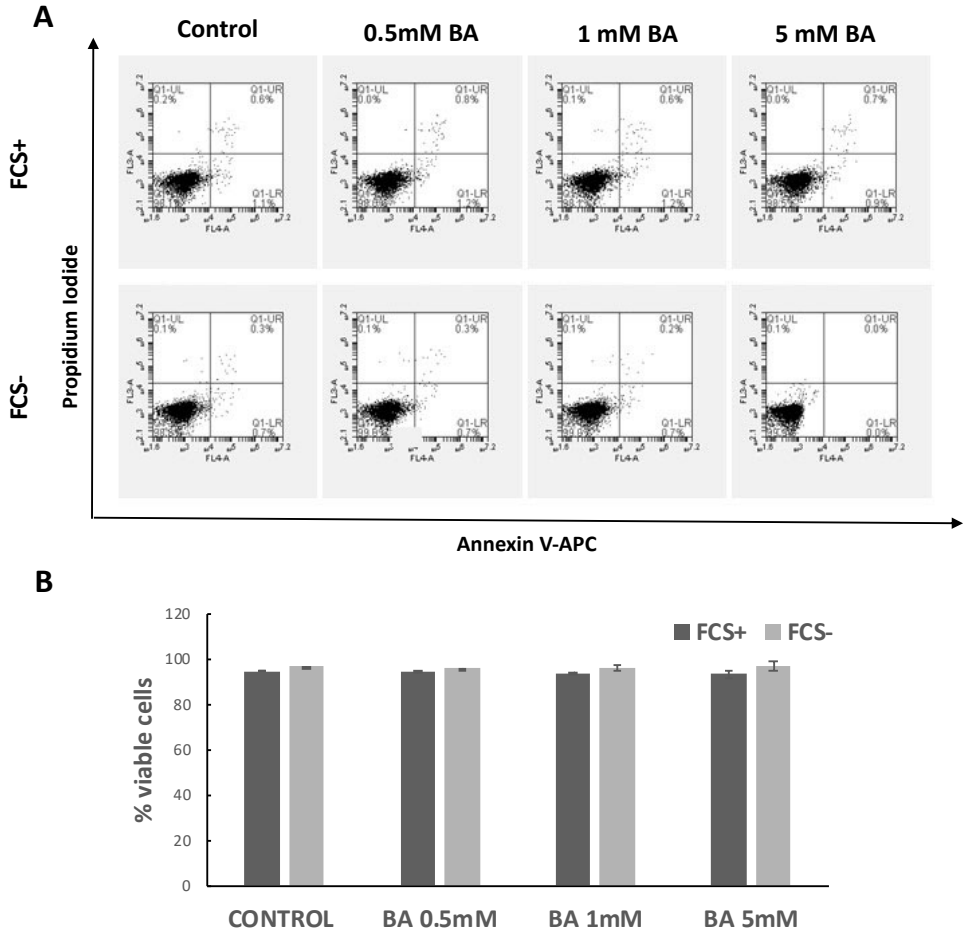

Figure 4.8. Analysis of viability of THP-1 cells incubated in RPMI with or without 10% FCS after 1hour treatment with Benzyl Alcohol (BA).

(A) Flow cytometry histograms show the percentage of apoptotic (Annexin V-APC positive) and necrotic (Propidium Iodide positive) cells in THP-1 cells treated for 1hr with Benzyl Alcohol; (B) Histograms show the average and SE of the percentage of viable (Annexin V and PI negative populations) THP-1 cells cultured in medium containing or not serum and treated for 1 hour with Benzyl Alcohol. In all the conditions, THP-1 cells showed viability of above 90% in the cultures.

We previously showed that monocytic cells expressing WIP migrated significantly faster and covered a longer distance after exposure to mild hyperthermia (40°C). In this experiment, we aimed to evaluate the effect of membrane fluidity perturbation on THP-1 migration. For this purpose, we filmed parental cells for two hours after treatment with the indicated drug concentrations and we were able to demonstrate that both Benzyl Alcohol (Figure 4.9) and Arimoclomol (Figure 4.10) increased the migratory capability of THP-1 cells in terms of velocity and distance travelled in a concentration dependent manner. When treated with Benzyl Alcohol the migratory boost resulted to be concentration dependent, while maximal cell response to Arimoclomol was obtained at a concentration of 0.5μM.

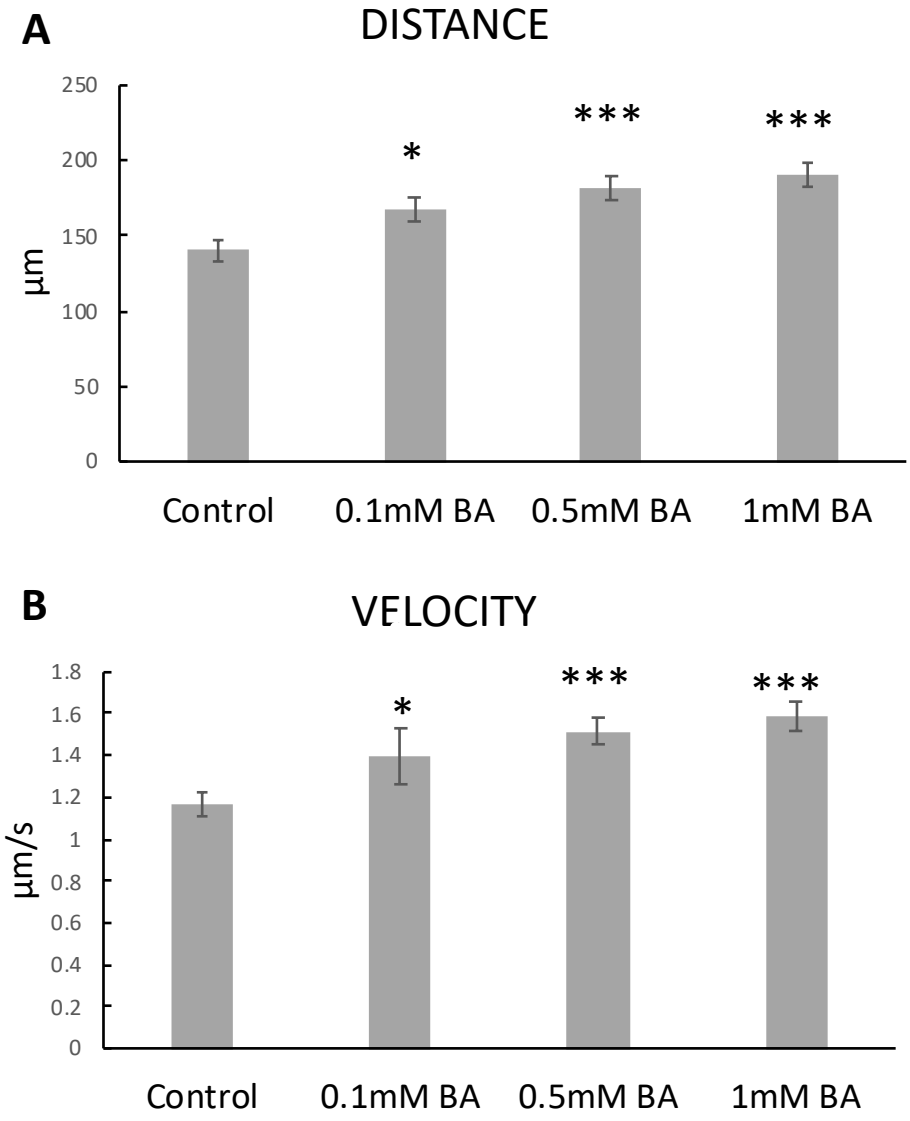

Figure 4.9. Analysis of THP-1 cells migration (velocity and distance travelled) in response to Benzyl Alcohol treatment.

THP-1 cells were seeded on fibronectin-coated plates in the presence of 1 ng/ml TGFb1 and incubated for 16 hours with different Benzyl Alconol concentrations. The following day, time lapse videos of cells were generated by taking phase contrast micrographs every minute for 2 hours at 37°C (A) Histogram shows the average and SE of the total distance travelled in two hours by tracked cells; (B) Histogram shows the average and SE of cell velocity (µm/second) of tracked cells (n>60). t-student test vs control group (*P<0.05, **P<0.01, ***P<0.001);

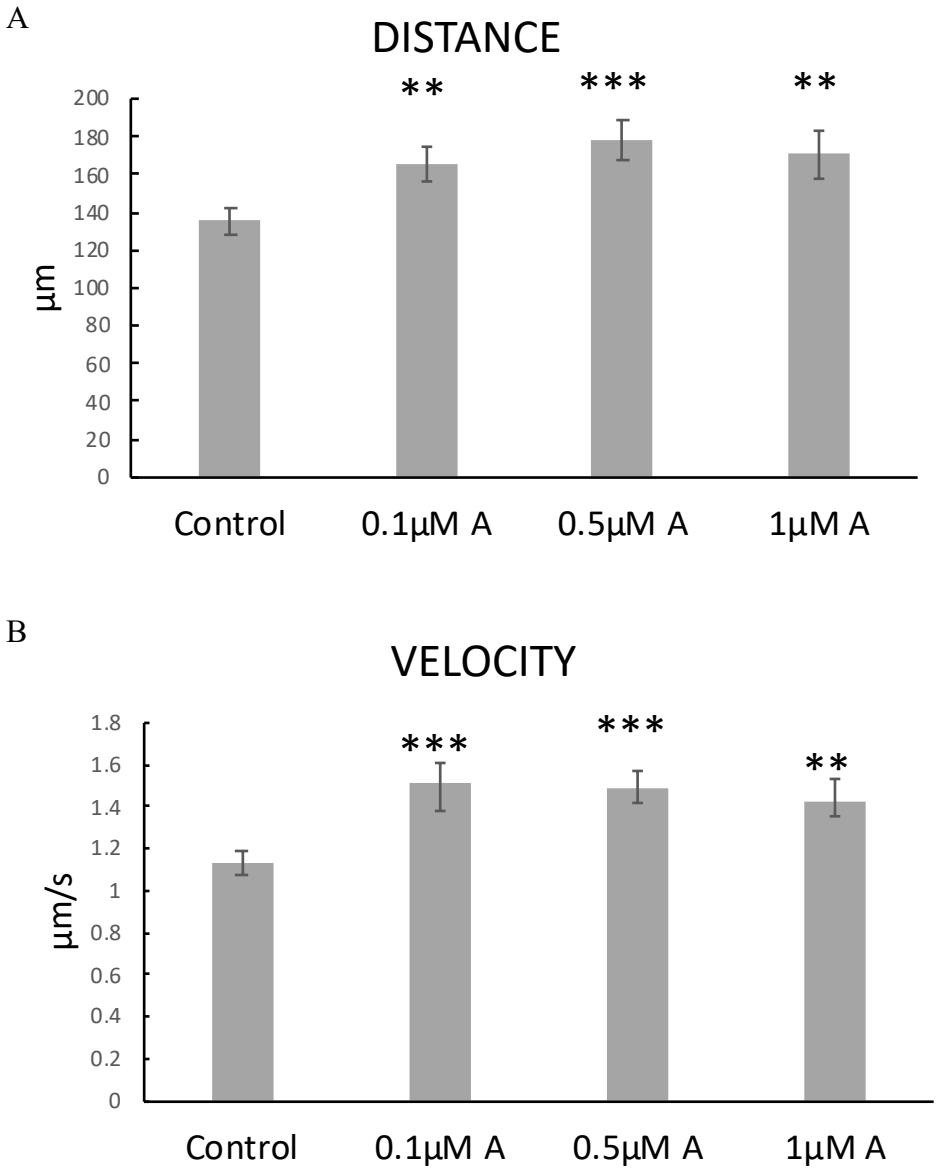

Figure 4.10. Analysis of THP-1 cells migration (velocity and distance travelled) in response to Arimoclomol treatment.

THP-1 cells were seeded on fibronectin-coated plates in the presence of 1 ng/ml TGFb1. After 6 hours, Arimoclomol was added to the culture at different concentrations and cells were incubated for 16 hours. The following day, time lapse videos of cells were generated by taking phase contrast micrographs every minute for 2 hours at 37°C. (A) Histogram shows the average and SE of the total distance travelled in two hours by tracked cells; (B) Histogram shows the average and SE of cell velocity (µm/second) of tracked cells (n>60). t-student test vs control group (**P<0.01, ***P<0.001);*

Furthermore, we evaluated THP-1 cells ability to transmigrate in the presence of the chemoattractant MCP-1 after 1-hour treatment with different concentrations of Benzyl Alcohol. The basal chemotaxis of THP-1 cells to MCP-1 was significantly increased by the pre-incubation with 1- and 5-mM Benzyl Alcohol in a concentration dependent-manner, indicating a role of membrane of fluidity in enhancing chemotaxis (Figure 4.11) as well as the general capacity for migration.

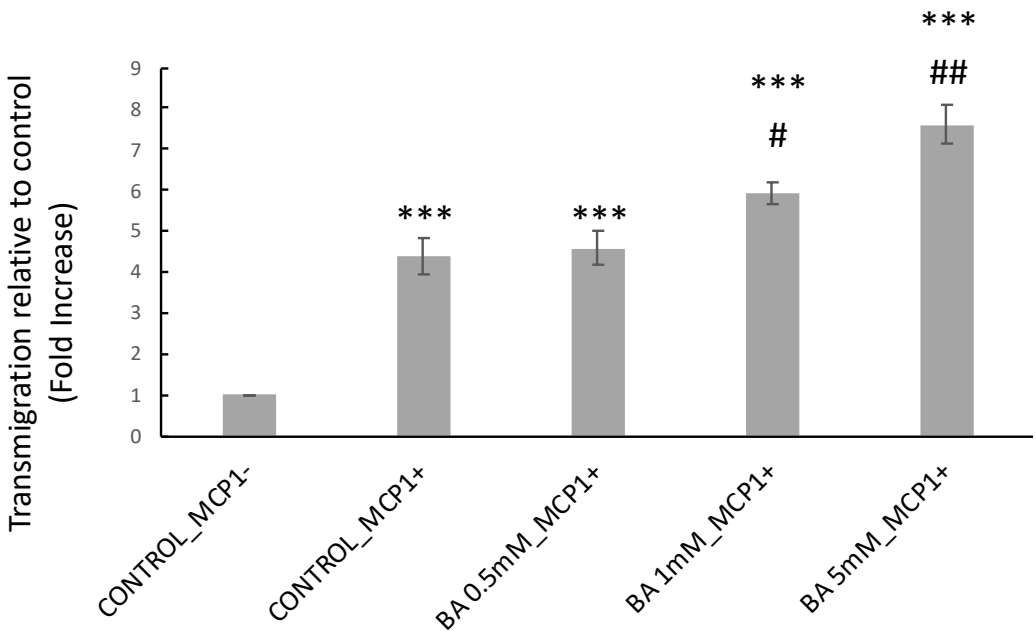

Figure 4.11. Chemotaxis towards MCP-1 of THP-1 cells treated with Benzyl Alcohol.

Bar graph shows average and SE of the percentage of transmigrated cells towards the bottom of the well in each condition. Incubation of THP-1 cells with 1 mM or 5 mM Benzyl Alcohol (BA) enhanced chemotaxis of THP-1 cells towards MCP-1, while no significant difference was found at 0.5mM BA. Data are representative of 4 biological replicates. Unpaired t-Student test was applied. #, t-student test vs control group MCP+; * t-student test vs control group MCP-1 (***P<0.001, #P<0.05, ##P<0.01).

Another striking effect observed when incubating cells at 40°C was the increment in the number of cells able to form podosomes. Podosomes are fundamental for movement of myeloid cells as they are needed to establish an anchor to the substratum to gain directionality and start migration (Linder *et al.*, 2005). We analysed podosome formation in THP-1 cells treated with increasing concentrations of Benzyl Alcohol and Arimoclomol and not surprisingly we found that, as after hyperthermia, the

observed enhancement in migration potential corresponded to a rise in the number of cells presenting podosomes (Figures 4.12 and 4.13). The more significant outcomes were observed after 16 hours treatment with 1 μM Arimoclomol (more than 10% increase in the number of cells assembling podosomes) and 1-hour treatment with 0.5 mM Benzyl Alcohol (almost 20% increase in the number of cells assembling podosomes) (Figure 4.13).

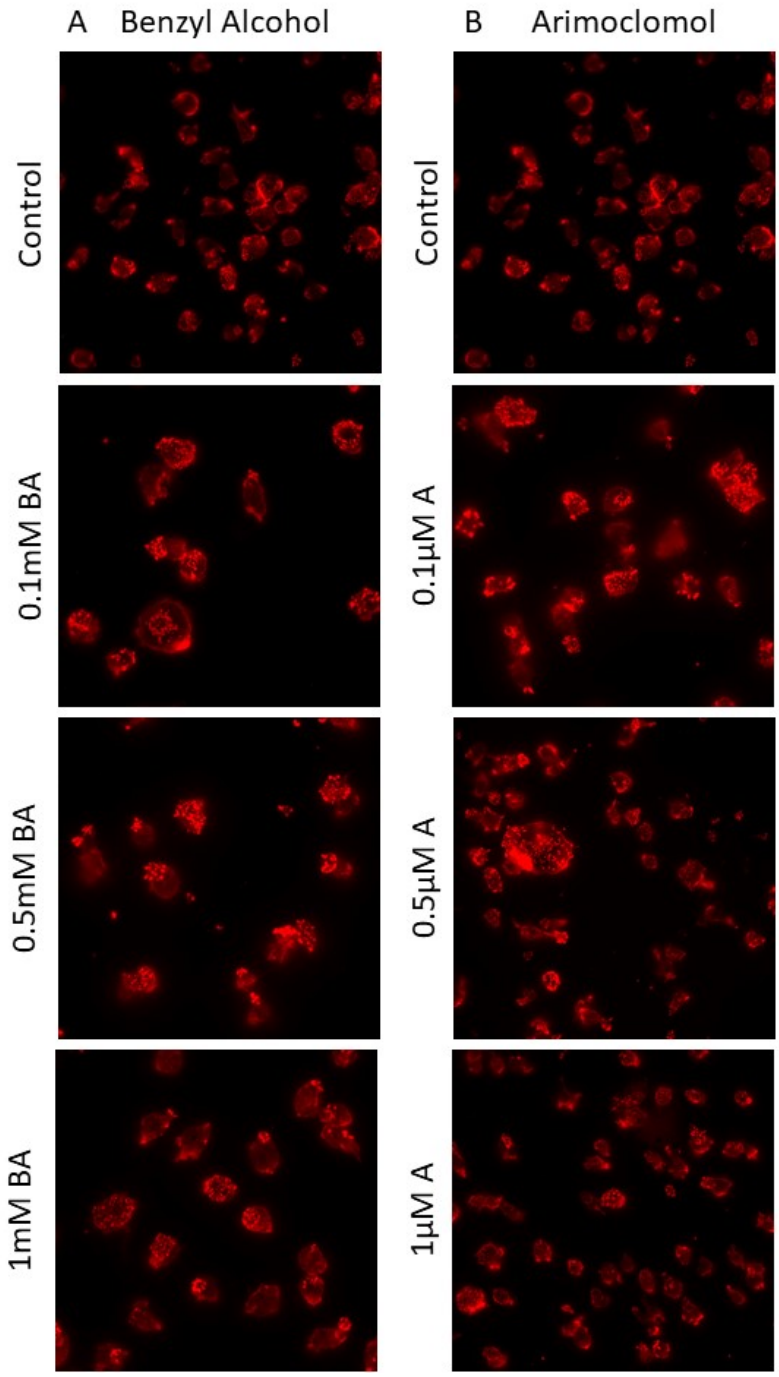

Figure 4.12. Representative micrographs showing podosomes formation after 1hour treatment with Benzyl alcohol or 16 hours treatment with Arimoclomol in THP-1 cells.

(A) THP-1 cells were cultured for 16 hours at 37°C on fibronectin coated coverslips in the presence of 1 ng/ml TGFβ-1. The following day cells were treated for one hour with different concentration of Benzyl Alcohol (BA) and then fixed and stained with Alexa 568 nm-labelled phalloidin. Micrographs show filamentous actin distribution in one representative field for each condition (Bar 10 um); (B) THP-1 cells were cultured at 37°C on fibronectin coated coverslips in the presence of 1 ng/ml TGFβ-1. Following cells adhesion to the substrate (6h), cells were incubated for 16 hours with different concentrations of Arimoclomol. The following day cells fixed and stained with Alexa 568 nm-labelled phalloidin. Micrographs show filamentous actin distribution in one representative field for each condition (Bar 10 um).

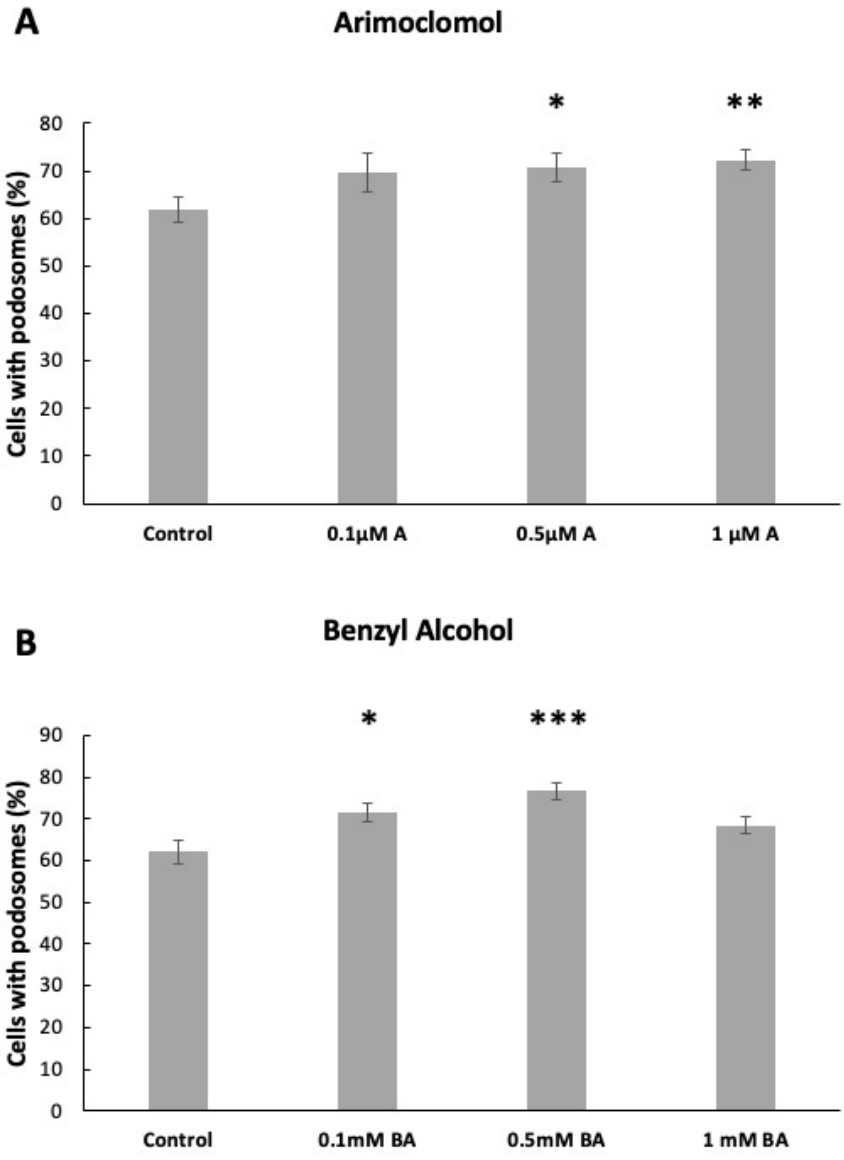

Figure 4.13. Analysis of podosomes formation in THP-1 cells after treatment with membrane fluidizer drugs, Arimoclomol and Benzyl Alcohol.

Quantitative analysis of number of cells with podosomes. Bar graph shows the average and SE of the number of cells with podosomes in THP-1 cultured for 16 hours at 37°C on fibronectin coated coverslips with 1ng/ml TGFβ and treated with different concentrations of (A) Arimocolomol (16 hours) or (B) Benzyl Alcohol (1 hour). Data were obtained analysing 10 fields, acquired from at least 2 different coverslips per condition at 60x magnification. *, t-student test vs control group (*P<0.05, *P<0.01, ***P<0.001);

Extracellular matrix degradation was also affected by membrane fluidity perturbation. Cells treated with 0.5 μM Arimoclomol showed significantly higher degradation capability and podosomes were perfectly localized in areas of degradation (Figure 4.14, 4.15). Although more podosomes were assembled at 1 μM Arimoclomol, degradation appeared in equal measure as in the control. Therefore, we hypothesized that podosomes might not be totally functional at this concentration, as they look thinner and cells size was slightly reduced.

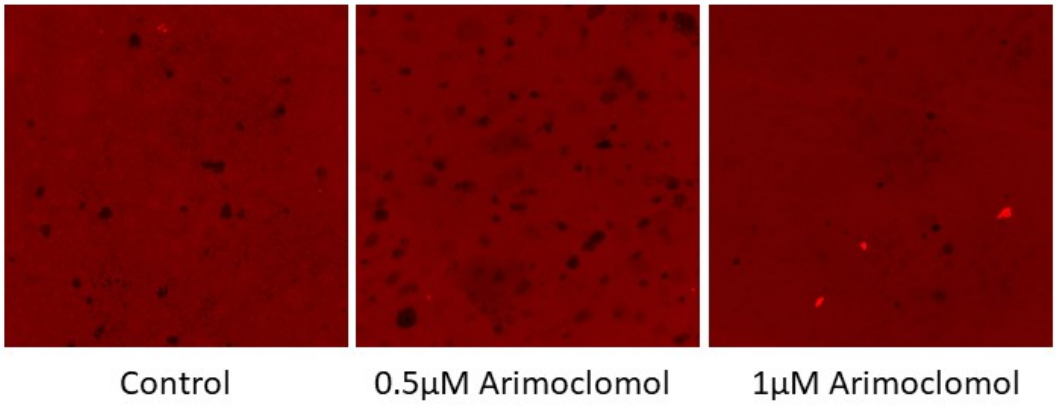

Figure 4.14. Representative fluorescent images of gelatin degradation by THP-1 treated with Arimoclomol.

THP-1 cells were cultured on red fluorescent gelatin coated coverslips with 1ng/ml TFGβ1 and allowed to adhere to the substrate. After 6 hours incubation at 37°C, 0.5 μM or 1 μM Arimoclomol was added to the cells. Treatment was performed for 16 hours at 37°C and followed by cells fixation and staining. Matrix degradation is visualized as an area devoid of fluorescence. Images are representative of matrix degradation in each condition. Images were acquired using a 60x objective.

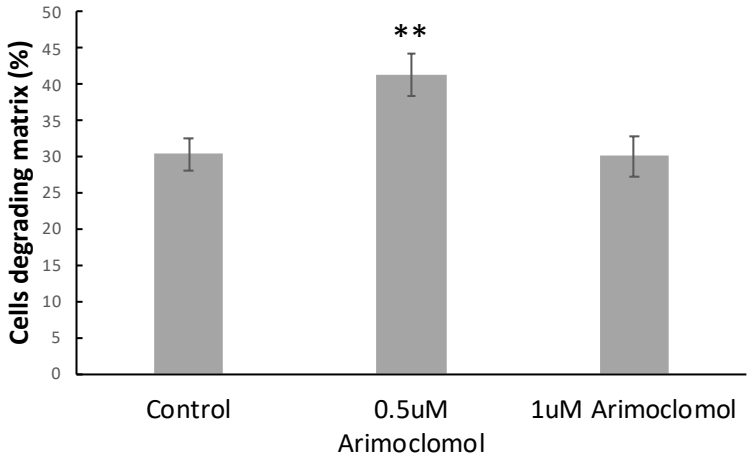

Figure 4.15. Quantitative analysis of THP-1 cells degrading matrix after treatment with Arimoclomol.

Bar graph shows the average and SE of the percentage of THP-1 cells presenting an area of gelatin degradation underneath after 16 hours treatment with different concentrations of Arimoclomol. Data were obtained from 10 fields acquired from at least 2 different coverslips per condition at 60x magnification. Graphs are representative of similar results obtained in three different experiments. Unpaired t test was applied. *, t-student test vs control group (**P<0.01);

4.4.4 Changes in mobility of membrane lipids of THP-1 cells in response to treatment with membrane fluidizing drugs

Finally, the effect of membrane fluidizer drugs on lipids mobility in parental and KD cells was investigated. THP-1 and WIP KD THP-1 cells were treated with membrane fluidizing drugs Benzyl Alcohol and Arimoclomol before analysis with laser scanning microscopy for possible changes in RICS and GP. The time point for analysis of RICS and GP was the same as for the analysis of the migratory and invasive properties of THP-1 cells in response to the same drugs, described above. Treatment of parental cells with either Benzyl Alcohol or Arimoclomol did not induce statistically significant changes in RICS or GP at the basal end of cells where they attach on the substratum in parental or WIP KD THP-1 cells (Figure 4.16, 4.17A). These results suggest no detectable changes in membrane fluidity at the basal end of cells compared to levels of fluidity at 37 C in parental or WIP KD THP-1 cells in response to the membrane fluidisers used in the study, at the time point used for analysis.

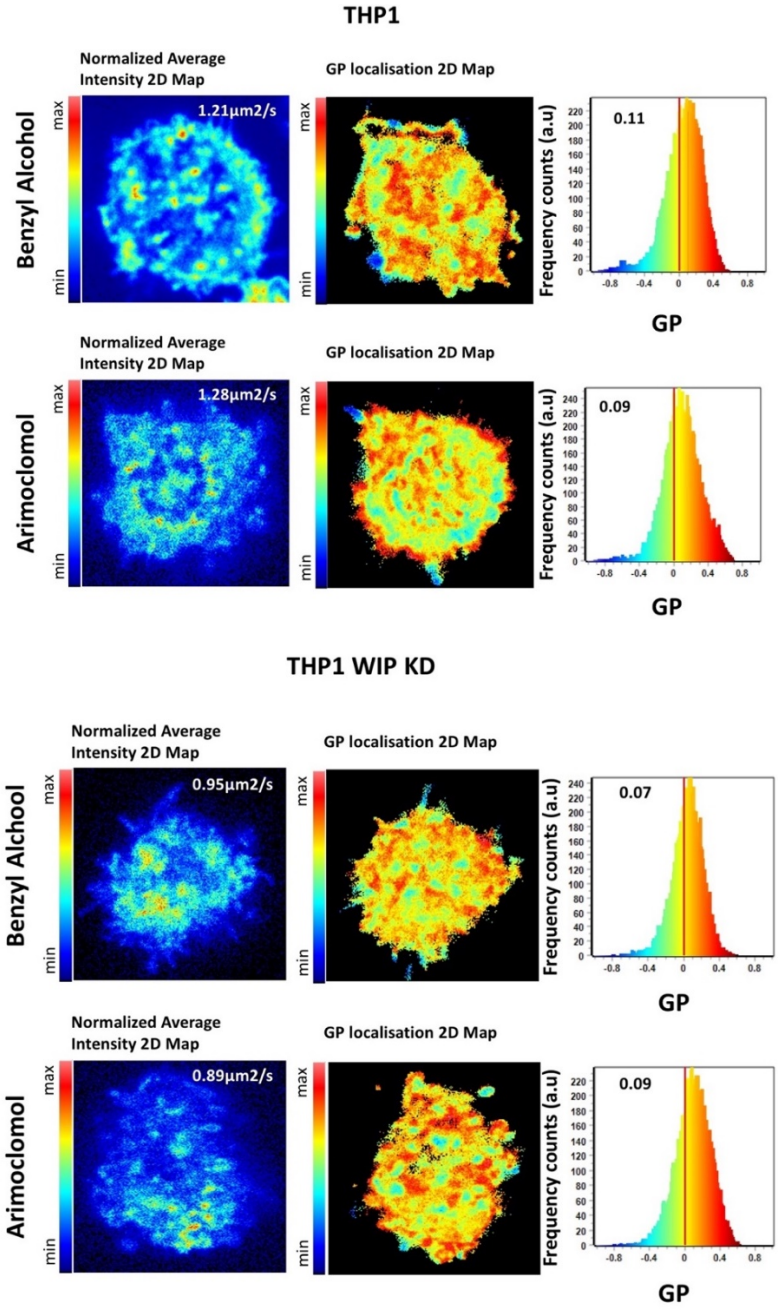

Figure 4.16. RICS and GP analyses in parental and WIP KD cells treated with different membrane fluidizer drugs.

THP-1 and WIP KD THP-1 cells were grown for 24h on fibronectin coated chambers in the presence of 1 ng/ml TGFβ-1 while being stained with 1 µM di-4-ANEPDHQ (ThermoFisher Scientific). The following day cells were stained with 1 µM SiR-Actin (SPIROCHROME) by incubation for 1 hour before imaging at 37°C. Cells were treated with 0.5mM Benzyl Alcohol (1 hour during the staining with SiR-Actin) or 0.5 µM Arimoclomol (16 hours during the staining with 1 µM di-4-ANEPDHQ) before imaging. RICS analysis was performed over 200 frames, while 5 frames per cell were averaged in the GP analysis. From the left: representative maximum intensity projection maps and coefficient of diffusion, GP Localization 2D map and GP distribution histogram in the different conditions. In all the drug treatments, parental cells slightly increased rigidity, both increasing general polarization and decreasing diffusion. No difference in diffusion or polarization was found in the WIP KD cells treated with drugs compared to KD cells at 37°C.

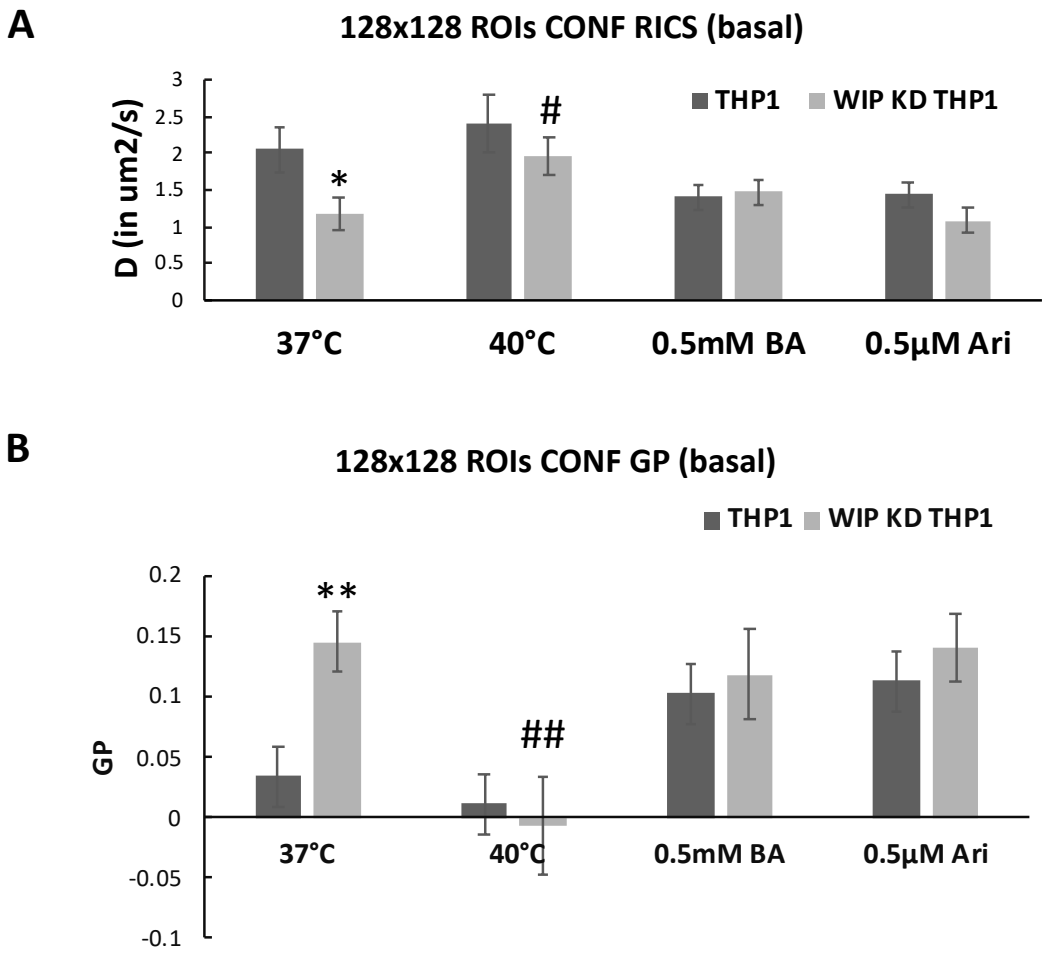

Figure 4.17. Bar graphs show average and SE of the Coefficient of diffusion and General Polarization obtained analysing at least 5 cells per condition after staining with di-4-ANEPDHQ.

(A) RICS analysis was performed over 200 frames (approximately 7 minutes). Histograms compare diffusion between parental and WIP KD cells at 37°C and cells treated with the indicated concentration of Benzyl Alcohol an Arimoclomol. *(B)* GP analysis was performed averaging 5 frames per cell. Histograms compare GP between parental and WIP KD cells at 37°C and cells treated with the indicated concentration of Benzyl Alcohol an Arimoclomol. Unpaired t-Student test was applied. #, t-student test vs control group at 37°C; * t-student test vs parental THP-1 in the respective condition (*P<0.05, ##P<0.01).

4.4.5 WIP regulates the expression of genes associated with lipid metabolism

To further elucidate the role of WIP in controlling cell response to hyperthermia, we performed total m-RNA sequencing in parental and WIP KD THP-1 cells after 16 hours incubation at 37°C and 40°C. Significant changes in levels of expression of several genes were detected in the absence of WIP or were induced by the increment in temperature (Figure 4.18).

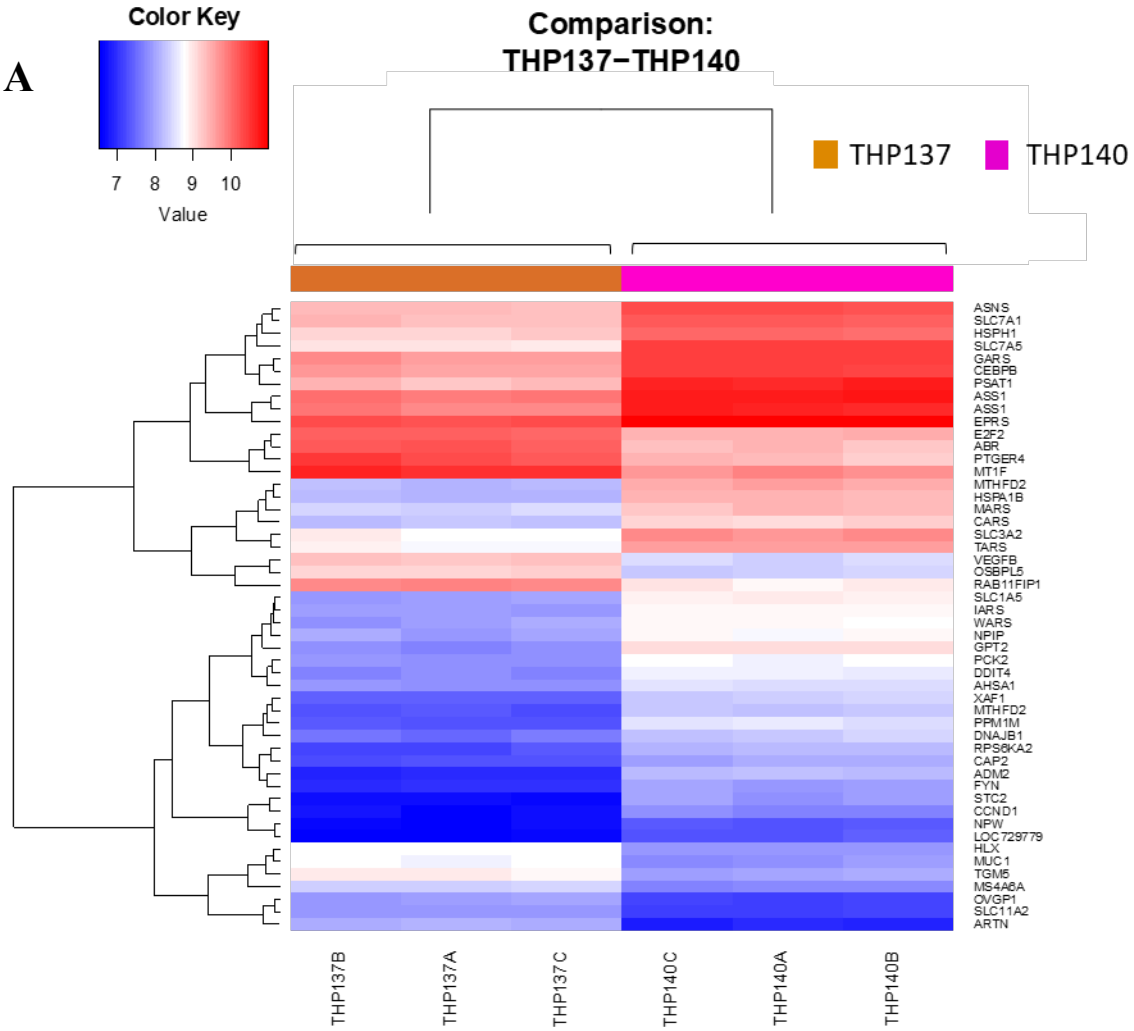

B

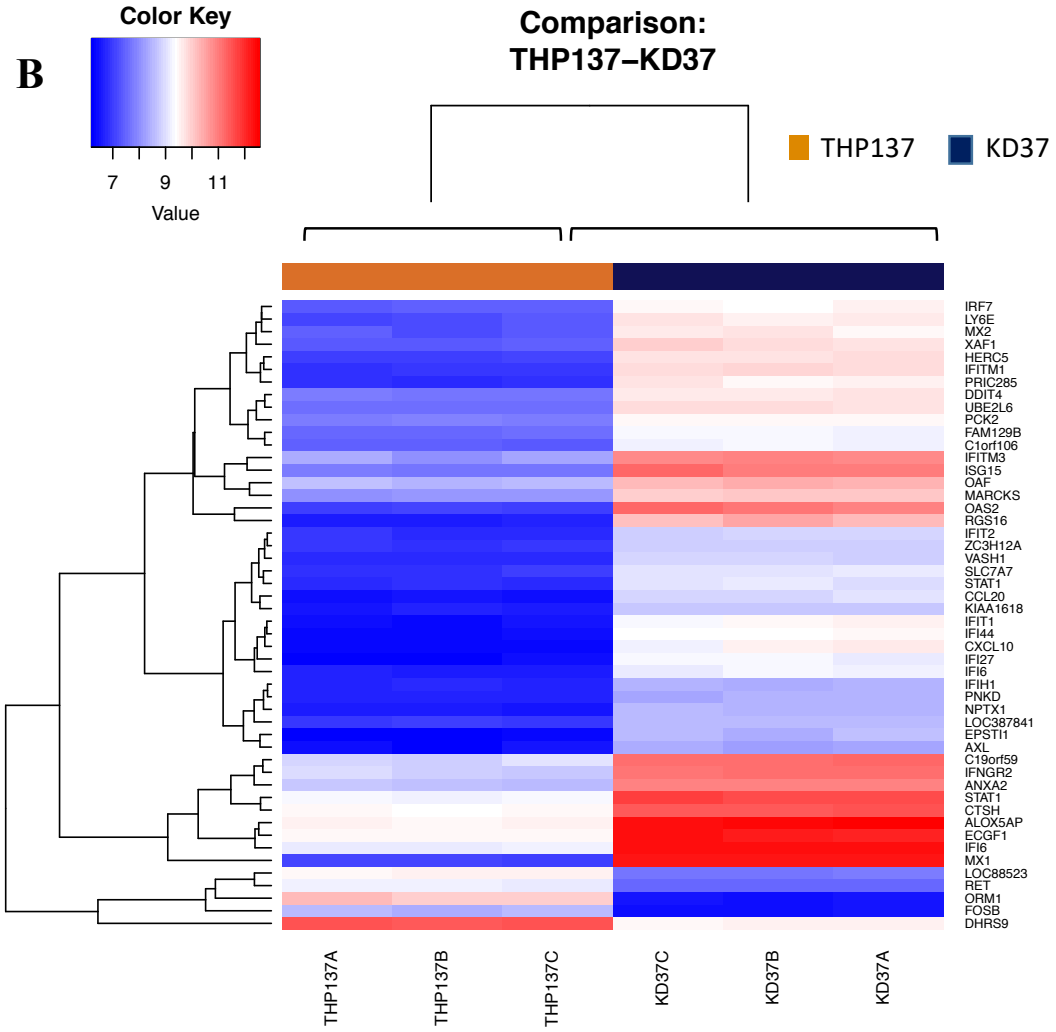
Color Key
7
9
11
Value
Comparison:
THP137–KD37
THP137
KD37
IRF7
LY6E
MX2
XAF1
HERC5
IFITM1
PRIC285
DDIT4
UBE2L6
PCK2
FAM129B
C1orf106
IFITM3
ISG15
OAF
MARCKS
OAS2
RGS16
IFIT2
ZC3H12A
VASH1
SLC7A7
STAT1
CCL20
KIAA1618
IFIT1
IFI44
CXCL10
IFI27
IFI6
IFIH1
PNKD
NPTX1
LOC387841
EPSTI1
AXL
C19orf59
IFNGR2
ANXA2
STAT1
CTSH
ALOX5AP
ECGF1
IFI6
MX1
LOC88523
RET
ORM1
FOSB
DHRS9
THP137A
THP137B
THP137C
KD37C
KD37B
KD37A

C

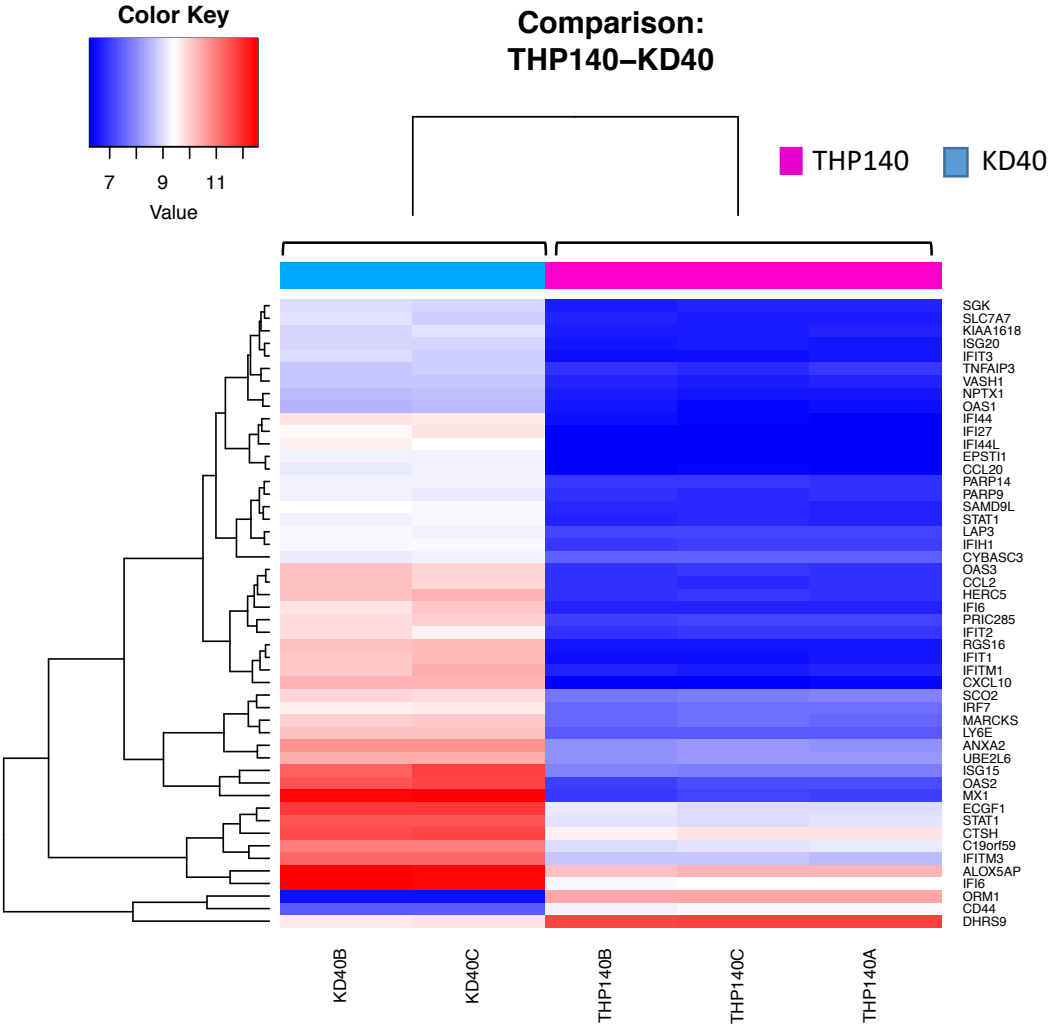
Color Key
7
9
11
Value
Comparison:
THP140–KD40
THP140
KD40
SGK
SLC7A7
KIAA1618
ISG20
IFIT3
TNFAIP3
VASH1
NPTX1
OAS1
IFI44
IFI27
IFI44L
EPSTI1
CCL20
PARP14
PARP9
SAMD9L
STAT1
LAP3
IFIH1
CYBASC3
OAS3
CCL2
HERC5
IFI6
PRIC285
IFIT2
RGS16
IFIT1
IFITM1
CXCL10
SCO2
IRF7
MARCKS
LY6E
ANXA2
UBE2L6
ISG15
OAS2
MX1
ECGF1
STAT1
CTSH
C19orf59
IFITM3
ALOX5AP
IFI6
ORM1
CD44
DHRS9
KD40B
KD40C
THP140B
THP140C
THP140A

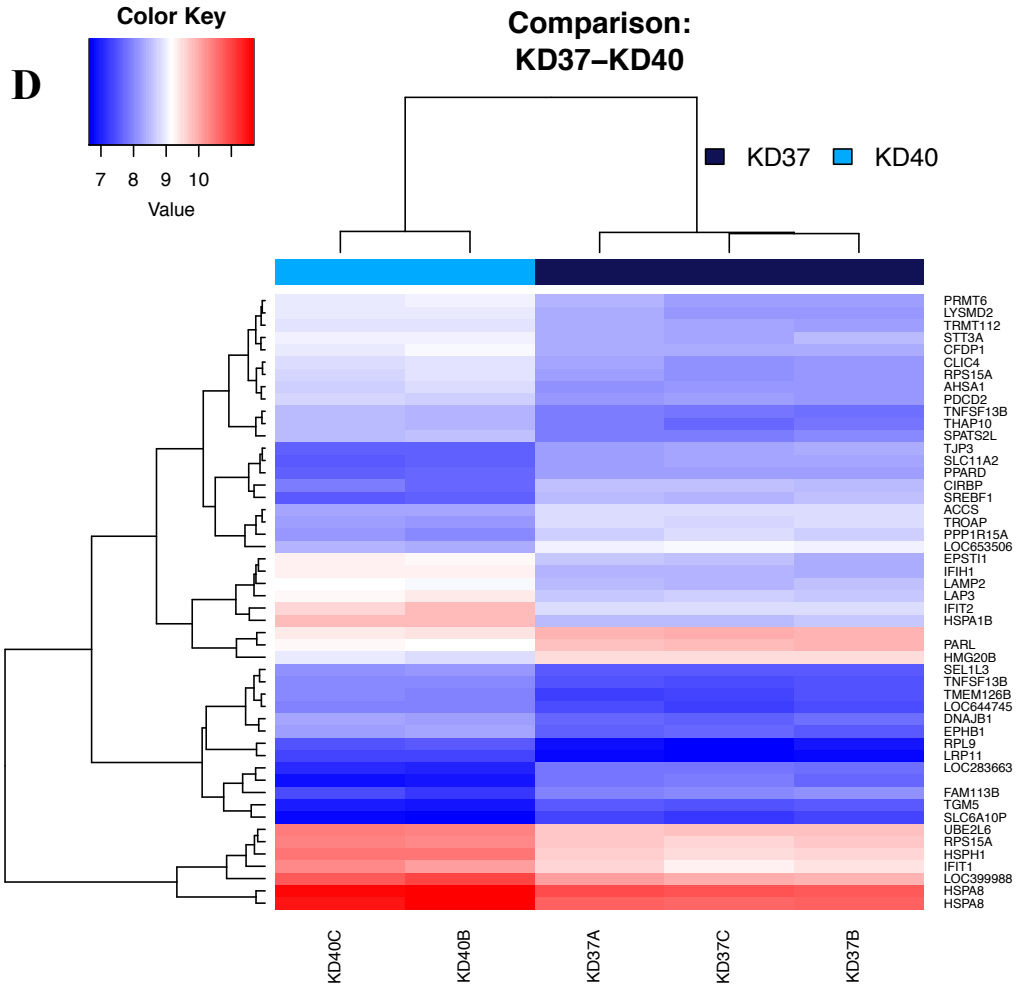

Figure 4.18. Heat maps for the 50 genes whose expression varied most significantly between the groups indicated.

(A) Heat map of the 50 most significant genes in THP-1 at 37°C versus THP-1 at 40°C; (B) Heat map of the 50 most significant genes in THP-1 at 37°C versus WIP KD THP-1 at 37°C; (C) Heat map of the 50 most significant genes in WIP KD THP-1 at 37°C versus WIP KD THP-1 at 40°C; (D) Heat map of the 50 most significant genes in THP-1 at 40°C versus WIP KD THP-1 at 40°C.

To assess groups of genes affected, gene ontology (GO) enrichment for biological processes (BP) was observed using the functional analysis package in Bioconductor "GOstats". On each comparison, genes with an absolute fold change > 1.5 and p-value < 0.05 were considered to be differentially expressed. The computations were done conditionally based on the structure of the GO graph in order to obtain more precise

p-values (adjusted p-value). Several processes involved in lipid transport and metabolism resulted to be significantly dysregulated in the WIP deficient cells as shown below (Table 4.1). In particular, genes involved in cholesterol transport and efflux, phospholipid efflux and high-density lipoprotein remodelling seemed to be over or under expressed in the WIP KD cells, indicating that WIP must have a role in controlling lipid metabolism in monocytic cells.

THP1 37°C vs WIP KD THP1 37°C				
GOBPID	**Count**	**Term**	**Pvalue.adj**	**Genes**
GO:0043691	6	reverse cholesterol transport	0.009017756	ABCA1, APOC2, APOE, LIPG, SCARB1, ABCG1
GO:0033700	4	phospholipid efflux	0.014228833	ABCA1, APOC1, APOC2, ABCG1
GO:0032371	8	regulation of sterol transport	0.025723985	ABCA1, APOC1, APOC2, APOE, NFKBIA, PPARG, LIPG, ABCG1
GO:0033993	29	response to lipid	0.038095112	CITED2, ADCY3, CST3, CREBRF, DEFB1, DSG2, EGR1, FOSB, GRN, GSTM3, ANXA1, ANXA3, IL4R, LDHA, NTSR1, NR4A2, PPARD, CCND1, SRC, TGFBR1, TGFBR2, C3, NR2C1, CA2, TRIM25, PAQR8, URI1, SOCS2, ABCG1
GO:0034375	5	high-density lipoprotein particle remodeling	0.049923957	APOC1, APOE, LIPG, SCARB1, ABCG1
THP1 40°C vs WIP KD THP1 40°C				
GOBPID	**Count**	**Term**	**Pvalue.adj**	**Genes**
GO:0032371	9	regulation of sterol transport	0.012314748	ABCA7, ABCA1, APOC1, APOC2, APOE, NFKB1, NFKBIA, LIPG, ABCG1
GO:0043691	6	reverse cholesterol transport	0.014742156	ABCA1, APOC2, APOE, LIPG, SCARB1, ABCG1
GO:0033700	4	phospholipid efflux	0.02466983	ABCA1, APOC1, APOC2, ABCG1
GO:0010875	5	positive regulation of cholesterol efflux	0.035729533	ABCA7, ABCA1, APOE, NFKBIA, ABCG1
GO:0032375	3	negative regulation of cholesterol transport	0.044266952	APOC1, APOC2, NFKB1
GO:0042362	5	fat-soluble vitamin biosynthetic process	0.048350201	CYP27A1, GFI1, IL1B, NFKB1, TNF

Table 4.1. Table shows biological processes significantly differentiated among the two groups indicated, identified using Gene Ontology.

The top table shows the differences in biological processes found between parental and KD cells at 37°C while the bottom table shows differences at 40°C. P-values are adjusted on the structure of the GO graph1. The last column indicates the names of the genes that were differentially regulated in each pathway.

Additionally, other genes involved in lipid synthesis were found to be differentially expressed in WIP KD cells or in response to hyperthermia. Among these lipids, the most interesting ones include: the sterol regulatory element binding transcription factor 1 (SRBF1), that plays a role in proteolytic release of cholesterol form membranes (Horton, Goldstein and Brown, 2002), fatty acid synthase (FASN) involved in de novo fatty acid synthesis (Stoiber *et al.*, 2018) and Neutral Sphingomyelinase Activation Associate Factor (NSMAF) (Table 4.2). Furthermore, the genes coding for ankyrin repeats containing proteins and oxysterol-binding proteins (OSBP) were found differentially expressed. These proteins were identified by blasting the *Saccharomyces cerevisiae* protein Mga2, involved in lipid modification in response to changes in membrane fluidity (Ballweg *et al.*, 2019), with homologous proteins in humans. Among those proteins, the ones that resulted more differentially expressed were ARAP3 (ankyrin repeats containing protein) and ORP5 (coded by gene OSBPL5). The extent of upregulation or downregulation is indicated in Table 4.2.

	THP-1 vs WIP KD THP-1 (37°C)				
Gene	**Fold Change**	**Regulation**	**P-Value**	**mean_WT**	**mean_KD**
SREBF1	-1.319	-	0.00100725	6.84252	7.24197
FASN	1.2065	-	0.0473317	11.58412	11.31327
NSMAF	1.8998	U	2.5732E-06	9.6113	8.68543
OSBPL5	1.6457	U	1.43E-05	8.5153	7.79659
ARAP3	-3.0957	D	9.44E-09	7.32784	8.95808
	THP-1 (37°C) vs THP-1 (40°C)				
Gene	**Fold Change**	**Regulation**	**P-Value**	**mean_37°C**	**mean_40°C**
SREBF1	1.2831	-	0.00027486	8.30514	7.94553
FASN	1.5138	U	5.58E-06	11.58412	10.9859
NSMAF	1.4224	-	1.01E-05	9.6113	9.10296
OSBPL5	1.711	U	7.40E-08	9.11055	8.33568
ARAP3	-1.505	D	4.40E-06	7.32784	7.9176
	THP-1 vs WIP KD THP-1 (40°C)				
Gene	**Fold Change**	**Regulation**	**P-Value**	**mean_WT**	**mean_KD**
SREBF1	1.2903	-	0.00041013	7.94553	7.57784
FASN	1.0461	-	0.692034	10.9859	10.92089
NSMAF	1.4325	-	3.12E-05	9.10296	8.58443
OSBPL5	1.4303	-	1.99E-05	8.0368	7.52052
ARAP3	-1.8001	D	5.84E-08	7.19956	8.179
	WIP KD THP-1 (37°C) vs WIP KD THP-1 (40°C)				
Gene	**Fold Change**	**Regulation**	**P-Value**	**mean_37°C**	**mean_40°C**
SREBF1	1.8909	U	8.07E-06	8.49688	7.57784
FASN	1.3126	-	0.0607885	11.31327	10.92089
NSMAF	1.0725	-	0.458575	8.68543	8.58443
OSBPL5	1.2109	-	0.00695297	7.79659	7.52052
ARAP3	1.1427	-	0.0997679	8.95808	8.76566

Table 4.2. Lipid metabolism genes expression in THP-1 and WIP KD THP-1 cells at 37°C and 40°C.

Data were obtained through mRNA sequencing. The first column shows the name of the genes identified, followed by the fold change value and regulation results, where D, U and – represents a downregulation, upregulation or no differential regulation, respectively. The fourth column represents the p-value obtained from three biological replicates and the fifth and sixth columns specify the mean expression value in the population indicated. Each sub-table compares different groups. From top to bottom: WT vs KD at 37°C, WT at 37°C vs WT at 40°C, WT vs KD at 40°C, WIP KD at 37°C vs WIP KD at 40°C.

4.5 Discussion

Many stimuli are involved in the activation of the Heat Shock Response, including heat, oxidative stress or bacterial infections (Akerfelt, Morimoto and Sistonen, 2010). The first cell element to perceive the shock is the plasma membrane, which creates a crosstalk between the extracellular and intracellular signals to start the response. Membrane composition is highly heterogenous and its physical properties are strictly dependent on lipid organization. Fluidity, in particular, was found to be essential in determining cells fate in response to environmental stresses (Maxfield and Tabas, 2005; Lladó *et al.*, 2014). Numerous pathologies, from cardiovascular diseases to cancer (Luostarinen, Boberg and Saldeen, 1993; Rashid *et al.*, 1997; Swinnen *et al.*, 2000; Mason and Jacob, 2003; Perona and Ruizgutierrez, 2005), are associated with modifications in lipid composition, since a disruption in lipids organization can lead to defects in protein-lipids interactions in channels, receptor and enzymes present in the cell membranes (Spector and Yorek, 1985). Cholesterol metabolism is one of the main pathways altered in cancer cells. In fact, tumour growth and cell cycle progression require cholesterol esterification (Maxfield and Tabas, 2005; Mulas *et al.*, 2011). Our gene expression profiling showed that, in the absence of WIP, several biological processes involving cholesterol, such as cholesterol transport and efflux, are altered. In particular, SREBPs, involved in lipid synthesis and cholesterol release from plasma membrane (Brown and Goldstein, 1997;Horton, Goldstein and Brown, 2002) is found to be downregulated in WIP KD cells. Interestingly SREBPs expression is dependent on the presence of HSP90 (Kuan *et al.*, 2017). Another recently identified role of SREBP is the regulation of transcription of FASN (Horton, Goldstein and Brown, 2002), whose level were also varied in the WIP KD cells line. Furthermore, cholesterol can regulate the activity of Rho family GTPases, which are

responsible for the formation of several actin adhesion structures, including podosomes (Ory *et al.*, 2008). When the amount of cholesterol is reduced, cells decrease Rac activation and consequently actin polymerization to form protrusions (Maxfield and Tabas, 2005). Our findings highlight the importance of WIP as lipid metabolism modulator and once again indicate a connection between lipids composition and actin dynamics. The WIP role in linking lipids and actin reorganization through adjustment of GTPase activity was previously described in neurons. Reduction of sphingomyelin in WIP KO neurons leads to enhanced RhoA activity and increased F-actin in dendritic spines. These events are obtained by upregulation of Neutral Sphingomyelinase (N-SMase) gene (Franco-Villanueva *et al.*, 2014). We observed a downregulation in NMSAF levels in WIP KD cells, corroborating the role of WIP in regulating SM levels. Interestingly, the abundance of SM in lipid rafts has regulatory power over integrin-based adhesion (Evans *et al.*, 2003; Eich *et al.*, 2016).

Several processes, including cell migration (Maxfield and Tabas, 2005) and adhesion to the extracellular matrix (Ziegler *et al.*, 2014) are originated through plasma membrane remodelling. In our previous chapter, we showed that WIP is responsible for controlling cell migration following mild hyperthermia, and it now suggesting the idea that WIP or WASP can control gene expression (Taylor *et al.*, 2010; Ramesh *et al.*, 2014). Taken together, our data indicate that WIP plays a major role in controlling cell response to heat stress through the regulation of lipid composition and organisation at sites of attachment. To further investigate this, we used lipidomics and found that incubation of monocytic cells at 40°C, to mimic mild febrile temperatures or local inflammation, resulted in changes in their lipid composition that were WIP dependent. We performed then an identification of a pool of some of those lipids and

established that those differentially regulated in WIP KD cells and whose levels also significantly increased in response to hyperthermia in parental THP-1 cells were highly saturated glycerophospholipids. Parental cells increased the amount of some saturated fatty acids and reduced the non-saturated ones, a common response seen in various organisms (e.g. plants, yeasts, bacteria and mammalian cells) to compensate the initial heat-induced increase in membrane fluidity (van Dooremalen and Ellers, 2010; Balogh *et al.*, 2013). However, WIP KD cells showed altered levels of the same glycerophospholipids at 37°C and 40°C. Interestingly, the *Saccharomyces cerevisiae* actin-associated protein Vrp1 (verprolin, End5) is related to WIP and is required for adaptation and viability of this yeast at a higher temperature (Thanabalu and Munn, 2001), further supporting the role of WIP as a thermosensor in eukaryotic cells. Additionally, we identified two genes differentially expressed in WIP KD cells as homologues of Mga2 in *Saccharomyces cerevisiae.* Mga2 works as a thermosensor and mediates lipid synthesis following sensing of modification in membrane fluidity and pressure (Martin, Oh and Jiang, 2007; Ballweg *et al.*, 2019). The fact that Mga2 homologous genes in humans are varied in WIP KD cells is a further indication of WIP as a possible regulator of membrane fluidity in response to heath. Furthermore, the protein encoded by OSBPL5, ORP5, whose level are upregulated in WIP KD cells, can modulate the expression of phosphatidylserine (Kattan *et al.*, 2019), that can consequently determine SM fate in lipid rafts (Airola and Hannun, 2013). Another possible homologue protein of Mga2, the ankyrin-repeats containing protein ARAP3 colocalizes in podosomes (Yu *et al.*, 2013), where it plays a role in controlling turnover dynamics (McCormick *et al.*, 2019). Interestingly, ARAP3 is overexpressed in THP-1 cells exposed to hyperthermia, correlating with the data obtained in the previous chapter showing higher podosomal turnover dynamics at 40°C.

Taken together, these data indicated a possible role of WIP in delivering changes in the lipid membrane composition in response to hyperthermia that may be involved in modulating membrane fluidity, a previously described critical factor in signal transduction in response to changes in temperature. We then decided to explore the role played by temperature and WIP on regulating membrane fluidity by analysing changes in lipid packing and spatiotemporal mobility. The results obtained in the two analysis were extremely consistent. At physiological temperature, parental cells basal plane, where cells attach on the substratum, was more fluidic than in WIP KD cells and analysis in smaller regions of interest highlighted that lipids located in podosome regions are less packed and more diffusive than in non-podosomal areas. These findings suggest a role of WIP in regulating the formation of lipid domains at the sites of cell attachment. Furthermore, the fact that changes were only revealed at the basal plane, while no difference was found on the apical plane, confirms the relevance of WIP in remodelling the plasma membrane at cell adhesions to the matrix and regulating cell motility (Keren, 2011). Increment is membrane fluidity following 30 minutes exposure to mild hyperthermia was observed in WIP KD cells only, indicating that this timeframe is sufficient for parental cells adjustment and maintenance of homeostasis of the fluidity of the cell membrane. Cells can respond to heat stress in different ways, however immune cells as monocytes are known to own adaptive mechanisms to respond to fever, gaining survival advantage. Similarly, DCs exposed to elevated temperature, even for short periods, enhances cells immune capability and induces maturation through the expression of HSP90 (Basu and Srivastava, 2003; Liso *et al.*, 2017). Therefore, it is likely that these cells can quickly adapt to the temperature induce stress by enabling changes in lipids composition to compensate the increment in fluidity, and that this adjustment is largely regulated by WIP.

To further demonstrate the role of membrane fluidisation as a possible trigger to induce myeloid cell migration in response to mild hyperthermia, we performed studies to determine possible changes in the pattern of myeloid cell migration in response to membrane fluidisation using drugs. It has been previously shown by 1,6-diphenyl-1,3,5-hexatriene (DPH) anisotropy that the membrane fluidizer drug Benzyl Alcohol can increase fluidity in K562 cells in a similar way as during a thermal shift up to 42°C. In addition, the chemically induced membrane fluidization activated HSP response, indicating that changes in fluidity are used by cells to sense stress (Balogh *et al.*, 2005). A similar effect can be caused by treatment with Arimoclomol (Hesselink JM, 2016; Fog *et al.*, 2018). Incubation with Benzyl Alcohol and Arimoclomol enhanced parental cells migration and chemotaxis, podosomes formation and matrix degradation capability.

However, in our study the membrane fluidity of THP-1 cells treated with benzyl alcohol or arimoclomol was not increased as previously described in the granulocytes-like cell line K562 (Balogh *et al.*, 2005). A plausible explanation might be that monocytic cells have a strong capacity of adaptation to maintain homeostasis due to their function in the immune response to fever, leading to a fast compensation of changes in membrane fluidity. Secondly, the concentrations of benzyl alcohol or arimoclomol used in our studies is lower to the one used in previous literature, since THP-1 cells were not able to tolerate higher concentrations. We observed a tendency (although statistically not significant) in parental cells in decreasing diffusion and increasing GP after drugs treatment, possibly indicating that cells were compensating the increased fluidity induced by drugs as seen following hyperthermia (likely by changing the composition of membrane phospholipids). The observed increment in the proportion of membrane lipids with high fatty acid saturation in response to

hyperthermia can contribute to the enhanced migratory response in parental THP-1 cells. Interestingly, HSP90 was previously associated with podosome formation and amplification of N-WASP-induced actin polymerization (Suetsugu and Takenawa, 2003; Park, Suetsugu and Takenawa, 2005), and it is also upregulated in THP-1 cells exposed to hyperthermia. Taken together, our findings suggest that following hyperthermia, WIP delivers changes in monocytic cells' membrane fluidity leading to increased HSP90-WASP/WIP-dependent actin polymerization that may be required for the enhancement of the migratory response during febrile and local inflammation.

Chapter 5: The role of the nuclear shuttling of the Wiskott Aldrich Syndrome protein (WASP) in leukocytes migration in response to mild hyperthermia

5 The role of the nuclear shuttling of the Wiskott Aldrich Syndrome protein (WASP) in leukocyte migration in response to mild hyperthermia

5.1 Introduction

In the previous two chapters, we identified WIP as a mediator of immune cells migratory and invasive response to mild hyperthermia by delivering changes in the lipid composition of the plasma membrane. WIP role as a "keeper" of WASP from degradation has been widely studied. In the absence of WIP, WASP is unstable and degraded by calpains and proteasome, determining a fail in podosome assembly and migratory defects (de la Fuente *et al.*, 2007). The strict association between the two proteins makes it challenging to discriminate which one is actually the main player of the effects described in the previous chapters.

WASP, the haematopoietic form of the ubiquitously expressed N-WASP, is localized in the podosome core alongside other actin related proteins (ARPs) and is one of the main actin nucleators. Following the release of its autoinhibited conformation, downstream activation of the Rho GTPase Cdc42, WASP can bind actin monomers and interact with the ARP2/3 complex through the VCA domain to start *de novo* polymerization of actin filaments (Higgs and Pollard, 1999; Millard, Sharp and Machesky, 2004). The *WAS* gene is situated on the short arm of the X chromosome and WASP protein is proline-rich and 502 amino acids long. The 137-bp region upstream of the transcription start site determines WASP limited expression in hematopoietic cells (Derry, Ochs and Francke, 1994; Kurisu and Takenawa, 2009). Mutations in the gene coding for WASP lead to the Wiskott Aldrich Syndrome (WAS), a haematological disorder, characterized by eczema, microthrombocytopenia

and immunodeficiency (Snapper and Rosen, 1999; Imai *et al.*, 2004; Worth and Thrasher, 2015). If left untreated, WAS patients will rarely reach adulthood and will die in their teenage years due to recurrent infections, bone marrow failure or cancer (Remold-O'Donnell, Rosen and Kenney, 1996). The pathogenesis of the disease is unclear, with cases of both immunodeficiency and immune system hyperactivation. Also, the severity of the disease is heterogenous among patients (Mahlaoui *et al.*, 2013; Notarangelo, 2013). In general, immune cells from WAS patients show cytoskeleton abnormalities affecting several stages of the immune response, including migration, trans endothelial migration, antigen processing processes, change of shape to mediate phagocytosis and direct cells signalling (Moulding *et al.*, 2013). In classical WAS disease, myeloid and dendritic cells display defects in chemotaxis, lack of podosomes necessary for adhesion to surrounding tissues and inability to polarize and maintain directional protrusions during migration (Jones *et al.*, 2002; Tsuboi, 2007; Monypenny *et al.*, 2011). Although some cells will eventually succeed in the migration process, later on, they can develop phagocytosis or antigen presenting deficiencies (Jones *et al.*, 2002; Westerberg *et al.*, 2003; Zhang *et al.*, 2006; Tsuboi, 2007; Monypenny *et al.*, 2011).

For a long time, the actin-polymerising activity of WASP has been thought to be a major contributor to the cellular pathology of WAS, including defective leukocyte trafficking. However, only 7% of the mutations in WAS patients are localised in the actin-regulatory domain of WASP (VCA domain) and the majority of such mutations result in the milder form of the disease called X-linked thrombocytopenia (Kwan *et al.*, 1995; Wengler *et al.*, 1995; Zhu *et al.*, 1995). In 80% of studied WAS patients, the syndrome arises from missense mutations in two recently identified functional nuclear export signals (NES) and nuclear localisation signal (NLS) (Taylor *et al.*, 2010). The

identification of the nuclear entry and exit sequences employed by WASP and the fact that WASP can localize in the nucleus of myeloid cells are significant evidence that WASP may play a role in regulating gene expression, although its role remains unclear. Recently, it was shown that WASP is responsible for the epigenetic control of histone methylation on genes involved in adaptive immunity through a nuclear ARP2/3-VCA independent function (Sadhukhan *et al.*, 2014), and that it plays a fundamental role in the differentiation of all the hematopoietic cell lineages (Parolini *et al.*, 1997). Likewise, other actin related proteins were found to be involved in controlling gene expression. For instance, the WASP interacting protein (WIP) can regulate N-WASP nuclear translocation interfering with cytoskeleton dynamics in rat fibroblasts (Sadhukhan *et al.*, 2014) and regulates gene expression indirectly through the regulation of actin dynamics, which in turn determine the nuclear localisation of the transcription co-factor MRTF-A (Parolini *et al.*, 1997).

5.2 Hypothesis and aims

Our previous data showed a correlation between hyperthermia, increased invasive migration of THP-1 cells and changes in the expression of motility related genes modulated by WIP. This suggests a possible direct modulation of gene transcription by the nuclear localisation of WASP and/or WIP in response to hyperthermia. It is clear that WASP must have other roles, additionally to controlling actin polymerization. Therefore, in this study we generated eGFP-tagged WASP constructs that are deleted of WASP NES1, NLS or VCA domains and expressed these constructs in the immune cell line THP-1 modified to mimic WAS disease (WASP CRISPR cells), in order to:

- investigate whether the nuclear localisation signal of WASP is involved in the invasive mode of migration of immune cells both at physiological temperature and in response to mild hyperthermia;
- verify whether WIP or WASP is the main orchestrator of the increased migratory and invasive phenotype observed in response to hyperthermia.

5.3 Materials and methods

5.3.1 PCR amplification from plasmids

WAS deletions sequences were amplified using vector pCMV6-AC-GFP (gift from Prof Vyas) as a template, while the eGFP fragment was obtained from a previously owned plasmid. Specific primer sequences, in which appropriate restriction sites were incorporated, were designed (Table 5.1).

	Primer FW	Primer RV	Restriction Enzymes (in bold)
WASPΔNLS	ATGGACGAGCTGTACAAGtccggccgc**tctaga**gaaagcaccATGAGTGGGGGCCCAATG	tagcta**ggtacc**tttaTCAGTCATCCCATTCATC	XbaI-KpnI
WASPΔNES	ATGGACGAGCTGTACAAGtccggccgc**tctaga**gaaagcaccATGAGTGGGGGCCCAATG	tagcta**ggtacc**tttaTCAGTCATCCCATTCATC	XbaI-KpnI
WASPΔVCA	ATGGACGAGCTGTACAAGtccggccgc**tctaga**gaaagcaccATGAGTGGGGGCCCAATG	tagcta**ggtacc**tttaACCAGAGCAGGAGGGAGT	XbaI-KpnI
eGFP	tagcta **ggatcc**cccctagcgctaccggtcgccacc ATGGTGAGCAAGGGC	CATTGGGCCCCCACTCATggtgctttc**tctaga**gcggccggaCTTGTACAGCTCGTCCAT	BamHI-XbaI

Table 5.1. PCR primers for cloning including specific restriction enzymes.

FW and RV primers contains 5' non-hybridizing sequences containing restriction sequences (in bold) and 15-25nts of hybridizing area (in capital). In addition, each primer presents a clamp region of six random nucleotides at the 5' ends to avoid enzymes digestion at DNA ends. Forward primers present a Kozak consensus sequence to improve initiation of amplification while reverse primers contain a stop consensus sequence.

The amplification reactions were performed with and without 5% DMSO to increase the success rate. Also, annealing temperature was varied using a range between 54-64°C. Reactions were obtained in a finale volume of 25ul and set up, using New England Biolabs High Fidelity Kit, as follow:

- Water: up to 25ul
- Phusion Buffer GC 5X: 5ul
- 10mM dNTPs: 0.5ul
- Primer FW (10uM): 1.25ul
- Primer RV (10uM): 1.25ul
- Template DNA: 1ul
- DMSO (Optional): 1.25ul
- Phusion DNA Polymerase: 0.25ul

PCR mixes were loaded on a BIORAD T100 Thermocycler with the following cycling instructions (Table 5.2):

Cycle STEP	**TEMP**	**TIME**	**Cycles**
Initial Denaturation	98°C	30s	1x
Denaturation	98°C	10s	31x
Annealing	Varied	30s	
Extension	72°C	30s/kb	
Final Extension	72°C	10 min	1x
Maintenance	4°C	Hold	1x

Table 5.2. PCR cycling protocol

5.3.2 Agarose gel electrophoresis

The amplification products were analysed through electrophoresis in 1% Agarose (TopVision Agarose Tablets, 0.5g each) gel in 1X TAE (Tris Acetate EDTA, BIORAD), with 0.01% Syber Safe (Thermofisher). PCR products were stained with 6x Orange DNA Loading Dye (Thermofisher). O'GeneRuler 1 kb (Thermofisher) was used as DNA Ladder to identify the length of the fragment and to verify the specificity of the reaction. The run was performed on a horizontal electrophoresis cell in 1x TAE buffer (Tris Acetate EDTA, BIORAD) at 100 V for 30 minutes. After the run, the gel was visualized and photographed using a GelDoc XR trans illuminator system (BIORAD) (Figure 5.2A). Gel slices containing the fragments of interest were excised and cleaned up using GeneJET DNA extraction Kit following manufacturer instructions (Thermofisher).

5.3.3 pTOPO subcloning

Purified fragments were incubated for 10 minutes at 72°C with 1 unit of Taq polymerase (New England Biolabs) to add 3' deoxyadenines. The plasmid pCR II-TOPO (Invitrogen) is supplied linearized and presents overhanging 3' deoxythymidine. This allows to directly insert the amplified product into the plasmid by incubating 4 µl of the purified PCR products with 1 µl of salt solution provided with the kit and 1 µl of TOPO vector for 30 minutes at room temperature. The product of the sub cloning was then immediately used to transform NEB® 5-alpha Competent *E. coli* cells, following manufacturer directions.

5.3.4 Miniprep and Digestion

Positive colonies were selected, and plasmids were purified using a QIAprep Spin Miniprep kit (QIAGEN).

All the restriction enzymes were purchased from New England Biolabs and digestions were performed following New England Biolabs guidelines. Following digestion, the pHRsin18cpptegfpwap vector was incubated at 37°C for 20 minutes with Alkaline Phosphatase (Thermofisher) to catalyse the release of 5'- and 3'- phosphate groups from DNA to avoid vector re-ligation. Digested fragments were subjected to electrophoreses, excised and cleaned up as described above.

5.3.5 Three pieces ligation

The purified and digested fragments were mixed as follow and incubated for 16 hours at 16°C:

- 1ul BamHI-KpnI digested pHRsin18cpptegfpwap;
- 3.5ul BamHI-XbaI digested eGFP;
- 3.5ul XbaI-KpnI digested WASP del mutants;
- 1u T4 Ligase (NEB);
- 1ul Ligation Buffer (NEB).

The ligation products were used to transform NEB® 5-alpha Competent *E. coli*. Positive colonies were selected and purified (QIAprep Spin Miniprep kit, QIAGEN).

5.3.6 Generation of WASP deletion mutants cell lines using lentiviral vectors

THP-1 WASP CRISPR cell lines expressing eGFP-WT WASP, or the newly generated eGFP-WASP deletion mutant proteins were generated using the pHRsin18cpptegfpwasp deletions lentiviral vectors plasmid produced in our lab as transfer vectors. Lentiviral particles were produced in 6-wells plates in HEK 293T cells by co-transfecting 1.5 µg transfer vector with 1.1 µg pCMV^R8.91 (packaging plasmid) and 0.4 µg pMD.G (envelope plasmid). The three plasmids were mixed in 150 mM NaCl to a final volume of 100 µl and diluted in equal volume of 150 mM NaCl containing 6 µl Jet-PEI (Polyplus). After 30 minutes incubation of the mixture at room temperature, the Jet-PEI/DNA mix was added to the culture medium in the cell cultures. The following day, the culture medium containing the transfection mix was replaced with fresh media and the supernatant containing lentiviral particles harvested after 24 hours. The supernatant was filtered through a 0.45 µm-pore-size filter to remove cell debris and stored at -80°C until transduction. $2x10^5$ THP-1 WASP CRISPR cells (gift from Prof Adrian Thrasher, UCL, London, UK) were transduced with the corresponding DNA by incubation with 500 µl of lentiviral supernatant. A second cycle of infection was performed at 24 h. At 48 hours from the second infection cycle, a cell population expressing homogenous levels of eGFP were sorted using BD FACSDiva cell sorter at the facilities at the Flow Cytometry Core at the NIHR GST/KCL Biomedical Research Centre. FACS sorted cells were more than 90% eGFP positive cells after sorting (Figure 5.3).

Table 5.3. List of cell lines used in this study

Cell lines	Description	Source
THP-1	Human acute monocytic leukemia cell lines	ATCC
THP-1 WAS CRISPR	WASP KO cell lines derived from THP-1 cells obtained using CRISPR technology	Prof Adrian Thrasher
THP1 eWASP	THP-1 WAS CRISPR cells transfected with pHRsin18cpptegfpwasp to recover WASP expression	This study
THP1 eWASPΔNLS	THP-1 WAS CRISPR cells transfected with pHRsin18cpptegfpwaspdelNLS to express WASP depleted Nuclear localization signal	This study
THP1 eWASPΔNES	THP-1 WAS CRISPR cells transfected with pHRsin18cpptegfpwaspdelNES to express WASP depleted Nuclear Export signal 1	This study
THP1 eWASPΔVCA	THP-1 WAS CRISPR cells transfected with pHRsin18cpptegfpwaspdelVCA to express WASP depleted the Verprolin, cofilin, acidic (VCA) domain	This study

5.4 Results

5.4.1 Generation of eGFP-WASP deletion mutants' plasmids

WASP domains deletion mutant plasmids were a gift from Prof Vyas and were received in vector pCMV6-AC-GFP. WAS gene deletions in the areas of interest were previously described (Sadhukhan *et al.*, 2014) and are the following (Figure 5.1):

- WASPΔNLS: coding DNA for WASP protein lacking the Nuclear Localization Signal;
- WASPΔNES: coding DNA for WASP protein lacking the Nuclear Export Signal 1;
- WASPΔVCA: coding DNA for WASP protein lacking the Verprolin, cofilin, acidic (VCA) domain;

atgagtgggggcccaatgggaggaaggcccgggggccgaggagcaccagcggttcagcagaacataccctccaccc
tcctccaggaccacgagaaccagcgactctttgagatgcttggacgaaaatgcttgacgctggccactgcagttgttcagc
tgtacctggcgctgccccctggagctgagcactggaccaaggagcattgtggggctgtgtgcttcgtgaaggataaccc
ccagaagtcctacttcatccgcctttacggccttcaggctggtcggctgctctgggaacaggagctgtactcacagcttgtc
tactccacccccacccccttcttccacaccttcgctggagatgactgccaagcggggctgaactttgcagacgaggacga
ggcccaggccttccgggccctcgtgcaggagaagatacaaaaaaggaatcagaggcaaagtggagacagacgccag
ctacccccaccaccaacaccagccaatgaagagagaagaggagggctcccacccctgcccctgcatccaggtggaga
ccaaggaggccctccagtgggtccgctctccctggggctggcgacagtggacatccagaaccctgacatcacgagttc
acgataccgtgggctcccagcacctggacctagccagctgataagaaacgctcagggaagaagaagatcagcaaag
ctgatattggtgcacccagtggattcaagcatgtcagccacgtggggtgggacccccagaatggatttgacgtgaacaac
ctcgacccagatctgcggagtctgttctccagggcaggaatcagcgaggcccagctcaccgacgccgagacctctaaa
cttatctacgacttcattgaggaccagggtgggctggaggctgtgcggcaggagatgaggcgccaggagccacttccg
ccgcccccaccgccatctcgaggagggaaccagctcccccggcccccctattgtgggggtaacaagggtcgttctggt
ccactgcccccctgtaccttttggggattgccccacccccaccaacaccccggggaccccccacccccaggccgaggggg
ccctccaccaccaccccctccagctactggacgttctggaccactgccccctccacccccctggagctggtgggccaccc
atgccaccaccaccgccaccaccgccaccgccgcccagctccgggaatggaccagcccctcccccactcctcctgct
ctggtgcctgccgggggcctggcccctggtgggggtcggggagcgcttttggatcaaatccggcagggaattcagctg
aacaagacccctggggccccagagagctcagcgctgcagccaccacctcagagctcagagggactggtgggggccc
tgatgcacgtgatgcagaagagaagcagagccatccactcctccgacgaaggggaggaccaggctggcgatgaagat
gaagatgatgaatgggatgactga

Figure 5.1. WAS gene sequence.

WAS sequences coding for WASP Nuclear Export Signal 1 (NES1), WASP Nuclear Localization Signal (NLS) and WASP Verprolin, cofilin, acidic domain (VCA) are highlighted in green, red and purple, respectively.

WAS deletions sequences of interest were amplified from vector pCMV6-AC-GFP while the eGFP fragment was obtained from a previously owned plasmid. Amplification reactions were performed using primers that incorporated restriction enzymes to allow for later ligation of the amplified fragment. Following amplification, the fragments obtained were electrophoresed and then purified from the agarose gel (Figure 5.2A). The purified fragments were sub cloned into pTOPO and immediately used to transform NEB® 5-alpha Competent *E. coli* cells. Plasmids were selected and purified form positive colonies.

Plasmids obtained were double digested with BamHI-XbaI (eGFP) or XbaI-KpnI (WASP deletion mutants) (Figure 5.2C), while the pHRsin18cpptegfpwap vector, obtained from Prof Adrian Thrasher of the Institute of Child Health, was digested with BamHI-KpnI to remove the full length eGFP WASP sequence present (Figure 5.2B). The purified and digested fragments were mixed up to obtain a three pieces ligation product, that was again used to transform NEB® 5-alpha Competent *E. coli*. Positive colonies were selected and purified. Control digestions were performed (Figure 5.2D) and plasmids were sent for sequencing to DBS Genomics (Durham University) to verify the corresponding coding DNA sequences.

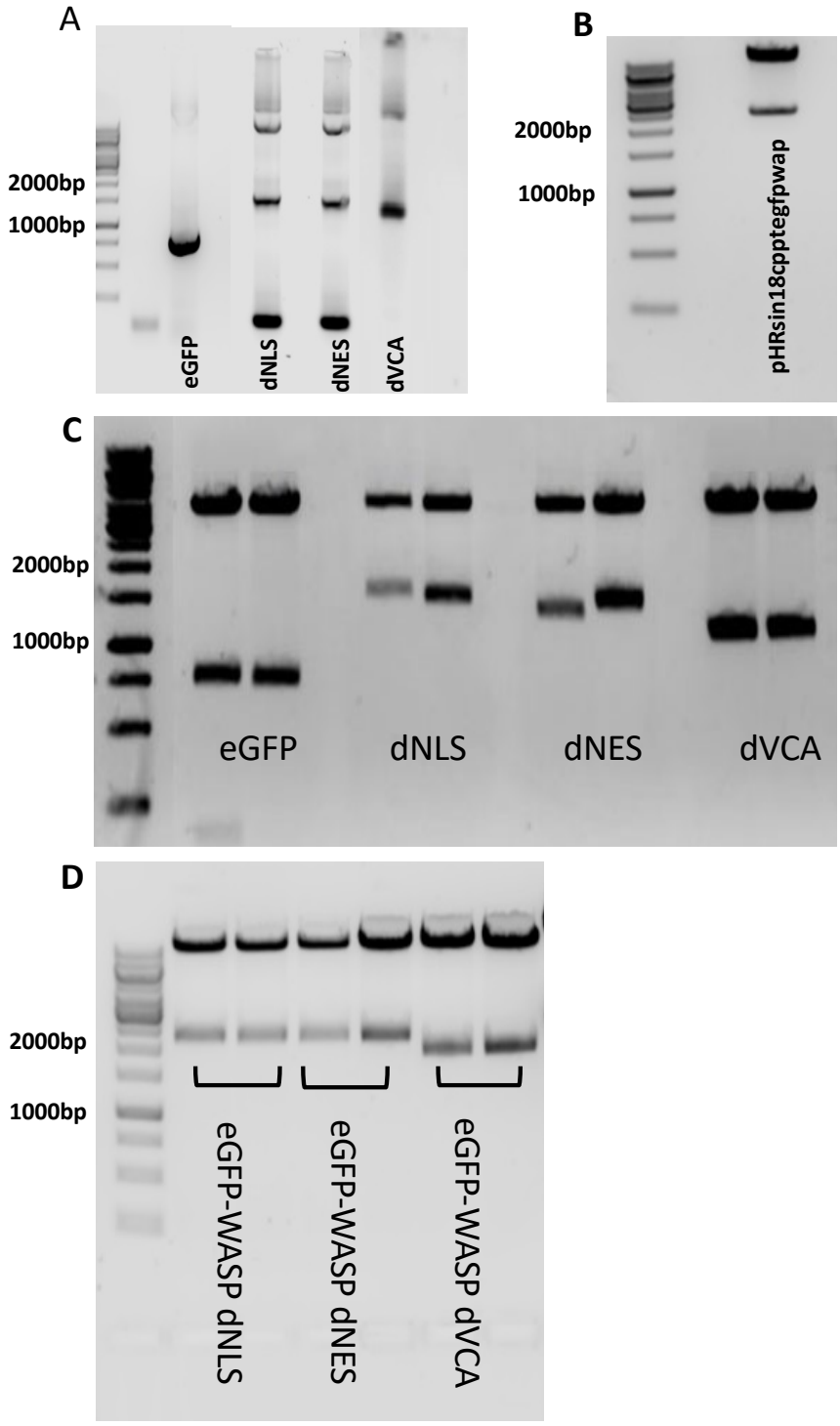

Figure 5.2. eGFP-WASP deletion mutants cloning in pHRsin18cpptegfpwasp vector.

(A) PCR product obtained from amplification of WAS deletions mutants from vector pCMV6-AC-GFP and eGFP fragment from a previously owned plasmid. Bands of appropriate size are visualized (eGFP:700bp, WAS dNLS and dNES: 1500bp and WAS dVCA: 1300bp); (B) pHRsin18cpptegfpwap vector digestion with BamHI-KpnI. eGFP-WASP full length sequence (2200bp) was excided from the plasmid; (C) eGFP digestion with BamHI-XbaI and WAS mutants digestions with XbaI and KpnI from pCR II-TOPO vector. Bands of appropriate size are visualized (eGFP:700bp, WAS dNLS and dNES: 1500bp and WAS dVCA: 1300bp); (D) eGFP WAS deletion mutants were cloned in pHRsin18cpptegfpwap. The resulting vectors were digested with BamHi/KpnI. Bands of appropriate size are visualized (eGFP-WAS dNLS and dNES: 2200bp and WAS dVCA: 2100bp).

5.4.2 Generation of eGFP-WASP deletion mutants cell lines

The produced plasmids were used to generate lentiviral particles and transduce THP-1 WASP CRISPR cell lines (gift from Prof Adrian Thrasher). To select a cell population expressing homogenous levels of eGFP, cells were sorted using BD FACSDiva cell sorter at the facilities at the Flow Cytometry Core at the NIHR GST/KCL Biomedical Research Centre. FACS sorted cells were more than 90% eGFP positive cells after sorting (Figure 5.3).

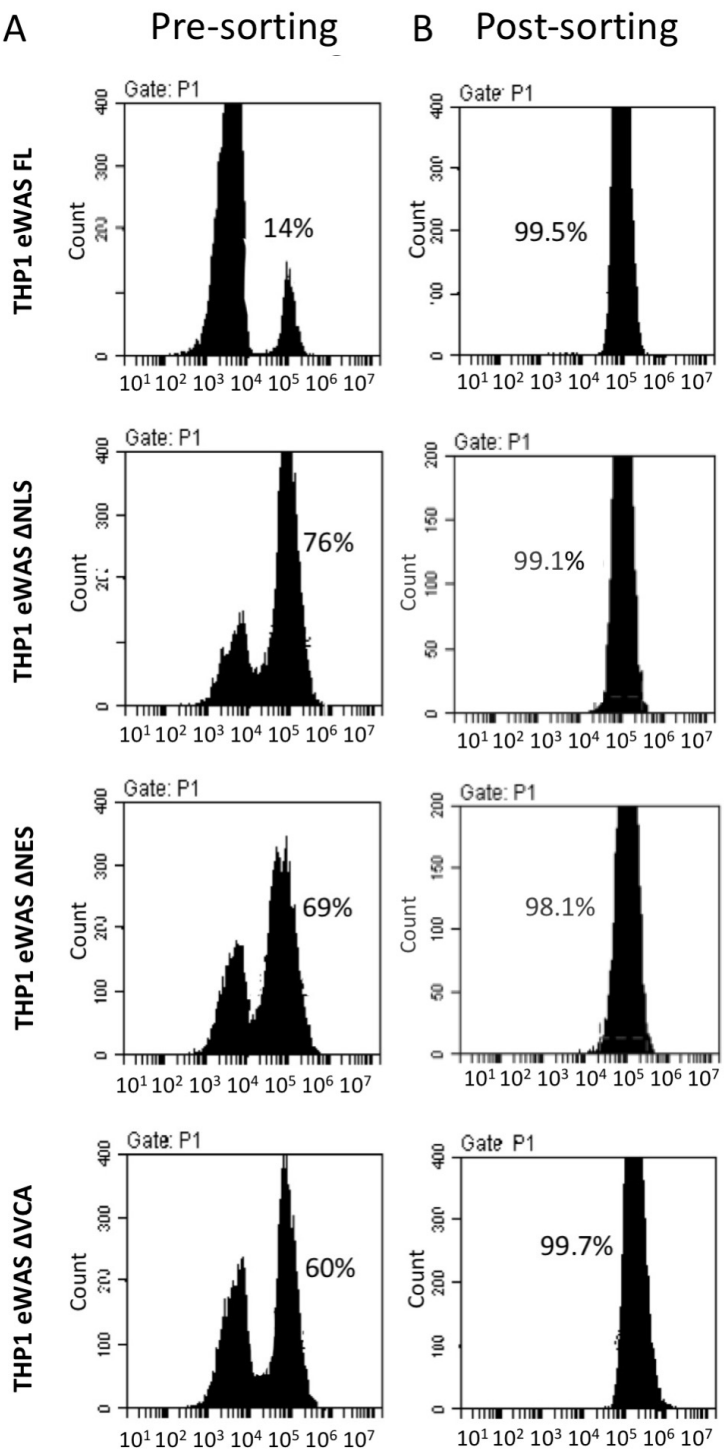

Figure 5.3. Percentages of eGFP positive THP-1 eGFP-WAS FL and THP-1 eWAS deletion mutants cells before and after FACS sorting.

THP-1 WASP CRISPR cells were transfected with a lentiviral vector carrying pHRsin18cppte-GFP-WASP full length, pHRsin18cppt-eGFP-WASPΔNLS, pHRsin18cppt-eGFP-WASPΔNES or pHRsin18cpptegfpwaspΔVCA. (A) Flow cytometer histograms showing the number of cells expressing eGFP-WASP before sorting. After the initial transduction the percentage of eGFP positive cells was between 13% and 70%. (B) FACS sorting allowed to select a population of homogenously expressing the eGFP-tagged proteins of interest.

5.4.3 Role of the nuclear shuttling of WASP in expression of F-actin related proteins

It was shown that various actin-related proteins, including WASP, are able to localize in the nucleus of immune cells (Olave, Reck-Peterson and Crabtree, 2002; Wu *et al.*, 2004; Zheng *et al.*, 2009). The gene/protein sequences involved in WASP shuttling in T cells were identified (Taylor *et al.*, 2010). In this study, we generated THP-1 CRISPR WASP cells in which eGFP-Full length (FL) WASP or WASP deletion mutants that failed to express specific sequences involved in WASP translocation or actin binding were expressed. Following subcellular fractionation, we observed the effect of the absence of these specific domains in WASP shuttling in THP-1 cells and on their migratory phenotype. As expected, WASP nuclear localization was significantly reduced by the lack of the NLS domain in THP-1 cells (Figure 5.4). In fact, we noticed a higher accumulation of WASP in the cytoplasm of these cells compared to parental cells expressing full length WASP constructs. Unexpectedly, no difference was found between parental and WASPΔNES1 cells, probably due the presence in WASP sequence of a second Nuclear Export Sequence (NES2) that may be able to compensate for the missing domain. Finally, WASP accumulation in the nucleus was increased by approximately 7 times when the protein is not able to bind actin and start polymerization, due to the deletion of WASP VCA domain (Figure 5.4).

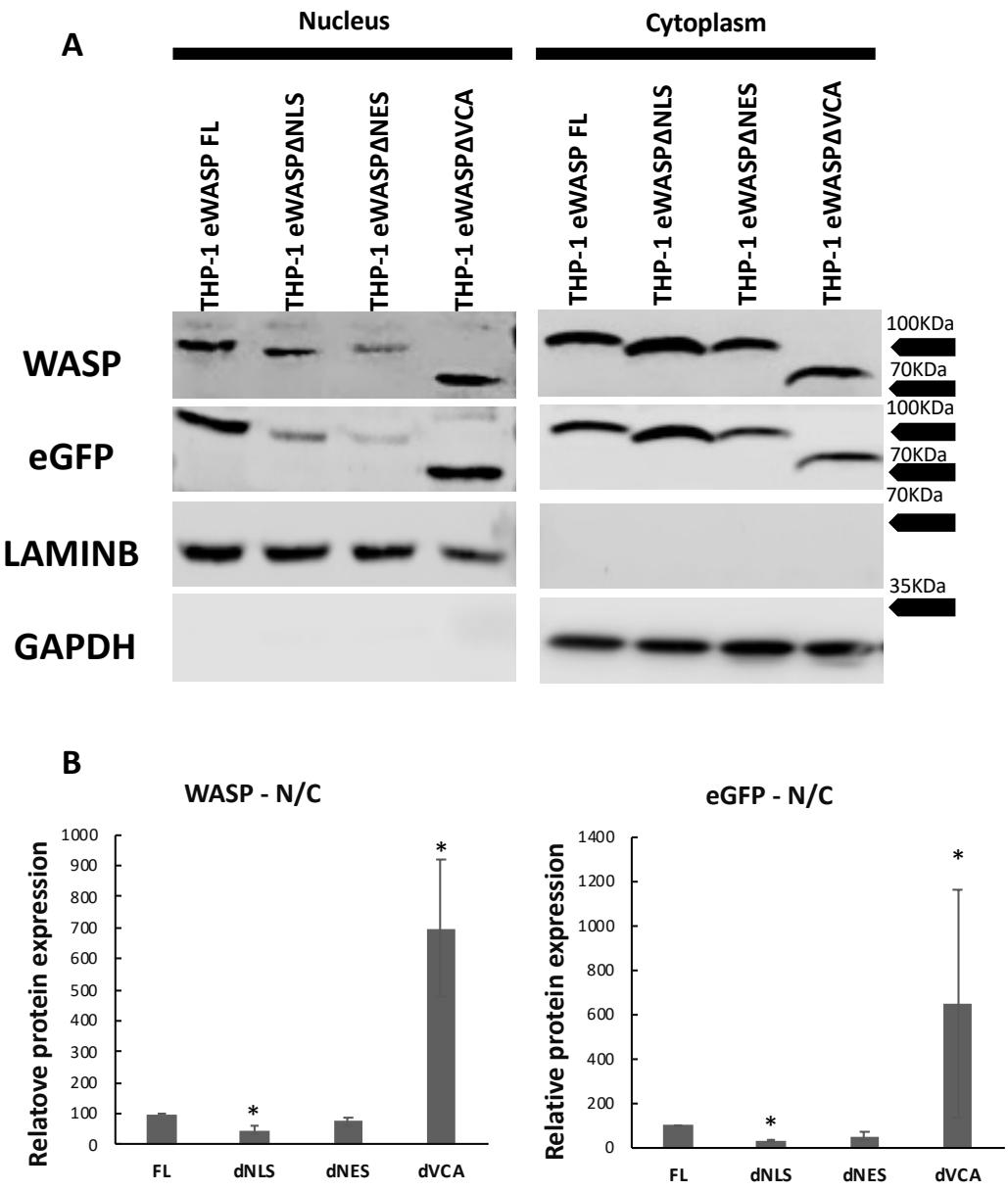

Figure 5.4. Analysis of WASP nuclear translocation in THP-1 eWAS deletion mutants cells.

(A) Representative blots of nuclear and cytoplasmic fractions of THP-1 eWAS deletion mutants. Nucleus/cytoplasm separation was performed after 16 hours incubation on fibronectin coated dishes in the presence of 1ng/ml TGFβ-1. Separated lysates were used for Western Blotting. LaminB and GAPDH were used as separation and loading controls. Antibodies anti WASP and eGFP were used to investigate the role of the deleted WAS sequence on WASP translocation to the nucleus. Deletion of WASP NLS caused lower nuclear localization of WASP and higher accumulation in the cytoplasm. THP-1 eGFP-WASΔNES showed lower WASP expression in the cytoplasm, however no nuclear accumulation was detected. Interestingly, THP-1 cells lacking the VCA domain showed an evident WASP translocation in the nucleus. (B) Bar graphs show average and SE of each protein relative expression calculated as a ratio between protein levels in the nucleus and protein levels in the cytoplasm. Data are representative of two biological replicates. Unpaired two tail t-test was applied (*P<0.05 vs THP-1 eGFP-WAS FL). Arrows on blots indicate protein ladder closest band (10 to 250 kDa, ThermoFisher Scientific).

Total protein expression was also investigated in the WASP deletion mutants cells exposed for 16 hours to mild hyperthermia (Figure 5.5). Both WASP and eGFP protein levels were comparable between the FL and the WASP mutant lacking the NLS, while a small but not significant decrease in the total level of both WASP and eGFP expression was observed in the mutants lacking the NES1 or the VCA domain (Figure 5.5B, 5.5C). No difference in WASP or eGFP expression was found after exposure to mild hyperthermia (Figure 5.5A, B, C). ARP2/3 and vinculin expression was similar in all the cell lines and not influenced by temperature (Figure 5.5A, D, E). Interestingly, we found that phosphorylation of Thr202/Tyr204 in protein kinase ERK (both ERK1 and ERK2 isoforms), that is activated downstream to the integrin pathway (Aplin *et al.*, 2001; Lai *et al.*, 2001; Yee, Weaver and Hammer, 2008), was increased at 40°C independently of the presence of the WASP NLS, NES or VCA domains (Figure 5.5A, F, G). Additionally, the levels of Heat Shock protein 90 (HSP90), previously associated with podosomes formation (Suetsugu and Takenawa, 2003), are upregulated in THP-1 cells exposed to hyperthermia independently of the presence of the WASP NLS, NES or VCA domains (Figure 5.5A, H). Taken together our results show that the upregulation of HSP90 and of ERK in response to mild hyperthermia is independent of the NLS, NES and VCA domains of WASP.

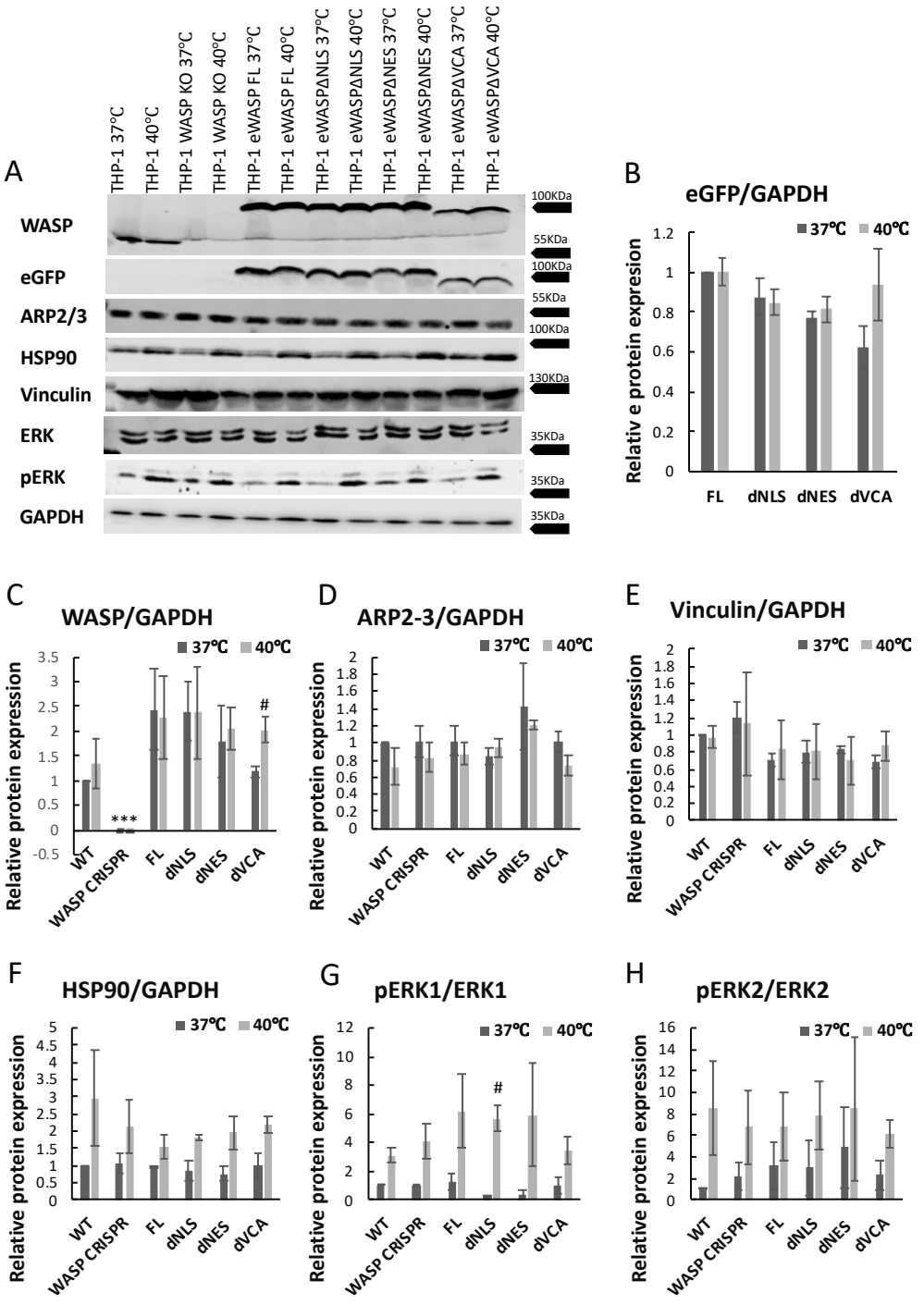

Figure 5.5. Analysis of protein expression in THP-1 WAS deletion mutants' cells.

Representative blots of total cell lysates of THP-1, THP-1 WASP CRISPR (WASP KO) and THP-1 eWAS deletion mutants after 16 hours incubation on fibronectin coated dishes in the presence of 1ng/ml TGFβ-1 at 37 °C and 40°C. GAPDH was used as loading control. (A) Representative Immunoblot of WASP, eGFP, ARP2/3, HSP90, Vinculin, ERK and pERK proteins expression in THP-1 cells cultured at 37°C and 40°C. (B-C-D-E-F-G) Bar graphs show average and SE of each protein relative expression and are representative of two biological replicates. Relative protein expression is normalized for GAPDH. #, t-student test vs control group at 37°C (#P<0.05); * t-student test vs corresponding parental THP-1 cells at 37°C or 40°C (*P<0.05). Arrows on blots indicate protein ladder closest band (10 to 250 kDa, ThermoFisher Scientific).

5.4.4 Role of nuclear shuttling of WASP in morphology and podosomes formation in THP-1 cells

We next investigated how nuclear shuttling would affect THP-1 cells morphology and the distribution of F-actin. THP-1 WASP CRISPR cells failed to assemble podosomes as previously described in other myeloid cells (Olivier *et al.*, 2006) (Figure 5.6). Podosome formation was fully restored in THP-1 cells transfected with the full-length (FL) WASP sequence. Expression of eGFP-WASPΔVCA failed to restore podosome formation indicating that the actin polymerising activity is required for podosome assembly. THP-1 WASP CRISPR cells expressing eGFP-WASPΔNLS cells were able to assemble podosomes, however, they appeared smaller in size, more fused and less discrete. The expression of eGFP-WASPΔNES failed to recover podosome formation, resembling the phenotype already described in both WASP and WIP KO cell lines (Jones, 2008) (Figure 5.6).

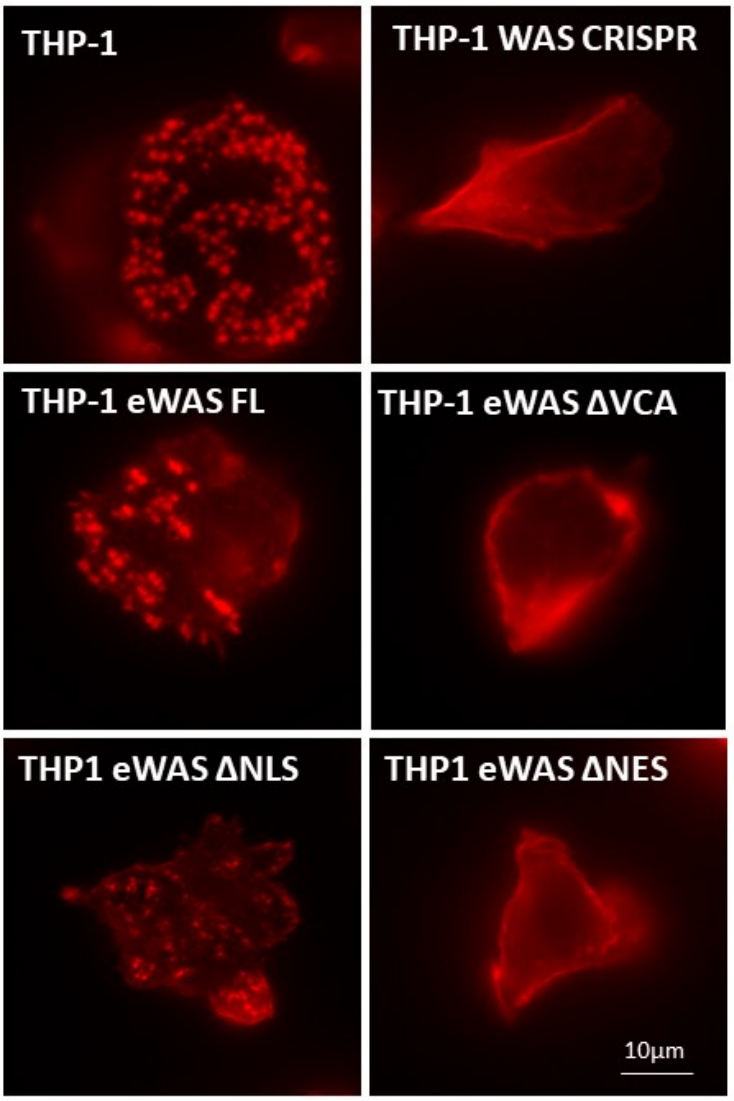

Figure 5.6. Representative micrographs showing THP-1 WAS deletion mutants morphology.

THP-1, THP-1 WAS CRISPR, THP-1 eGFP-WAS FL, THP-1 eGFP-WASPΔNLS, THP-1 eGFP-WASPΔNES and THP-1 eGFP-WASPΔVCA cells were cultured for 16 hours at 37°C on fibronectin coated coverslips in the presence of 1 ng/ml TGFβ-1 and stained with Alexa 568 nm-labelled phalloidin. Micrographs show filamentous actin distribution in one representative cell for each mutation (Bar 10 mm).

We showed in previous chapters that mild hyperthermia promotes podosome formation in THP-1 cells. In this experiment, we tested how hyperthermia affected podosome formation in WASP mutant cell lines (Figures 5.7 and 5.8). Although exposure to mild hyperthermia of WASP CRISPR cells resulted in a significant increase in cells displaying podosomes when compared to cells incubated at 37°C, the percentage of cells with podosomes was still 4.8-fold lower when compared to parental cells (Figure 5.8). Expression of full length eGFP-WASP restored the increased formation of podosomes in response to mild hyperthermia at same levels as parental cells. Deletion of WASP NLS did not impair the enhanced formation of podosomes in response to mild hyperthermia, although podosomes still appeared smaller and more fused when compared to parental cells and THP-1 WASP CRISPR cells expressing full length eGFP-WASP. Similarly to WASP CRISPR cells, podosome assembly increased in eGFP-WASPΔNES cells in response to mild hyperthermia but the percentage of cells displaying podosomes remained 3.2-fold lower when compared to parental cells. The lack of the VCA domain in WASP resulted in failure to increase podosome formation in response to hyperthermia. Taken together, our results indicate that the VCA domains of WASP may play a critical role for the detection of mild hyperthermia in THP-1 cells. Our data also shows that the NES1 and VCA domains are required for podosome initiation and the NLS domain for complete maturation of podosomes required for full functionality.

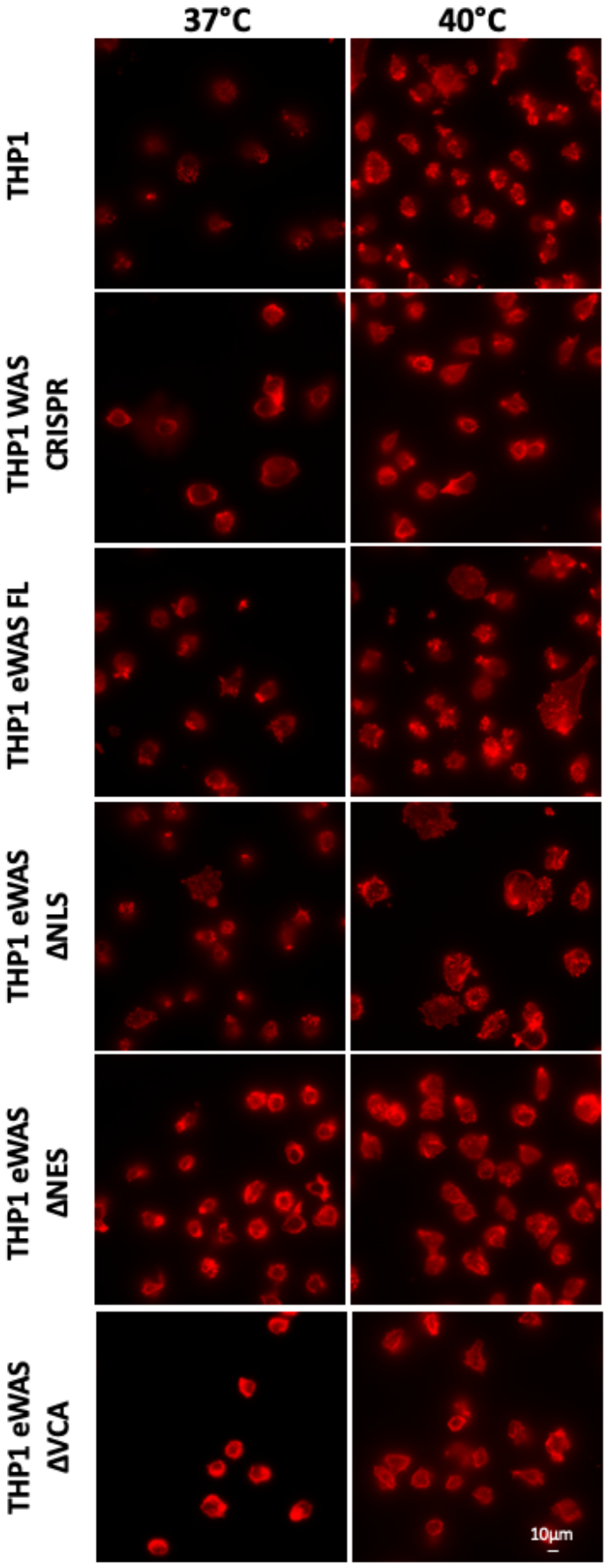

Figure 5.7. Representative micrographs showing podosomes formation in response to exposure to 40ºC in THP-1, THP-1 WASP CRISPR, THP-1 eWASP FL, THP-1 eWASPΔNLS, THP-1 eWASPΔNES and THP-1 eWASPΔVCA.

THP-1 cells were cultured for 16 hours at 37°C or 40°C on fibronectin coated coverslips in the presence of 1ng/ml TGFβ-1 and stained with Alexa 568 nm-labelled phalloidin. Micrographs show filamentous actin distribution in one representative field for each condition (Bar 10 mm).

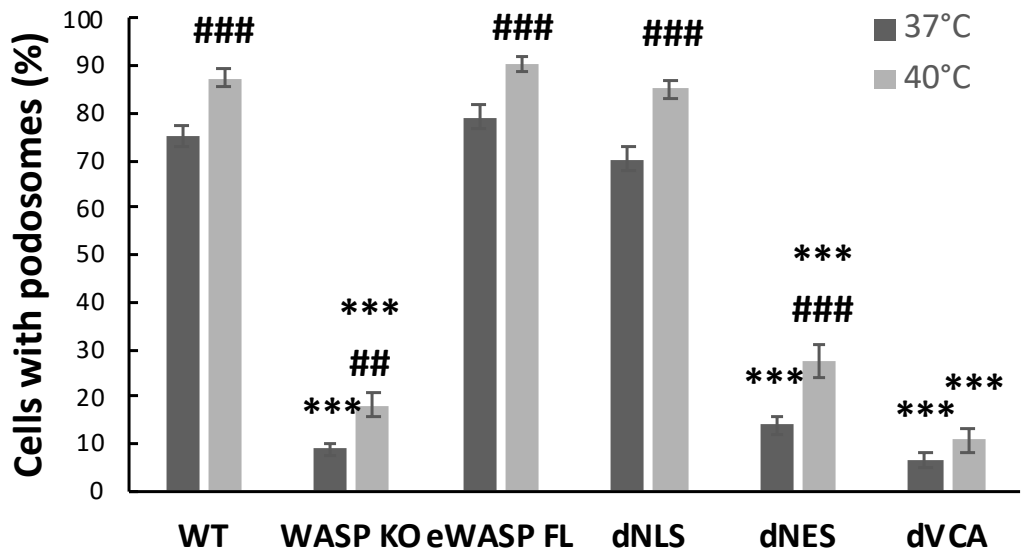

Figure 5.8. Analysis of podosome formation in response to mild hyperthermia in THP-1 WASPCRISPR cells expressing eGFP-WASP deletion mutants for the NES, NLS and VCA domains.

Bar graph shows the average and SE of number of cells with podosomes in THP-1, THP-1 WASP CRISPR, THP-1 eGFP-WASP FL, THP-1 eWASPΔNLS, THP-1 eWASPΔNES and THP-1 eWASPΔVCA cells cultured for 16 hours at 37°C and 40°C on fibronectin coated coverslips with 1ng/ml TGFβ. Data were obtained analysing 10 fields, acquired from at least 2 coverslips per condition at 60x magnification. Data are representative of three biological replicates. #, t-student test vs control group at 37°C (##P<0.01. ###P<0.001); * t-student test vs parental THP-1 cells at 37°C or 40°C (***P<0.001).

Role of nuclear shuttling of WASP in the chemotactic capability and migratory response to hyperthermia of THP-1 cells.

Chemotaxis plays an important role in the immune response (Luster, 2001) and leukocyte migration strictly depends on the dynamic assemble of actin adhesive structures (Calle *et al.*, 2006). WAS patients are generally more prone to develop infectious diseases (Buchbinder, Nugent and Fillipovich, 2014) and this may be addressed to defects in the capability of their immune cells to be recruited to fight pathogens. Therefore, in the next experiment we investigated the role played by the different WASP domains responsible of WASP shuttling to the nucleus in responding to chemotactic factors as MCP-1. While parental and WASP CRISPR THP-1 expressing full length eGFP-WASP cells showed chemotaxis to MCP-1, expression of

the eGFP-WASP mutants lacking the NLS, NES or VCA domains resulted in inhibition of chemotaxis. (Figure 5.9).

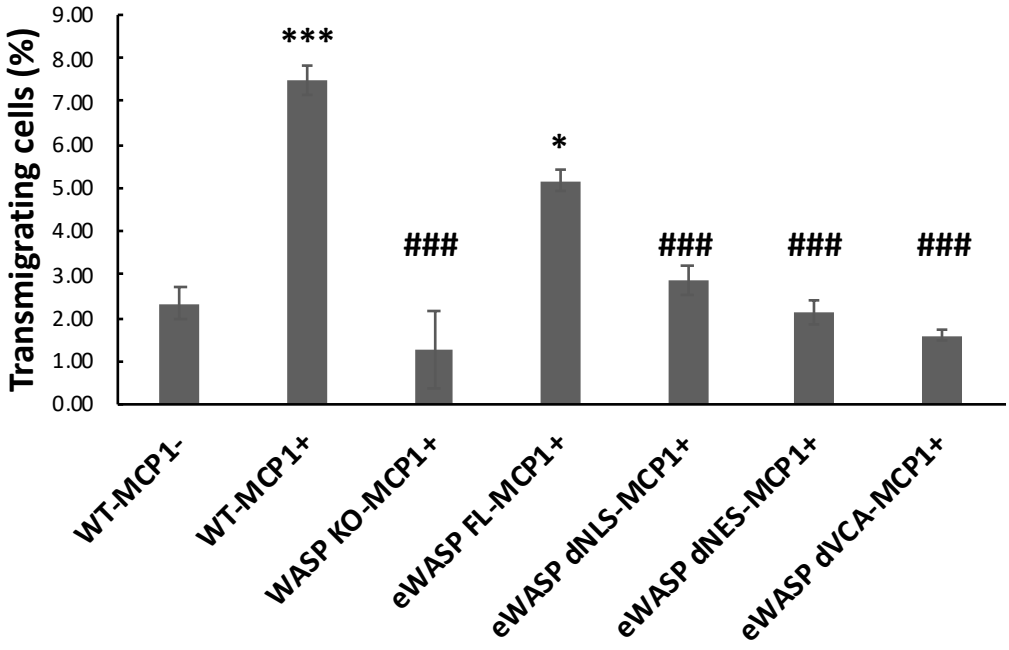

Figure 5.9. Analysis of chemotaxis to MCP-1 of THP-1 WASP CRISPR cells expressing e-WASP deletion mutants for the NES, NLS and VCA domains.

Bar graphs show average and SE of percentage of transmigrated cells towards the lower part of the transwell insert in each condition in the presence of the chemoattractant protein MCP-1 for one hour (50 ng/ml). Unpaired t-Student test was applied. #, t-student test vs control group MCP+; * t-student test vs control group MCP1-.

Furthermore, when migrating randomly on fibronectin coated surfaces, velocity and distance travelled was not affected by the lack of WASP or WASP specific domains at physiological temperatures. However, in response to hyperthermia, an increase in general migration was observed only in parental cells and THP-1 WASP CRISPR cells expressing full length eGFP-WASP, but not in those expressing the mutants lacking the NLS, NES or VCA domains or in WASP KO cells (Figure 5.10).

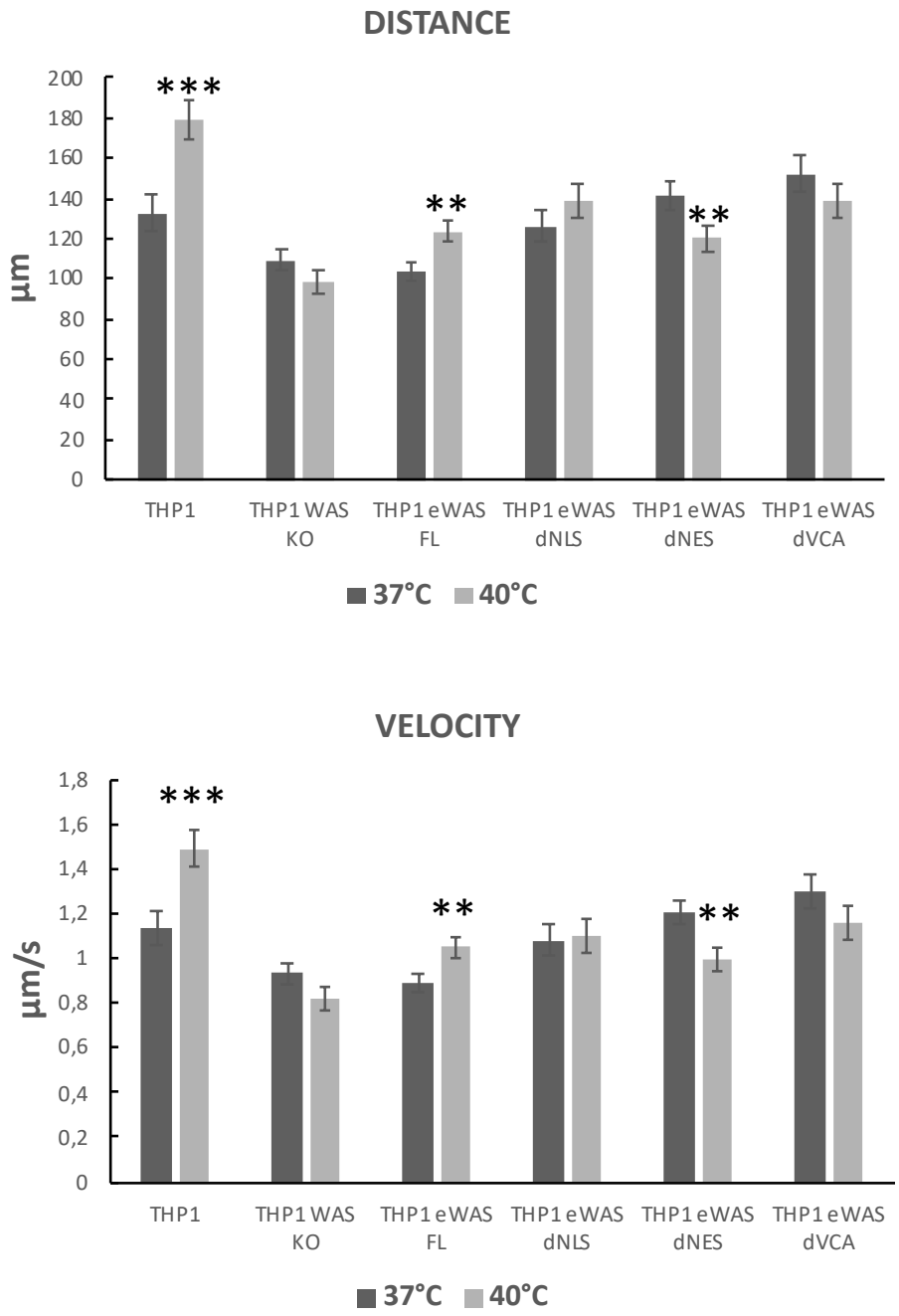

Figure 5.10. Analysis of velocity and distance travelled during random migration of THP-1 WASP CRISPR cells expressing eGFP-WASP deletion mutants for the NES, NLS and VCA domains in response to exposure to mild hyperthermia (40°C).

THP-1, THP-1 WASP CRISPR, THP-1 WASP CRISPR cells expressing full length e-WASP, e-WASPΔNLS, e-WASPΔNES and e-WASPΔVCA were seeded on fibronectin-coated plates in the presence of 1 ng/ml TGFb1 for 16 hours. Time lapse videos of cells were generated by taking phase contrast micrographs every 5 minutes for 2 hours at 37°C or 40°C. (A) Histograms show the average and SE of the total distance travelled in two hours by each tracked cell; (B) Histograms show the average and SE of the velocity (µm/second) of each tracked cells in one frame (n>60).***P<0.001, **P<0.01, unpaired two tail t-Student test 37°C vs 40°C. #, t-student test vs parental cells incubated at the corresponding temperature (#P<0.001, ###P<0.001). Data are representative of three biological replicates.

5.4.5 Role of nuclear shuttling of WASP in matrix degradation capability

Matrix degradation is also defective in immune cells from patients with WAS disease, generally due to the absence of podosomes and failure in metalloproteinase secretion (Mizutani *et al.*, 2002; Bañón-Rodríguez *et al.*, 2011). To address the role played by the NLS and NES1 domains of WASP in matrix degradation, cells were seeded for 16 hours on red fluorescent gelatine coated coverslips. At 37°C the results obtained reflected our data on podosome formation with only cells assembling podosomes (parental THP-1 cells, THP-1 WASP CRISPR cells expressing full length eGFP-WASP or eGFP-WASPΔNLS) being able to degrade matrix (Figures 5.11 and 5.12). Exposure to mild hyperthermia resulted in an increase in matrix degradation capability in parental cells and in THP-1 WASP CRISPR cells expressing full length eGFP-WASP cells only, while no difference was found in THP-1 WASP CRISPR cells expressing eGFP-WASPΔNLS.

Taken together, our data indicate that the domains regulating the nuclear localisation of WASP (NLS and NES1) regulate the migratory and invasive response of myeloid cells in response to external environmental stimuli including chemotactic factors and mild hyperthermia.

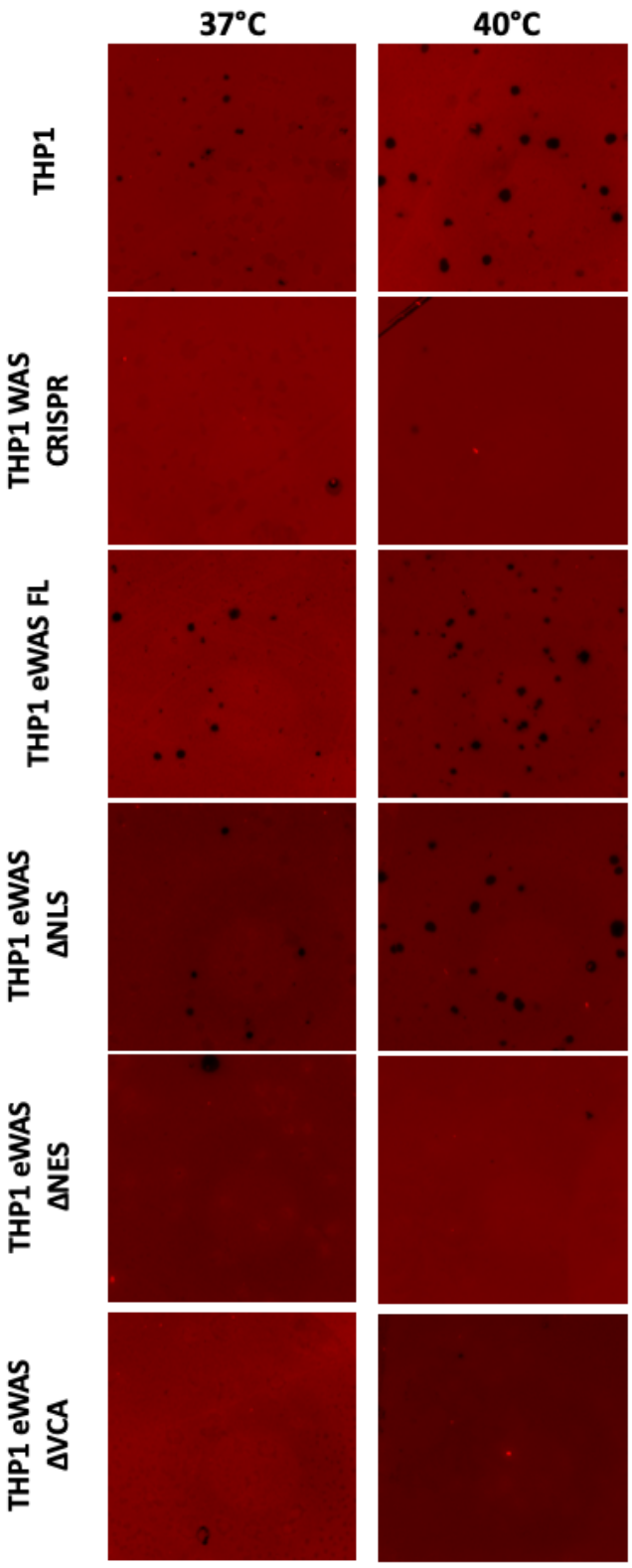

Figure 5.11. Representative fluorescent images of gelatin degradation by THP-1 WASP CRISPR cells expressing eGFP-WASP deletion mutants for the NES, NLS and VCA domains.

Cells were cultured for 16 hours at 37°C or 40°C on red fluorescent gelatin coated coverslips in the presence of 1ng/ml TFGβ. This method allows to visualize the regions where cells degrade matrix to create an area devoid of fluorescence. Images are representative of matrix degradation in each condition.

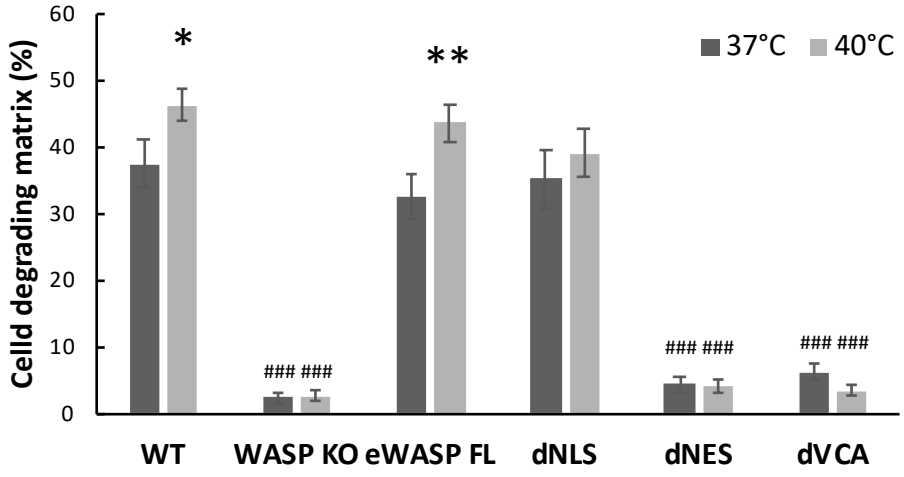

Figure 5.12. Quantitative analysis of matrix degradation of THP-1 WASP CRISPR cells expressing eGFP-WASP deletion mutants for the NES, NLS and VCA domains.

Bar graph shows the average and SE of percentage of THP-1, THP-1 WASP CRISPR, THP-1 e-WASP, THP-1 e-WASPΔNLS, THP-1 e-WASPΔNES and THP-1 e-WASPΔVCA cells able to degrade matrix. Data were obtained from 10 fields acquired from at least 2 coverslips per condition at 60x magnification. Graphs are representative of similar results obtained in three different experiments. Unpaired t test was applied.*, t-student test vs corresponding experimental group at 37°C (**P<0.01, *P<0.05). #, t-student test vs parental cells incubated at the corresponding temperature (###P<0.001).

5.5 Discussion

Formation of actin-based structures and cytoskeleton remodelling are necessary events in cell migration and adhesion. How actin related proteins (ARPs) work together to coordinate the formation of these structures is still largely unknown. In this study, we underlined the importance of understanding the role played by the ARP WASP dual compartmentalization in the cytoplasm and in the nucleus in the migration of myeloid cells using THP-1 cells as a model. Hundreds of mutations in the *WAS* gene have been described (Chandra *et al.*, 1993). They can lead to a phenotypic spectrum of defects in the hematopoietic lineage varying from mild to severe (Jin *et al.*, 2004). Although immune cells in WAS patients present evident defects in functions dependent on actin cytoskeleton remodelling (Ochs *et al.*, 1980; Kenney *et al.*, 1986), only a few of these mutations localise in the actin binding domain of WASP (Kelly *et al.*, 2006) suggesting that additional functions of WASP non-related to its actin polymerising activity may be involved in the pathogenesis of WAS disease. In this chapter, we generated THP-1 cell lines expressing forms of WASP lacking the NLS, NES1 or VCA domains to investigate the role played by WASP nucleus-cytoplasmic shuttling in regulating myeloid cell migration and invasion in response to mild hyperthermia.

WASP cytoplasmic role in podosome assembly has been extensively described (Linder *et al.*, 1999; Mizutani *et al.*, 2002), however, only lately is becoming apparent the importance of this protein in regulating gene expression through its translocation to the nucleus (Taylor *et al.*, 2010). Interestingly, we found that at physiological temperature (37°C) when WASP nuclear localization is impeded, monocytic cells are still able to assemble functional podosomes that can degrade matrix despite of a not completely normal F-actin organisation (smaller in size compared to podosomes formed in parental THP-1 cells). However, although podosome assembly was

enhanced in these cells upon exposure to mild hyperthermia, their ability to migrate or degrade matrix was not significantly increased. Additionally, the lack of the NLS domain of WASP also impaired chemotaxis to MCP-1. Taken together, our data indicate that the nuclear localisation of WASP facilitates myeloid cell migration in response to external stimuli that promote cell migration and recruitment to sites of inflammation including chemotactic cues and mild hyperthermia.

Unpublished data in our research group show that WASP is required for formation of tyrosine phosphorylated complexes with the histone H2AZ, which is the regulator of the expression of temperature responsive genes in plants (Deal and Henikoff, 2010). It is tempting to speculate that WASP may regulate H2AZ functions that might be necessary to induce the immune boost mediated by mild hyperthermia at sites of inflammation or during fever. However, further studies will be required to confirm and understand this process. Recently, WASP nuclear transcriptional role was revealed for the first time. WASP can function as a gene-specific transcriptional cofactor and controls epigenetically the expression of genes involved in the differentiation of Th1 cells (Taylor *et al.*, 2010). It was striking that the defects occurred independently of its actin polymerising activity (Sadhukhan *et al.*, 2014). The epigenetic control played by WASP was dependent on its association with histone H3K4 trimethylase, further supporting possible WASP/histones interactions. Furthermore, there are evidences that nuclear proteins as EZH2, a histone H3K27 methylase, have cytoplasmic roles in remodelling F-actin cytoskeleton in T cells (Su *et al.*, 2005). The activity of WASP or WASP family proteins in the nucleus is also conserved in other species: it is fundamental for organogenesis in *Drosophila* (Rodriguez-Mesa *et al.*, 2012), infectivity in Baculoviruses (Goley *et al.*, 2006) and oocyte development in *Xenopus* (Miyamoto *et al.*, 2013). The fact that WASP nuclear

role is evolutionary maintained in so diverse organisms further supports a key role in WASP function that deserves further investigation.

In THP-1 mutants lacking the NES1, WASP was still able to localize in the cytoplasm. WASP sequence presents an additional putative export signal known as NES2. It was shown that WASP cytosolic localization was not impaired in T cells lacking the NES1, addressing NES2 as the only responsible of the export process (Sadhukhan *et al.*, 2014). Therefore, we can conclude that similarly to T cells, in monocytes the NES1 does not play an essential role in WASP shuttling. However, WASP cytoplasmic functions were strongly disturbed. For instance, in these mutants, podosomes failed to form correlating with defects in migration and capacity for matrix degradation similarly to the absence of WASP in the WASP CRISPR cells or in cells expressing WASP lacking the VCA domain. While general migration at physiological temperatures was not affected, these cells failed to enhance velocity and distance travelled in response to hyperthermia. Further studies will be required to investigate in depth the role played by the NES1 sequence in actin remodelling. Interestingly, blasting the putative depleted NES1 sequence, we found that the NES1 aminoacidic sequence (LFEMLGRKCLTL) occupies the position 35 to 46 in WASP sequence, overlapping with the beginning of the WH1 domain (39-148). A mutation in the WH1 domain transcription might be the cause of the defective actin polymerization, since this domain is essential for WASP/WIP complex formation. However, the WASP/WIP complex is probably only partially disrupted since WASP total expression is slightly decreased, while, in case of the total absence of WIP binding, WASP would be degraded as shown in chapter 3. Furthermore, it was shown that WASP mutants for the WH1 domain cannot bind EP400, a catalyser of chromatin conversion from unmodified H2A to heterotypic H2AZ-marked chromatin in the nucleus (Sarkar *et al.*,

2014). It may be possible that WASP mutants lacking the NES1, and in turn presenting a mutation in the WH1 domain, may not covert H2A into H2AZ. Therefore, WASP nuclear role in complex with H2AZ might be disrupted, leading to a failure in activating temperature responsive genes and therefore, a lack of response to the temperature-induced stimuli. Further studies should be performed to investigate this possibility.

Our data also indicated that the actin polymerising activity of WASP can regulate its nuclear localisation since depletion of the WASP VCA domain resulted in accumulation of WASP in the nucleus. This correlated with our data in Chapter 3 (Figure 3.13) showing that disassembly of F-actin induced by treatment with Cytochalasin D resulted in nuclear accumulation of WASP. Interestingly, when actin polymerization is impaired due to cytochalasin D treatment, both WASP and ARP2/3 actively translocate in the nucleus of THP-1 cells. Additionally, deletion of the VCA domain of WASP in THP-1 cells resulted in a partial downregulation of total WASP levels. The interaction of the carboxy-end of WASP, where the VCA lies, and the CRIB domain keeps WASP in an autoinhibited hairpin conformation that also avoids degradation of WASP by the proteasome or calpains. It is possible that deletion of the VCA domain may destabilise the closed conformation of this WASP mutant construct making it more accessible for calpain and or proteasome degradation, leading to the observed reduced WASP levels in THP-1 cells expressing the WASPΔVCA mutant.

Not only WASP, but other actin related proteins can localise in the nucleus where they exert transcriptional roles. In particular, N-WASP nuclear localization was found to be controlled by phosphorylation of tyrosine residues. Unphosphorylated N-WASP localize in the nucleus leading to a decreased expression of HSP90, by interaction with Heat shock transcription factors (HSTF). HSP90 is essential for Src kinases activity,

therefore downregulating HSP90 delivers a feedback mechanism to drive N-WASP in the nucleus (Suetsugu and Takenawa, 2003). N-WASP was found to be involved in several other nuclear processes as part of a complex with PSF-NonO, RNA pol II and actin. When N-WASP actin polymerization activity is defective, due to the absence of the VCA domain or due to the presence of actin inhibitors drugs as Cytochalasin D, global transcription defects were observed, highlighting the essential role of N-WASP in polymerizing nuclear actin and working as a transcriptional regulator (Wu *et al.*, 2006). Furthermore, the junction-mediating and regulatory protein (JMY), that belongs to a class of proteins that can nucleate actin independently from the presence of the ARP2/3 complex, was found to play an important nuclear role. Interestingly, JMY-mediated p53 transcription is inhibited when cells are treated with actin inhibitors drugs. In fact, JMY shuttling in the nucleus in response to DNA damage, to activate p53 mediated cell apoptosis, is controlled by actin dynamics in the cytoplasm. Upon DNA damage, actin polymerization is enhanced and monomeric actin is sequestered in the growing filament, freeing the WH2 domain of JMY and in turn allowing activation of the NLS (Zuchero *et al.*, 2009). Finally, the lately discovered member of the WAS family, WASH, was found to have an essential role in modelling *Drosophila* nuclear architecture by interaction with Lamin B. Depletion of this complex induced global chromatin redistribution and histones modifications, interfering with nuclear morphology (Verboon *et al.*, 2015)

Taken together, these latest findings fit with our current data on WASP nuclear shuttling, indicating that an important transcription role might be played by WASP in the nucleus through histones interaction to control the cellular response to hyperthermia and that there is a strict connection between actin polymerization

activity and nuclear transcription. Further studies are needed to clarify these possible roles of WASP.

Chapter 6: Discussion

6 Discussion

Many studies showed that mild hyperthermia, as during a local inflammatory event, can stimulate immunity, affecting both innate and adaptive immunity cells (Ingersoll *et al.*, 2011; Evans, Repasky and Fisher, 2015). However, the mechanisms driving the recruitment and activation of immune cells following hyperthermia are still poorly understood. This thesis focused on delineating the WASP/WIP complex as the orchestrator of the activation and recruitment to the site of inflammation of immune cells, in particular myeloid cells (monocytes and dendritic cells), mediated by the external stimulus of mild hyperthermia. The main events considered in this study are migratory and invasive capability, regulation of gene expression and remodelling of membrane lipid composition. We found that each one of these events can be influenced by hyperthermia through regulation by the WASP/WIP complex and that these processes are interconnected within each other. In monocytes and dendritic cells, the WIP/WASP complex is essential to assemble actin rich, highly dynamic, dot shaped migratory structures known as podosomes (Jones, 2008). Therefore, it is not surprising that any regulation mediated by this complex would involve reorganization and redevelopment of these structures. It is important to highlight that WIP deficiency causes WASP deficiency (de la Fuente *et al.*, 2007), leading to difficulties in discriminating which of these two proteins plays a major role. Although it might seem immediate to address WASP as the main player of the incremented immune response, it is also well known that WIP is involved in numerous processes in a WASP independent manner. In fact, when WASP levels are restored in a WIP deficient cell line, actin polymerization is still impaired and takes place in inappropriate site (Chou *et al.*, 2006). Furthermore, 80% of the mutations in patients with symptomatic WAS

are localized in the WIP binding site of WASP (Volkman *et al.*, 2002). For all these reasons, in this thesis we investigated the role of both WIP and WASP.

The investigation of the role of WIP/WASP into the response to hyperthermia was triggered by preliminary data showing that both WIP and WASP can form tyrosine-phosphorylated complexes with the histone H2AZ (Dr Calle's unpublished data), whose role in controlling the expression of temperature responsive genes in plants by regulation of RNA polymerase II access to the chromatin was previously described (Deal and Henikoff, 2010). This finding suggested that the WIP/WASP unit may modulate leukocyte response to hyperthermia by a possible regulation of gene expression. Interestingly, the role of both WASP and WIP in controlling gene transcription has been previously described, with the first one being a regulator of histone methylation of adaptive immunity genes (Sadhukhan *et al.*, 2014) and the latter a regulator of transcription factors as a result of actin remodelling (Ramesh *et al.*, 2014). Additionally, the WIP homologue in *Saccharomyces cerevisiae*, Vrp1p, is essential to maintain survival and sustain cytoskeletal dynamics when exposed to higher temperatures (Thanabalu and Munn, 2001). These evidences made us prone to further investigate whether the WASP/WIP complex could work as a functional unit to link actin cytoskeleton remodelling and gene regulation in response to mild hyperthermia, exploring the potential mechanism employed in in the regulation of the increased leukocyte migration to sites of inflammation in response to heat.

We first verified whether mild hyperthermia would induce an increase in THP-1 and primary mouse dendritic cells migratory and chemotactic response. It is known that heat stress can promote lymphocyte trafficking and adhesion (Chen and Evans, 2005), macrophage proliferation (Mescher, 2017) and neutrophil recruitment to distant infected tissues (Takada *et al.*, 2000; Tulapurkar *et al.*, 2012). The mechanisms

delivering this improved immune response are poorly understood, however, it was demonstrated that HSPs can orchestrate many of these reactions. In particular, HSPs upregulation following heat stress increases NK cells cytotoxicity (Dayanc *et al.*, 2008), macrophage activation by controlling production of cytokines and nitric oxide (Pritchard, Li and Repasky, 2005; Gupta *et al.*, 2013; Repasky, Evans and Dewhirst, 2013) and improves T-cell adhesion by modulating with the expression of adhesion molecules (Chen and Evans, 2005; Park *et al.*, 2005). However, what is still unclear and, therefore was investigated in this thesis, is the effect of heat on the cytoskeletal remodelling process necessary for the improved migratory phenotype. We observed an increment in invasive migration in myeloid cells exposed to hyperthermia. This invasive migratory phenotype was obtained in the absence of pathogens or inflammatory cytokines, resembling cells recruitment during early stages of inflammation. Increased migration correlated with higher formation of more robust podosomes. It is likely that the higher assembly of podosomes can improve several steps of diapedesis by enhanced adhesive capability, promoting leukocyte adhesion to the endothelium, and enhanced matrix degradation, facilitating crossing of tissue boundaries. Chemotaxis was also accelerated by cells higher response towards MCP-1, a cytokine produced at the sites of inflammation, during mild hyperthermia. Once reached the site of inflammation, podosomes are not further required since myeloid cells need to increase their phagocytic capacity to fight infections. Here, podosomes are disassembled, as observed in dendritic cells activated by TLR signalling and prostaglandins (West *et al.*, 2008; Gawden-Bone *et al.*, 2014), and actin polymerization is deployed towards the formation of phagocytic cups (West *et al.*, 2004). Phagocytosis was also shown to be improved by mild hyperthermia, however this event was not further studied in this thesis (Postic *et al.*, 1966; Djaldetti and

Bessler, 2015). Given the key role of WIP and WASP in the process of podosome formation through regulation of F-actin and integrin dynamics (Chou *et al.*, 2006; Jones, 2008; Vijayakumar *et al.*, 2015), it is not surprising that in the absence of these proteins, cells fail to increase their migratory capacity in response to hyperthermia, accordingly. However, it is also possible that WIP mediates changes in cytoskeletal dynamics in response to hyperthermia through additional mechanisms than cortactin and/or WASP-mediated actin polymerisation.

WIP was recently associated with the ability to control sphingomyelin levels at the plasma membrane, which regulated the remodelling of F-actin assembly in neurons dendritic spines (Franco-Villanueva *et al.*, 2014). We hypothesised that in leukocytes WIP may also regulate the lipid composition of the plasma membrane involved in signalling towards cytoskeletal remodelling. Additionally, a novel theory ("Membrane Sensor Hypothesis") addresses the perturbation in the membrane lipid fluidity as a mechanism to sense thermal stress (Török *et al.*, 2014). In particular, heat stress can interfere with the normal physical properties of the membrane by altering its fluidity and, in turn, leading to changes in lipid reorganization and composition necessary to maintain homeostasis. Following sensing of the heat stress and lipid modification, an activation cascade of events can lead to expression of HSPs, determining cell fate (Fan-Xin *et al.*, 2012; Hsu and Yoshioka, 2015). Interestingly, we observed that parental THP-1 cells can counteract the increment in fluidity of the membrane at adhesion sites caused by hyperthermia. However, in the absence of WIP, the plasma membrane in THP-1 cells, which appears already more rigid at physiological temperatures, cannot counteract the increment in fluidity following hyperthermia. This correlated with altered lipid composition in the plasma membrane in WIP KD cells, including some species whose proportion increased or decreased in

parental cells in response to exposure to mild hyperthermia. Taken together, these results show that WIP regulates the lipid composition in the plasma membrane and this may explain the role of WIP in regulating the fluidity of the plasma membrane at adhesion sites and maintaining homeostasis during exposure to mild hyperthermia. Additionally, our data confirmed that increasing membrane fluidity using drugs, also leads to increased migration and podosome formation in THP-1 cells. This finding correlates with recent work showing that membrane fluidity can influence haematopoietic cells adhesion and migration through clustering of adhesion complexes and lipid rafts (Matsuzaki *et al.*, 2018). Additionally, lipid composition and membrane fluidity can influence cells migratory phenotype, as seen in cancer cells where increased membrane fluidity, due to ceramide depletion, can determine epithelial-mesenchymal transition (Edmond *et al.*, 2015). Similarly, drugs capable of altering membrane fluidity represent a promising cancer treatment able to prevent metastasis diffusion (Glatzel *et al.*, 2018; Stoiber *et al.*, 2018).

We then explored whether the changes in cytoskeletal remodelling and/or in the lipid composition in response to mild hyperthermia in THP-1 cells could be explained by the previously described role of WIP in regulating the pattern of gene expression. In neurons, WIP regulates the levels of sphingomyelin through upregulation of the Neutral Sphingomyelinase gene (Franco-Villanueva *et al.*, 2014) and it has been previously shown a role of WIP in regulation of gene expression through the organisation of F-actin (Ramesh *et al.*, 2014). We found that WIP is required for the regulation of expression of HSP90, a key protein that we confirmed to be upregulated in response to mild hyperthermia. The increased expression of HSP90 in response to mild hyperthermia may, in turn, cooperate with WIP in regulating expression of lipid related genes. HSP90 was proved to regulate gene

expression by epigenetic mechanisms when cells are exposed to an unfriendly environment through association with histone deacetylases and DNA methylases (Erlejman *et al.*, 2014; Mazaira *et al.*, 2018). Among the transcription factors regulated by HSP90, sterol regulatory element binding proteins (SREBPs) were identified. HSP90 protect SREBPs from proteasome degradation and inhibition of HSP90 leads to downregulation of SREBPs target genes (Kuan *et al.*, 2017). These genes are involved in modulating lipid biosynthesis and cholesterol levels through proteolytic release from membranes (Brown and Goldstein, 1997; Horton, Goldstein and Brown, 2002). Interestingly, we found that SREBF1 (sterol regulatory element binding transcription factor 1) gene is downregulated in WIP KD, but not in parental cells, exposed to hyperthermia, indicating possible defects in controlling proteolytic release of cholesterol from membrane in response to hyperthermia. SREBPs role in fatty acid synthesis through activation of transcription of FASN was also described (Horton, Goldstein and Brown, 2002). Contrarily to what observed for SREBF1, we found FASN to be downregulated in parental THP-1 and not WIP KD cells during heat stress. Furthermore, several genes involved in cholesterol transport and uptake such as apolipoproteins are upregulated or downregulated in response to hyperthermia in a WIP dependent manner. Overexpression of HSP90, caused by mild hyperthermia, might also be a further factor responsible of the increased podosome assembly given the previously described role of HSP90 as a podosome component (Park, Suetsugu and Takenawa, 2005). Thermal therapy is employed to stimulate tumour immunity through changes in membrane fluidity and upregulation of HSPs (Gao *et al.*, 2016), fitting with our data of increased motility and invasiveness observed in parental monocytes and dendritic cells exposed to hyperthermia. Additionally, HSP90 was previously associated with podosome formation through regulation by Src kinase and

stabilization of N-WASP (Park, Suetsugu and Takenawa, 2005). A further pathway activated by HSPs is the ERK pathway (Dou, Yuan and Zhu, 2005). We found that ERK phosphorylation was increased in monocytic cells in response to hyperthermia. ERK can be activated downstream of integrins and interacts with proteins involved in protrusion development and migration (Dou, Yuan and Zhu, 2005). However, HSP90 overexpression was also observed in WIP deficient cells at physiological temperature. While podosome assembly cannot occur in these cells due the absence of actin nucleator proteins, HSP90 overexpression can lead to increased secretion of cytokines such as IL-1β and the hyper inflammatory phenotype. This possibility is supported by our findings as in WIP KD cells we also detected an increment in the expression of the gene coding for IL-1β. Our results also indicate that WIP has a WASP-independent role in controlling HSP90 expression, since WASP KO cells do not overexpress HSP90 at physiological temperatures compared to parental cells.

As described above, we observed that WIP can mediate the expression of several genes involved in formation of specialized lipid signalling domains in THP-1 cells. Interestingly, the activation and organisation of cell adhesion receptors, such as integrins in podosomes, is dependent on the formation of specialised lipid microdomains, rafts or caveolae. For instance, the expression of the integrin lymphocyte function-associated antigen 1 (LFA1), that is present in podosomes and it is involved in monocytes binding to ICAM-1 (Evans *et al.*, 2003), depends on sphingomyelin (SM) levels (Eich *et al.*, 2016). Upon SM conversion into ceramide by Sphingomyelinase (SMase), LFA-1 binding to ICAM-1 is reduced significantly, as seen for β2 integrins in neutrophils (Feldhaus *et al.*, 2002). This event is due to exclusion of LFA1 from glycosphingolipids enriched domains in the absence of SM, indicating an important role of SM and lipid rafts in controlling adhesion (Eich *et al.*,

2016). The actin-related functions of WIP may be essential for rafts and membrane microdomain organisation. A link between actin reorganization and lipid rafts formation was already described in T-cells (Villalba *et al.*, 2001) and in the formation of immune synapses in B-cells (Bolger-Munro *et al.*, 2019). Furthermore, WASP is recruited in lipid rafts in CD28 activated T cells playing an important role in lipid rafts movement (Dupré *et al.*, 2002). WIP may also play a role in the organisation of these lipid domains as several genes involved in generation and organisation of sphingomyelin/ceramide containing rafts were altered in WIP KD cells. As mentioned above, previous studies have shown that WIP regulates the levels of SM in neurons by modulating the levels of neutral sphingomyelinase (Franco-Villanueva *et al.*, 2014). Although we did not observe WIP-dependent changes in the levels of transcript of neutral sphingomyelinase by m-RNA sequencing analysis, we detected significant higher levels of the transcript for Neutral-SMase Activating Factor (NSMAF) in THP-1 parental cells vs WIP KD cells, suggesting a possible WIP-dependent regulation of SM levels. We also found that OSBPL5, the gene coding for the oxysterol-binding protein ORP5, is downregulated in WIP KD cells vs THP-1 parental cells and in parental cells in response to hyperthermia. ORP5 is a possible homologue of Mga2, a transmembrane receptor used by *Saccharomyces cerevisiae* to detect changes in membrane fluidity and pressure in the ER in response to increased temperature (Martin, Oh and Jiang, 2007; Ballweg *et al.*, 2019). OSBPL5 can also affect the levels of phosphatidylserine (PS) in the inner plasma membrane (Kattan *et al.*, 2019), which in turn can stimulate the activity of N-SMase (Liu *et al.*, 1998; Airola and Hannun, 2013; Avota, de Lira and Schneider-Schaulies, 2019) hence, affecting formation of rafts at the plasma membrane. This pattern of expression of NSMAF and OSBPL5 suggests a role of WIP in regulating raft organisation in response to hyperthermia.

These results also suggest that WIP may maintain low levels of SM at 37°C, which may only increase when cells are exposed to hyperthermia. These results prone to future studies to determine raft organisation in response to hyperthermia and the possible role of WIP in this process.

Taken together, these results show that WIP regulates the expression of enzymes required for maintenance of membrane lipid content and for the regulation of sphingomyelin, which will affect formation of rafts and caveolae in response to increased hyperthermia.

In summary, we found that WIP regulates the overall lipid composition of cell membrane and the fluidity of the plasma membrane at adhesion sites in THP-1 cells. We also found that WIP is required for the adequate expression of genes involved in modulating the lipid composition of cellular membranes. WIP regulation of the expression of the identified genes may explain the changes in lipid composition and fluidity of the cell membrane, but further experiments will be needed to confirm this. The composition and organisation of these lipids may determine: a) the clustering and activation of cell adhesion molecules and other membrane receptors involved in podosome formation at 37°C and b) the podosome increased dynamics and activity in response to mild hyperthermia at 40°C leading to increased overall invasive migration and chemotaxis.

Since WIP KD cells also express limited levels of WASP (Chou *et al.*, 2006; Ramesh *et al.*, 2014; Vijayakumar *et al.*, 2015), we decided to explore whether the observed increased migration and invasive capacity in response to hyperthermia was also dependent on WASP. Our data indicated that WASP binding to the Arp2/3 complex and actin, required for actin polymerisation, is essential for the increased migratory phenotype of THP-1 cells in response to hyperthermia. Additionally, we

found that the NLS of WASP is also essential in this process. However, further studies will be required to determine whether the WIP-dependent changes in the expression of the genes involved in the thermo-modulation of lipid saturation or raft/membrane microdomain organisation in THP-1 cells may also be dependent on the nuclear localisation of WASP or the functionality of other WASP domains. As previously mentioned, the pilot data that triggered the investigations in this thesis showed that in the absence of WASP or WIP, DCs failed to form Tyr-phosphorylated complexes containing the histone H2A.Z. It would be interesting to investigate whether the regulation of these histone complexes may be dependent on the nuclear localisation of WASP. In T-cells, WASP interaction with histone H3K4 trimethylase is essential for WASP epigenetic activity as a modulator of histone methylation (Taylor *et al.*, 2010; Sadhukhan *et al.*, 2014). It may be possible that using similar mechanisms, WASP may regulate gene expression in response to hyperthermia in myeloid cells.

WIP may regulate gene expression through additional mechanisms. A mechanism that should be further explored is the regulation of gene expression by the co-transcription factor, serum response factor (SRF) / myocardin-related transcription factor A (MRTFA). The regulation of actin dynamics by WIP can control the nuclear localisation of MRTFA (Ramesh *et al.*, 2014). Additionally, our results showed that exposure to mild hyperthermia induces a WIP/WASP-dependent translocation of the ARP2/3 complex to the nucleus in a similar way as when actin polymerization is prevented. In the absence of WIP/WASP in WIP KD cells, the hyperthermic stimulus is not sufficient to translocate the ARP2/3 complex to the nucleus, where it might play a role in regulating expression of cytoskeleton remodelling genes. Interestingly, the ARP2/3 complex in the nucleus is a regulator of transcription through regulation of RNA pol II (Yoo, Wu and Guan, 2007). Further studies should determine what specific

genes that are modulated in response to hyperthermia are dependent on the increased nuclear localisation of the Arp2/3 complex.

The fact that similar outcomes were observed in both WIP and WASP mutants throughout our work, indicates that WASP deficiency alone is a sufficient in order to induce the poor responsiveness to hyperthermia. However, studies were not performed to identify the possible role of WASP in controlling membrane lipids remodelling. Then, based on our current data it is not possible to know whether WIP or WASP are the main orchestrator of the lipid's reorganization. Furthermore, while WIP KD cells presented a higher expression of HSP90 at physiological temperature, this was not observed in WASP KO cells, indicating a WASP-independent role played by WIP in controlling HSP90 expression and possibly specific signalling response induced by hyperthermia.

In summary, our overall results pinpoint WIP as a regulator of lipid reorganization and cell adhesion dynamics leading to increased monocytic cell migration in response to hyperthermia. However, the mechanism employed by WIP to regulate the observed changes in gene expression in response to hyperthermia, especially of those genes involved in raft and caveolae formation, will require further investigations.

Chapter 7: Conclusions

7 Conclusions

The following conclusions can be drawn in this thesis:

- In response to mild hyperthermia, myeloid cells increase their migratory and invasive capability, thanks to the increased assembly of podosomes with high turnover in a WIP/WASP dependent manner.
- WASP regulates the migratory burst in response to hyperthermia through its actin polymerising activity as well as by its nuclear localization domain.
- Changes in membrane fluidity caused by hyperthermia are modulated by WIP and they induce the migratory and invasive phenotype in myeloid cells. Specifically, podosomal areas in the basal adhesion plane of cells present a more fluidic lipid membrane regulated at physiological temperature and sustained under hyperthermia by WIP function.
- WIP regulates the lipid composition of the plasma membrane of THP-1 cells, including those lipids whose levels change in response to mild hyperthermia.
- WIP may regulate the lipid composition and membrane fluidity of the plasma membrane through regulation of transcription of genes involved in organisation of lipid rafts, including NSMAF, OSBPL5 and regulators of the cholesterol pathway.
- WIP may regulate the response to hyperthermia by controlling the expression of HSP90. This process is independent of the presence of WASP.
- Possible identified mechanisms regulated by WIP to control gene expression in response to mild hyperthermia include: a) WIP-dependent translocation of the Arp2/3 complex into the nucleus; and b) the nuclear localisation of WASP.

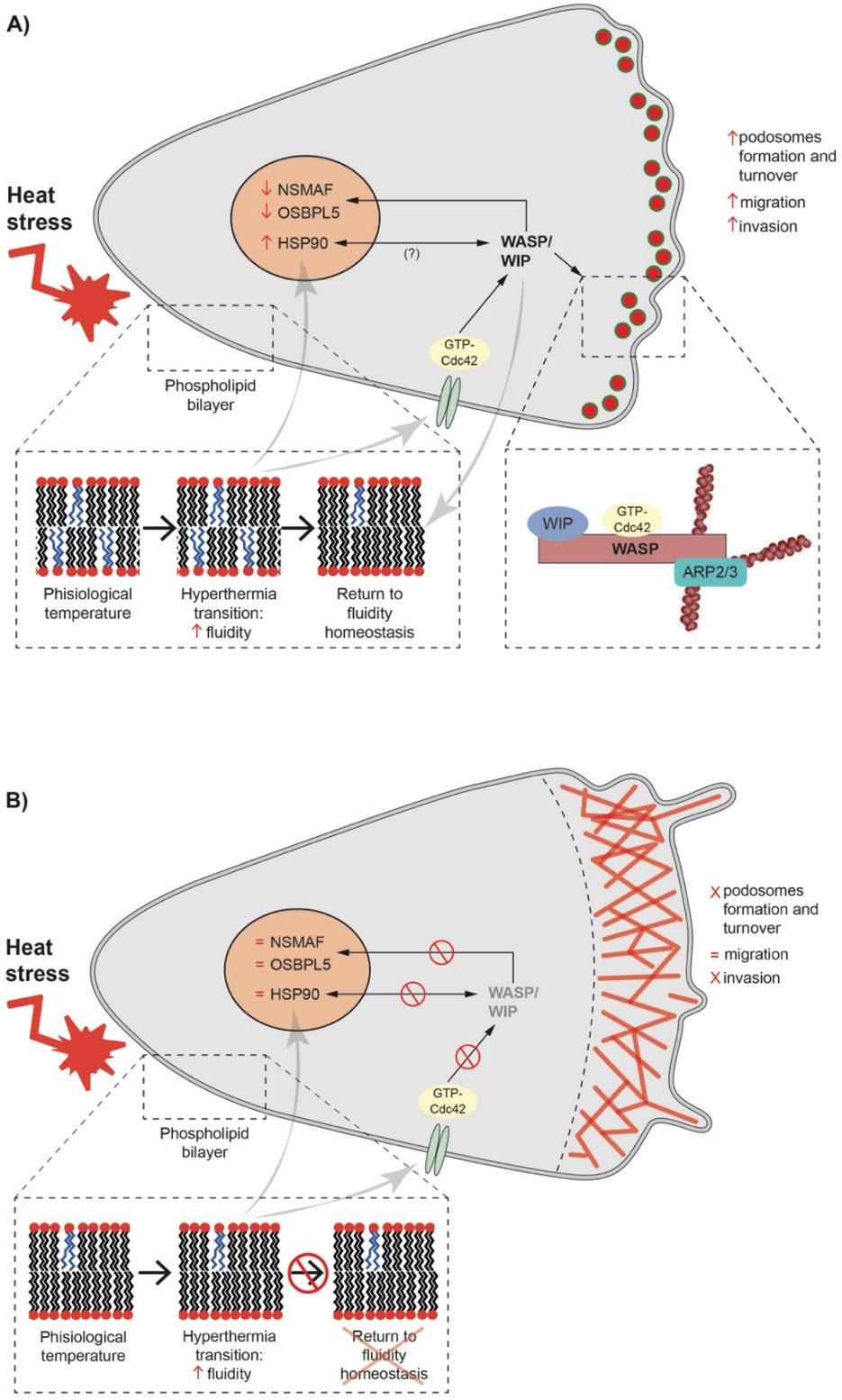

Figure 7.1. Schematic representation of THP-1 and WIP KD THP-1 cells response to hyperthermia.

(A) THP-1 cells present actin rich podosmes (red) surrounded by defined vinculin rings (green) assembled at the cell leading edge. They respond to hyperthermia by increasing migratory and invasive capability. This result is achieved thanks to actin cytoskeleton remodelling by the WIP/WASP complex and trough WIP/WASP nuclear localization. In the nucleus, WIP and WASP can play a role in

regulating the expression of lipid biosynthesis genes as NSMAF and OSBPL5 and, therefore, regulate the lipid composition of the plasma membrane, maintaining membrane fluidity homeostasis by decreasing lipid saturation levels. Alternatively, in response to hyperthermia, membrane fluidization leads to increased expression of HSP90. HSP90 can bind to the WIP/WASP complex, stabilizing podosomes formation and inducing the improved migratory and invasive phenotype. (B) WIP KD THP-1 cells present at physiological temperatures a more rigid plasma membrane due to the absence of the more fluidic podosomal regions, replaced by focal adhesions (red) assembled at the cell leading edge. As seen in parental cells, hyperthermia causes a transient increment in membrane fluidity, independently of changes in membrane lipids. However, the absence of the WIP/WASP complex determines a failure in returning to membrane fluidity homoeostasis. Migration is not augmented in response to hyperthermia and podosomes formation and matrix degradation capability are defective in these cells.

Chapter 8: Appendix

8 Appendix

8.1 Dendritic cells isolation

DCs slides and lysates were obtained from Dr. Calle's archives. DCs were generated from mouse spleens obtained from 6- to 8-week-old WT and WIP KO mice as previously described (Calle *et al.*, 2006). Spleens were homogenised to obtain a cell suspension. Following two washes with RPMI 1% FCS, cells were resuspended in RPMI supplemented with 10% foetal bovine serum (FBS), 1 mM pyruvate (Sigma, UK), 1x non-essential amino acids (Sigma, UK), 2 mM glutamine (Sigma, UK), 50 βM 2-ME (Gibco BRL), 20 ng/ml recombinant mouse GM-CSF (R&D Systems) and 1ng/ml recombinant human TGF- β (R&D Systems). Cells were seeded at a density of $2x10^6$ cells/ml in 75 cm^2 culture flasks at 37°C in a 5% CO2 atmosphere. Cells were re-plated and medium replaced at day 8 and 80-90% of the culture was differentiated into DCs at day 17-18.

8.2 Gene expression profiling

Raw data of the analysis were extracted with Illumina's GenomeStudio data analysis software in the form of GenomeStudio's Final Report (sample probe profile). These data were analysed using the R/Bioconductor statistical computing environment (www.r-project.org, www.bioconductor.org). Using the lumi Bioconductor package (Du, Kibbe and Lin, 2008), raw expression data were background corrected, log2 transformed and normalized. Probes not identified in at least one sample (p-value > 0.01) were discounted for subsequent analyses as they represent non expressed transcripts. For the detection of differentially expressed genes, a linear model was

fitted to the data and empirical Bayes moderated t-statistics were calculated using the limma package (Smyth, 2004) from Bioconductor.

Adjustment of p-values was done by the determination of false discovery rates (FDR) using Benjami-Hochberg procedure. Samples were assigned to groups and clustered as in figure 4.1A for the purpose of the comparison. Although some variability was observed among the samples, biological replicates resulted to be highly reproducible as shown in the Principal Component Analysis (PCA, 4.1B). Sample "KD40A" was excluded from the analysis due to low quality.

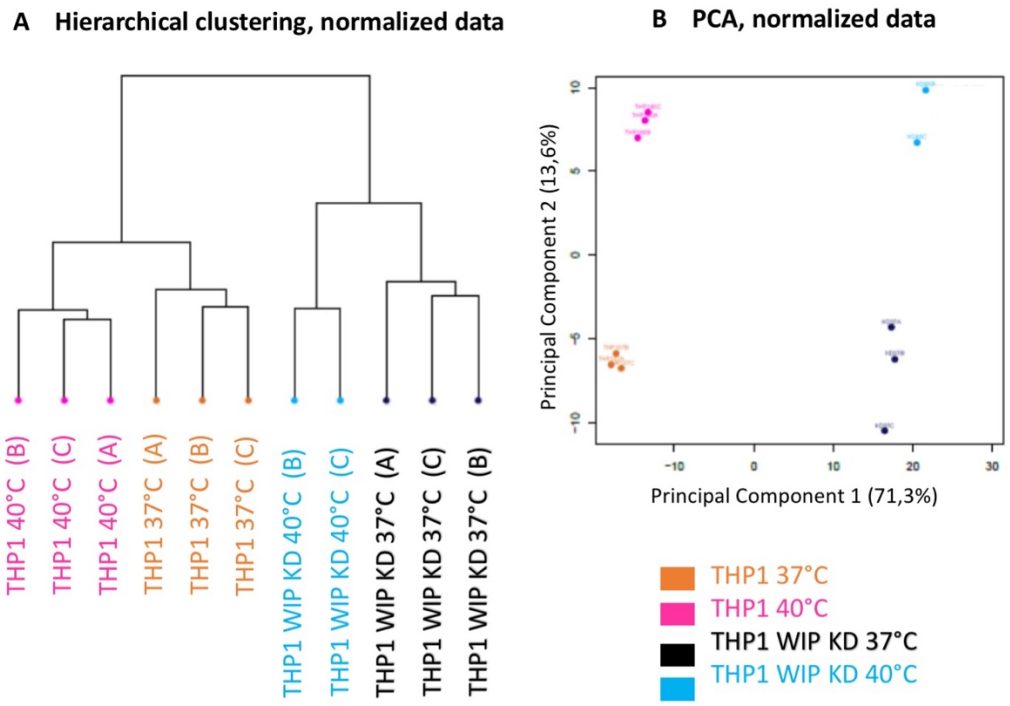

Figure 8.1. Hierarchical clustering (A) and principal component analysis (PCA) plot (B) on normalized data.

8.3 Lipidomics

8.3.1 Isolation of cell membranes

Samples were homogenized using a Teflon-glass grinder (Heidolph RZR 2020) in 20 volumes of homogenized buffer (1 mM EGTA, 3 mM MgCl2, and 50 mMTris-HCl, pH 7.4) supplemented with 250 mM sucrose. The crude homogenate was subjected to a 1000x g for 8 min, and the resultant supernatant was centrifuged again at 18000x g for 15 min (4°C, Microfuge 22R centrifuge, Beckman Coulter). The pellet was washed in 20 volumes of homogenized buffer using an Ultra-Turrax (T10 basic, IKA) and re-centrifuged under the same conditions. The homogenate aliquots were stored at -80 °C until they were used. Protein concentration was measured by the Bradford method and adjusted to the required concentrations.

8.3.2 Cell membrane microarray development

Membrane homogenates were resuspended in buffer and printed (4 nL per spot, 3-5 replicates per sample) onto glass slides using a non-contact microarrayer (Nano_plotter NP 2.1). Microarrays were stored at -20°C until they were used.

8.3.3 MALDI-MS

The arrays were covered with a suitable matrix with the aid of a standard glass sublimator (Ace Glass 8233), producing a uniform film of aprox. 0.2 mg/cm2. As sublimation is a dry method, it prevents lipid delocalization, which is important in this device, taking into account the proximity of the spots in the array. 1,5-diaminonaphtalene (DAN) was used for negative-ion mode. Once introduced in the spectrometer, the arrays were scanned as in a MALDI-imaging experiment. The area of the array was explored following a grid of coordinates separated 150 mm. As the spot of the arrays had a diameter of 450 mm, this means that nine pixels were recorded

at each spot. The mass spectrometer used in this work was an LTQ-Orbitrap XL (Thermo Scientific, San José, CA, USA), equipped with a MALDI source with a N2 laser (60 Hz, 100 mJ/pulse maximum power output). The laser spot is an ellipsoid of aprox. 50-60 mm x 140-160 mm. Thus, the size of the spots in the array were chosen as to avoid laser shot overlapping. Two microscans of ten shots at 25µJ of laser energy were used to produce the spectrum of each pixel. Mass resolution was set to 60000 at m/z = 400 in an 550-2000 observation window, in negative-ion modes. The spectra were analysed as in a MALDI-imaging experiment: the whole set of data were loaded as a single experiment. Therefore, data loading included spectra normalization by total ion current (TIC), spectra alignment and peak picking, filtering all the m/z with intensity < 0.5 % of the strongest peak in the spectrum. Statistical analysis was carried out using an in-house made statistical algorithm, based on rank compete (see below) and built in Matlab (MathWorks, Natick, USA), for segmentation, Excel and Unscrambler 9.7 (Camo Analytics, Oslo, Norway), for Principal components analysis.

8.3.4 Statistical Analysis

Segmentation of the pixels in the image of the array was done using a segmentation algorithm, RankCompete, based on the properties of Markov Chains to define Random Walker competing to divide the imaging experiment into two segments. Using this algorithm as splitting algorithm in a modification of a Hierarchical Divisive Analysis, a reliable and robust segmentation of the data was achieved. By definition, the RankCompete algorithm divides the experiment into two segments. However, the data from the array may contain a variable number of segments. Therefore, we used a variation of the Divisive Analysis algorithm (DIANA) to create a variable number of walkers. Thus, the final software is a segmentation algorithm based on DIANA and

using RankCompete as split function. Once the segments were obtained, the correlation between them was obtained and the value was used to assign a color to each segment using a color scale and 1-correlation between the segments. In this way, the two segments that present the lowest correlation occupy the two extremes of the scale and those segments with more similar average spectra receive colors that are closer in the scale. Because membranes spectra are much better than cells spectra, all the mean comparisons have been done using only membranes spectra. Mean comparisons between the samples is shown in a Heatmap, each mass channel is normalized to sum one and its intensity is represented by a colour in a scale, from green to red, 0 values are shown in black. Correlations between pairs of average spectra are shown as a linear regression between the intensities of each mass channel.

8.3.5 Lipid identification

Lipid identification in MALDI-IMS was based on a direct comparison of the m/z and the lipids in the software lipid database (>33,000 species plus their adducts) and with those in the lipid maps database (www.lipidmaps.org). Mass accuracy was always better than 5 parts per million (ppm) and it was typically better than 3 ppm.

9 References

Abraham, V. *et al.* (2016) 'Influence of PECAM-1 ligand interactions on PECAM-1-dependent cell motility and filopodia extension', *Physiol Rep*, 4(22). doi: 10.14814/phy2.13030e13030.

Airola, M. V. and Hannun, Y. A. (2013) 'Sphingolipid Metabolism and Neutral Sphingomyelinases', in *Handbook of experimental pharmacology*, pp. 57–76. doi: 10.1007/978-3-7091-1368-4_3.

Aizawa, H., Sutoh, K. and Yahara, I. (1996) 'Overexpression of cofilin stimulates bundling of actin filaments, membrane ruffling, and cell movement in Dictyostelium.', *The Journal of cell biology*, 132(3), pp. 335–44. doi: 10.1083/jcb.132.3.335.

Akerfelt, M., Morimoto, R. I. and Sistonen, L. (2010) 'Heat shock factors: integrators of cell stress, development and lifespan.', *Nature reviews. Molecular cell biology*. NIH Public Access, 11(8), pp. 545–55. doi: 10.1038/nrm2938.

Albiges-Rizo, C. *et al.* (2009) 'Actin machinery and mechanosensitivity in invadopodia, podosomes and focal adhesions.', *Journal of cell science*. The Company of Biologists Ltd, 122(Pt 17), pp. 3037–49. doi: 10.1242/jcs.052704.

Albrechtsen, R. *et al.* (2011) 'Extracellular engagement of ADAM12 induces clusters of invadopodia with localized ectodomain shedding activity', *Experimental Cell Research*, 317(2), pp. 195–209. doi: 10.1016/j.yexcr.2010.10.003.

Alekhina, O., Burstein, E. and Billadeau, D. D. (2017) 'Cellular functions of WASP family proteins at a glance', *Journal of Cell Science*, 130(14), pp. 2235–2241. doi: 10.1242/jcs.199570.

Alexander, N. R. *et al.* (2008) 'Extracellular Matrix Rigidity Promotes Invadopodia Activity', *Current Biology*. Cell Press, 18(17), pp. 1295–1299. doi: 10.1016/J.CUB.2008.07.090.

Allen, W. E. *et al.* (1998) 'A role for Cdc42 in macrophage chemotaxis.', *The Journal of cell biology*. Rockefeller University Press, 141(5), pp. 1147–57. doi: 10.1083/JCB.141.5.1147.

Almeida, M. C. *et al.* (2006) 'Cold-seeking behavior as a thermoregulatory strategy in systemic inflammation', *European Journal of Neuroscience*, 23(12), pp. 3359–3367. doi: 10.1111/j.1460-9568.2006.04854.x.

Alper, O. and Bowden, E. T. (2005) 'Novel insights into c-Src.', *Current pharmaceutical design*, 11(9), pp. 1119–30.

Aman, A. and Piotrowski, T. (2010) 'Cell migration during morphogenesis', *Developmental Biology*, 341(1), pp. 20–33. doi: 10.1016/j.ydbio.2009.11.014.

Andersen, A. S. *et al.* (2016) 'Podosome Formation and Development in Monocytes Restricted by the Nanoscale Spatial Distribution of ICAM1', *Nano Letters*. American Chemical Society, 16(3), pp. 2114–2121. doi: 10.1021/acs.nanolett.6b00519.

Antón, I. M. and Jones, G. E. (2006) 'WIP: A multifunctional protein involved in actin cytoskeleton regulation', *European Journal of Cell Biology*. doi: 10.1016/j.ejcb.2005.08.004.

Aplin, A. E. *et al.* (2001) 'Integrin-mediated adhesion regulates ERK nuclear translocation and phosphorylation of Elk-1.', *The Journal of cell biology*. The Rockefeller University Press, 153(2), pp. 273–82.

Armour, E. P. *et al.* (1993) 'Sensitivity of human cells to mild hyperthermia.', *Cancer research*, 53(12), pp. 2740–4.

Artym, V. V. *et al.* (2006) 'Dynamic Interactions of Cortactin and Membrane Type 1 Matrix Metalloproteinase at Invadopodia: Defining the Stages of Invadopodia Formation and Function', *Cancer Research*, 66(6), pp. 3034–3043. doi: 10.1158/0008-5472.CAN-05-2177.

Aspenströ, P. (2005) ‘The verprolin family of proteins: Regulators of cell morphogenesis and endocytosis’. doi: 10.1016/j.febslet.2005.08.053.

Aspenström, P. (2002) ‘The WASP-binding protein WIRE has a role in the regulation of the actin filament system downstream of the platelet-derived growth factor receptor.’, *Experimental cell research*, 279(1), pp. 21–33.

Aspenström, P. (2004) ‘The mammalian verprolin homologue WIRE participates in receptor-mediated endocytosis and regulation of the actin filament system by distinct mechanisms.’, *Experimental cell research*, 298(2), pp. 485–98. doi: 10.1016/j.yexcr.2004.04.050.

Atherton, P. *et al.* (2015) ‘Vinculin controls talin engagement with the actomyosin machinery’, *Nature Communications*. Nature Publishing Group, 6(1), p. 10038. doi: 10.1038/ncomms10038.

Auffray, C. *et al.* (2007) ‘Monitoring of Blood Vessels and Tissues by a Population of Monocytes with Patrolling Behavior’, *Science*, 317(5838), pp. 666–670. doi: 10.1126/science.1142883.

Avota, E., de Lira, M. N. and Schneider-Schaulies, S. (2019) ‘Sphingomyelin Breakdown in T Cells: Role of Membrane Compartmentalization in T Cell Signaling and Interference by a Pathogen.’, *Frontiers in cell and developmental biology*. Frontiers Media SA, 7, p. 152. doi: 10.3389/fcell.2019.00152.

Baba, Y. *et al.* (1999) ‘Involvement of wiskott-aldrich syndrome protein in B-cell cytoplasmic tyrosine kinase pathway.’, *Blood*, 93(6), pp. 2003–12.

Badolato, R. *et al.* (1998) ‘Monocytes from Wiskott-Aldrich patients display reduced chemotaxis and lack of cell polarization in response to monocyte chemoattractant protein-1 and formyl-methionyl-leucyl-phenylalanine.’, *Journal of immunology (Baltimore, Md. : 1950)*. American Association of Immunologists, 161(2), pp. 1026–

33. doi: 10.4049/jimmunol.165.1.221.

Badowski, C. *et al.* (2008) 'Paxillin Phosphorylation Controls Invadopodia/Podosomes Spatiotemporal Organization', *Molecular Biology of the Cell*. Edited by M. Ginsberg, 19(2), pp. 633–645. doi: 10.1091/mbc.e06-01-0088.

Ballweg, S. *et al.* (2019) 'Regulation of lipid saturation without sensing membrane fluidity', *bioRxiv*. Cold Spring Harbor Laboratory, p. 706556. doi: 10.1101/706556.

Balogh, G. *et al.* (2013) 'Key role of lipids in heat stress management', *FEBS Letters*. No longer published by Elsevier, 587(13), pp. 1970–1980. doi: 10.1016/J.FEBSLET.2013.05.016.

Balogh, G. *et al.* (2005) 'The hyperfluidization of mammalian cell membranes acts as a signal to initiate the heat shock protein response'. doi: 10.1111/j.1742-4658.2005.04999.x.

Bañón-Rodríguez, I. *et al.* (2011) 'The cortactin-binding domain of WIP is essential for podosome formation and extracellular matrix degradation by murine dendritic cells', *European Journal of Cell Biology*. doi: 10.1016/j.ejcb.2010.09.001.

Barczyk, M., Carracedo, S. and Gullberg, D. (2010) 'Integrins', *Cell and Tissue Research*. Springer-Verlag, 339(1), pp. 269–280. doi: 10.1007/s00441-009-0834-6.

Baronzio, G. F. *et al.* (2006) 'Effects of Local and Whole Body Hyperthermia on Immunity', in *Hyperthermia in Cancer Treatment: A Primer*. Boston, MA: Springer US, pp. 247–275. doi: 10.1007/978-0-387-33441-7_20.

Basu, S. and Srivastava, P. K. (2003) 'Fever-like temperature induces maturation of dendritic cells through induction of hsp90.', *International immunology*, 15(9), pp. 1053–61.

Berdeaux, R. L. *et al.* (2004) 'Active Rho is localized to podosomes induced by oncogenic Src and is required for their assembly and function.', *The Journal of cell*

biology. The Rockefeller University Press, 166(3), pp. 317–23. doi: 10.1083/jcb.200312168.

Berman, A. E., Kozlova, N. I. and Morozevich, G. E. (2003) 'Integrins: structure and signaling.', *Biochemistry. Biokhimiia*, 68(12), pp. 1284–99.

Bernabé-Rubio, M. *et al.* (2019) 'The ciliary membrane of polarized epithelial cells stems from a midbody remnant-associated membrane patch with condensed nanodomains', *bioRxiv*. Cold Spring Harbor Laboratory, p. 667642. doi: 10.1101/667642.

Bernadó, P. *et al.* (2008) 'Structural Characterization of the Active and Inactive States of Src Kinase in Solution by Small-Angle X-ray Scattering', *Journal of Molecular Biology*, 376(2), pp. 492–505. doi: 10.1016/j.jmb.2007.11.066.

Bernheim, H. A. and Kluger, M. J. (1976) 'Fever: effect of drug-induced antipyresis on survival.', *Science (New York, N.Y.)*, 193(4249), pp. 237–9.

Bershadsky, A. *et al.* (2006) 'Assembly and mechanosensory function of focal adhesions: experiments and models', *European Journal of Cell Biology*, 85(3–4), pp. 165–173. doi: 10.1016/j.ejcb.2005.11.001.

Bevers, E. M. and Williamson, P. L. (2016) 'Getting to the Outer Leaflet: Physiology of Phosphatidylserine Exposure at the Plasma Membrane', *Physiological Reviews*. American Physiological Society Bethesda, MD, 96(2), pp. 605–645. doi: 10.1152/physrev.00020.2015.

Beyersdorf, N., Kerkau, T. and Hünig, T. (2015) 'CD28 co-stimulation in T-cell homeostasis: a recent perspective.', *ImmunoTargets and therapy*. Dove Press, 4, pp. 111–22. doi: 10.2147/ITT.S61647.

Bhadriraju, K. *et al.* (2007) 'Activation of ROCK by RhoA is regulated by cell adhesion, shape, and cytoskeletal tension', *Experimental Cell Research*, 313(16), pp.

3616–3623. doi: 10.1016/j.yexcr.2007.07.002.

Birkedal-Hansen, H. *et al.* (1993) *Matrix Metalloproteinases: A Review**, *Critical Reviews in Oral Biology and Medicine*.

Block, M. *et al.* (2008) 'Podosome-type adhesions and focal adhesions, so alike yet so different', *European Journal of Cell Biology*, 87(8–9), pp. 491–506. doi: 10.1016/j.ejcb.2008.02.012.

Blom, M. *et al.* (2015) 'RhoD is a Golgi component with a role in anterograde protein transport from the ER to the plasma membrane', *Experimental Cell Research*, 333(2), pp. 208–219. doi: 10.1016/j.yexcr.2015.02.023.

Blundell, M. P. *et al.* (2009) 'Phosphorylation of WASp is a key regulator of activity and stability in vivo.', *Proceedings of the National Academy of Sciences of the United States of America*. National Academy of Sciences, 106(37), pp. 15738–43. doi: 10.1073/pnas.0904346106.

Bois, P. R. J. *et al.* (2006) 'The Vinculin Binding Sites of Talin and α-Actinin Are Sufficient to Activate Vinculin', *Journal of Biological Chemistry*. American Society for Biochemistry and Molecular Biology, 281(11), pp. 7228–7236. doi: 10.1074/JBC.M510397200.

Bolger-Munro, M. *et al.* (2019) 'Arp2/3 complex-driven spatial patterning of the BCR enhances immune synapse formation, BCR signaling and B cell activation.', *eLife*. eLife Sciences Publications, Ltd, 8. doi: 10.7554/eLife.44574.

Bompard, G. and Caron, E. (2004) 'Regulation of WASP/WAVE proteins: making a long story short.', *The Journal of cell biology*. The Rockefeller University Press, 166(7), pp. 957–62. doi: 10.1083/jcb.200403127.

Borghi, N. *et al.* (2010) 'Regulation of cell motile behavior by crosstalk between cadherin- and integrin-mediated adhesions.', *Proceedings of the National Academy of*

Sciences of the United States of America. National Academy of Sciences, 107(30), pp. 13324–9. doi: 10.1073/pnas.1002662107.

Bouma, G. *et al.* (2011) 'Cytoskeletal remodeling mediated by WASp in dendritic cells is necessary for normal immune synapse formation and T-cell priming.', *Blood*. American Society of Hematology, 118(9), pp. 2492–501. doi: 10.1182/blood-2011-03-340265.

Bouma, G., Burns, S. and Thrasher, A. J. (2007) 'Impaired T-cell priming in vivo resulting from dysfunction of WASp-deficient dendritic cells', *Blood*, 110(13), pp. 4278–4284. doi: 10.1182/blood-2007-06-096875.

Bouzigon, R. *et al.* (2016) 'Whole- and partial-body cryostimulation/cryotherapy: Current technologies and practical applications', *Journal of Thermal Biology*, 61, pp. 67–81. doi: 10.1016/j.jtherbio.2016.08.009.

Bowden, E. T. *et al.* (1999) 'An invasion-related complex of cortactin, paxillin and PKCμ associates with invadopodia at sites of extracellular matrix degradation', *Oncogene*, 18(31), pp. 4440–4449. doi: 10.1038/sj.onc.1202827.

Branch, K. M., Hoshino, D. and Weaver, A. M. (2012) 'Adhesion rings surround invadopodia and promote maturation', *Biology Open*, 1(8), pp. 711–722. doi: 10.1242/bio.20121867.

Bravo-Cordero, J. J., Hodgson, L. and Condeelis, J. (2012) 'Directed cell invasion and migration during metastasis.', *Current opinion in cell biology*. NIH Public Access, 24(2), pp. 277–83. doi: 10.1016/j.ceb.2011.12.004.

Brown, C. M. *et al.* (2008) 'Raster image correlation spectroscopy (RICS) for measuring fast protein dynamics and concentrations with a commercial laser scanning confocal microscope.', *Journal of microscopy*. NIH Public Access, 229(Pt 1), pp. 78–91. doi: 10.1111/j.1365-2818.2007.01871.x.

Brown, M. S. and Goldstein, J. L. (1997) ‘The SREBP pathway: regulation of cholesterol metabolism by proteolysis of a membrane-bound transcription factor.’, *Cell*. Elsevier, 89(3), pp. 331–40. doi: 10.1016/s0092-8674(00)80213-5.

van Bruggen, I., Robertson, T. A. and Papadimitriou, J. M. (1991) ‘The effect of mild hyperthermia on the morphology and function of murine resident peritoneal macrophages.’, *Experimental and molecular pathology*, 55(2), pp. 119–34.

Buchbinder, D., Nugent, D. J. and Fillipovich, A. H. (2014) ‘Wiskott-Aldrich syndrome: diagnosis, current management, and emerging treatments.’, *The application of clinical genetics*. Dove Press, 7, pp. 55–66. doi: 10.2147/TACG.S58444.

Buchman, T. G. (2002) ‘The community of the self’, *Nature*, 420(6912), pp. 246–251. doi: 10.1038/nature01260.

Burger, K. L. *et al.* (2011) ‘The podosome marker protein Tks5 regulates macrophage invasive behavior.’, *Cytoskeleton (Hoboken, N.J.)*. NIH Public Access, 68(12), pp. 694–711. doi: 10.1002/cm.20545.

Burkhardt Daniel A Hammer, J. K. *et al.* (2011) ‘Chemotaxis in Dendritic Cells Podosome Array Organization and Aldrich Syndrome Protein To Promote − 1 Functions in Concert with the Wiskott Hematopoietic Lineage Cell-Specific Protein’. doi: 10.4049/jimmunol.1003102.

Burns, S. *et al.* (2001) ‘Configuration of human dendritic cell cytoskeleton by Rho GTPases, the WAS protein, and differentiation’, *Blood*. American Society of Hematology, 98(4), pp. 1142–1149. doi: 10.1182/BLOOD.V98.4.1142.

Burns, Siobhan *et al.* (2004) ‘Maturation of DC is associated with changes in motile characteristics and adherence’, *Cell Motility and the Cytoskeleton*, 57(2), pp. 118–132. doi: 10.1002/cm.10163.

Burns, S. *et al.* (2004) 'Mechanisms of WASp-mediated hematologic and immunologic disease', *Blood*, 104(12), pp. 3454–3462. doi: 10.1182/blood-2004-04-1678.

Burns, S. and Thrasher, A. J. (2004) 'Dendritic Cells: The Bare Bones of Immunity', *Current Biology*, 14, pp. 965–967. doi: 10.1016/j.cub.2004.10.044.

Calle, Y. *et al.* (2004) 'WASp deficiency in mice results in failure to form osteoclast sealing zones and defects in bone resorption', *Blood*, 103(9), pp. 3552–3561. doi: 10.1182/blood-2003-04-1259.

Calle, Yolanda *et al.* (2004) 'Wiskott-Aldrich syndrome protein and the cytoskeletal dynamics of dendritic cells', *The Journal of Pathology*. John Wiley & Sons, Ltd, 204(4), pp. 460–469. doi: 10.1002/path.1651.

Calle, Y. *et al.* (2006) 'Inhibition of calpain stabilises podosomes and impairs dendritic cell motility', *Journal of Cell Science*. The Company of Biologists Ltd, 119(11), pp. 2375–2385. doi: 10.1242/jcs.02939.

Calle, Y. *et al.* (2006) 'The leukocyte podosome', *European Journal of Cell Biology*, 85(3–4), pp. 151–157. doi: 10.1016/j.ejcb.2005.09.003.

Campbell, I. D. and Humphries, M. J. (2011) 'Integrin structure, activation, and interactions.', *Cold Spring Harbor perspectives in biology*. Cold Spring Harbor Laboratory Press, 3(3), p. a004994. doi: 10.1101/cshperspect.a004994.

Campellone, K. G. *et al.* (2008) 'WHAMM Is an Arp2/3 Complex Activator That Binds Microtubules and Functions in ER to Golgi Transport', *Cell*, 134(1), pp. 148–161. doi: 10.1016/j.cell.2008.05.032.

Cebecauer, M. *et al.* (2010) 'Signalling complexes and clusters: functional advantages and methodological hurdles', *Journal of Cell Science*, 123(3), pp. 309–320. doi: 10.1242/jcs.061739.

Chadwick, D. and Goode, J. (2004) *Mammalian TRP channels as molecular targets*. John Wiley & Sons.

Chan, C., Beltzner, C. C. and Pollard, T. D. (2009) 'Cofilin Dissociates Arp2/3 Complex and Branches from Actin Filaments', *Current Biology*, 19(7), pp. 537–545. doi: 10.1016/j.cub.2009.02.060.

Chandra, S. *et al.* (1993) *WAS-Related Disorders*, *GeneReviews®*.

Chellaiah, M. A. *et al.* (2000) 'Rho-A Is Critical for Osteoclast Podosome Organization, Motility, and Bone Resorption', *Journal of Biological Chemistry*, 275(16), pp. 11993–12002. doi: 10.1074/jbc.275.16.11993.

Chen, Q. *et al.* (2009) 'Thermal Facilitation of Lymphocyte Trafficking Involves Temporal Induction of Intravascular ICAM-1', *Microcirculation*, 16(2), pp. 143–158. doi: 10.1080/10739680802353850.

Chen, B. *et al.* (2014) 'Biochemical reconstitution of the WAVE regulatory complex.', *Methods in enzymology*. NIH Public Access, 540, pp. 55–72. doi: 10.1016/B978-0-12-397924-7.00004-2.

Chen, B. *et al.* (2017) 'Rac1 GTPase activates the WAVE regulatory complex through two distinct binding sites', *eLife*, 6. doi: 10.7554/eLife.29795.

Chen, H. *et al.* (2009) 'Extracellular Signal-Regulated Kinase Signaling Pathway Regulates Breast Cancer Cell Migration by Maintaining slug Expression', *Cancer Research*, 69(24), pp. 9228–9235. doi: 10.1158/0008-5472.CAN-09-1950.

Chen, Q. *et al.* (2006) 'Fever-range thermal stress promotes lymphocyte trafficking across high endothelial venules via an interleukin 6 trans-signaling mechanism', *Nature Immunology*, 7(12), pp. 1299–1308. doi: 10.1038/ni1406.

Chen, Q. and Evans, S. S. (2005) 'Thermal regulation of lymphocyte trafficking: Hot spots of the immune response', in *International Journal of Hyperthermia*. doi:

10.1080/02656730500271734.

Chen, W. T. *et al.* (1984) 'Expression of transformation-associated protease(s) that degrade fibronectin at cell contact sites.', *The Journal of cell biology*, 98(4), pp. 1546–55.

Chereau, D. *et al.* (2005) 'Actin-bound structures of Wiskott-Aldrich syndrome protein (WASP)-homology domain 2 and the implications for filament assembly', *Proceedings of the National Academy of Sciences*, 102(46), pp. 16644–16649. doi: 10.1073/pnas.0507021102.

Chomarat, P. *et al.* (2000) 'IL-6 switches the differentiation of monocytes from dendritic cells to macrophages', *Nature Immunology*. Nature Publishing Group, 1(6), pp. 510–514. doi: 10.1038/82763.

Chong, L. D. *et al.* (1994) 'The small GTP-binding protein Rho regulates a phosphatidylinositol 4-phosphate 5-kinase in mammalian cells', *Cell*, 79(3), pp. 507–513. doi: 10.1016/0092-8674(94)90259-3.

Chou, H.-C. *et al.* (2006) 'WIP regulates the stability and localization of WASP to podosomes in migrating dendritic cells.', *Current biology : CB*. Elsevier, 16(23), pp. 2337–44. doi: 10.1016/j.cub.2006.10.037.

Clark, E. S. *et al.* (2007) 'Cortactin is an essential regulator of matrix metalloproteinase secretion and extracellular matrix degradation in invadopodia.', *Cancer research*. American Association for Cancer Research, 67(9), pp. 4227–35. doi: 10.1158/0008-5472.CAN-06-3928.

Clark, E. S. and Weaver, A. M. (2008) 'A new role for cortactin in invadopodia: regulation of protease secretion.', *European journal of cell biology*. NIH Public Access, 87(8–9), pp. 581–90. doi: 10.1016/j.ejcb.2008.01.008.

Collin, O. *et al.* (2006) 'Spatiotemporal dynamics of actin-rich adhesion

microdomains: influence of substrate flexibility', *Journal of Cell Science*. The Company of Biologists Ltd, 119(9), pp. 1914–1925. doi: 10.1242/JCS.02838.

Cory, G. O. C. *et al.* (2002) 'Phosphorylation of tyrosine 291 enhances the ability of WASp to stimulate actin polymerization and filopodium formation. Wiskott-Aldrich Syndrome protein.', *The Journal of biological chemistry*. American Society for Biochemistry and Molecular Biology, 277(47), pp. 45115–21. doi: 10.1074/jbc.M203346200.

Cosen-Binker, L. I. and Kapus, A. (2006) 'Cortactin: The Gray Eminence of the Cytoskeleton', *Physiology*, 21(5), pp. 352–361. doi: 10.1152/physiol.00012.2006.

Coskun, Ü. and Simons, K. (2011) 'Cell Membranes: The Lipid Perspective', *Structure*. Cell Press, 19(11), pp. 1543–1548. doi: 10.1016/J.STR.2011.10.010.

Cougoule, C. *et al.* (2010) 'Three-dimensional migration of macrophages requires Hck for podosome organization and extracellular matrix proteolysis', *Blood*, 115(7), pp. 1444–1452. doi: 10.1182/blood-2009-04-218735.

Cougoule, C. *et al.* (2012) 'Blood leukocytes and macrophages of various phenotypes have distinct abilities to form podosomes and to migrate in 3D environments', *European Journal of Cell Biology*. Urban & Fischer, 91(11–12), pp. 938–949. doi: 10.1016/J.EJCB.2012.07.002.

Covert, J. B. and Reynolds, W. W. (1977) 'Survival value of fever in fish.', *Nature*, 267(5606), pp. 43–5.

Cox, E. A., Sastry, S. K. and Huttenlocher, A. (2001) 'Integrin-mediated Adhesion Regulates Cell Polarity and Membrane Protrusion through the Rho Family of GTPases', *Molecular Biology of the Cell*. Edited by W. J. Nelson, 12(2), pp. 265–277. doi: 10.1091/mbc.12.2.265.

Cox, S. *et al.* (2012) 'Bayesian localization microscopy reveals nanoscale podosome

dynamics', *Nature Methods*, 9(2), pp. 195–200. doi: 10.1038/nmeth.1812.

Cramer, L. P. (1999) 'Organization and polarity of actin filament networks in cells: implications for the mechanism of myosin-based cell motility.', *Biochemical Society symposium*, 65, pp. 173–205.

de Curtis, I. (2019) 'The Rac3 GTPase in Neuronal Development, Neurodevelopmental Disorders, and Cancer', *Cells*. Multidisciplinary Digital Publishing Institute, 8(9), p. 1063. doi: 10.3390/cells8091063.

Danson, C. M. *et al.* (2007) 'Phosphorylation of WAVE2 by MAP kinases regulates persistent cell migration and polarity', *Journal of Cell Science*, 120(23), pp. 4144–4154. doi: 10.1242/jcs.013714.

Dawaliby, R. *et al.* (2015) 'Phosphatidylethanolamine is a Key Regulator of Membrane Fluidity in Eukaryotic Cells*'. doi: 10.1074/jbc.M115.706523.

Dayanc, B. E. *et al.* (2008) 'Dissecting the role of hyperthermia in natural killer cell mediated anti-tumor responses', *International Journal of Hyperthermia*. Taylor & Francis, 24(1), pp. 41–56. doi: 10.1080/02656730701858297.

Deal, R. B. and Henikoff, S. (2010) 'Gene regulation: A chromatin thermostat.', *Nature*. NIH Public Access, 463(7283), pp. 887–8. doi: 10.1038/463887a.

DeMali, K. A. and Burridge, K. (2003) 'Coupling membrane protrusion and cell adhesion.', *Journal of cell science*. The Company of Biologists Ltd, 116(Pt 12), pp. 2389–97. doi: 10.1242/jcs.00605.

Derry, J. M., Ochs, H. D. and Francke, U. (1994) 'Isolation of a novel gene mutated in Wiskott-Aldrich syndrome.', *Cell*. Elsevier, 78(4), pp. 635–44. doi: 10.1016/0092-8674(94)90528-2.

Destaing, O. *et al.* (2003) 'Podosomes Display Actin Turnover and Dynamic Self-Organization in Osteoclasts Expressing Actin-Green Fluorescent Protein', *Molecular*

Biology of the Cell. Edited by T. D. Pollard, 14(2), pp. 407–416. doi: 10.1091/mbc.e02-07-0389.

Destaing, O. *et al.* (2008) 'The tyrosine kinase activity of c-Src regulates actin dynamics and organization of podosomes in osteoclasts.', *Molecular biology of the cell*. American Society for Cell Biology, 19(1), pp. 394–404. doi: 10.1091/mbc.e07-03-0227.

Destaing, O. *et al.* (2010) 'β1A integrin is a master regulator of invadosome organization and function.', *Molecular biology of the cell*. American Society for Cell Biology, 21(23), pp. 4108–19. doi: 10.1091/mbc.E10-07-0580.

Dhaka, A., Viswanath, V. and Patapoutian, A. (2006) 'TRP ION CHANNELS AND TEMPERATURE SENSATION', *Annual Review of Neuroscience*. Annual Reviews, 29(1), pp. 135–161. doi: 10.1146/annurev.neuro.29.051605.112958.

Dindia, L. *et al.* (2013) 'Rapid cortisol signaling in response to acute stress involves changes in plasma membrane order in rainbow trout liver', *American Journal of Physiology-Endocrinology and Metabolism*. American Physiological Society Bethesda, MD, 304(11), pp. E1157–E1166. doi: 10.1152/ajpendo.00500.2012.

Disanza, A. and Scita, G. (2008) 'Cytoskeletal Regulation: Coordinating Actin and Microtubule Dynamics in Membrane Trafficking', *Current Biology*. Cell Press, 18(18), pp. R873–R875. doi: 10.1016/J.CUB.2008.07.059.

Djaldetti, M. and Bessler, H. (2015) 'High temperature affects the phagocytic activity of human peripheral blood mononuclear cells', *Scandinavian Journal of Clinical and Laboratory Investigation*. Taylor & Francis, 75(6), pp. 482–486. doi: 10.3109/00365513.2015.1052550.

van Dooremalen, C. and Ellers, J. (2010) 'A moderate change in temperature induces changes in fatty acid composition of storage and membrane lipids in a soil arthropod',

Journal of Insect Physiology. Pergamon, 56(2), pp. 178–184. doi: 10.1016/J.JINSPHYS.2009.10.002.

Dou, F., Yuan, L.-D. and Zhu, J.-J. (2005) 'Heat Shock Protein 90 Indirectly Regulates ERK Activity by Affecting Raf Protein Metabolism', *Acta Biochimica et Biophysica Sinica*, 37(7), pp. 501–505. doi: 10.1111/j.1745-7270.2005.00069.x.

Dovas, A. *et al.* (2009) 'Regulation of podosome dynamics by WASp phosphorylation: implication in matrix degradation and chemotaxis in macrophages.', *Journal of cell science*. The Company of Biologists Ltd, 122(Pt 21), pp. 3873–82. doi: 10.1242/jcs.051755.

Dowhan, W. and Bogdanov, M. (2002) 'Chapter 1 Functional roles of lipids in membranes', *New Comprehensive Biochemistry*. Elsevier, 36, pp. 1–35. doi: 10.1016/S0167-7306(02)36003-4.

van den Dries, K. *et al.* (2013) 'Interplay between myosin IIA-mediated contractility and actin network integrity orchestrates podosome composition and oscillations', *Nature Communications*. Nature Publishing Group, 4(1), p. 1412. doi: 10.1038/ncomms2402.

van den Dries, K., Bolomini-Vittori, M. and Cambi, A. (2014) 'Spatiotemporal organization and mechanosensory function of podosomes.', *Cell adhesion & migration*. Taylor & Francis, 8(3), pp. 268–72. doi: 10.4161/CAM.28182.

Du, P., Kibbe, W. A. and Lin, S. M. (2008) 'lumi: a pipeline for processing Illumina microarray', *Bioinformatics*, 24(13), pp. 1547–1548. doi: 10.1093/bioinformatics/btn224.

Dupré, L. *et al.* (2002) 'Wiskott-Aldrich syndrome protein regulates lipid raft dynamics during immunological synapse formation.', *Immunity*, 17(2), pp. 157–66.

Earn, D. J. D., Andrews, P. W. and Bolker, B. M. (2014) 'Population-level effects of

suppressing fever', *Proceedings of the Royal Society B: Biological Sciences*, 281(1778), pp. 20132570–20132570. doi: 10.1098/rspb.2013.2570.

Edmond, V. *et al.* (2015) 'Downregulation of ceramide synthase-6 during epithelial-to-mesenchymal transition reduces plasma membrane fluidity and cancer cell motility', *Oncogene*, 34(8), pp. 996–1005. doi: 10.1038/onc.2014.55.

Eich, C. *et al.* (2016) 'Changes in membrane sphingolipid composition modulate dynamics and adhesion of integrin nanoclusters', *Scientific Reports*. Nature Publishing Group, 6(1), p. 20693. doi: 10.1038/srep20693.

Ejsing, C. S. *et al.* (2009) 'Global analysis of the yeast lipidome by quantitative shotgun mass spectrometry', *Proceedings of the National Academy of Sciences*, 106(7), pp. 2136–2141. doi: 10.1073/pnas.0811700106.

Ellis, G. S. *et al.* (2005) 'G-CSF, but not corticosterone, mediates circulating neutrophilia induced by febrile-range hyperthermia', *Journal of Applied Physiology*, 98(5), pp. 1799–1804. doi: 10.1152/japplphysiol.01376.2004.

Erlejman, A. G. *et al.* (2014) 'Regulatory role of the 90-kDa-heat-shock protein (Hsp90) and associated factors on gene expression', *Biochimica et Biophysica Acta (BBA) - Gene Regulatory Mechanisms*. Elsevier, 1839(2), pp. 71–87. doi: 10.1016/J.BBAGRM.2013.12.006.

Etienne-Manneville, S. and Hall, A. (2002) 'Rho GTPases in cell biology', *Nature*. Nature Publishing Group, 420(6916), pp. 629–635. doi: 10.1038/nature01148.

Evans, J. G. *et al.* (2003) 'Macrophage podosomes assemble at the leading lamella by growth and fragmentation.', *The Journal of cell biology*. The Rockefeller University Press, 161(4), pp. 697–705. doi: 10.1083/jcb.200212037.

Evans, S. S. *et al.* (1999) 'Dynamic association of L-selectin with the lymphocyte cytoskeletal matrix.', *Journal of immunology (Baltimore, Md. : 1950)*, 162(6), pp.

3615–24.

Evans, S. S. *et al.* (2001) ‘Fever-range hyperthermia dynamically regulates lymphocyte delivery to high endothelial venules.’, *Blood*, 97(9), pp. 2727–33.

Evans, S. S., Repasky, E. A. and Fisher, D. T. (2015) ‘Fever and the thermal regulation of immunity: The immune system feels the heat’, *Nature Reviews Immunology*. doi: 10.1038/nri3843.

Fan-Xin, M. *et al.* (2012) ‘Experimental Physiology Heat shock factor 1 regulates the expression of the TRPV1 gene in the rat preoptic-anterior hypothalamus area during lipopolysaccharide-induced fever’, *Exp Physiol*, 97, pp. 730–740. doi: 10.1113/expphysiol.2011.064204.

Farina, F. *et al.* (2016) ‘The centrosome is an actin-organizing centre’, *Nature Cell Biology*. Nature Publishing Group, 18(1), pp. 65–75. doi: 10.1038/ncb3285.

Feldhaus, M. J. *et al.* (2002) ‘Ceramide Generation *in Situ* Alters Leukocyte Cytoskeletal Organization and β_2 -Integrin Function and Causes Complete Degranulation’, *Journal of Biological Chemistry*, 277(6), pp. 4285–4293. doi: 10.1074/jbc.M106653200.

Fieren, M. W. J. A. (2012) ‘The Local Inflammatory Responses to Infection of the Peritoneal Cavity in Humans: Their Regulation by Cytokines, Macrophages, and Other Leukocytes’, *Mediators of Inflammation*. Hindawi, 2012, pp. 1–9. doi: 10.1155/2012/976241.

Fog, C. K. *et al.* (2018) ‘The heat shock protein amplifier arimoclomol improves refolding, maturation and lysosomal activity of glucocerebrosidase’, *EBioMedicine*. Elsevier, 38, pp. 142–153. doi: 10.1016/J.EBIOM.2018.11.037.

Forni, G. *et al.* (1995) ‘Molecular approaches to cancer immunotherapy.’, *Cytokines and molecular therapy*, 1(4), pp. 225–48.

Forsdyke, D. R. (1999) ‘Heat shock proteins as mediators of aggregation-induced “danger” signals: implications of the slow evolutionary fine-tuning of sequences for the antigenicity of cancer cells.’, *Cell stress & chaperones*, 4(4), pp. 205–10.

Foxall, E. *et al.* (2019) ‘PAK4 Kinase Activity Plays a Crucial Role in the Podosome Ring of Myeloid Cells.’, *Cell reports*. Elsevier, 29(11), pp. 3385-3393.e6. doi: 10.1016/j.celrep.2019.11.016.

Fraley, S. I. *et al.* (2010) ‘A distinctive role for focal adhesion proteins in three-dimensional cell motility.’, *Nature cell biology*. NIH Public Access, 12(6), pp. 598–604. doi: 10.1038/ncb2062.

Franco-Villanueva, A. *et al.* (2014) ‘WIP modulates dendritic spine actin cytoskeleton by transcriptional control of lipid metabolic enzymes’, *Human Molecular Genetics*, 23(16), pp. 4383–4395. doi: 10.1093/hmg/ddu155.

Franco-Villanueva, A., Wandosell, F. and Antón, I. M. (2015) ‘Neuritic complexity of hippocampal neurons depends on WIP-mediated mTORC1 and Abl family kinases activities’, *Brain and Behavior*, 5(11), p. n/a-n/a. doi: 10.1002/brb3.359.

Frankowski, H. *et al.* (2012) ‘Use of gel zymography to examine matrix metalloproteinase (gelatinase) expression in brain tissue or in primary glial cultures.’, *Methods in molecular biology (Clifton, N.J.)*. NIH Public Access, 814, pp. 221–33. doi: 10.1007/978-1-61779-452-0_15.

Fried, S. *et al.* (2014) ‘WIP: more than a WASp-interacting protein’, *Journal of Leukocyte Biology*, 96(5), pp. 713–727. doi: 10.1189/jlb.2RU0314-162R.

Friedl, P. and Wolf, K. (2010) ‘Plasticity of cell migration: a multiscale tuning model’, *The Journal of Cell Biology*, 188(1), pp. 11–19. doi: 10.1083/jcb.200909003.

Friedlander, G. *et al.* (1987) ‘Benzyl alcohol increases membrane fluidity and modulates cyclic AMP synthesis in intact renal epithelial cells.’, *Biochimica et*

biophysica acta, 903(2), pp. 341–8.

Fujiwara, N. and Kobayashi, K. (2005) 'Macrophages in Inflammation', *Current Drug Target -Inflammation & Allergy*, 4(3), pp. 281–286. doi: 10.2174/1568010054022024.

Fukuoka, M. *et al.* (2001) 'A novel neural Wiskott-Aldrich syndrome protein (N-WASP) binding protein, WISH, induces Arp2/3 complex activation independent of Cdc42.', *The Journal of cell biology*. Rockefeller University Press, 152(3), pp. 471–82. doi: 10.1083/JCB.152.3.471.

Gálvez, B. G. *et al.* (2002) 'ECM regulates MT1-MMP localization with β1 or αvβ3 integrins at distinct cell compartments modulating its internalization and activity on human endothelial cells', *The Journal of Cell Biology*, 159(3), pp. 509–521. doi: 10.1083/jcb.200205026.

Gandhi, M. *et al.* (2010) 'GMF Is a Cofilin Homolog that Binds Arp2/3 Complex to Stimulate Filament Debranching and Inhibit Actin Nucleation', *Current Biology*, 20(9), pp. 861–867. doi: 10.1016/j.cub.2010.03.026.

Gao, S. *et al.* (2016) 'Local hyperthermia in head and neck cancer: mechanism, application and advance.', *Oncotarget*. Impact Journals, LLC, 7(35), pp. 57367–57378. doi: 10.18632/oncotarget.10350.

García, E. *et al.* (2016) 'WIP and WICH/WIRE co-ordinately control invadopodium formation and maturation in human breast cancer cell invasion.', *Scientific reports*. Nature Publishing Group, 6, p. 23590. doi: 10.1038/srep23590.

Garcia, E. and Bernardino De La Serna, J. (2018) 'Dissecting single-cell molecular spatiotemporal mobility and clustering at Focal Adhesions in polarised cells by fluorescence fluctuation spectroscopy methods'. doi: 10.1101/220491.

García, E. and Machesky, L. M. (2012) 'WIP: WASP-interacting proteins at invadopodia and podosomes', *European Journal of Cell Biology*. Urban & Fischer,

91(11–12), pp. 869–877. doi: 10.1016/J.EJCB.2012.06.002.

Gawden-Bone, C. *et al.* (2010) 'Dendritic cell podosomes are protrusive and invade the extracellular matrix using metalloproteinase MMP-14', *Journal of Cell Science*, 123(9), pp. 1427–1437. doi: 10.1242/jcs.056515.

Gawden-Bone, C. *et al.* (2014) 'A crucial role for β2 integrins in podosome formation, dynamics and Toll-like-receptor-signaled disassembly in dendritic cells.', *Journal of cell science*. Company of Biologists, 127(Pt 19), pp. 4213–24. doi: 10.1242/jcs.151167.

Geblinger, D. *et al.* (2010) 'Nano-topography sensing by osteoclasts.', *Journal of cell science*. The Company of Biologists Ltd, 123(Pt 9), pp. 1503–10. doi: 10.1242/jcs.060954.

Gerhardt, T. and Ley, K. (2015) 'Monocyte trafficking across the vessel wall', *Cardiovascular Research*. Narnia, 107(3), pp. 321–330. doi: 10.1093/cvr/cvv147.

GILL, S. and PARKS, W. (2008) 'Metalloproteinases and their inhibitors: Regulators of wound healing', *The International Journal of Biochemistry & Cell Biology*, 40(6–7), pp. 1334–1347. doi: 10.1016/j.biocel.2007.10.024.

Gilmore, A. P. and Burridge, K. (1996) 'Regulation of vinculin binding to talin and actin by phosphatidyl-inositol-4-5-bisphosphate', *Nature*. Nature Publishing Group, 381(6582), pp. 531–535. doi: 10.1038/381531a0.

Gimona, M. *et al.* (2008) 'Assembly and biological role of podosomes and invadopodia', *Current Opinion in Cell Biology*, 20(2), pp. 235–241. doi: 10.1016/j.ceb.2008.01.005.

Gimona, M. and Buccione, R. (2006) 'Adhesions that mediate invasion', *The International Journal of Biochemistry & Cell Biology*. Pergamon, 38(11), pp. 1875–1892. doi: 10.1016/J.BIOCEL.2006.05.003.

Ginhoux, F. and Jung, S. (2014) 'Monocytes and macrophages: developmental pathways and tissue homeostasis', *Nature Reviews Immunology*. Nature Publishing Group, 14(6), pp. 392–404. doi: 10.1038/nri3671.

Girard, J.-P., Moussion, C. and Förster, R. (2012) 'HEVs, lymphatics and homeostatic immune cell trafficking in lymph nodes', *Nature Reviews Immunology*, 12(11), pp. 762–773. doi: 10.1038/nri3298.

Glatzel, D. K. *et al.* (2018) 'Acetyl-CoA carboxylase 1 regulates endothelial cell migration by shifting the phospholipid composition', *Journal of Lipid Research*, 59(2), pp. 298–311. doi: 10.1194/jlr.M080101.

Gligorijevic, B. *et al.* (2012) 'N-WASP-mediated invadopodium formation is involved in intravasation and lung metastasis of mammary tumors', *Journal of Cell Science*, 125(3), pp. 724–734. doi: 10.1242/jcs.092726.

Van Goethem, E. *et al.* (2010) 'Matrix Architecture Dictates Three-Dimensional Migration Modes of Human Macrophages: Differential Involvement of Proteases and Podosome-Like Structures', *The Journal of Immunology*, 184(2), pp. 1049–1061. doi: 10.4049/jimmunol.0902223.

Van Goethem, E. *et al.* (2011) 'Macrophage podosomes go 3D', *European Journal of Cell Biology*, 90(2–3), pp. 224–236. doi: 10.1016/j.ejcb.2010.07.011.

Goley, E. D. *et al.* (2004) 'Critical Conformational Changes in the Arp2/3 Complex Are Induced by Nucleotide and Nucleation Promoting Factor', *Molecular Cell*. Cell Press, 16(2), pp. 269–279. doi: 10.1016/J.MOLCEL.2004.09.018.

Goley, E. D. *et al.* (2006) 'Dynamic nuclear actin assembly by Arp2/3 complex and a baculovirus WASP-like protein.', *Science (New York, N.Y.)*. American Association for the Advancement of Science, 314(5798), pp. 464–7. doi: 10.1126/science.1133348.

Goley, E. D. and Welch, M. D. (2006) 'The ARP2/3 complex: an actin nucleator

comes of age', *Nature Reviews Molecular Cell Biology*, 7(10), pp. 713–726. doi: 10.1038/nrm2026.

Gombos, I. and Vígh, L. (2015) 'Membrane fluidity in the center of fever-enhanced immunity.', *Cell cycle (Georgetown, Tex.)*. Taylor & Francis, 14(19), pp. 3014–5. doi: 10.1080/15384101.2015.1069506.

Gomez, T. S. *et al.* (2012) 'Trafficking defects in *WASH*- knockout fibroblasts originate from collapsed endosomal and lysosomal networks', *Molecular Biology of the Cell*. Edited by J. Klumperman, 23(16), pp. 3215–3228. doi: 10.1091/mbc.e12-02-0101.

Gomez, T. S. and Billadeau, D. D. (2009) 'A FAM21-Containing WASH Complex Regulates Retromer-Dependent Sorting', *Developmental Cell*, 17(5), pp. 699–711. doi: 10.1016/j.devcel.2009.09.009.

Götz, A. and Jessberger, R. (2013) 'Dendritic Cell Podosome Dynamics Does Not Depend on the F-actin Regulator SWAP-70', *PLoS ONE*. Edited by Y. Komarova. Public Library of Science, 8(3), p. e60642. doi: 10.1371/journal.pone.0060642.

Griera, M. *et al.* (2014) 'Integrin linked kinase (ILK) regulates podosome maturation and stability in dendritic cells', *The International Journal of Biochemistry & Cell Biology*. Pergamon, 50, pp. 47–54. doi: 10.1016/J.BIOCEL.2014.01.021.

Griffith, J. W., Sokol, C. L. and Luster, A. D. (2014) 'Chemokines and Chemokine Receptors: Positioning Cells for Host Defense and Immunity', *Annual Review of Immunology*, 32(1), pp. 659–702. doi: 10.1146/annurev-immunol-032713-120145.

Gu, Y. *et al.* (2002) 'Rac2, a hematopoiesis-specific Rho GTPase, specifically regulates mast cell protease gene expression in bone marrow-derived mast cells.', *Molecular and cellular biology*, 22(21), pp. 7645–57.

Guerriero, C. J. and Weisz, O. A. (2007) 'N-WASP inhibitor wiskostatin

nonselectively perturbs membrane transport by decreasing cellular ATP levels', *American Journal of Physiology-Cell Physiology*. American Physiological Society, 292(4), pp. C1562–C1566. doi: 10.1152/ajpcell.00426.2006.

Guiet, R. *et al.* (2012) 'Macrophage mesenchymal migration requires podosome stabilization by filamin A.', *The Journal of biological chemistry*. American Society for Biochemistry and Molecular Biology, 287(16), pp. 13051–62. doi: 10.1074/jbc.M111.307124.

Gupta, A. *et al.* (2013) 'Toll-like receptor agonists and febrile range hyperthermia synergize to induce heat shock protein 70 expression and extracellular release.', *The Journal of biological chemistry*. American Society for Biochemistry and Molecular Biology, 288(4), pp. 2756–66. doi: 10.1074/jbc.M112.427336.

Gupta, D. *et al.* (2014) 'Differentiation and Characterization of Myeloid Cells', in *Current Protocols in Immunology*. Hoboken, NJ, USA: John Wiley & Sons, Inc., pp. 22F.5.1-22F.5.28. doi: 10.1002/0471142735.im22f05s104.

den Haan, J. M. M., Arens, R. and van Zelm, M. C. (2014) 'The activation of the adaptive immune system: Cross-talk between antigen-presenting cells, T cells and B cells', *Immunology Letters*, 162(2), pp. 103–112. doi: 10.1016/j.imlet.2014.10.011.

Hao, Y.-H. *et al.* (2013) 'Regulation of WASH-Dependent Actin Polymerization and Protein Trafficking by Ubiquitination', *Cell*, 152(5), pp. 1051–1064. doi: 10.1016/j.cell.2013.01.051.

Harayama, T. and Riezman, H. (2018) 'Understanding the diversity of membrane lipid composition', *Nature Reviews Molecular Cell Biology*. Nature Publishing Group, 19(5), pp. 281–296. doi: 10.1038/nrm.2017.138.

Hatzfeld-Charbonnier, A. S. *et al.* (2007) 'Influence of heat stress on human monocyte-derived dendritic cell functions with immunotherapeutic potential for

antitumor vaccines.', *Journal of leukocyte biology*. Inserm, 81(5), pp. 1179–87. doi: 10.1189/jlb.0506347.

He, H.-T. and Marguet, D. (2008) 'T-cell antigen receptor triggering and lipid rafts: a matter of space and time scales. Talking Point on the involvement of lipid rafts in T-cell activation', *EMBO reports*, 9(6), pp. 525–530. doi: 10.1038/embor.2008.78.

Heasman, S. J. and Ridley, A. J. (2008) 'Mammalian Rho GTPases: new insights into their functions from in vivo studies', *Nature Reviews Molecular Cell Biology*, 9(9), pp. 690–701. doi: 10.1038/nrm2476.

Hesselink JM, K. (2016) 'Bimoclomol and Arimoclomol: HSP-co-Inducers for the Treatment of Protein Misfolding Disorders, Neuropathy and Neuropathic Pain', *Journal of Pain & Relief*. OMICS International, 06(01), pp. 1–5. doi: 10.4172/2167-0846.1000279.

Higgs, H. N. and Pollard, T. D. (1999) 'Regulation of actin polymerization by Arp2/3 complex and WASp/Scar proteins.', *The Journal of biological chemistry*. American Society for Biochemistry and Molecular Biology, 274(46), pp. 32531–4. doi: 10.1074/JBC.274.46.32531.

Higgs, H. N. and Pollard, T. D. (2000) 'Activation by Cdc42 and PIP(2) of Wiskott-Aldrich syndrome protein (WASp) stimulates actin nucleation by Arp2/3 complex.', *The Journal of cell biology*. The Rockefeller University Press, 150(6), pp. 1311–20.

Ho, H.-Y. H. *et al.* (2004) 'Toca-1 Mediates Cdc42-Dependent Actin Nucleation by Activating the N-WASP-WIP Complex', *Cell*, 118(2), pp. 203–216. doi: 10.1016/j.cell.2004.06.027.

Ho, H. Y. *et al.* (2001) 'CR16 forms a complex with N-WASP in brain and is a novel member of a conserved proline-rich actin-binding protein family.', *Proceedings of the National Academy of Sciences of the United States of America*. National Academy of

Sciences, 98(20), pp. 11306–11. doi: 10.1073/pnas.211420498.

Holt, M. R. *et al.* (2008) 'Quantifying cell-matrix adhesion dynamics in living cells using interference reflection microscopy', *Journal of Microscopy*. Wiley/Blackwell (10.1111), 232(1), pp. 73–81. doi: 10.1111/j.1365-2818.2008.02069.x.

Hong, J. *et al.* (2011) 'Phosphorylation of Serine 68 of Twist1 by MAPKs Stabilizes Twist1 Protein and Promotes Breast Cancer Cell Invasiveness', *Cancer Research*, 71(11), pp. 3980–3990. doi: 10.1158/0008-5472.CAN-10-2914.

Horton, Jay D, Goldstein, J. L. and Brown, M. S. (2002) 'SREBPs: activators of the complete program of cholesterol and fatty acid synthesis in the liver.', *The Journal of clinical investigation*. American Society for Clinical Investigation, 109(9), pp. 1125–31. doi: 10.1172/JCI15593.

Horton, Jay D., Goldstein, J. L. and Brown, M. S. (2002) 'SREBPs: activators of the complete program of cholesterol and fatty acid synthesis in the liver', *Journal of Clinical Investigation*, 109(9), pp. 1125–1131. doi: 10.1172/JCI200215593.

Horváth, I. *et al.* (1998) 'Membrane physical state controls the signaling mechanism of the heat shock response in Synechocystis PCC 6803: identification of hsp17 as a fluidity gene.', *Proceedings of the National Academy of Sciences of the United States of America*. National Academy of Sciences, 95(7), pp. 3513–8. doi: 10.1073/PNAS.95.7.3513.

Hsu, W.-L. and Yoshioka, T. (2015) 'Role of TRP channels in the induction of heat shock proteins (Hsps) by heating skin', *BIOPHYSICS*, 11(0), pp. 25–32. doi: 10.2142/biophysics.11.25.

Huang, C. *et al.* (1997) 'Down-regulation of the filamentous actin cross-linking activity of cortactin by Src-mediated tyrosine phosphorylation.', *The Journal of biological chemistry*, 272(21), pp. 13911–5.

Hubler, M. J. and Kennedy, A. J. (2016) 'Role of lipids in the metabolism and activation of immune cells.', *The Journal of nutritional biochemistry*. NIH Public Access, 34, pp. 1–7. doi: 10.1016/j.jnutbio.2015.11.002.

Humphries, M. J., Symonds, E. J. H. and Mould, A. P. (2003) 'Mapping functional residues onto integrin crystal structures.', *Current opinion in structural biology*, 13(2), pp. 236–43.

Huo, Y., Hafezi-Moghadam, A. and Ley, K. (2000) 'Role of Vascular Cell Adhesion Molecule-1 and Fibronectin Connecting Segment-1 in Monocyte Rolling and Adhesion on Early Atherosclerotic Lesions', *Circulation Research*. Lippincott Williams & Wilkins, 87(2), pp. 153–159. doi: 10.1161/01.RES.87.2.153.

Huttenlocher, A. and Horwitz, A. R. (2011) 'Integrins in Cell Migration', *Cold Spring Harbor Perspectives in Biology*. Cold Spring Harbor Laboratory Press, 3(9). doi: 10.1101/CSHPERSPECT.A005074.

Huttenlocher, A., Sandborg, R. R. and Horwitz, A. F. (1995) 'Adhesion in cell migration', *Current Opinion in Cell Biology*. Elsevier Current Trends, 7(5), pp. 697–706. doi: 10.1016/0955-0674(95)80112-X.

Hwang, S.-L. *et al.* (2005) 'Expression of Rac3 in human brain tumors', *Journal of Clinical Neuroscience*. Churchill Livingstone, 12(5), pp. 571–574. doi: 10.1016/J.JOCN.2004.08.013.

Imai, K. *et al.* (2004) 'Clinical course of patients with WASP gene mutations.', *Blood*. American Society of Hematology, 103(2), pp. 456–64. doi: 10.1182/blood-2003-05-1480.

Ingersoll, M. A. *et al.* (2011) 'Monocyte trafficking in acute and chronic inflammation', *Trends in Immunology*, 32(10), pp. 470–477. doi: 10.1016/j.it.2011.05.001.

Ingólfsson, H. I. *et al.* (2014) 'Lipid Organization of the Plasma Membrane', *Journal of the American Chemical Society*. American Chemical Society, 136(41), pp. 14554–14559. doi: 10.1021/ja507832e.

Iqbal, A. J., Fisher, E. A. and Greaves, D. R. (2016) 'Inflammation-a Critical Appreciation of the Role of Myeloid Cells.', *Microbiology spectrum*. NIH Public Access, 4(5). doi: 10.1128/microbiolspec.MCHD-0027-2016.

Irtegun, S. *et al.* (2013) 'Tyrosine 416 Is Phosphorylated in the Closed, Repressed Conformation of c-Src', *PLoS ONE*. Edited by P. Lewis. Public Library of Science, 8(7), p. e71035. doi: 10.1371/journal.pone.0071035.

Isaac, B. M. *et al.* (2010) 'N-WASP has the ability to compensate for the loss of WASP in macrophage podosome formation and chemotaxis', *Experimental Cell Research*, 316(20), pp. 3406–3416. doi: 10.1016/j.yexcr.2010.06.011.

Italiani, P. and Boraschi, D. (2014) 'From Monocytes to M1/M2 Macrophages: Phenotypical vs. Functional Differentiation.', *Frontiers in immunology*. Frontiers Media SA, 5, p. 514. doi: 10.3389/fimmu.2014.00514.

Jacobson, K. and Liu, P. (2016) 'Complexity Revealed: A Hierarchy of Clustered Membrane Proteins.', *Biophysical journal*. The Biophysical Society, 111(1), pp. 1–2. doi: 10.1016/j.bpj.2016.05.045.

Janatpour, M. J. *et al.* (2001) 'Tumor necrosis factor-dependent segmental control of MIG expression by high endothelial venules in inflamed lymph nodes regulates monocyte recruitment.', *The Journal of experimental medicine*, 194(9), pp. 1375–84.

Jerry, L. M. and Sullivan, A. K. (1976) 'The lymphocyte plasma membrane: locus of control in the immune response.', *In vitro*, 12(3), pp. 236–59.

Jia, D. *et al.* (2010) 'WASH and WAVE actin regulators of the Wiskott-Aldrich syndrome protein (WASP) family are controlled by analogous structurally related

complexes.', *Proceedings of the National Academy of Sciences of the United States of America*. National Academy of Sciences, 107(23), pp. 10442–7. doi: 10.1073/pnas.0913293107.

Jiang, Q. *et al.* (1999) 'Exposure to febrile temperature upregulates expression of pyrogenic cytokines in endotoxin-challenged mice.', *The American journal of physiology*, 276(6 Pt 2), pp. R1653-60.

Jin, L. *et al.* (2005) 'Cholesterol-enriched lipid domains can be visualized by di-4-ANEPPDHQ with linear and nonlinear optics.', *Biophysical journal*. The Biophysical Society, 89(1), pp. L04-6. doi: 10.1529/biophysj.105.064816.

Jin, Y. *et al.* (2004) 'Mutations of the Wiskott-Aldrich Syndrome Protein (WASP): hotspots, effect on transcription, and translation and phenotype/genotype correlation', *Blood*, 104(13), pp. 4010–4019. doi: 10.1182/blood-2003-05-1592.

Jones, G. E. *et al.* (2002) 'Restoration of podosomes and chemotaxis in Wiskott-Aldrich syndrome macrophages following induced expression of WASp.', *The international journal of biochemistry & cell biology*, 34(7), pp. 806–15.

Jones, G. E. (2008) 'WASP and WIP regulate podosomes in migrating leukocytes', *Journal of Microscopy*, 231, pp. 494–505.

Karsunky, H. *et al.* (2003) 'Flt3 ligand regulates dendritic cell development from Flt3+ lymphoid and myeloid-committed progenitors to Flt3+ dendritic cells in vivo.', *The Journal of experimental medicine*. Rockefeller University Press, 198(2), pp. 305–13. doi: 10.1084/jem.20030323.

Kattan, W. E. *et al.* (2019) 'Targeting plasma membrane phosphatidylserine content to inhibit oncogenic KRAS function.', *Life science alliance*. Life Science Alliance LLC, 2(5). doi: 10.26508/lsa.201900431.

Kawamoto, H. and Minato, N. (2004) 'Myeloid cells', *The International Journal of*

Biochemistry & Cell Biology. Pergamon, 36(8), pp. 1374–1379. doi: 10.1016/J.BIOCEL.2004.01.020.

Kelly, A. E. *et al.* (2006) 'Actin binding to the central domain of WASP/Scar proteins plays a critical role in the activation of the Arp2/3 complex.', *The Journal of biological chemistry*. NIH Public Access, 281(15), pp. 10589–97. doi: 10.1074/jbc.M507470200.

Kenney, D. *et al.* (1986) 'Morphological abnormalities in the lymphocytes of patients with the Wiskott-Aldrich syndrome', *Blood*, 68(6).

Keren, K. (2011) 'Cell motility: the integrating role of the plasma membrane.', *European biophysics journal : EBJ*. Springer, 40(9), pp. 1013–27. doi: 10.1007/s00249-011-0741-0.

Kim, A. S. *et al.* (2000) 'Autoinhibition and activation mechanisms of the Wiskott–Aldrich syndrome protein', *Nature*, 404(6774), pp. 151–158. doi: 10.1038/35004513.

Kim, B.-K. *et al.* (2016) 'Heat shock protein 90 is involved in IL-17-mediated skin inflammation following thermal stimulation', *International Journal of Molecular Medicine*, 38(2), pp. 650–658. doi: 10.3892/ijmm.2016.2627.

Kim, D.-H. and Wirtz, D. (2013) 'Focal adhesion size uniquely predicts cell migration.', *FASEB journal : official publication of the Federation of American Societies for Experimental Biology*. The Federation of American Societies for Experimental Biology, 27(4), pp. 1351–61. doi: 10.1096/fj.12-220160.

Kinley, A. W. *et al.* (2003) 'Cortactin interacts with WIP in regulating Arp2/3 activation and membrane protrusion.', *Current biology : CB*, 13(5), pp. 384–93.

Kiosses, W. B. *et al.* (1999) 'A role for p21-activated kinase in endothelial cell migration.', *The Journal of cell biology*, 147(4), pp. 831–44. doi: 10.1083/jcb.147.4.831.

Klemke, R. L. *et al.* (1997) 'Regulation of Cell Motility by Mitogen-activated Protein Kinase', *The Journal of Cell Biology*, 137(2), pp. 481–492. doi: 10.1083/jcb.137.2.481.

Knight, B. *et al.* (2000) 'Visualizing muscle cell migration in situ.', *Current biology : CB*, 10(10), pp. 576–85.

Knippertz, I. *et al.* (2011) 'Mild hyperthermia enhances human monocyte-derived dendritic cell functions and offers potential for applications in vaccination strategies', *International Journal of Hyperthermia*, 27(6), pp. 591–603. doi: 10.3109/02656736.2011.589234.

Kondo, M. (2010) 'Lymphoid and myeloid lineage commitment in multipotent hematopoietic progenitors.', *Immunological reviews*. NIH Public Access, 238(1), pp. 37–46. doi: 10.1111/j.1600-065X.2010.00963.x.

Kuan, Y.-C. *et al.* (2017) 'Heat Shock Protein 90 Modulates Lipid Homeostasis by Regulating the Stability and Function of Sterol Regulatory Element-binding Protein (SREBP) and SREBP Cleavage-activating Protein.', *The Journal of biological chemistry*. American Society for Biochemistry and Molecular Biology, 292(7), pp. 3016–3028. doi: 10.1074/jbc.M116.767277.

Kurisu, S. and Takenawa, T. (2009) 'The WASP and WAVE family proteins.', *Genome biology*. BioMed Central, 10(6), p. 226. doi: 10.1186/gb-2009-10-6-226.

Kwan, S. P. *et al.* (1995) 'Identification of mutations in the Wiskott-Aldrich syndrome gene and characterization of a polymorphic dinucleotide repeat at DXS6940, adjacent to the disease gene.', *Proceedings of the National Academy of Sciences of the United States of America*. National Academy of Sciences, 92(10), pp. 4706–10. doi: 10.1073/PNAS.92.10.4706.

de la Fuente, M. A. *et al.* (2007) 'WIP is a chaperone for Wiskott–Aldrich syndrome

protein (WASP)'.

Lai, C. F. *et al.* (2001) 'Erk is essential for growth, differentiation, integrin expression, and cell function in human osteoblastic cells.', *The Journal of biological chemistry*. American Society for Biochemistry and Molecular Biology, 276(17), pp. 14443–50. doi: 10.1074/jbc.M010021200.

Lai, F. P. L. *et al.* (2009) 'Cortactin promotes migration and platelet-derived growth factor-induced actin reorganization by signaling to Rho-GTPases.', *Molecular biology of the cell*. American Society for Cell Biology, 20(14), pp. 3209–23. doi: 10.1091/mbc.E08-12-1180.

Lanzardo, S. *et al.* (2007) 'A role for WASP Interacting Protein, WIP, in fibroblast adhesion, spreading and migration', *The International Journal of Biochemistry & Cell Biology*. Pergamon, 39(1), pp. 262–274. doi: 10.1016/J.BIOCEL.2006.08.011.

Larkindale, J. and Huang, B. (2004) 'Changes of lipid composition and saturation level in leaves and roots for heat-stressed and heat-acclimated creeping bentgrass (Agrostis stolonifera)', *Environmental and Experimental Botany*. Elsevier, 51(1), pp. 57–67. doi: 10.1016/S0098-8472(03)00060-1.

Laszlo, A. (1992) *The effects of hyperthermia on mammalian cell structure and function*, *Cell Prolif*.

Launey, Y. *et al.* (2011) 'Clinical review: Fever in septic ICU patients - friend or foe?', *Critical Care*, 15(3), p. 222. doi: 10.1186/cc10097.

Leber, T. M. and Balkwill, F. R. (1997) 'Zymography: A Single-Step Staining Method for Quantitation of Proteolytic Activity on Substrate Gels', *Analytical Biochemistry*, 249(1), pp. 24–28. doi: 10.1006/abio.1997.2170.

Lee, J. *et al.* (2015) 'Restricted dendritic cell and monocyte progenitors in human cord blood and bone marrow', *Journal of Experimental Medicine*. Rockefeller University

Press, 212(3), pp. 385–399. doi: 10.1084/JEM.20141442.

Lee, P. P. *et al.* (2017) 'Wiskott-Aldrich syndrome protein regulates autophagy and inflammasome activity in innate immune cells', *Nature Communications*, 8(1), p. 1576. doi: 10.1038/s41467-017-01676-0.

Lefor, A. T. *et al.* (1994) 'Hyperthermia increases intercellular adhesion molecule-1 expression and lymphocyte adhesion to endothelial cells.', *Surgery*, 116(2), pp. 214–20; discussion 220-1.

Leon, B. and Ardavin, C. (2008) 'Monocyte migration to inflamed skin and lymph nodes is differentially controlled by L-selectin and PSGL-1', *Blood*, 111(6), pp. 3126–3130. doi: 10.1182/blood-2007-07-100610.

Lepock, J. R. (1982) 'Involvement of Membranes in Cellular Responses to Hyperthermia', *Radiation Research*. Radiation Research Society, 92(3), p. 433. doi: 10.2307/3575914.

Lepock, J. R. *et al.* (1983) 'Thermotropic lipid and protein transitions in chinese hamster lung cell membranes: relationship to hyperthermic cell killing.', *Canadian journal of biochemistry and cell biology = Revue canadienne de biochimie et biologie cellulaire*, 61(6), pp. 421–7.

Leuschner, F. *et al.* (2011) 'Therapeutic siRNA silencing in inflammatory monocytes in mice', *Nature Biotechnology*. Nature Publishing Group, 29(11), pp. 1005–1010. doi: 10.1038/nbt.1989.

Lew, D. J. (2002) 'Formin' actin filament bundles', *Nature Cell Biology*. Nature Publishing Group, 4(2), pp. E29–E30. doi: 10.1038/ncb0202-e29.

Ley, K. *et al.* (2007) 'Getting to the site of inflammation: the leukocyte adhesion cascade updated', *Nature Reviews Immunology*. Nature Publishing Group, 7(9), pp. 678–689. doi: 10.1038/nri2156.

Lillemeier, B. F. *et al.* (2010) 'TCR and Lat are expressed on separate protein islands on T cell membranes and concatenate during activation', *Nature Immunology*, 11(1), pp. 90–96. doi: 10.1038/ni.1832.

Lillemeier, B. F. and Davis, M. M. (2011) 'Probing the Plasma Membrane Structure of Immune Cells Through the Analysis of Membrane Sheets by Electron Microscopy', *Methods in molecular biology (Clifton, N.J.)*. NIH Public Access, 748, p. 169. doi: 10.1007/978-1-61779-139-0_12.

Linder, S. *et al.* (1999) 'Wiskott-Aldrich syndrome protein regulates podosomes in primary human macrophages.', *Proceedings of the National Academy of Sciences of the United States of America*. National Academy of Sciences, 96(17), pp. 9648–53. doi: 10.1073/PNAS.96.17.9648.

Linder, S. *et al.* (2000) 'The polarization defect of Wiskott-Aldrich syndrome macrophages is linked to dislocalization of the Arp2/3 complex.', *Journal of immunology (Baltimore, Md. : 1950)*, 165(1), pp. 221–5.

Linder, S. *et al.* (2005) 'Podosomes at a glance.', *Journal of cell science*. The Company of Biologists Ltd, 118(Pt 10), pp. 2079–82. doi: 10.1242/jcs.02390.

Linder, S. (2007) 'The matrix corroded: podosomes and invadopodia in extracellular matrix degradation', *Trends in Cell Biology*. Elsevier Current Trends, 17(3), pp. 107–117.

Linder, S. (2009) 'Invadosomes at a glance.', *Journal of cell science*. The Company of Biologists Ltd, 122(Pt 17), pp. 3009–13. doi: 10.1242/jcs.032631.

Linder, S. and Aepfelbacher, M. (2003) 'Podosomes: adhesion hot-spots of invasive cells', *Trends in Cell Biology*. Elsevier Current Trends, 13(7), pp. 376–385. doi: 10.1016/S0962-8924(03)00128-4.

Linder, S., Wiesner, C. and Himmel, M. (2011) 'Degrading Devices: Invadosomes in

Proteolytic Cell Invasion', *Annual Review of Cell and Developmental Biology*. Annual Reviews , 27(1), pp. 185–211. doi: 10.1146/annurev-cellbio-092910-154216.

Lingwood, D. and Simons, K. (2010) 'Lipid rafts as a membrane-organizing principle.', *Science (New York, N.Y.)*. American Association for the Advancement of Science, 327(5961), pp. 46–50. doi: 10.1126/science.1174621.

Liso, A. *et al.* (2017) 'Human monocyte-derived dendritic cells exposed to hyperthermia show a distinct gene expression profile and selective upregulation of IGFBP6.', *Oncotarget*. Impact Journals, LLC, 8(37), pp. 60826–60840. doi: 10.18632/oncotarget.18338.

Liu, B. *et al.* (1998) 'Purification and Characterization of a Membrane Bound Neutral pH Optimum Magnesium-dependent and Phosphatidylserine-stimulated Sphingomyelinase from Rat Brain', *Journal of Biological Chemistry*, 273(51), pp. 34472–34479. doi: 10.1074/jbc.273.51.34472.

Liu, E. *et al.* (2012) 'Naturally occurring hypothermia is more advantageous than fever in severe forms of lipopolysaccharide- and Escherichia coli-induced systemic inflammation', *American Journal of Physiology-Regulatory, Integrative and Comparative Physiology*, 302(12), pp. R1372–R1383. doi: 10.1152/ajpregu.00023.2012.

Liu, S., Kapoor, M. and Leask, A. (2009) 'Rac1 expression by fibroblasts is required for tissue repair in vivo.', *The American journal of pathology*. American Society for Investigative Pathology, 174(5), pp. 1847–56. doi: 10.2353/ajpath.2009.080779.

Liu, T. *et al.* (2017) 'Structural Insights of WHAMM's Interaction with Microtubules by Cryo-EM', *Journal of Molecular Biology*. Academic Press, 429(9), pp. 1352–1363. doi: 10.1016/J.JMB.2017.03.022.

Livne, A. and Geiger, B. (2016) 'The inner workings of stress fibers - from contractile

machinery to focal adhesions and back.', *Journal of cell science*. The Company of Biologists Ltd, 129(7), pp. 1293–304. doi: 10.1242/jcs.180927.

Lladó, V. *et al.* (2014) 'Regulation of the cancer cell membrane lipid composition by NaCHOleate: Effects on cell signaling and therapeutical relevance in glioma', *Biochimica et Biophysica Acta (BBA) - Biomembranes*. Elsevier, 1838(6), pp. 1619–1627. doi: 10.1016/J.BBAMEM.2014.01.027.

llić, D. *et al.* (1995) 'Reduced cell motility and enhanced focal adhesion contact formation in cells from FAK-deficient mice', *Nature*. Nature Publishing Group, 377(6549), pp. 539–544. doi: 10.1038/377539a0.

Lorenz, M. *et al.* (2004) 'Imaging Sites of N-WASP Activity in Lamellipodia and Invadopodia of Carcinoma Cells', *Current Biology*, 14(8), pp. 697–703. doi: 10.1016/j.cub.2004.04.008.

Luan, Q. *et al.* (2018) 'Identification of Wiskott-Aldrich syndrome protein (WASP) binding sites on the branched actin filament nucleator Arp2/3 complex.', *Proceedings of the National Academy of Sciences of the United States of America*. National Academy of Sciences, 115(7), pp. E1409–E1418. doi: 10.1073/pnas.1716622115.

Luo, B.-H., Carman, C. V. and Springer, T. A. (2007) 'Structural Basis of Integrin Regulation and Signaling', *Annual Review of Immunology*. Annual Reviews, 25(1), pp. 619–647. doi: 10.1146/annurev.immunol.25.022106.141618.

Luostarinen, R., Boberg, M. and Saldeen, T. (1993) 'Fatty acid composition in total phospholipids of human coronary arteries in sudden cardiac death.', *Atherosclerosis*, 99(2), pp. 187–93.

Luscinskas, F. W. *et al.* (1994) 'Monocyte rolling, arrest and spreading on IL-4-activated vascular endothelium under flow is mediated via sequential action of L-selectin, beta 1-integrins, and beta 2-integrins.', *The Journal of cell biology*.

Rockefeller University Press, 125(6), pp. 1417–27. doi: 10.1083/JCB.125.6.1417.

Luster, A. D. (2001) *Chemotaxis: Role in Immune Response*.

Luxenburg, C. *et al.* (2006) 'Involvement of the Src-cortactin pathway in podosome formation and turnover during polarization of cultured osteoclasts', *Journal of Cell Science*, 119(23), pp. 4878–4888. doi: 10.1242/jcs.03271.

Luxenburg, C. *et al.* (2007) 'The Architecture of the Adhesive Apparatus of Cultured Osteoclasts: From Podosome Formation to Sealing Zone Assembly', *PLoS ONE*. Edited by N. Cordes. Public Library of Science, 2(1), p. e179. doi: 10.1371/journal.pone.0000179.

Mace, T. A. *et al.* (2012) 'Effector CD8 $^{+}$ T cell IFN- γ production and cytotoxicity are enhanced by mild hyperthermia', *International Journal of Hyperthermia*, 28(1), pp. 9–18. doi: 10.3109/02656736.2011.616182.

MacGrath, S. M. and Koleske, A. J. (2012) 'Cortactin in cell migration and cancer at a glance.', *Journal of cell science*. The Company of Biologists Ltd, 125(Pt 7), pp. 1621–6. doi: 10.1242/jcs.093781.

Macpherson, L. *et al.* (2012) 'Tyrosine phosphorylation of WASP promotes calpain-mediated podosome disassembly.', *Haematologica*. Ferrata Storti Foundation, 97(5), pp. 687–91. doi: 10.3324/haematol.2011.048868.

Mahlaoui, N. *et al.* (2013) 'Characteristics and outcome of early-onset, severe forms of Wiskott-Aldrich syndrome', *Blood*. American Society of Hematology, 121(9), pp. 1510–1516. doi: 10.1182/BLOOD-2012-08-448118.

Mansilla, M. C. *et al.* (2004) 'Control of membrane lipid fluidity by molecular thermosensors.', *Journal of bacteriology*. American Society for Microbiology Journals, 186(20), pp. 6681–8. doi: 10.1128/JB.186.20.6681-6688.2004.

Martín-Fontecha, A. *et al.* (2004) 'Induced recruitment of NK cells to lymph nodes

provides IFN-γ for TH1 priming', *Nature Immunology*, 5(12), pp. 1260–1265. doi: 10.1038/ni1138.

Martin, C. E., Oh, C.-S. and Jiang, Y. (2007) 'Regulation of long chain unsaturated fatty acid synthesis in yeast', *Biochimica et Biophysica Acta (BBA) - Molecular and Cell Biology of Lipids*. Elsevier, 1771(3), pp. 271–285. doi: 10.1016/J.BBALIP.2006.06.010.

Martinez-Quiles, N. *et al.* (2001) 'WIP regulates N-WASP-mediated actin polymerization and filopodium formation.', *Nature cell biology*, 3(5), pp. 484–91. doi: 10.1038/35074551.

Martinez-Quiles, N. *et al.* (2004) 'Erk/Src Phosphorylation of Cortactin Acts as a Switch On-Switch Off Mechanism That Controls Its Ability To Activate N-WASP', *Molecular and Cellular Biology*, 24(12), pp. 5269–5280. doi: 10.1128/MCB.24.12.5269-5280.2004.

Maslin, C. *et al.* (2005) 'Transendothelial Migration of Monocytes: The Underlying Molecular Mechanisms and Consequences of HIV-1 Infection', *Current HIV Research*, 3(4), pp. 303–317. doi: 10.2174/157016205774370401.

Mason, R. P. and Jacob, R. F. (2003) 'Membrane Microdomains and Vascular Biology', *Circulation*, 107(17), pp. 2270–2273. doi: 10.1161/01.CIR.0000062607.02451.B6.

Matsuzaki, T. *et al.* (2018) 'Defining Lineage-Specific Membrane Fluidity Signatures that Regulate Adhesion Kinetics', *Stem Cell Reports*, 11(4), pp. 852–860. doi: 10.1016/j.stemcr.2018.08.010.

Maxfield, F. R. and Tabas, I. (2005) 'Role of cholesterol and lipid organization in disease', *Nature*, 438(7068), pp. 612–621. doi: 10.1038/nature04399.

May, J. A. *et al.* (1998) 'GPIIb-IIIa antagonists cause rapid disaggregation of platelets

pre-treated with cytochalasin D. Evidence that the stability of platelet aggregates depends on normal cytoskeletal assembly', *Platelets*, 9(3–4), pp. 227–232. doi: 10.1080/09537109876744.

Mazaira, G. I. *et al.* (2018) 'Gene expression regulation by heat-shock proteins: the cardinal roles of HSF1 and Hsp90.', *Biochemical Society transactions*. Portland Press Limited, 46(1), pp. 51–65. doi: 10.1042/BST20170335.

McCormick, B. *et al.* (2019) 'A Negative Feedback Loop Regulates Integrin Inactivation and Promotes Neutrophil Recruitment to Inflammatory Sites', *The Journal of Immunology*, 203(6), pp. 1579–1588. doi: 10.4049/jimmunol.1900443.

Medeiros, N. I. *et al.* (2017) 'Differential Expression of Matrix Metalloproteinases 2, 9 and Cytokines by Neutrophils and Monocytes in the Clinical Forms of Chagas Disease', *PLOS Neglected Tropical Diseases*. Edited by H. B. Tanowitz. Public Library of Science, 11(1), p. e0005284. doi: 10.1371/journal.pntd.0005284.

Medzhitov, R. (2010) 'Inflammation 2010: New Adventures of an Old Flame', *Cell*. Cell Press, 140(6), pp. 771–776. doi: 10.1016/J.CELL.2010.03.006.

van Meer, G. and de Kroon, A. I. P. M. (2011) 'Lipid map of the mammalian cell.', *Journal of cell science*. The Company of Biologists Ltd, 124(Pt 1), pp. 5–8. doi: 10.1242/jcs.071233.

van Meer, G., Voelker, D. R. and Feigenson, G. W. (2008) 'Membrane lipids: where they are and how they behave.', *Nature reviews. Molecular cell biology*. NIH Public Access, 9(2), pp. 112–24. doi: 10.1038/nrm2330.

Megha and London, E. (2004) 'Ceramide Selectively Displaces Cholesterol from Ordered Lipid Domains (Rafts)', *Journal of Biological Chemistry*, 279(11), pp. 9997–10004. doi: 10.1074/jbc.M309992200.

Meirson, T. and Gil-Henn, H. (2018) 'Targeting invadopodia for blocking breast

cancer metastasis', *Drug Resistance Updates*, 39, pp. 1–17. doi: 10.1016/j.drup.2018.05.002.

Mellor, H. (2010) 'The role of formins in filopodia formation', *Biochimica et Biophysica Acta (BBA) - Molecular Cell Research*, 1803(2), pp. 191–200. doi: 10.1016/j.bbamcr.2008.12.018.

Mendoza, M. C. *et al.* (2011) 'ERK-MAPK Drives Lamellipodia Protrusion by Activating the WAVE2 Regulatory Complex', *Molecular Cell*, 41(6), pp. 661–671. doi: 10.1016/j.molcel.2011.02.031.

Mersich, A. T. *et al.* (2010) 'The formin FRL1 (FMNL1) is an essential component of macrophage podosomes', *Cytoskeleton*, 67(9), pp. 573–585. doi: 10.1002/cm.20468.

Mescher, A. L. (2017) 'Macrophages and fibroblasts during inflammation and tissue repair in models of organ regeneration', *Regeneration*, 4(2), pp. 39–53. doi: 10.1002/reg2.77.

de Meyer, F. and Smit, B. (2009) 'Effect of cholesterol on the structure of a phospholipid bilayer.', *Proceedings of the National Academy of Sciences of the United States of America*. National Academy of Sciences, 106(10), pp. 3654–8. doi: 10.1073/pnas.0809959106.

Midis, G. P., Fabian, D. F. and Lefor, A. T. (1992) 'Lymphocyte migration to tumors after hyperthermia and immunotherapy.', *The Journal of surgical research*, 52(5), pp. 530–6.

Miki, H. *et al.* (2000) 'IRSp53 is an essential intermediate between Rac and WAVE in the regulation of membrane ruffling.', *Nature*, 408(6813), pp. 732–5. doi: 10.1038/35047107.

Mikucki, M. E. *et al.* (2013) 'Preconditioning thermal therapy: Flipping the switch on IL-6 for anti-tumour immunity', *International Journal of Hyperthermia*. doi:

10.3109/02656736.2013.807440.

Millard, T. H., Sharp, S. J. and Machesky, L. M. (2004) ‘Signalling to actin assembly via the WASP (Wiskott-Aldrich syndrome protein)-family proteins and the Arp2/3 complex.’, *The Biochemical journal*. Portland Press Ltd, 380(Pt 1), pp. 1–17. doi: 10.1042/BJ20040176.

Miller, G. J., Dunn, S. D. and Ball, E. H. (2001) ‘Interaction of the N- and C-terminal domains of vinculin. Characterization and mapping studies.’, *The Journal of biological chemistry*. American Society for Biochemistry and Molecular Biology, 276(15), pp. 11729–34. doi: 10.1074/jbc.M008646200.

Miller, M. W. and Ziskin, M. C. (1989) ‘Biological consequences of hyperthermia’, *Ultrasound in Medicine & Biology*. Elsevier, 15(8), pp. 707–722. doi: 10.1016/0301-5629(89)90111-7.

Mitra, S. K. and Schlaepfer, D. D. (2006) ‘Integrin-regulated FAK–Src signaling in normal and cancer cells’, *Current Opinion in Cell Biology*, 18(5), pp. 516–523. doi: 10.1016/j.ceb.2006.08.011.

Miyamoto, K. *et al.* (2013) ‘Nuclear Wave1 Is Required for Reprogramming Transcription in Oocytes and for Normal Development’, *Science*. American Association for the Advancement of Science, 341(6149), pp. 1002–1005. doi: 10.1126/SCIENCE.1240376.

Mizutani, K. *et al.* (2002) ‘Essential role of neural Wiskott-Aldrich syndrome protein in podosome formation and degradation of extracellular matrix in src-transformed fibroblasts.’, *Cancer research*, 62(3), pp. 669–74.

Mohd Rafiq, N. *et al.* (2017) ‘Myosin II-Dependent Suppression of Podosomes by an ARNO-ARF1 Signaling Axis’, *Biophysical Journal*. Elsevier, 112(3), p. 429a. doi: 10.1016/j.bpj.2016.11.2294.

Monick, M. M. *et al.* (2002) 'Interaction of matrix with integrin receptors is required for optimal LPS-induced MAP kinase activation', *American Journal of Physiology-Lung Cellular and Molecular Physiology*, 283(2), pp. L390–L402. doi: 10.1152/ajplung.00437.2001.

Monypenny, J. *et al.* (2011) 'Role of WASP in cell polarity and podosome dynamics of myeloid cells.', *European journal of cell biology*. Elsevier, 90(2–3), pp. 198–204. doi: 10.1016/j.ejcb.2010.05.009.

Morenilla-Palao, C. *et al.* (2009) 'Lipid raft segregation modulates TRPM8 channel activity.', *The Journal of biological chemistry*. American Society for Biochemistry and Molecular Biology, 284(14), pp. 9215–24. doi: 10.1074/jbc.M807228200.

Moulding, D. A. *et al.* (2013) 'Actin cytoskeletal defects in immunodeficiency.', *Immunological reviews*. Wiley-Blackwell, 256(1), pp. 282–99. doi: 10.1111/imr.12114.

Mulas, M. F. *et al.* (2011) 'Cholesterol esterification during differentiation of mouse erythroleukemia (Friend) cells.', *Hematology reports*. PAGEPress, 3(2), p. e19. doi: 10.4081/hr.2011.e19.

Muller, W. A. (2011) 'Mechanisms of leukocyte transendothelial migration.', *Annual review of pathology*. NIH Public Access, 6, pp. 323–44. doi: 10.1146/annurev-pathol-011110-130224.

Muller, W. A. *et al.* (1993) '*PECAM-1 Is Required for Transendothelial Migration of Leukocytes'*. J Exp Med, 178(2):449-60.

Mullins, R. D., Heuser, J. A. and Pollard, T. D. (1998) 'The interaction of Arp2/3 complex with actin: nucleation, high affinity pointed end capping, and formation of branching networks of filaments.', *Proceedings of the National Academy of Sciences of the United States of America*. National Academy of Sciences, 95(11), pp. 6181–6.

Multhoff, G. *et al.* (1995) 'CD3- large granular lymphocytes recognize a heat-inducible immunogenic determinant associated with the 72-kD heat shock protein on human sarcoma cells.', *Blood*, 86(4), pp. 1374–82.

Munro, S. (2003) 'Lipid Rafts', *Cell*, 115(4), pp. 377–388. doi: 10.1016/S0092-8674(03)00882-1.

Murata, N. and 10s, D. A. (1997) *Membrane Fluidity and Temperature Perception'*, *Plant Phvsiol*.

Nakano, K. *et al.* (2010) 'GMF is an evolutionarily developed Adf/cofilin-super family protein involved in the Arp2/3 complex-mediated organization of the actin cytoskeleton', *Cytoskeleton*, 67(6), p. n/a-n/a. doi: 10.1002/cm.20451.

Nobes, C. D. and Hall, A. (1995) 'Rho, Rac, and Cdc42 GTPases regulate the assembly of multimolecular focal complexes associated with actin stress fibers, lamellipodia, and filopodia', *Cell*. Cell Press, 81(1), pp. 53–62. doi: 10.1016/0092-8674(95)90370-4.

Nobes, C. D. and Hall, A. (1999) 'Rho GTPases control polarity, protrusion, and adhesion during cell movement.', *The Journal of cell biology*, 144(6), pp. 1235–44. doi: 10.1083/jcb.144.6.1235.

Nolen, B. J. *et al.* (2009) 'Characterization of two classes of small molecule inhibitors of Arp2/3 complex', *Nature*, 460(7258), pp. 1031–1034. doi: 10.1038/nature08231.

de Noronha, S. *et al.* (2005) 'Impaired dendritic-cell homing in vivo in the absence of Wiskott-Aldrich syndrome protein', *Blood*, 105(4), pp. 1590–1597. doi: 10.1182/blood-2004-06-2332.

Notarangelo, L. D. (2013) 'In Wiskott-Aldrich syndrome, platelet count matters', *Blood*, 121(9), pp. 1484–1485. doi: 10.1182/blood-2013-01-475913.

O'Neill, G. M. (2009) 'The coordination between actin filaments and adhesion in

mesenchymal migration.', *Cell adhesion & migration*. Taylor & Francis, 3(4), pp. 355–7.

Ochs, H. *et al.* (1980) 'The Wiskott-Aldrich syndrome: studies of lymphocytes, granulocytes, and platelets', *Blood*, 55(2).

Ochs, H. D. and Thrasher, A. J. (2006) 'The Wiskott-Aldrich syndrome.', *The Journal of allergy and clinical immunology*. Elsevier, 117(4), pp. 725–38; quiz 739. doi: 10.1016/j.jaci.2006.02.005.

Ohnishi, K. *et al.* (1998) 'Matrix metalloproteinase-mediated extracellular matrix protein degradation in human pulmonary emphysema.', *Laboratory investigation; a journal of technical methods and pathology*, 78(9), pp. 1077–87.

Oikawa, T. *et al.* (2013) 'IRSp53 Mediates Podosome Formation via VASP in NIH-Src Cells', *PLoS ONE*. Edited by N. A. Hotchin. Public Library of Science, 8(3), p. e60528. doi: 10.1371/journal.pone.0060528.

Oikawa, T. and Takenawa, T. (2009) 'PtdIns(3,4)P2 instigates focal adhesions to generate podosomes.', *Cell adhesion & migration*. Taylor & Francis, 3(2), pp. 195–7. doi: 10.4161/cam.3.2.7510.

Okamoto, T. *et al.* (2018) 'Reduced substrate stiffness promotes M2-like macrophage activation and enhances peroxisome proliferator-activated receptor γ expression', *Experimental Cell Research*. Academic Press, 367(2), pp. 264–273. doi: 10.1016/J.YEXCR.2018.04.005.

Olave, I. A., Reck-Peterson, S. L. and Crabtree, G. R. (2002) 'Nuclear Actin and Actin-Related Proteins in Chromatin Remodeling', *Annual Review of Biochemistry*, 71(1), pp. 755–781. doi: 10.1146/annurev.biochem.71.110601.135507.

Olivier, A. *et al.* (2006) 'A Partial Down-regulation of WASP Is Sufficient to Inhibit Podosome Formation in Dendritic Cells', *Molecular Therapy*. Cell Press, 13(4), pp.

729–737. doi: 10.1016/J.YMTHE.2005.11.003.

Ory, S. *et al.* (2008) 'Rho GTPases in osteoclasts: Orchestrators of podosome arrangement', *European Journal of Cell Biology*, 87(8–9), pp. 469–477. doi: 10.1016/j.ejcb.2008.03.002.

Ostberg, J. R. *et al.* (2000) 'Regulatory effects of fever-range whole-body hyperthermia on the LPS-induced acute inflammatory response.', *Journal of leukocyte biology*, 68(6), pp. 815–20.

Ostberg, J. R. *et al.* (2001) 'Regulatory potential of fever-range whole body hyperthermia on Langerhans cells and lymphocytes in an antigen-dependent cellular immune response.', *Journal of immunology (Baltimore, Md. : 1950)*, 167(5), pp. 2666–70.

Ostberg, J. R. *et al.* (2007) 'Enhancement of natural killer (NK) cell cytotoxicity by fever-range thermal stress is dependent on NKG2D function and is associated with plasma membrane NKG2D clustering and increased expression of MICA on target cells', *Journal of Leukocyte Biology*, 82(5), pp. 1322–1331. doi: 10.1189/jlb.1106699.

Ostberg, J. R., Ertel, B. R. and Lanphere, J. A. (2005) 'An important role for granulocytes in the thermal regulation of colon tumor growth.', *Immunological investigations*, 34(3), pp. 259–72.

Ostberg, J. R. and Repasky, E. A. (2000) 'Comparison of the effects of two different whole body hyperthermia protocols on the distribution of murine leukocyte populations.', *International journal of hyperthermia : the official journal of European Society for Hyperthermic Oncology, North American Hyperthermia Group*, 16(1), pp. 29–43.

Owen, D. M. *et al.* (2010) 'Dynamic organization of lymphocyte plasma membrane: lessons from advanced imaging methods.', *Immunology*. Wiley-Blackwell, 131(1), pp.

1–8. doi: 10.1111/j.1365-2567.2010.03319.x.

Pan, Y.-R. *et al.* (2013) 'Protein tyrosine phosphatase SHP2 suppresses podosome rosette formation in Src-transformed fibroblasts', *Journal of Cell Science*, 126(2), pp. 657–666. doi: 10.1242/jcs.116624.

Pant, K. *et al.* (2006) 'Cortactin Binding to F-actin Revealed by Electron Microscopy and 3D Reconstruction', *Journal of Molecular Biology*. Academic Press, 359(4), pp. 840–847. doi: 10.1016/J.JMB.2006.03.065.

Panzer, L. *et al.* (2016) 'The formins FHOD1 and INF2 regulate inter- and intra-structural contractility of podosomes.', *Journal of cell science*. The Company of Biologists Ltd, 129(2), pp. 298–313. doi: 10.1242/jcs.177691.

Parekh, A. and Weaver, A. M. (2016) 'Regulation of invadopodia by mechanical signaling.', *Experimental cell research*. NIH Public Access, 343(1), pp. 89–95. doi: 10.1016/j.yexcr.2015.10.038.

Parfitt, D. A. *et al.* (2014) 'The heat-shock response co-inducer arimoclomol protects against retinal degeneration in rhodopsin retinitis pigmentosa', *Cell Death & Disease*, 5(5), pp. e1236–e1236. doi: 10.1038/cddis.2014.214.

Park, H. G. *et al.* (2005) 'Cellular responses to mild heat stress', *Cellular and Molecular Life Sciences*. Birkhäuser-Verlag, 62(1), pp. 10–23. doi: 10.1007/s00018-004-4208-7.

Park, S. J. *et al.* (2007) 'HSP90 cross-links branched actin filaments induced by N-WASP and the Arp2/3 complex', *Genes to Cells*, 12(5), pp. 611–622. doi: 10.1111/j.1365-2443.2007.01081.x.

Park, S. J., Suetsugu, S. and Takenawa, T. (2005) 'Interaction of HSP90 to N-WASP leads to activation and protection from proteasome-dependent degradation.', *The EMBO journal*, 24(8), pp. 1557–70. doi: 10.1038/sj.emboj.7600586.

Parolini, O. *et al.* (1997) 'Expression of Wiskott-Aldrich syndrome protein (WASP) gene during hematopoietic differentiation.', *Blood*, 90(1), pp. 70–5.

Parsons, J. T., Horwitz, A. R. and Schwartz, M. A. (2010) 'Cell adhesion: integrating cytoskeletal dynamics and cellular tension.', *Nature reviews. Molecular cell biology*. NIH Public Access, 11(9), pp. 633–43. doi: 10.1038/nrm2957.

Parsons, S. J. and Parsons, J. T. (2004) 'Src family kinases, key regulators of signal transduction', *Oncogene*. Nature Publishing Group, 23(48), pp. 7906–7909. doi: 10.1038/sj.onc.1208160.

Pasapera, A. M. *et al.* (2010) 'Myosin II activity regulates vinculin recruitment to focal adhesions through FAK-mediated paxillin phosphorylation.', *The Journal of cell biology*. Rockefeller University Press, 188(6), pp. 877–90. doi: 10.1083/jcb.200906012.

Peláez, R. *et al.* (2017) 'β3 integrin expression is required for invadopodia-mediated ECM degradation in lung carcinoma cells', *PLOS ONE*. Edited by J. W. Lee. Public Library of Science, 12(8), p. e0181579. doi: 10.1371/journal.pone.0181579.

Peng, X. *et al.* (2012) 'Cell adhesion nucleation regulated by substrate stiffness: A Monte Carlo study', *Journal of Biomechanics*, 45(1), pp. 116–122. doi: 10.1016/j.jbiomech.2011.09.013.

PERONA, J. and RUIZGUTIERREZ, V. (2005) 'Triacylglycerol molecular species are depleted to different extents in the myocardium of spontaneously hypertensive rats fed two oleic acid?rich oils', *American Journal of Hypertension*, 18(1), pp. 72–80. doi: 10.1016/j.amjhyper.2004.11.012.

Petrella, A. *et al.* (1998) 'A 5' regulatory sequence containing two Ets motifs controls the expression of the Wiskott-Aldrich syndrome protein (WASP) gene in human hematopoietic cells.', *Blood*, 91(12), pp. 4554–60.

Pfaff, M. and Jurdic, P. (2001) ‘Podosomes in osteoclast-like cells: structural analysis and cooperative roles of paxillin, proline-rich tyrosine kinase 2 (Pyk2) and integrin alphaVbeta3.’, *Journal of cell science*, 114(Pt 15), pp. 2775–86.

Picker, L. J. and Butcher, E. C. (1992) ‘Physiological and Molecular Mechanisms of Lymphocyte Homing’, *Annual Review of Immunology*, 10(1), pp. 561–591. doi: 10.1146/annurev.iy.10.040192.003021.

Pike, L. J. (2003) ‘Lipid rafts: bringing order to chaos.’, *Journal of lipid research*. American Society for Biochemistry and Molecular Biology, 44(4), pp. 655–67. doi: 10.1194/jlr.R200021-JLR200.

Pilpel, Y. and Segal, M. (2005) ‘Rapid WAVE dynamics in dendritic spines of cultured hippocampal neurons is mediated by actin polymerization’, *Journal of Neurochemistry*, 95(5), pp. 1401–1410. doi: 10.1111/j.1471-4159.2005.03467.x.

Pollard, T. D., Blanchoin, L. and Mullins, R. D. (2000) ‘Molecular mechanisms controlling actin filament dynamics in nonmuscle cells.’, *Annual review of biophysics and biomolecular structure*, 29(1), pp. 545–76. doi: 10.1146/annurev.biophys.29.1.545.

Porcheray, F. *et al.* (2005) ‘Macrophage activation switching: an asset for the resolution of inflammation’, *Clinical and Experimental Immunology*. John Wiley & Sons, Ltd, 0(0), p. 051006055454001. doi: 10.1111/j.1365-2249.2005.02934.x.

Pörn, M. I., Ares, M. P. and Slotte, J. P. (1993) ‘Degradation of plasma membrane phosphatidylcholine appears not to affect the cellular cholesterol distribution.’, *Journal of lipid research*, 34(8), pp. 1385–92.

Posern, G., Sotiropoulos, A. and Treisman, R. (2002) ‘Mutant Actins Demonstrate a Role for Unpolymerized Actin in Control of Transcription by Serum Response Factor’, *Molecular Biology of the Cell*, 13(12), pp. 4167–4178. doi: 10.1091/mbc.02-

05-0068.

Postic, B. *et al.* (1966) ‘Effect of temperature on the induction of interferons by endotoxin and virus.’, *Journal of bacteriology*, 91(3), pp. 1277–81.

Prats, C. *et al.* (2016) ‘Local Inflammation, Dissemination and Coalescence of Lesions Are Key for the Progression toward Active Tuberculosis: The Bubble Model’, *Frontiers in Microbiology*. Frontiers, 7, p. 33. doi: 10.3389/fmicb.2016.00033.

Price, L. S. *et al.* (1998) ‘Activation of Rac and Cdc42 by integrins mediates cell spreading.’, *Molecular biology of the cell*, 9(7), pp. 1863–71. doi: 10.1091/mbc.9.7.1863.

Pritchard, M. T., Li, Z. and Repasky, E. A. (2005) ‘Nitric oxide production is regulated by fever-range thermal stimulation of murine macrophages’, *Journal of Leukocyte Biology*, 78(3), pp. 630–638. doi: 10.1189/jlb.0404220.

Proudfoot, A. E. I. *et al.* (2003) ‘Glycosaminoglycan binding and oligomerization are essential for the in vivo activity of certain chemokines’, *Proceedings of the National Academy of Sciences*, 100(4), pp. 1885–1890. doi: 10.1073/pnas.0334864100.

Pruenster, M. *et al.* (2009) ‘The Duffy antigen receptor for chemokines transports chemokines and supports their promigratory activity’, *Nature Immunology*. Nature Publishing Group, 10(1), pp. 101–108. doi: 10.1038/ni.1675.

Qu, F., Guilak, F. and Mauck, R. L. (2019) ‘Cell migration: implications for repair and regeneration in joint disease’, *Nature Reviews Rheumatology*. Nature Publishing Group, 15(3), pp. 167–179. doi: 10.1038/s41584-018-0151-0.

Ra, H.-J. and Parks, W. C. (2007) ‘Control of matrix metalloproteinase catalytic activity.’, *Matrix biology : journal of the International Society for Matrix Biology*. NIH Public Access, 26(8), pp. 587–96. doi: 10.1016/j.matbio.2007.07.001.

Ramesh, N. *et al.* (2014) ‘Binding of the WASP/N-WASP-Interacting Protein WIP to

Actin Regulates Focal Adhesion Assembly and Adhesion', *Molecular and Cellular Biology*. doi: 10.1128/MCB.00017-14.

Rashid, A. *et al.* (1997) 'Elevated expression of fatty acid synthase and fatty acid synthetic activity in colorectal neoplasia.', *The American journal of pathology*. American Society for Investigative Pathology, 150(1), pp. 201–8. A

Remold-O'Donnell, E., Rosen, F. and Kenney, D. (1996) 'Defects in Wiskott-Aldrich syndrome blood cells', *Blood*, 87(7).

Repasky, E. A., Evans, S. S. and Dewhirst, M. W. (2013) 'Temperature Matters! And Why It Should Matter to Tumor Immunologists', *Cancer Immunology Research*. doi: 10.1158/2326-6066.CIR-13-0118.

Rice, P. *et al.* (2005) 'Febrile-range hyperthermia augments neutrophil accumulation and enhances lung injury in experimental gram-negative bacterial pneumonia.', *Journal of immunology (Baltimore, Md. : 1950)*, 174(6), pp. 3676–85. A

Ridley, A. (2001) *Rho GTPases and cell migration*.

Ridley, A. (2000) 'Rho GTPases. Integrating integrin signaling.', *The Journal of cell biology*, 150(4), pp. F107-9. doi: 10.1083/jcb.150.4.f107.

Riveline, D. *et al.* (2001) 'Focal contacts as mechanosensors: externally applied local mechanical force induces growth of focal contacts by an mDia1-dependent and ROCK-independent mechanism.', *The Journal of cell biology*. Rockefeller University Press, 153(6), pp. 1175–86. doi: 10.1083/JCB.153.6.1175.

Roberts, A. W. *et al.* (1999) 'Deficiency of the hematopoietic cell-specific Rho family GTPase Rac2 is characterized by abnormalities in neutrophil function and host defense.', *Immunity*, 10(2), pp. 183–96.

Rodriguez-Mesa, E. *et al.* (2012) 'Developmental expression of Drosophila Wiskott-Aldrich Syndrome family proteins', *Developmental Dynamics*, 241(3), pp. 608–626.

doi: 10.1002/dvdy.23742.

Rohatgi, R. *et al.* (2001) 'Nck and phosphatidylinositol 4,5-bisphosphate synergistically activate actin polymerization through the N-WASP-Arp2/3 pathway.', *The Journal of biological chemistry*. American Society for Biochemistry and Molecular Biology, 276(28), pp. 26448–52. doi: 10.1074/jbc.M103856200.

Rossow, M. J. *et al.* (2010) 'Raster image correlation spectroscopy in live cells', *Nature Protocols*, 5(11), pp. 1761–1774. doi: 10.1038/nprot.2010.122.

Rottner, K., Hall, A. and Small, J. V (1999) 'Interplay between Rac and Rho in the control of substrate contact dynamics.', *Current biology : CB*, 9(12), pp. 640–8. doi: 10.1016/s0960-9822(99)80286-3.

Rouiller, I. *et al.* (2008) 'The structural basis of actin filament branching by the Arp2/3 complex', *The Journal of Cell Biology*, 180(5), pp. 887–895. doi: 10.1083/jcb.200709092.

Royal, I. *et al.* (2000) 'Activation of cdc42, rac, PAK, and rho-kinase in response to hepatocyte growth factor differentially regulates epithelial cell colony spreading and dissociation.', *Molecular biology of the cell*, 11(5), pp. 1709–25. doi: 10.1091/mbc.11.5.1709.

Ryan, M. and Levy, M. M. (2003) 'Clinical review: fever in intensive care unit patients.', *Critical Care*, 7(3), p. 221. doi: 10.1186/cc1879.

Sadhukhan, S. *et al.* (2014) 'Nuclear Role of WASp in Gene Transcription Is Uncoupled from Its ARP2/3-Dependent Cytoplasmic Role in Actin Polymerization', *The Journal of Immunology*, 193(1), pp. 150–160. doi: 10.4049/jimmunol.1302923.

Saita, E. A. and de Mendoza, D. (2015) 'Thermosensing via transmembrane protein–lipid interactions', *Biochimica et Biophysica Acta (BBA) - Biomembranes*. Elsevier, 1848(9), pp. 1757–1764. doi: 10.1016/J.BBAMEM.2015.04.005.

Sanjay, A. *et al.* (2001) 'Cbl associates with Pyk2 and Src to regulate Src kinase activity, alpha(v)beta(3) integrin-mediated signaling, cell adhesion, and osteoclast motility.', *The Journal of cell biology*, 152(1), pp. 181–95.

Sarkar, K. *et al.* (2014) 'Disruption of hSWI/SNF complexes in T cells by WAS mutations distinguishes X-linked thrombocytopenia from Wiskott-Aldrich syndrome', *Blood*. doi: 10.1182/blood-2014-07-587642.

Sawhney, R. S. *et al.* (2006) 'Integrin α2-mediated ERK and Calpain Activation Play a Critical Role in Cell Adhesion and Motility via Focal Adhesion Kinase Signaling', *Journal of Biological Chemistry*. American Society for Biochemistry and Molecular Biology, 281(13), pp. 8497–8510. doi: 10.1074/JBC.M600787200.

Schachtner, H. *et al.* (2013) 'Megakaryocytes assemble podosomes that degrade matrix and protrude through basement membrane', *Blood*, 121(13), pp. 2542–2552. doi: 10.1182/blood-2012-07-443457.

Schachtner, Hannah *et al.* (2013) 'Podosomes in adhesion, migration, mechanosensing and matrix remodeling', *Cytoskeleton*, 70(10), pp. 572–589. doi: 10.1002/cm.21119.

Schenkel, A. R., Mamdouh, Z. and Muller, W. A. (2004) 'Locomotion of monocytes on endothelium is a critical step during extravasation', *Nature Immunology*, 5(4), pp. 393–400. doi: 10.1038/ni1051.

Schlitzer, A., McGovern, N. and Ginhoux, F. (2015) 'Dendritic cells and monocyte-derived cells: Two complementary and integrated functional systems', *Seminars in Cell & Developmental Biology*, 41, pp. 9–22. doi: 10.1016/j.semcdb.2015.03.011.

Schmid, M. C. and Varner, J. A. (2007) 'Myeloid cell trafficking and tumor angiogenesis.', *Cancer letters*. NIH Public Access, 250(1), pp. 1–8. doi: 10.1016/j.canlet.2006.09.002.

Schulman, C. I. *et al.* (2005) 'The Effect of Antipyretic Therapy upon Outcomes in

Critically Ill Patients: A Randomized, Prospective Study', *Surgical Infections*, 6(4), pp. 369–375. doi: 10.1089/sur.2005.6.369.

Schumann, J. (2012) *The Impact of Macrophage Membrane Lipid Composition on Innate Immune Response Mechanisms*.

Schumann, K. *et al.* (2010) 'Immobilized Chemokine Fields and Soluble Chemokine Gradients Cooperatively Shape Migration Patterns of Dendritic Cells', *Immunity*, 32(5), pp. 703–713. doi: 10.1016/j.immuni.2010.04.017.

Schwartz, M. A. (2010) 'Integrins and extracellular matrix in mechanotransduction.', *Cold Spring Harbor perspectives in biology*. Cold Spring Harbor Laboratory Press, 2(12), p. a005066. doi: 10.1101/cshperspect.a005066.

Sengupta, P. and Garrity, P. (2013) 'Sensing temperature.', *Current biology : CB*. NIH Public Access, 23(8), pp. R304-7. doi: 10.1016/j.cub.2013.03.009.

Serbina, N. V and Pamer, E. G. (2006) 'Monocyte emigration from bone marrow during bacterial infection requires signals mediated by chemokine receptor CCR2', *Nature Immunology*, 7(3), pp. 311–317. doi: 10.1038/ni1309.

Shafaq-Zadah, M. *et al.* (2016) 'Persistent cell migration and adhesion rely on retrograde transport of β1 integrin', *Nature Cell Biology*, 18(1), pp. 54–64. doi: 10.1038/ncb3287.

Shankavaram, U. T. *et al.* (2001) 'Monocyte membrane type 1-matrix metalloproteinase. Prostaglandin-dependent regulation and role in metalloproteinase-2 activation.', *The Journal of biological chemistry*. American Society for Biochemistry and Molecular Biology, 276(22), pp. 19027–32. doi: 10.1074/jbc.M009562200.

Shi, C. and Pamer, E. G. (2011) 'Monocyte recruitment during infection and inflammation.', *Nature reviews. Immunology*. NIH Public Access, 11(11), pp. 762–

74. doi: 10.1038/nri3070.

Shvetsov, A. *et al.* (2009) 'The actin-binding domain of cortactin is dynamic and unstructured and affects lateral and longitudinal contacts in F-actin.', *Cell motility and the cytoskeleton*. NIH Public Access, 66(2), pp. 90–8. doi: 10.1002/cm.20328.

Siar, C. H. *et al.* (2016) 'Invadopodia proteins, cortactin, N-WASP and WIP differentially promote local invasiveness in ameloblastoma', *Journal of Oral Pathology & Medicine*, 45(8), pp. 591–598. doi: 10.1111/jop.12417.

Simard, J. P. *et al.* (2011) 'Overexpression of HSP70 inhibits cofilin phosphorylation and promotes lymphocyte migration in heat-stressed cells', *Journal of Cell Science*. doi: 10.1242/jcs.081745.

Simons, K. and Ikonen, E. (1997) 'Functional rafts in cell membranes', *Nature*. Nature Publishing Group, 387(6633), pp. 569–572. doi: 10.1038/42408.

Sims, J. D., McCready, J. and Jay, D. G. (2011) 'Extracellular Heat Shock Protein (Hsp)70 and Hsp90α Assist in Matrix Metalloproteinase-2 Activation and Breast Cancer Cell Migration and Invasion', *PLoS ONE*. Edited by D. Gullberg, 6(4), p. e18848. doi: 10.1371/journal.pone.0018848.

Singer, S. J. and Nicolson, G. L. (1972) 'The fluid mosaic model of the structure of cell membranes.', *Science (New York, N.Y.)*, 175(4023), pp. 720–31.

Singh, I. S. *et al.* (2008) 'Heat shock co-activates interleukin-8 transcription.', *American journal of respiratory cell and molecular biology*. American Thoracic Society, 39(2), pp. 235–42. doi: 10.1165/rcmb.2007-0294OC.

Singh, I. S. and Hasday, J. D. (2013) 'Fever, hyperthermia and the heat shock response', *International Journal of Hyperthermia*, 29(5), pp. 423–435. doi: 10.3109/02656736.2013.808766.

Sit, S.-T. and Manser, E. (2011) 'Rho GTPases and their role in organizing the actin

cytoskeleton.', *Journal of cell science*. The Company of Biologists Ltd, 124(Pt 5), pp. 679–83. doi: 10.1242/jcs.064964.

Smyth, G. K. (2004) 'Linear Models and Empirical Bayes Methods for Assessing Differential Expression in Microarray Experiments', *Statistical Applications in Genetics and Molecular Biology*, 3(1), pp. 1–25. doi: 10.2202/1544-6115.1027.

Snapper, S. B. and Rosen, F. S. (1999) 'THE WISKOTT-ALDRICH SYNDROME PROTEIN (WASP): Roles in Signaling and Cytoskeletal Organization', *Annual Review of Immunology*. Annual Reviews 4139 El Camino Way, P.O. Box 10139, Palo Alto, CA 94303-0139, USA , 17(1), pp. 905–929. doi: 10.1146/annurev.immunol.17.1.905.

Sotiropoulos, A. *et al.* (1999) 'Signal-regulated activation of serum response factor is mediated by changes in actin dynamics.', *Cell*, 98(2), pp. 159–69.

Spector, A. A. and Yorek, M. A. (1985) *Membrane lipid composition and cellular function*, *Journal of Lipid Research*.

Starnes, T. W., Cortesio, C. L. and Huttenlocher, A. (2011) 'Imaging podosome dynamics and matrix degradation.', *Methods in molecular biology (Clifton, N.J.)*. NIH Public Access, 769, pp. 111–36. doi: 10.1007/978-1-61779-207-6_9.

Staszowska, A. D. *et al.* (2017) 'Investigation of podosome ring protein arrangement using localization microscopy images', *Methods*. Academic Press, 115, pp. 9–16. doi: 10.1016/J.YMETH.2016.11.005.

Stehbens, S. J. and Wittmann, T. (2014) 'Analysis of focal adhesion turnover: a quantitative live-cell imaging example.', *Methods in cell biology*. NIH Public Access, 123, pp. 335–46. doi: 10.1016/B978-0-12-420138-5.00018-5.

Stewart, P. L. and Nemerow, G. R. (2007) 'Cell integrins: commonly used receptors for diverse viral pathogens', *Trends in Microbiology*, 15(11), pp. 500–507. doi:

10.1016/j.tim.2007.10.001.

Stoiber, K. *et al.* (2018) 'Targeting de novo lipogenesis as a novel approach in anti-cancer therapy', *British Journal of Cancer*, 118(1), pp. 43–51. doi: 10.1038/bjc.2017.374.

Stovold, C. F., Millard, T. H. and Machesky, L. M. (2005) 'Inclusion of Scar/WAVE3 in a similar complex to Scar/WAVE1 and 2', *BMC Cell Biology*. BioMed Central, 6(1), p. 11. doi: 10.1186/1471-2121-6-11.

Stradal, T. *et al.* (2001) 'The Abl interactor proteins localize to sites of actin polymerization at the tips of lamellipodia and filopodia.', *Current biology : CB*, 11(11), pp. 891–5.

Strobl, H. *et al.* (1997) 'flt3 ligand in cooperation with transforming growth factor-beta1 potentiates in vitro development of Langerhans-type dendritic cells and allows single-cell dendritic cell cluster formation under serum-free conditions.', *Blood*. American Society of Hematology, 90(4), pp. 1425–34.

Su, I. *et al.* (2005) 'Polycomb Group Protein Ezh2 Controls Actin Polymerization and Cell Signaling', *Cell*, 121(3), pp. 425–436. doi: 10.1016/j.cell.2005.02.029.

Su, W.-H. *et al.* (2002) 'Differential movements of VE-cadherin and PECAM-1 during transmigration of polymorphonuclear leukocytes through human umbilical vein endothelium.', *Blood*. American Society of Hematology, 100(10), pp. 3597–603. doi: 10.1182/blood-2002-01-0303.

Subauste, M. C. *et al.* (2004) 'Vinculin modulation of paxillin-FAK interactions regulates ERK to control survival and motility.', *The Journal of cell biology*. Rockefeller University Press, 165(3), pp. 371–81. doi: 10.1083/jcb.200308011.

Suetsugu, S. and Takenawa, T. (2003) 'Translocation of N-WASP by nuclear localization and export signals into the nucleus modulates expression of HSP90.', *The*

Journal of biological chemistry. American Society for Biochemistry and Molecular Biology, 278(43), pp. 42515–23. doi: 10.1074/jbc.M302177200.

Sugihara, K. *et al.* (1998) 'Rac1 is required for the formation of three germ layers during gastrulation', *Oncogene*, 17(26), pp. 3427–3433. doi: 10.1038/sj.onc.1202595.

Suh, B., Biophys., B. H.-A. R. and 2008, undefined (2008) 'PIP2 Is a Necessary Cofactor for Ion Channel Function: How and Why?'.

Swinnen, J. V *et al.* (2000) 'Selective activation of the fatty acid synthesis pathway in human prostate cancer.', *International journal of cancer*, 88(2), pp. 176–9.

Taberner, F. J. *et al.* (2015) 'TRP channels interaction with lipids and its implications in disease', *Biochimica et Biophysica Acta (BBA) - Biomembranes*. Elsevier, 1848(9), pp. 1818–1827. doi: 10.1016/J.BBAMEM.2015.03.022.

Tahtamouni, L. *et al.* (2019) 'Molecular Regulation of Cancer Cell Migration, Invasion, and Metastasis', *Analytical Cellular Pathology*, 2019, pp. 1–2. doi: 10.1155/2019/1356508.

Takada, Y. *et al.* (2000) 'Granulocyte-colony stimulating factor enhances anti-tumour effect of hyperthermia.', *International journal of hyperthermia : the official journal of European Society for Hyperthermic Oncology, North American Hyperthermia Group*, 16(3), pp. 275–86.

Tal, O. *et al.* (2011) 'DC mobilization from the skin requires docking to immobilized CCL21 on lymphatic endothelium and intralymphatic crawling', *The Journal of Experimental Medicine*, 208(10), pp. 2141–2153. doi: 10.1084/jem.20102392.

Tarone, G. *et al.* (1985) 'Rous sarcoma virus-transformed fibroblasts adhere primarily at discrete protrusions of the ventral membrane called podosomes.', *Experimental cell research*, 159(1), pp. 141–57.

Taylor, M. D. *et al.* (2010) 'Nuclear role of WASp in the pathogenesis of dysregulated

TH1 immunity in human Wiskott-Aldrich syndrome.', *Science translational medicine*. NIH Public Access, 2(37), p. 37ra44. doi: 10.1126/scitranslmed.3000813.

Teti, A. *et al.* (1992) 'Protein kinase C affects microfilaments, bone resorption, and [Ca2+]o sensing in cultured osteoclasts', *American Journal of Physiology-Cell Physiology*, 263(1), pp. C130–C139. doi: 10.1152/ajpcell.1992.263.1.C130.

Thanabalu, T. and Munn, A. L. (2001) 'Functions of Vrp1p in cytokines and actin patches are distinct and neither requires a WH2/V domain', *The EMBO Journal*, 20(24), pp. 79–89.

Thomas, S. G. *et al.* (2017) 'The actin binding proteins cortactin and HS1 are dispensable for platelet actin nodule and megakaryocyte podosome formation.', *Platelets*. Taylor & Francis, 28(4), pp. 372–379. doi: 10.1080/09537104.2016.1235688.

Toraya-Brown, S. and Fiering, S. (2014) 'Local tumour hyperthermia as immunotherapy for metastatic cancer', *International Journal of Hyperthermia*, 30(8), pp. 531–539. doi: 10.3109/02656736.2014.968640.

Török, Z. *et al.* (2003) 'Heat shock protein coinducers with no effect on protein denaturation specifically modulate the membrane lipid phase.', *Proceedings of the National Academy of Sciences of the United States of America*. National Academy of Sciences, 100(6), pp. 3131–6. doi: 10.1073/pnas.0438003100.

Török, Z. *et al.* (2014) 'Plasma membranes as heat stress sensors: From lipid-controlled molecular switches to therapeutic applications', *Biochimica et Biophysica Acta (BBA) - Biomembranes*. Elsevier, 1838(6), pp. 1594–1618. doi: 10.1016/J.BBAMEM.2013.12.015.

Toth, M. and Fridman, R. (2001) 'Assessment of Gelatinases (MMP-2 and MMP-9) by Gelatin Zymography', in *Metastasis Research Protocols*. New Jersey: Humana

Press, pp. 163–174. doi: 10.1385/1-59259-136-1:163.

Trepat, X., Chen, Z. and Jacobson, K. (2012) 'Cell migration.', *Comprehensive Physiology*. NIH Public Access, 2(4), pp. 2369–92. doi: 10.1002/cphy.c110012.

Troeberg, L. and Nagase, H. (2003) 'Measurement of Matrix Metalloproteinase Activities in the Medium of Cultured Synoviocytes Using Zymography', in *Inflammation Protocols*. New Jersey: Humana Press, pp. 77–88. doi: 10.1385/1-59259-374-7:77.

Tsou, C.-L. *et al.* (2007) 'Critical roles for CCR2 and MCP-3 in monocyte mobilization from bone marrow and recruitment to inflammatory sites', *Journal of Clinical Investigation*, 117(4), pp. 902–909. doi: 10.1172/JCI29919.

Tsuboi, S. (2006) 'A complex of Wiskott-Aldrich syndrome protein with mammalian verprolins plays an important role in monocyte chemotaxis.', *Journal of immunology (Baltimore, Md. : 1950)*, 176(11), pp. 6576–85.

Tsuboi, S. (2007) 'Requirement for a complex of Wiskott-Aldrich syndrome protein (WASP) with WASP interacting protein in podosome formation in macrophages.', *Journal of immunology (Baltimore, Md. : 1950)*, 178(5), pp. 2987–95.

Tsuboi, S. *et al.* (2009) 'FBP17 Mediates a Common Molecular Step in the Formation of Podosomes and Phagocytic Cups in Macrophages', *Journal of Biological Chemistry*, 284(13), pp. 8548–8556. doi: 10.1074/jbc.M805638200.

Tulapurkar, M. E. *et al.* (2012) 'Febrile-Range Hyperthermia Modifies Endothelial and Neutrophilic Functions to Promote Extravasation', *American Journal of Respiratory Cell and Molecular Biology*, 46(6), pp. 807–814. doi: 10.1165/rcmb.2011-0378OC.

Turner, C. E., Glenney, J. R. and Burridge, K. (1990) 'Paxillin: a new vinculin-binding protein present in focal adhesions.', *The Journal of cell biology*, 111(3), pp. 1059–68.

Tyler, J. J., Allwood, E. G. and Ayscough, K. R. (2016) 'WASP family proteins, more than Arp2/3 activators.', *Biochemical Society transactions*. Portland Press Ltd, 44(5), pp. 1339–1345. doi: 10.1042/BST20160176.

Uruno, T. *et al.* (2001) 'Activation of Arp2/3 complex-mediated actin polymerization by cortactin', *Nature Cell Biology*. Nature Publishing Group, 3(3), pp. 259–266. doi: 10.1038/35060051.

Uruno, T., Zhang, P., *et al.* (2003) 'Haematopoietic lineage cell-specific protein 1 (HS1) promotes actin-related protein (Arp) 2/3 complex-mediated actin polymerization.', *The Biochemical journal*. Portland Press Ltd, 371(Pt 2), pp. 485–93. doi: 10.1042/BJ20021791.

Uruno, T., Liu, J., *et al.* (2003) 'Sequential interaction of actin-related proteins 2 and 3 (Arp2/3) complex with neural Wiscott-Aldrich syndrome protein (N-WASP) and cortactin during branched actin filament network formation.', *The Journal of biological chemistry*. American Society for Biochemistry and Molecular Biology, 278(28), pp. 26086–93. doi: 10.1074/jbc.M301997200.

Varon, C. *et al.* (2006) 'Transforming Growth Factor Induces Rosettes of Podosomes in Primary Aortic Endothelial Cells', *Molecular and Cellular Biology*, 26(9), pp. 3582–3594. doi: 10.1128/MCB.26.9.3582-3594.2006.

Varshney, P., Yadav, V. and Saini, N. (2016) 'Lipid rafts in immune signalling: current progress and future perspective.', *Immunology*. Wiley-Blackwell, 149(1), pp. 13–24. doi: 10.1111/imm.12617.

Vaughn, L. K., Bernheim, H. A. and Kluger, M. J. (1974) 'Fever in the lizard Dipsosaurus dorsalis.', *Nature*, 252(5483), pp. 473–4.

Verboon, J. M. *et al.* (2015) 'Wash Interacts with Lamin and Affects Global Nuclear Organization', *Current Biology*, 25(6), pp. 804–810. doi: 10.1016/j.cub.2015.01.052.

Vetterkind, S. *et al.* (2002) 'The rat homologue of Wiskott-Aldrich syndrome protein (WASP)-interacting protein (WIP) associates with actin filaments, recruits N-WASP from the nucleus, and mediates mobilization of actin from stress fibers in favor of filopodia formation.', *The Journal of biological chemistry*, 277(1), pp. 87–95. doi: 10.1074/jbc.M104555200.

Vidal, C. *et al.* (2002) 'Cdc42/Rac1-dependent activation of the p21-activated kinase (PAK) regulates human platelet lamellipodia spreading: implication of the cortical-actin binding protein cortactin.', *Blood*. American Society of Hematology, 100(13), pp. 4462–9. doi: 10.1182/blood.V100.13.4462.

Vígh, L. *et al.* (1997) 'Bimoclomol: a nontoxic, hydroxylamine derivative with stress protein-inducing activity and cytoprotective effects.', *Nature medicine*, 3(10), pp. 1150–4.

Vijayakumar, V. *et al.* (2015) 'Tyrosine phosphorylation of WIP releases bound WASP and impairs podosome assembly in macrophages'.

Villalba, M. *et al.* (2001) 'Vav1/Rac-dependent actin cytoskeleton reorganization is required for lipid raft clustering in T cells.', *The Journal of cell biology*. Rockefeller University Press, 155(3), pp. 331–8. doi: 10.1083/jcb.200107080.

Voets, T. *et al.* (2004) 'The principle of temperature-dependent gating in cold- and heat-sensitive TRP channels', *Nature*. Nature Publishing Group, 430(7001), pp. 748–754. doi: 10.1038/nature02732.

Volkman, B. F. *et al.* (2002) 'Structure of the N-WASP EVH1 domain-WIP complex: insight into the molecular basis of Wiskott-Aldrich Syndrome.', *Cell*, 111(4), pp. 565–76.

Walde, M. *et al.* (2014) 'Vinculin Binding Angle in Podosomes Revealed by High Resolution Microscopy', *PLoS ONE*. Edited by C. Gottardi. Public Library of Science,

9(2), p. e88251. doi: 10.1371/journal.pone.0088251.

Wang, W. C. *et al.* (1998) 'Fever-range hyperthermia enhances L-selectin-dependent adhesion of lymphocytes to vascular endothelium.', *Journal of immunology (Baltimore, Md. : 1950)*. American Association of Immunologists, 160(2), pp. 961–9. doi: 10.4049/jimmunol.167.5.2666.

Wang, Y. and McNiven, M. A. (2012) 'Invasive matrix degradation at focal adhesions occurs via protease recruitment by a FAK-p130Cas complex.', *The Journal of cell biology*. Rockefeller University Press, 196(3), pp. 375–85. doi: 10.1083/jcb.201105153.

Watling, J. R. *et al.* (2008) 'Mechanisms of thermoregulation in plants.', *Plant signaling & behavior*. Taylor & Francis, 3(8), pp. 595–7.

Weaver, A. M. *et al.* (2001) 'Cortactin promotes and stabilizes Arp2/3-induced actin filament network formation.', *Current biology : CB*, 11(5), pp. 370–4.

Weaver, A. M. (2006) 'Invadopodia: Specialized Cell Structures for Cancer Invasion', *Clinical & Experimental Metastasis*. Springer Netherlands, 23(2), pp. 97–105. doi: 10.1007/s10585-006-9014-1.

Weiskopf, K. *et al.* (2016) 'Myeloid Cell Origins, Differentiation, and Clinical Implications.', *Microbiology spectrum*. NIH Public Access, 4(5). doi: 10.1128/microbiolspec.MCHD-0031-2016.

Wengler, G. S. *et al.* (1995) 'High prevalence of nonsense, frame shift, and splice-site mutations in 16 patients with full-blown Wiskott-Aldrich syndrome.', *Blood*. American Society of Hematology, 86(10), pp. 3648–54.

Wernimont, S. A. *et al.* (2008) 'Adhesions ring: a structural comparison between podosomes and the immune synapse.', *European journal of cell biology*. NIH Public Access, 87(8–9), pp. 507–15. doi: 10.1016/j.ejcb.2008.01.011.

West, M. A. *et al.* (2004) 'Enhanced dendritic cell antigen capture via toll-like receptor-induced actin remodeling.', *Science (New York, N.Y.)*. American Association for the Advancement of Science, 305(5687), pp. 1153–7. doi: 10.1126/science.1099153.

West, M. A. *et al.* (2008) 'TLR ligand-induced podosome disassembly in dendritic cells is ADAM17 dependent.', *The Journal of cell biology*. The Rockefeller University Press, 182(5), pp. 993–1005. doi: 10.1083/jcb.200801022.

Westerberg, L. *et al.* (2003) 'Efficient antigen presentation of soluble, but not particulate, antigen in the absence of Wiskott-Aldrich syndrome protein.', *Immunology*, 109(3), pp. 384–91.

Wheeler, A. P. *et al.* (2006) 'Rac1 and Rac2 regulate macrophage morphology but are not essential for migration', *Journal of Cell Science*, 119(13), pp. 2749–2757. doi: 10.1242/jcs.03024.

Wiesner, C. *et al.* (2014) 'Podosomes in space', *Cell Adhesion & Migration*. Taylor & Francis, 8(3), pp. 179–191. doi: 10.4161/cam.28116.

Williams, K. C. *et al.* (2019) 'Invadopodia are chemosensing protrusions that guide cancer cell extravasation to promote brain tropism in metastasis', *Oncogene*. Nature Publishing Group, p. 1. doi: 10.1038/s41388-018-0667-4.

Worth, A. J. and Thrasher, A. J. (2015) 'Current and emerging treatment options for Wiskott–Aldrich syndrome', *Expert Review of Clinical Immunology*, 11(9), pp. 1015–1032. doi: 10.1586/1744666X.2015.1062366.

Wozniak, M. A. *et al.* (2004) 'Focal adhesion regulation of cell behavior', *Biochimica et Biophysica Acta (BBA) - Molecular Cell Research*. Elsevier, 1692(2–3), pp. 103–119. doi: 10.1016/J.BBAMCR.2004.04.007.

Wu, H. and Parsons, J. T. (1993) 'Cortactin, an 80/85-kilodalton pp60src substrate, is

a filamentous actin-binding protein enriched in the cell cortex.', *The Journal of cell biology*. Rockefeller University Press, 120(6), pp. 1417–26. doi: 10.1083/JCB.120.6.1417.

Wu, X. *et al.* (2004) 'Focal Adhesion Kinase Regulation of N-WASP Subcellular Localization and Function', *Journal of Biological Chemistry*, 279(10), pp. 9565–9576. doi: 10.1074/jbc.M310739200.

Wu, X. *et al.* (2006) 'Regulation of RNA-polymerase-II-dependent transcription by N-WASP and its nuclear-binding partners', *Nature Cell Biology*. Nature Publishing Group, 8(7), pp. 756–763. doi: 10.1038/ncb1433.

Xu, Y. Z. *et al.* (2018) 'c-Src kinase is involved in the tyrosine phosphorylation and activity of SLC11A1 in differentiating macrophages', *PLOS ONE*. Edited by M. Salvi. Public Library of Science, 13(5), p. e0196230. doi: 10.1371/journal.pone.0196230.

Yamaguchi, H. *et al.* (2005) 'Molecular mechanisms of invadopodium formation: the role of the N-WASP-Arp2/3 complex pathway and cofilin.', *The Journal of cell biology*. The Rockefeller University Press, 168(3), pp. 441–52. doi: 10.1083/jcb.200407076.

Yang, J. *et al.* (2014) 'Monocyte and macrophage differentiation: circulation inflammatory monocyte as biomarker for inflammatory diseases.', *Biomarker research*. BioMed Central, 2(1), p. 1. doi: 10.1186/2050-7771-2-1.

Yao, M. *et al.* (2015) 'Mechanical activation of vinculin binding to talin locks talin in an unfolded conformation', *Scientific Reports*. Nature Publishing Group, 4(1), p. 4610. doi: 10.1038/srep04610.

Yee, K. L., Weaver, V. M. and Hammer, D. A. (2008) 'Integrin-mediated signalling through the MAP-kinase pathway', *IET Systems Biology*, 2(1), pp. 8–15. doi: 10.1049/iet-syb:20060058.

Yoo, Y., Wu, X. and Guan, J.-L. (2007) 'A Novel Role of the Actin-nucleating Arp2/3 Complex in the Regulation of RNA Polymerase II-dependent Transcription', *Journal of Biological Chemistry*. American Society for Biochemistry and Molecular Biology, 282(10), pp. 7616–7623. doi: 10.1074/JBC.M607596200.

Yoshimura, T. *et al.* (1989) 'Human monocyte chemoattractant protein-1 (MCP-1). Full-length cDNA cloning, expression in mitogen-stimulated blood mononuclear leukocytes, and sequence similarity to mouse competence gene JE.', *FEBS letters*, 244(2), pp. 487–93.

Young, L. E., Heimsath, E. G. and Higgs, H. N. (2015) 'Cell type–dependent mechanisms for formin-mediated assembly of filopodia', *Molecular Biology of the Cell*. Edited by W. Bement, 26(25), pp. 4646–4659. doi: 10.1091/mbc.E15-09-0626.

Yu, C. *et al.* (2013) 'Integrin-matrix clusters form podosome-like adhesions in the absence of traction forces.', *Cell reports*, 5(5), pp. 1456–68. doi: 10.1016/j.celrep.2013.10.040.

Zhang, H. *et al.* (2006) 'Impaired Integrin-Dependent Function in Wiskott-Aldrich Syndrome Protein-Deficient Murine and Human Neutrophils', *Immunity*, 25(2), pp. 285–295. doi: 10.1016/j.immuni.2006.06.014.

Zheng, B. *et al.* (2009) 'Nuclear actin and actin-binding proteins in the regulation of transcription and gene expression', *FEBS Journal*, 276(10), pp. 2669–2685. doi: 10.1111/j.1742-4658.2009.06986.x.

Zhou, S. *et al.* (2006) 'Effects of tyrosine phosphorylation of cortactin on podosome formation in A7r5 vascular smooth muscle cells', *American Journal of Physiology-Cell Physiology*, 290(2), pp. C463–C471. doi: 10.1152/ajpcell.00350.2005.

Zhu, Q. *et al.* (1995) 'The Wiskott-Aldrich syndrome and X-linked congenital thrombocytopenia are caused by mutations of the same gene', *Blood*, 86(10).

Zhu, Y. *et al.* (2011) 'Regulation of Thermogenesis in Plants: The Interaction of Alternative Oxidase and Plant Uncoupling Mitochondrial Protein', *Journal of Integrative Plant Biology*, 53(1), pp. 7–13. doi: 10.1111/j.1744-7909.2010.01004.x.

Zicha, D. *et al.* (1998) 'Chemotaxis of macrophages is abolished in the Wiskott-Aldrich syndrome.', *British journal of haematology*, 101(4), pp. 659–65.

Ziegler-Heitbrock, L. *et al.* (2010) 'Nomenclature of monocytes and dendritic cells in blood', *Blood*, 116(16), pp. e74–e80. doi: 10.1182/blood-2010-02-258558.

Ziegler, Y. S. *et al.* (2014) 'Plasma membrane proteomics of human breast cancer cell lines identifies potential targets for breast cancer diagnosis and treatment.', *PloS one*. Public Library of Science, 9(7), p. e102341. doi: 10.1371/journal.pone.0102341.

van Zijl, F., Krupitza, G. and Mikulits, W. (2011) 'Initial steps of metastasis: cell invasion and endothelial transmigration.', *Mutation research*. Elsevier, 728(1–2), pp. 23–34. doi: 10.1016/j.mrrev.2011.05.002.

Zuchero, J. B. *et al.* (2009) 'p53-cofactor JMY is a multifunctional actin nucleation factor', *Nature Cell Biology*. Nature Publishing Group, 11(4), pp. 451–459. doi: 10.1038/ncb1852.